UNIVERSIDADE FEDERAL DE VIÇOSA

Produção de bio-óleo e biohidrogênio a partir de microalgas cultivadas em águas residuárias

Thiago Abrantes Silva
Doctor Scientiae

VIÇOSA - MINAS GERAIS
2025

THIAGO ABRANTES SILVA

Produção de bio-óleo e biohidrogênio a partir de microalgas cultivadas em águas residuárias

Tese apresentada à Universidade Federal de Viçosa, como parte das exigências do Programa de Pós-Graduação em Engenharia Civil, para obtenção do título de *Doctor Scientiae*.

Orientadora: Maria Lucia Calijuri

Coorientador: Alberto J. D. dos Reis

VIÇOSA - MINAS GERAIS
2025

Ficha catalográfica elaborada pela Biblioteca Central da Universidade Federal de Viçosa - Campus Viçosa

T
S586p
2025

Silva, Thiago Abrantes, 1992-
Produção de bio-óleo e biohidrogênio a partir de microalgas cultivadas em águas residuárias / Thiago Abrantes Silva. – Viçosa, MG, 2025.
1 tese eletrônica (221 f.): il. (algumas color.).

Inclui anexos.
Inclui apêndices.
Orientador: Maria Lúcia Calijuri.
Tese (doutorado) - Universidade Federal de Viçosa, Departamento de Engenharia Civil, 2025.
Inclui bibliografia.
DOI: https://doi.org/10.47328/ufvbbt.2025.305
Modo de acesso: World Wide Web.

1. Biocombustíveis. 2. Biomassa - Efeito das algas. 3. Resíduos industriais. 4. Hidrogênio como combustível. 5. Fermentação. I. Calijuri, Maria Lúcia, 1955-. II. Universidade Federal de Viçosa. Departamento de Engenharia Civil. Programa de Pós-Graduação em Engenharia Civil. III. Título.

CDD 22. ed. 662.88

Bibliotecário(a) responsável: Euzébio Luiz Pinto CRB-6/3317

THIAGO ABRANTES SILVA

Produção de bio-óleo e biohidrogênio a partir de microalgas cultivadas em águas residuárias

Tese apresentada à Universidade Federal de Viçosa, como parte das exigências do Programa de Pós-Graduação em Engenharia Civil, para obtenção do título de *Doctor Scientiae*.

APROVADA: 10 de março de 2025.

Assentimento:

_____

Thiago Abrantes Silva
Autor

_____

Maria Lucia Calijuri
Orientadora

À minha avó Amélia (*in memoriam*),
que me criou como filho.
Dedico.

AGRADECIMENTOS

Agradeço à minha mãe duas vezes, Amélia, que agora está no céu, mas estará sempre viva em meu coração e ao meu avô Sebastião por todo amor e carinho;
Agradeço à professora Maria Lúcia Calijuri, por toda a orientação, suporte e confiança durante essa jornada;
Ao Doutor Alberto José Delgado dos Reis do Laboratório Nacional de Energia e Geologia (LNEG), por todo suporte, paciência, esclarecimento de dúvidas e por ter viabilizado uma das experiências mais importantes da minha carreira;
À Professora Paula Assemany e ao Professor Eduardo Couto por todos os ensinamentos e as orientações. Aprendi e aprendo muito com eles;
À Paula Costa, Filipe Paradela, Paula Marques, Filipa, Graça e Natércia e demais colegas que fiz no LNEG por todo suporte durante o doutorado sanduíche;
Agradeço ao Professor Fábio de Ávila Rodrigues e ao Doutor Maurino Magno de Jesus Junior, por todo apoio e esclarecimento de dúvidas.
Ao professor Marcelo Zaiat, Professor Lucas Tadeus Fuess e Matheus Neves de Araujo, da Escola de Engenharia de São Carlos da Universidade de São Paulo (EESC-USP) pela paciência em explicar os mais diversos conceitos do universo do biohidrogênio;
À Alexia Saleme Aona de Paula Pereira e Iara Barbosa Magalhães, pela amizade e apoio imprescindível para a elaboração deste trabalho;
Ao Arthur, Matheus, Juliana, Jéssica, Ana Paula, Bruno, Letícia e Nayara por terem sido grandes amigos nessa jornada.
Às amigas que fiz em Lisboa, Bruna e Valéria, por terem feito a experiência que vivi lá ser muito mais interessante.
A toda a minha família, por todo o amor, sempre me dando forças para que eu chegasse até aqui;
Agradeço aos demais amigos e colegas do SIGEOnPA e aos estagiários do LESA. Sem eles nada disso teria sido possível.
Agradeço aos professores da Universidade Federal Viçosa (UFV) pelos valiosos ensinamentos e ensino de qualidade;
Ao Programa de Pós-Graduação em Engenharia Civil, pela oportunidade de realização deste doutorado;
Este trabalho foi realizado com o apoio das seguintes agências de pesquisa brasileiras: Coordenação de Aperfeiçoamento de Pessoal de Nível Superior – Brasil (CAPES) – Código de Financiamento 001, Fundação de Amparo à Pesquisa do Estado de Minas Gerais (FAPEMIG) e Conselho Nacional de Desenvolvimento Científico e Tecnológico (CNPq).

“Quem nunca cometeu um erro,
nunca tentou algo novo”
Albert Einstein

RESUMO

SILVA, Thiago Abrantes, D.Sc., Universidade Federal de Viçosa, março de 2025. **Produção de bio-óleo e biohidrogênio a partir de microalgas cultivadas em águas residuárias**. Orientadora: Maria Lucia Calijuri. Coorientador: Alberto José Delgado dos Reis.

A integração da produção de biomassa de microalgas com a geração de bio-óleo e biohidrogênio (bioH_2) apresenta uma abordagem potencialmente sustentável e inovadora para energia renovável e recuperação de recursos. Este estudo abrange o cultivo de microalgas em sistemas híbridos (reatores de biofilme integrados a lagoas de alta taxas) utilizando uma mistura de efluentes industriais e domésticos para maximizar a produtividade da biomassa. Frequências de raspagem a cada 2 dias proporcionaram a maior produtividade de biomassa (18,75 g de sólidos voláteis totais m^{-2} d^{-1}) e maior teor lipídico (15,45%), além de alcançar tratamento eficiente do efluente, com remoção de até 100% do nitrogênio amoniacal. A biomassa produzida foi utilizada em duas rotas de valorização. A primeira envolveu a liquefação hidrotermal (LHT) para produção de bio-óleo, com maiores produções de bio-óleo a 300°C por 30 minutos, resultando em um bio-óleo com teor de carbono de até 76,3% e poder calorífico de até 38,34 MJ kg^{-1}. O aprimoramento com catalisadores de cobalto-molibdênio (CoMo) aumentou a presença de hidrocarbonetos de cadeia longa, como o heptadecano, destacando seu potencial como biocombustível, embora ainda seja necessário um refinamento adicional para atender aos padrões de combustível, como por exemplo, maiores remoção de compostos nitrogenados. A segunda rota explorou a produção de bioH_2 por fermentação escura, precedida por um pré-tratamento hidrotérmico com fosfato de nióbio (NbP) para melhorar a fermentabilidade da biomassa. O pré-tratamento a 180°C por 10 minutos com 75% de NbP liberou 7.431 mg carboidratos totais (CHt) L^{-1}, melhorando os rendimentos de bioH2 (1,03 mmol H_2 mol^{-1} CHt) em comparação com a biomassa não tratada. Fermentação com pH 5,0 alcançou uma eficiência de conversão de carboidratos de 83,6%, destacando a sinergia entre o pré-tratamento e o controle de pH para uma hidrogenogênese mais eficiente. No geral, este trabalho destaca o potencial das microalgas cultivadas em efluentes como uma matéria-prima versátil para energia renovável, enfatizando a necessidade de otimização nos aspectos econômicos e ambientais para viabilizar a implementação em larga escala. Para ambas as rotas, a análise econômica revelou que a obtenção de biomassa de microalgas representa a maior parcela dos custos de produção, enquanto a análise do ciclo de vida (ACV)

demonstrou que a utilização de fontes de energia renováveis nos processos é fundamental para minimizar os impactos ambientais, reforçando a necessidade de estratégias de otimização para garantir a viabilidade sustentável e econômica em larga escala.

Palavras-chave: Tratamento de efluentes; Colheita de biomassa; Biocombustíveis; Liquefação hidrotérmica; Fermentação escura; Análise de viabilidade

ABSTRACT

SILVA, Thiago Abrantes, D.Sc., Universidade Federal de Viçosa, March, 2025. **Production of bio-oil and biohydrogen from microalgae cultivated in wastewater**. Adviser: Maria Lucia Calijuri. Co-adviser: Alberto José Delgado dos Reis.

The integration of microalgae biomass production with bio-oil and biohydrogen (bioH_2) generation presents a potentially sustainable and innovative approach to renewable energy and resource recovery. This study involves the cultivation of microalgae in hybrid systems (biofilm reactors integrated with high-rate algal ponds) using a mixture of industrial and domestic effluents to maximize biomass productivity. Scraping frequencies every two days resulted in the highest biomass productivity (18.75 g of total volatile solids m^{-2} d^{-1}) and lipid content (15.45%), while also achieving efficient wastewater treatment, with up to 100% removal of ammoniacal nitrogen. The produced biomass was utilized in two valorization pathways. The first involved hydrothermal liquefaction (HTL) for bio-oil production, with the highest bio-oil yields obtained at 300°C for 30 minutes, resulting in a bio-oil with up to 76.3% carbon content and a heating value of up to 38.34 MJ kg^{-1}. Upgrading with cobalt-molybdenum (CoMo) catalysts increased the presence of long-chain hydrocarbons, such as heptadecane, highlighting its potential as a biofuel. However, further refining is still necessary to meet fuel standards, particularly regarding the removal of nitrogenous compounds. The second pathway explored bioH_2 production through dark fermentation, preceded by a hydrothermal pretreatment with niobium phosphate (NbP) to enhance biomass fermentability. Pretreatment at 180°C for 10 minutes with 75% NbP released 7,431 mg of total carbohydrates (CHt) L^{-1}, improving bioH2 yields (1.03 mmol H_2 mol^{-1} CHt) compared to untreated biomass. Fermentation at pH 5.0 achieved a carbohydrate conversion efficiency of 83.6%, emphasizing the synergy between pretreatment and pH control for more efficient hydrogenogenesis. Overall, this study highlights the potential of microalgae cultivated in effluents as a feedstock for renewable energy, underscoring the need for economic and environmental optimization to enable large-scale implementation. For both pathways, the economic analysis revealed that microalgae biomass obtention represents the largest share of production costs, while the life cycle assessment (LCA) demonstrated that the use of renewable energy sources in the processes is crucial to minimizing environmental impacts. This reinforces the need for optimization strategies to ensure sustainable and economically viable large-scale deployment.

Keywords: Wastewater treatment; Biomass harvesting; Biofuels; Hydrothermal liquefaction; Dark fermentation; Feasibility analysis

LISTA DE TABELAS

LISTA DE FIGURAS

Sumário

APRESENTAÇÃO

Este documento está estruturado em seis capítulos. O primeiro apresenta uma revisão dos temas abordados no escopo da tese. Esse levantamento possibilitou identificar as principais pesquisas relacionadas ao cultivo de microalgas em águas residuárias, o uso de biofilmes para colheita de biomassa e a produção de bio-óleo e biohidrogênio a partir da biomassa de microalgas. O segundo capítulo explora a otimização do processo de colheita de biomassa, integrando reatores de biofilme a lagoas de alta taxa. O objetivo dessa otimização é assegurar uma recuperação eficaz da biomassa gerada, potencializando sua viabilidade para produção dos biocombustíveis propostos. O terceiro capítulo aborda a produção e refino de bio-óleo por processo de liquefação hidrotérmica (LHT). A pesquisa do terceiro capítulo foi realizada no Laboratório Nacional de Energia e Geologia (LNEG), em Portugal, sob orientação do Pesquisador Alberto José Delgado dos Reis no âmbito do Edital CAPES Nº 10/2022 do Programa de Doutorado Sanduíche no Exterior (PDSE). O quarto capítulo envolveu a avaliação do ciclo de vida e a avaliação econômica do processo de LHT e da produção de bio-óleo. O quinto capítulo tratou da produção de biohidrogênio por processo de fermentação escura utilizando a biomassa de microalgas como substrato. Por fim, o sexto capítulo envolveu a avaliação econômica e ambiental da produção de biohidrogênio.

Na abordagem da separação de biomassa utilizando reatores de biofilme, destaca-se o projeto "FAPEMIG TEC APQ 02527-18 - Edital 001/2018 Demanda Universal. Tecnologia Inovadora Aplicada ao Tratamento de Efluentes, Produção de Biomassa Algal e Valorização Energética", aprovado em 2021. O objetivo geral envolve o tratamento de efluente e a utilização como meio de cultivo para a produção de biomassa algal em lagoas de alta taxa adaptadas com reatores de biofilme. No que se refere a valorização energética, destacam-se os projetos "CNPq 405787/2022-7 - Biohidrogênio sustentável por meio de microalgas cultivadas em esgotos sanitários: Desempenho e estratégias inovadoras de produção", aprovado em 2022. O objetivo do projeto é avaliar a viabilidade energética, ambiental e econômica da produção de biohidrogênio por meio de biomassa de microalgas cultivada em águas residuárias. Destaca-se o projeto "Ciência por Elas (FAPEMIG APQ-03618-23) - Biorrefinarias Algais para a Produção Sustentável de Bioprodutos: Aspectos técnicos, econômicos e ambientais", aprovado em 2023. Dentre os objetivos do projeto, tem-se a produção de biohidrogênio por fermentação escura e a produção de bio-óleo por liquefação hidrotérmica. Por fim, destaca-se o projeto "REDES FAPEMIG (RED-00068-23) - Estratégias emergentes e disruptivas para o saneamento sustentável no estado de Minas

Gerais: Biorrefinaria de microalgas no contexto de redes de desenvolvimento tecnológico" aprovado em 2023. Dentre os objetivos do projeto, tem-se também a produção de biohidrogênio e bio-óleo, bem com a avaliação econômica e ambiental destes processos.

1. Introdução geral

A necessidade de alternativas sustentáveis para os combustíveis fósseis tem ganhado destaque no cenário global. Neste contexto, as microalgas surgem como uma matéria-prima promissora para a produção de biocombustíveis, devido à sua eficiência fotossintética e capacidade de tratar águas residuárias enquanto produzem biomassa (ASSIS et al., 2020; CHOUDHARY; MALIK; PANT, 2017). As microalgas, ao serem cultivadas em águas residuárias, promovem a remoção de nutrientes excessivos e contribuem para a sequestro de dióxido de carbono (CO_2), atuando simultaneamente no tratamento de efluentes e na mitigação de emissões de gases de efeito estufa.

Para garantir a produção de biomassa para produção de tais biocombustíveis é necessário otimizar a forma de colheita da biomassa. Nesse contexto, sistemas híbridos, como aqueles que incorporam lagoas de algas de alta taxa (LAT) e reatores de biofilme (RBs), têm mostrado potencial no tratamento de águas residuárias enquanto cultivam microalgas (ASSIS et al., 2020; BOELEE et al., 2014; GROSS et al., 2013). ASSIS et al. (2020) discutem que a integração de LAT e RB facilitou a colheita de biomassa, com a eficiência de colheita aumentando para 61% em comparação com 22% quando coletada apenas em LAT. GROSS et al. (2013) constataram uma produtividade de biomassa de 8.09 g m^{-2} d^{-1} em um sistema de LAT aprimorado com sistema de crescimento aderido, em comparação com 3.48 g m^{-2} d^{-1} em LAT apenas.

Com relação à produção de biocombustíveis, a liquefação hidrotérmica (LHT) é uma técnica termoquímica que converte biomassa úmida em bio-óleo em condições de alta pressão, usando água como solvente reacional (CASTELLO; HAIDER; ROSENDAHL, 2019). Neste processo, a água promove a degradação das macromoléculas orgânicas em compostos mais simples. Estes, por sua vez, podem ser repolimerizados, gerando o bio-óleo (GRANDE et al., 2021). Contudo, conforme apontado por COUTO et al. (2020), o bio-óleo produzido por meio das microalgas pode ter um alto teor de nitrogênio, o que aumenta o risco de emissões de óxidos de nitrogênio (NOx). Isso sinaliza a potencial necessidade de aprimoramento do bio-óleo produzido.

Operando a temperaturas entre 250°C e 374°C e pressões de 100 a 221 bar, o processo de LHT transforma a biomassa em quatro produtos principais: bio-óleo, hidrochar, compostos solúveis em água e gases. Vale ressaltar que o rendimento do bio-óleo pode ultrapassar o conteúdo lipídico original da biomassa (CASTELLO; HAIDER; ROSENDAHL, 2019). Uma vantagem econômica adicional é a redução dos custos de secagem da biomassa na fase de preparação.

A eficiência da LHT e a qualidade dos produtos derivados dependem fortemente das condições operacionais. Fatores como temperatura, tempo de reação, proporção de biomassa/água e a introdução de catalisadores são decisivos. Por exemplo, temperaturas a partir de 300°C tendem a favorecer maiores rendimentos de bio-óleo. No entanto, a temperatura ideal pode variar de acordo com a composição específica da biomassa (GOLLAKOTA; KISHORE; GU, 2018). Além disso, tempos de reação mais curtos, variando entre 15 e 60 minutos, mostraram-se mais eficazes em termos econômicos (ZHANG, 2010).

A adição de catalisadores também pode potencializar a técnica. Eles podem ser homogêneos, como ácidos ou bases, ou heterogêneos, predominantemente óxidos metálicos (COUTO; CALIJURI; ASSEMANY, 2020). JIN et al. (2019) enfatizam que a hidrodesoxigenação (HDO) é uma abordagem catalítica promissora para otimizar as propriedades do bio-óleo, alinhando-o melhor com os padrões de combustíveis tradicionais.

O biohidrogênio, por sua vez, é reconhecido por seu alto conteúdo energético (142 kJ g^{-1}), superando combustíveis convencionais. Um dos principais processos para produção de biohidrogênio é a fermentação escura. A produção de biohidrogênio via fermentação escura, um processo biotecnológico baseado na digestão anaeróbia, tem sido explorada como uma alternativa promissora (MAÑUNGA et al., 2022). Na fermentação escura, a biomassa de microalgas enquanto substrato gera uma mistura de gases, incluindo hidrogênio (H_2), monóxido de carbono (CO), dióxido de carbono (CO_2), metano (CH_4) e vapor de água (SINGH; DAS, 2020). Para otimizar essa produção, um pré-tratamento da biomassa pode ser necessário. O objetivo desse pré-tratamento é romper as células de microalgas, liberando carboidratos e tornando o processo de produção mais eficiente (AHMED et al., 2021). Existem vários métodos de pré-tratamento, incluindo ultrassônico, enzimático, químico e térmico, e o método mais adequado pode variar dependendo da espécie de microalga (CHOI et al., 2011; NGUYEN et al., 2010; PHANDUANG et al., 2019; XIA et al., 2013). Além disso, diversos aspectos, como pH e temperatura, desempenham um papel significativo na produção de biohidrogênio por meio de microalgas (BALA AMUTHA; MURUGESAN, 2011; CHANG, 2004; HEMSCHEMEIER; MELIS; HAPPE, 2009; ONCEL et al., 2014; RAZU; HOSSAIN; KHAN, 2019).

A análise econômica e ambiental de processos baseados em biomassa de microalgas é essencial para avaliar sua viabilidade. Segundo CASTRO et al. (2023), essas estimativas fornecem dados importantes sobre impactos ambientais e custos econômicos associados aos produtos

gerados. Os autores discutem ainda que a avaliação de custos de aquisição, operação e impactos ao longo do ciclo de vida identifica gargalos críticos, como o elevado consumo energético em etapas específicas, destacando a necessidade de otimização dos sistemas. Além disso, essas análises orientam a escolha de rotas mais sustentáveis, promovendo tecnologias que maximizem a recuperação de recursos e minimizem impactos ambientais, fornecendo suporte estratégico para o escalonamento de processos sustentáveis e economicamente viáveis.

Nesse contexto, o presente estudo visa avaliar a produção de bio-óleo e biohidrogênio a partir de microalgas cultivadas em águas residuárias em reatores híbridos. Adicionalmente, investiga-se a viabilidade econômica e ambiental dos processos propostos, com o objetivo de identificar as condições mais eficientes e sustentáveis para a produção de biocombustíveis, contribuindo para a integração de sistemas de tratamento de águas residuárias e processos de conversão de biomassa.

2. Hipóteses da pesquisa

- Raspagens menos frequentes em reatores de biofilme promovem maior produtividade de biomassa, além de favorecer o acúmulo de lipídios e carboidratos na biomassa, potencializando sua valorização energética.
- O pré-tratamento hidrotérmico da biomassa de microalgas, realizado com o uso do catalisador fosfato de nióbio, favorece a liberação de carboidratos fermentáveis, potencializando a produção de biohidrogênio (bioH_2) por meio da fermentação escura.
- A liquefação hidrotérmica da biomassa mencionada, seguida do aprimoramento catalítico do bio-óleo resultante, promove o aumento da fração de hidrocarbonetos no produto final.
- A substituição de insumos e a integração energética reduzem custos e impactos ambientais, aumentando a viabilidade da produção de bio-óleo e bioH_2 a partir de microalgas cultivadas e águas residuárias.

3. Objetivo geral

- Investigar o potencial da biomassa de microalgas produzida em sistema híbrido para a produção de biohidrogênio e bio-óleo.

3.1. Objetivos específicos

- Avaliar como diferentes frequências de raspagem em reatores de biofilme influenciam na produtividade da biomassa e na composição bioquímica da biomassa.
- Avaliar o potencial da biomassa de microalgas cultivada em sistema híbrido, utilizando efluentes mistos da indústria alimentícia e doméstico, como substrato para a produção de biohidrogênio.
- Investigar o potencial da biomassa de microalgas produzida no sistema híbrido, utilizando efluentes mistos da indústria alimentícia e doméstico, para a produção de bio-óleo.
- Avaliar os impactos ambientais via avaliação do ciclo de vida do sistema de cultivo, da produção de bio-óleo por meio da liquefação hidrotérmica e da produção de biohidrogênio por meio da fermentação escura;
- Avaliar economicamente a produção de bio-óleo por meio da liquefação hidrotérmica e da produção de biohidrogênio por meio da fermentação escura.

4. Capítulo I. Revisão Bibliográfica

A presente revisão explora o processo de produção de biocombustíveis a partir de microalgas cultivadas em águas residuárias, com ênfase especial no tratamento de efluentes, na otimização da produção e colheita de biomassa, e na subsequente conversão em bio-óleo e biohidrogênio. No âmbito da produção de biohidrogênio, a revisão aborda os fatores e desafios relacionados ao emprego de microalgas, além de discutir técnicas para potencializar essa produção. De forma complementar, é analisada a viabilidade ambiental e econômica da produção de biohidrogênio. No que diz respeito à produção de bio-óleo, a revisão explora o processo de liquefação hidrotérmica (LHT), uma técnica para a conversão da biomassa de microalgas em bio-óleo. Aspectos técnicos como as condições de operação do reator de LHT e a incorporação de catalisadores para otimizar a produção de bio-óleo também são abordados. Assim como para o biohidrogênio, a viabilidade ambiental e econômica da produção de bio-óleo é discutida.

4.1. Otimização da produção e colheita de biomassa de microalgas para produção de biocombustíveis

Dentre as estratégias para a produção e colheita otimizada de biomassa, os sistemas híbridos, que combinam lagoa de alta taxa e reator de biofilme, vêm ganhando destaque. Nesse método, as águas residuárias e a biomassa presentes na lagoa de alta taxa (LAT) são continuamente recirculadas através dos reatores de biofilme, possibilitando o crescimento de biofilme aderido a estes reatores (Figura 4.1). Os sistemas híbridos oferecem uma abordagem inovadora, não apenas potencializando a produção de microalgas, mas também reduzindo custos operacionais e aumentando a eficiência do processo (ASSIS et al., 2020). Nesse contexto, ao aderirem a uma superfície, as microalgas podem crescer em camadas, aproveitando ao máximo a área disponível, o que pode não ser alcançado em cultivos em suspensão tradicionais (ZHUANG et al., 2018). Além disso, uma das principais vantagens desses sistemas é a redução nos custos de separação e colheita da biomassa, visto que as microalgas crescem aderidas a uma superfície, facilitando sua colheita (ASSIS et al., 2020).

Figura 4.1. Sistema híbrido composto de lagoa de alta taxa e reatores de biofilme (ASSIS et al., 2020).

A colheita das microalgas em grandes volumes de água dos sistemas de cultura em suspensão é um grande desafio, devido à baixa densidade (entre 0,3 - 5g.L) e ao pequeno tamanho (2 - 40 μm) das células (GULTOM; HU, 2013). Para efetiva colheita dessa biomassa, fazem-se necessárias separações sólido-líquidos em mais de uma etapa física, como em tanques de sedimentação e centrífugas, tornando as operações de separação onerosas e demoradas (JEEVANANDAM et al., 2020). Nesse sentido, há um enorme interesse no desenvolvimento de sistemas de cultivo baseados na formação de biofilmes, em que a biomassa cresce aderida a um material de apoio e pode ser facilmente coletada (ASSIS et al., 2020).

No crescimento aderido, existe um meio suporte capaz de sustentar a biomassa, formando o biofilme. O meio suporte pode ser natural, artificial ou constituído pela própria biomassa aglomerada e pode também estar imerso no meio líquido (SEHAR; NAZ, 2016). O desenvolvimento de biofilme fotossintético ocorre, primeiramente, com a fixação de bactérias e microalgas, que excretam substâncias poliméricas extracelulares (EPS), responsáveis por modificarem o substrato e condicionarem a superfície para o crescimento de outros microrganismos (FLEMMING, 2016). Após o estabelecimento da matriz EPS, as células das algas começam a crescer rapidamente. A matriz do biofilme facilita a retenção e o compartilhamento de nutrientes, uma vez que existem relações simbióticas entre as bactérias e microalgas (BESEMER, 2015). Sistemas de crescimento aderido e formação de biofilme para cultivo de microalgas têm sido

relatados na literatura, apresentando como as principais vantagens: elevada concentração, menor sensibilidade aos efeitos de toxicidade, eficiência na assimilação de nutrientes, rápida formação de biomassa e redução nos custos de separação da biomassa (ASSIS et al., 2020; BERNER; HEIMANN; SHEEHAN, 2015; CHOUDHARY; MALIK; PANT, 2017; GROSS et al., 2013; MANTZOROU; VERVERIDIS, 2019). Na Tabela 4.1 são apresentados trabalhos que realizaram a avaliação da produtividade de biomassa de microalgas utilizando diversos materiais de suporte e meios de cultivo.

Tabela 4.1.Comparação da produtividade de biomassa de microalgas em diferentes materiais de suporte e meios de cultivo.

Material suporte	Meio de cultivo	Microalga	Produtividade de biomassa ($g.m^{-2}.d^{-1}$)	Referência
Tecido de algodão	Efluente doméstico	Cultura mista, predominância de *Chlorella vulgaris*	5,87	ASSIS et al. (2017)
Tecido de algodão	Efluente doméstico	Cultura mista, predominância de *Chlorella vulgaris*	3,25	ASSIS et al. (2020)
Malha de náilon	Efluente doméstico	Cultura mista (*Scenedesmus, Chlorella, Pediastrum, Nitzschia, Cosmarium*)	9,1	LEE et al. (2014)
Tecido de náilon	Efluente doméstico	Cultura mista	1,8	ASSIS et al. (2019)
Tecido de poliéster	Efluente doméstico	Cultura mista	1,57	ASSIS et al. (2019)
Tecido de algodão	Efluente doméstico	Cultura mista	1,91	ASSIS et al. (2019)
Espuma de poliestireno	Água residuária da bovinocultura	*Chlorella* sp.	2,57	JOHNSON; WEN (2010)

Os suportes utilizados para o crescimento das microalgas abrangem desde tecidos de algodão e náilon até espuma de poliestireno. Dentre os trabalhos apresentados, a maioria utilizou efluente doméstico como meio de cultivo, com exceção de um que empregou água residuária da

bovinocultura (JOHNSON; WEN, 2010). O gênero de microalgas *Chlorella* aparece frequentemente, em especial a espécie *Chlorella vulgaris* que foi predominante em estudos de ASSIS et al. (2017, 2020). No entanto, a produtividade de biomassa apresentou diferenças, variando de 1.57 g/m²d (ASSIS et al., 2019) em poliéster a 9.1 g/m²d (LEE et al., 2014) em malha de náilon. Os estudos mostram um foco contínuo nesta área de pesquisa, porém com resultados variados, destacando a necessidade de aprofundamento e otimização das variáveis envolvidas.

Logo, a avaliação da frequência de raspagem nos sistemas híbridos de cultivo de microalgas é importante para evitar o acúmulo excessivo de biomassa sobre os suportes, que pode reduzir a penetração de luz e limitar o crescimento das microalgas. Esse ajuste permite manter a eficiência fotossintética, evitar o desprendimento descontrolado do biofilme e garantir uma colheita regular e otimizada. Além disso, acredita-se que a raspagem periódica contribui para a produtividade sustentável do sistema, maximizando o aproveitamento do meio de cultivo e reduzindo os custos operacionais associados à separação da biomassa.

4.2. Produção de bio-óleo e biohidrogênio a partir de microalgas cultivadas em águas residuárias

Na busca por energias sustentáveis, tem-se o biohidrogênio e o bio-óleo de microalgas como alternativas promissoras. Com relação ao hidrogênio, sua produção a partir de microalgas enfrenta desafios técnicos e operacionais. Métodos diretos utilizam luz, enquanto os indiretos recorrem a processos termoquímicos e bioquímicos. Além disso, a característica bioquímica da biomassa de microalgas como substrato é decisiva e pré-tratamentos podem ser necessários para otimizar a liberação de carboidratos, principal substrato para as bactérias produtoras de hidrogênio. Para o bio-óleo, a LHT é uma técnica destacada, processando biomassa úmida e convertendo lipídios, carboidratos e proteínas. A eficiência da LHT é influenciada por variáveis como temperatura e uso de catalisadores. A seguir, os temas aqui abordados são aprofundados.

4.2.1. Produção de biohidrogênio por meio de microalgas

O hidrogênio é o elemento mais abundante no universo e um dos mais abundantes da crosta terrestre (ZOHURI, 2019). Além disso, apresenta o maior poder calorífico entre os combustíveis conhecidos, sendo em média igual a 142 $MJ.kg^{-1}$. Embora o hidrogênio apresente grande potencial em termos de poder calorífico, a sua obtenção na forma pura é complexa e onerosa. Os principais

processos estudados para este fim são reforma a vapor ou autotérmica e oxidação parcial (CAPPELLETTI; MARTELLI, 2017). Ressalta-se que tais processos envolvem custos e energia, sendo obstáculos que ainda precisam ser superados (KALAMARAS; EFSTATHIOU, 2013). Nesse contexto, faz-se necessário aprimorar as formas de produção de bioH_2. Dentre tais formas, estudos recentes abordam a produção a partir de biomassa de microalgas (AHMED et al., 2022; SHOW et al., 2019). Nesse contexto, a produção direta (BAN et al., 2018; BAN; LIN; LUO, 2019; ZIARA et al., 2019) e indireta (ADNAN et al., 2019; ADNAN; HOSSAIN, 2018; FLORIO et al., 2019; KIM; LOGAN, 2019; KRISHNAN et al., 2019) de bioH_2 são abordados.

O principal processo para produção direta de bioH_2 é a fotofermentação. Com relação à produção indireta, fermentação escura, gaseificação e pirólise têm sido utilizados como processos de conversão química e células microbianas têm sido utilizadas para os processos eletroquímicos de produção de bioH_2 (AHMED et al., 2022). Na Figura 4.2 é apresentado um fluxograma dos principais bioprocessos para produção de bioH_2 a partir de microalgas.

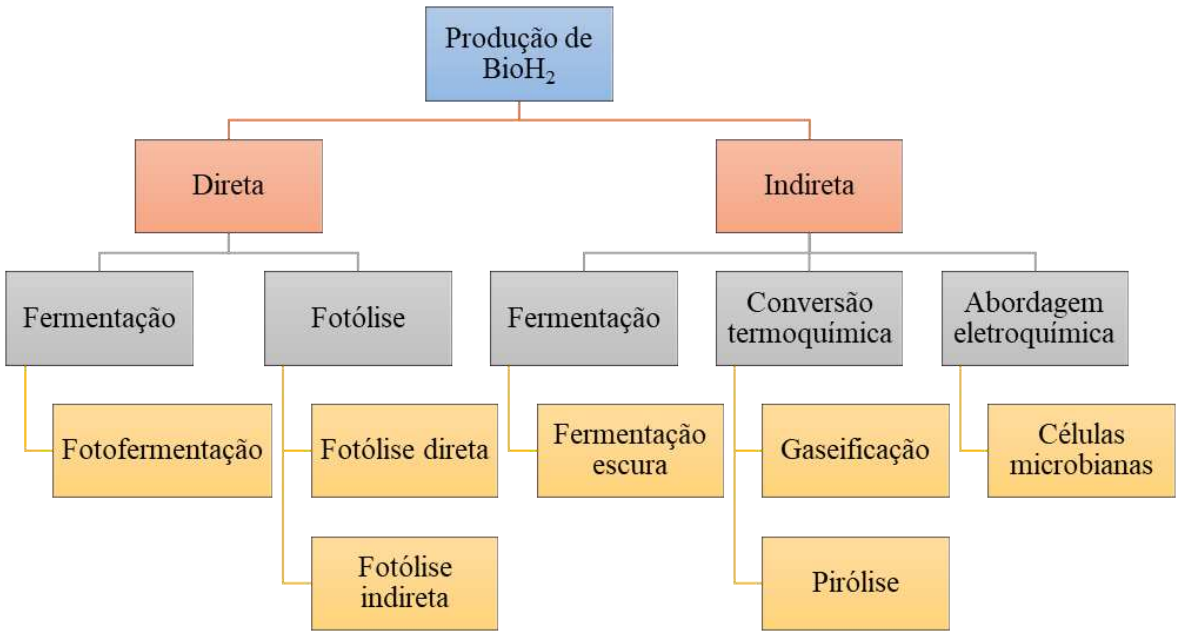

Figura 4.2. Bioprocessos para obtenção de bioH_2 a partir do cultivo de microalgas.

Na Tabela 4.2 são apresentados diferentes estudos que avaliaram a produção de biohidrogênio utilizando microalgas.

Tabela 4.2. Estudos que avaliaram a produção de biohidrogênio utilizando microalgas.

Microalga	Forma de produção	Produção de biohidrogênio	Referências
Chlorella vulgaris ESP6	Fermentação escura	1,15 mol mol SV^{-1}	LIU et al. (2012)
Chlorella vulgaris	Fermentação escura	19 ml H_2 g SV^{-1}	WIECZOREK; KUCUKER; KUCHTA (2014)
Chlorella vulgaris	Fermentação escura	190,90 mL H_2 g SV^{-1}	STANISLAUS et al. (2018)
Chlorella vulgaris FSP-E	Fermentação escura	2,87 mmol H_2 g SV^{-1}	CHEN; CHANG; CHANG (2016)
Chlorella sp.	Fotólise	10,31 ± 0,05 mL L^{-1}	SENGMEE et al. (2017)
Chlorella vulgaris	Fermentação escura	31,2 mL H_2 g CS^{-1}	YUN et al. (2012)
Tetradesmus sp.	Fermentação escura	40,27 mL H_2 g SV^{-1}	YANG et al. (2011)
Chlorella vulgaris	Fotofermentação	0,0019 g hL^{-1}	LAKSHMIKANDAN; MURUGESAN (2016)
Chlorella sp.	Fermentação escura	43,16 mL H_2 g SV^{-1}	SRIYOD; REUNGSANG; PLANGKLANG (2021)
Chlorella sp.	Fermentação escura	16,2 mL g SV^{-1}	LUNPROM et al. (2019)

Nota: SV = Sólidos voláteis, CS = Célula seca.

Dentre os trabalhos avaliados, a *Chlorella vulgaris* foi amplamente estudada em diferentes métodos de fermentação escura. LIU et al., (2012) relataram uma produção de 25,76 mL H_2 g SV^{-1} de *Chlorella vulgaris* ESP6, enquanto STANISLAUS et al., (2018) notaram uma produção de 190,90 mL H_2 g SV^{-1} utilizando a mesma espécie. CHEN; CHANG; CHANG (2016) reportaram uma produção de 2,87 mmol H_2 g^{-1} com *Chlorella vulgaris* FSP-E. Embora a fermentação escura seja o método mais utilizado para produção de biohidrogênio por meio das microalgas, SENGMEE et al., (2017), avaliaram a fotólise com a *Chlorella* sp. Os autores obtiveram uma produção de 10,31 mL L^{-1}. O estudo de YANG et al., (2011) com *Tetradesmus* sp. destaca que outras espécies também podem ser eficazes, com uma produção relatada de 40,27 mL H_2 g SV^{-1}, sugerindo que a

diversidade de microalgas pode ser explorada para otimização da produção de biohidrogênio. Em contraste, a fotofermentação foi menos produtiva, com LAKSHMIKANDAN; MURUGESAN (2016) relatando 0,0019 g hL^{-1} para *Chlorella vulgaris*. Por fim, estudos LUNPROM et al. (2019) integraram fermentação anaeróbia em estado sólido e fermentação escura para aumentar a produção de bioH_2 a partir de biomassa microalgal, alcançando 16,2 mL H_2 g^{-1} VS com alta eficiência de colheita (>90%). SRIYOD; REUNGSANG; PLANGKLANG (2021) otimizaram o pré-tratamento de *Chlorella* sp. com múltiplas enzimas (OSME), obtendo 43,16 mL H_2 g^{-1} SV, 39,63% superior à biomassa não tratada. OSME demonstrou ser alternativa eficiente aos processos sequenciais de hidrólise, convertendo biomassa em açúcares fermentáveis e bioH_2. A adição de nutrientes reduziu a eficiência do processo, destacando as condições otimizadas para produção sustentável.

4.2.2. Biohidrogênio a partir das microalgas: Produção direta

A produção direta de bioH_2 deve ocorrer em reator fechado, para garantir o armazenamento do gás produzido. Ademais, tal forma de produção é dependente de luz durante o cultivo de microalgas, em que a enzima hidrogenase é capaz de quebrar a molécula de água, produzindo bioH_2 (KHETKORN et al., 2017). A produção de bioH_2 se dá em fotobiorreatores, sendo os mais utilizados atualmente: tubular em cerca, tubular helicoidal, tubular horizontal, painel vertical, *air lift*, acordeão, tanque de agitação e coluna de bolhas (KHETKORN et al., 2017). Esses reatores estão, em sua maioria, desenvolvidos em escala laboratorial, necessitando mais estudos para o aumento da escala (SKJÅNES; REBOURS; LINDBLAD, 2013). Ademais, estudos mostram que um fotobiorreator adequado para produção de bioH_2 deve ter baixo tempo de detenção hidráulica sem remover a biomassa do reator (ARIMI et al., 2015).

Logo, os reatores supracitados visam aumentar a produção de bioH_2 por meio de seleção adequada de espécies de microalgas, técnicas de coleta e aspectos construtivos. É relevante conhecer a espécie de microalga utilizada afim de saber se seu código genético permite produzir esse biocombustível (AHMED et al., 2022). Dentre as espécies atualmente utilizadas tem-se *Chlorella sp., Spirulina obliquus, Spirulina platensis, Pseudomonas sp., Synechocystis sp., Rhodobacter sphaeroides, Chlamydomonas reinhardtii, Lysinibacillus sphaericus* e *Pseudomoas aeroginosa* (DUANGJAN et al., 2017).

4.2.3. Biohidrogênio a partir das microalgas: Produção indireta

Para a produção indireta do bioH_2, não há dependência de luz (SINGH; DAS, 2020). A biomassa é inserida em processos termoquímicos ou bioquímicos para produção do combustível. Quando a produção ocorre por processo bioquímico de fermentação, há geração de gás que pode conter dióxido de carbono (CO_2), gás metano (CH_4) e gás hidrogênio (H_2), podendo ser necessária posterior purificação (KUMAR; JONES; HANNA, 2009). Assim como na produção direta, o reator deve ser fechado para coleta e armazenamento do gás gerado.

4.2.3.1. Pré-tratamento para otimização da produção de biohidrogênio a partir das microalgas

A fim de otimizar a obtenção de bioH_2, a aplicação de pré-tratamentos à biomassa de microalgas pode ser necessária para garantir a produção adequada de bioH_2 em processos indiretos. Nesse contexto, tais tratamentos visam a ruptura das células para aumentar a disponibilidade de carboidratos (AHMED et al., 2022). Dentre os principais pré-tratamentos utilizados atualmente, tem-se o ultrassônico (CHOI et al., 2011), o enzimático (NGUYEN et al., 2010), o químico (PHANDUANG et al., 2019) e o térmico (XIA et al., 2013). Ressalta-se que, para algumas espécies de microalgas, o uso de ácido é mais adequado e enquanto para outras espécies cabe o tratamento alcalino. Os ácidos hidrolisam os polímeros da parede celular, resultando em sua ruptura. As bases, por sua vez, hidrolisam os lipídios da parede celular desintegrando sua estrutura (NAGARAJAN; CHANG; LEE, 2020).

4.2.3.2. Processos de produção indireta de biohidrogênio a partir das microalgas

Após o pré-tratamento, a biomassa pode ser inserida em diversos processos de conversão bioquímica, termoquímica ou eletroquímica. Na Tabela 4.3 são apresentadas vantagens e desvantagens desses processos de acordo com AHMED et al. (2022).

Tabela 4.3. Vantagens e desvantagens de diferentes tecnologias para produção de bioH_2.

Tecnologia	Vantagens	Desvantagens	Referência
Gaseificação	Processo consolidado	Produção de cinzas e alcatrão	AHMED et al. (2022)
Pirólise	Maior eficiência energética em comparação com a gaseificação	Processo complexo e caro; produção de cinzas e alcatrão	
Fermentação escura	Não necessita de luz ou oxigênio; consome pouca energia	Baixa produção de bioH_2; separação do gás produzido é um gargalo	
Células microbianas	Baixo tempo de detenção; rápida obtenção de H_2	Necessitam de energia elétrica continuamente; demandam mais estudos para escala	

Diante das diferentes tecnologias para produção de bioH_2, a fermentação escura destaca-se como uma alternativa promissora, especialmente para o uso de microalgas como substrato (AHMED et al., 2022). Essa tecnologia combina a simplicidade operacional com a possibilidade de integração em biorrefinarias, alinhando-se aos princípios de economia circular. No entanto, a eficiência da fermentação escura depende da disponibilidade de açúcares fermentáveis, mas as paredes celulares resistentes das microalgas, compostas de celulose e outras estruturas poliméricas, limitam o acesso dos microrganismos ao conteúdo intracelular (BHATIA et al., 2023). Para superar essa barreira, diversas estratégias de pré-tratamento têm sido investigadas. O pré-tratamento ácido-térmico, por exemplo, aumentou significativamente a recuperação de carboidratos em biomassa de *Scenedesmus obliquus*, alcançando 87,5% de recuperação, o que levou a um aumento de até 10 vezes na produção de biohidrogênio (de 9,8 para 97,6 mL g^{-1} SV) (SINGH; ROUT; DAS 2022).

A composição das microalgas pode variar amplamente dependendo das condições de cultivo, como disponibilidade de nutrientes e intensidade de luz. LACROUX et al. (2023) apontam que microalgas ricas em amido ou carboidratos simples, como *Chlamydomonas reinhardtii*, são preferíveis, pois apresentam maior conversão de carboidratos em bioH_2 durante a fermentação escura.

Estudos mostram que o controle do pH durante a fermentação pode modular as vias metabólicas e minimizar a formação de subprodutos inibitórios. Por exemplo, em estudo realizado

por ROGERI et al. (2023), o ajuste do pH favoreceu a fermentação butírica, resultando em maior produção de bioH_2.

A interação entre a biomassa de microalgas e consórcios bacterianos é um fator crítico no aumento da eficiência de processos bioquímicos. ANZOLA-ROJAS et al. (2025) destacaram que o gênero bacteriano *Thermoanaerobacterium*, frequentemente encontrado em sistemas fermentativos, pode alcançar uma taxa de conversão de glicose em H_2 de até 90% da fração molar, utilizando açúcares derivados de microalgas previamente hidrolisados, atingindo uma produção volumétrica de até 12,7 L H_2 m^{-2} d^{-1} em sistemas de eletrofermentação integrados.

O uso de microalgas em sistemas integrados de biorrefinaria oferece uma oportunidade para maximizar a recuperação de energia e valorizar subprodutos. LACROUX et al. (2023) demonstraram que os efluentes da fermentação escura, ricos em ácidos graxos voláteis como acetato (2897 mg L^{-1}), podem ser reutilizados no cultivo de microalgas heterotróficas ou utilizados como substrato na digestão anaeróbia para a produção de metano (CH_4). Além disso, avanços tecnológicos têm sido desenvolvidos para superar desafios relacionados à eficiência do processo. Estratégias adicionais incluem o uso de nanopartículas metálicas, como óxido de ferro (Fe_2O_3), para aumentar a eficiência das enzimas hidrogenases, reduzindo as limitações cinéticas e termodinâmicas da fermentação anaeróbia (LI et al., 2022).

Modificações genéticas de microalgas, como *Chlamydomonas reinhardtii*, têm mostrado promessas significativas, permitindo o aumento do acúmulo de carboidratos intracelulares para até 70% do peso seco em condições otimizadas (LI et al., 2022). Além disso, sistemas combinados de fermentação escura e fotobiorreatores têm explorado a reutilização de subprodutos como substratos, representando uma estratégia inovadora para transitar para uma economia circular (LI et al., 2022).

Em resumo, uma lacuna importante a ser preenchida é a otimização da produção de biohidrogênio por fermentação escura utilizando microalgas como substrato. Este estudo busca abordar essa lacuna, propondo estratégias para maximizar a eficiência do processo e consolidar essa tecnologia como uma alternativa viável e sustentável.

4.2.4. Viabilidade ambiental e econômica da produção de biohidrogênio a partir das microalgas

Como apresentado anteriormente, a obtenção do bioH_2 a partir das microalgas ainda é um desafio. Ademais, ainda existem poucos estudos ambientais e econômicos para determinar a viabilidade desse biocombustível. Dentre os trabalhos existentes, GHOLKAR et al. (2021) realizaram tais avaliações considerando a produção da microalga *Scenedesmus* sp., processando 12.790 kg de microalga.h^{-1}. Uma modelagem computacional foi realizada para avaliar a produção de bioH_2 a partir da biomassa de microalgas utilizando gaseificador como reator para a produção do biocombustível. Considerando condições experimentais ideais, a produção de H_2 do sistema foi de 12 kt ano^{-1}. Comparativamente, a produção convencional de H por eletrólise foi de cerca de 30 kt ano^{-1} (IEA, 2021). Embora a produção seja cerca de 60% do que o sistema convencional, o uso de microalgas é uma forma alternativa de produção desse combustível que está em constante aprimoramento. A análise ambiental mostrou que os principais impactos estiveram associados às mudanças climáticas devido à fonte de energia elétrica utilizada no gaseificador (75% combustíveis fósseis, 20% hidroeletricidade e 5% outras energias renováveis). Embora impactos ambientais tenham sido reportados, os autores relatam que a produção de bioH_2 é viável ambientalmente. Comparativamente, a produção de biometano no sistema apresentou impactos em termos de mudança climática 36,74 % maiores do que o bioH_2, demostrando o potencial desse biocombustível quando comparado ao biometano. Ainda assim, os autores sugerem a substituição da matriz energética para fontes como hidroeletricidade afim de diminuir impactos ambientais ao se utilizar fonte de energias não-renováveis. Ademais, os autores ressaltam que essa redução pode ser ainda maior se as microalgas forem cultivadas em águas residuárias.

Aliada a análise ambiental, faz-se necessário abordar a viabilidade econômica da produção de bioH_2 a partir das microalgas. Nesse contexto, a análise econômica realizada por GHOLKAR et al. (2021) mostrou que o custo de produção de microalgas é igual a USD 0,5 kg^{-1} microalga, com investimento total de USD 144,6 milhões de dólares. Ao se utilizar gaseificador, esse reator representou 11% dos gastos de material. Ademais, a eletricidade para o cultivo de microalgas representou 76% dos gastos de operação. Na produção direta, por sua vez, os fotobiorreatores são considerados muito caros em termos de implementação e custo operacional. Sendo este um grande desafio da geração de bioH_2 em grande escala a partir de microalgas cultivadas em águas residuárias (AHMED et al., 2022). Esses custos devem ser reduzidos para promover a aceitação dessas tecnologias pelas partes interessadas em diferentes níveis. É importante ressaltar que não

foram encontrados trabalhos que realizaram análise econômica e ambiental de outros bioprocessos para produção de bioH_2 a partir de microalgas.

Ademais, embora ainda sejam necessários mais estudos para viabilizar a produção de bioH_2 em escala comercial, a Agência Internacional de Energia (IEA) (IEA (INTERNATIONAL ENERGY AGENCY), 2006) estabelece como meta o custo comercial para a produção de hidrogênio no mercado competitivo em 0,30 USD.kg^{-1} H_2. Comparativamente, a referência de preço da gasolina é igual a 0,33 USD.kg^{-1} (SHOW et al., 2019). Nesse contexto, os estudos com foco em analisar as rotas e bioprocessos, os principais fatores que afetam a produção de bioH_2 e o atual cenário de viabilidade técnica, econômica e ambiental são importantes para garantir que esse biocombustível possa ser inserido no mercado de forma competitiva.

4.2.5. Bio-óleo como biocombustível

O principal processo para produção de bio-óleo a partir de microalgas é a LHT, que é um processo de conversão termoquímica que ocorre por meio do aquecimento da biomassa úmida em meio pressurizado (CASTELLO; HAIDER; ROSENDAHL, 2019). Nessas condições, a água existente na biomassa se mantém no estado líquido. Assim, a água participa de uma série de reações em cascata, que são responsáveis por degradar as macromoléculas orgânicas da biomassa em compostos menores, que em seguida, são repolimerizados, dando origem ao bio-óleo (GRANDE et al., 2021). Ressalta-se que existem outros processos termoquímicos que ocorrem na presença de água, que diferem da LHT em termos do produto principal a ser gerado e das condições de operação.

COUTO et al. (2020) apontam que o bio-óleo produzido na LHT possui de 70 a 95% do conteúdo energético do petróleo e suas propriedades físicas e químicas são altamente dependentes da composição da biomassa e das condições experimentais. Grande parte dos compostos presentes no bio-óleo é solúvel em acetona e diclorometano, sendo este último o principal solvente utilizado na separação dos produtos para quantificação do rendimento. Os autores apresentam ainda que uma caracterização parcial dos compostos existentes no bio-óleo pode ser realizada por meio de cromatografia gasosa, mas muitos compostos pesados podem permanecer não identificados em diferentes tipos de coluna. Ressalta-se que o principal problema relatado em relação ao bio-óleo da LHT de biomassa algal é o elevado conteúdo de nitrogênio, que não contribui para a elevação do poder calorífico e pode gerar emissões de NOx após a utilização.

4.2.6. O processo de LHT

A LHT ocorre em temperaturas que variam de 250°C a 374°C e pressões entre 100 e 221 bar. A biomassa utilizada como matéria-prima é convertida em quatro produtos, sendo o bio-óleo, hidrochar, produtos solúveis em água e gás. Durante o processo, não apenas os lipídeos participam das reações, mas também carboidratos e proteínas, sendo que muitas vezes o rendimento de bio-óleo é superior ao conteúdo lipídico da matéria prima (COUTO; CALIJURI; ASSEMANY, 2020). Isso ressalta a aplicabilidade do processo para diversos tipos de biomassa, como macroalgas, microalgas e bactérias com reduzida porcentagem de lipídeos (CASTELLO; HAIDER; ROSENDAHL, 2019). Adicionalmente, como a água participa das reações da LHT, os custos com secagem da biomassa podem ser reduzidos.

4.2.7. Condições de operação do reator de LHT

Como todos os processos termoquímicos, a LHT é fortemente influenciada pelas condições de operação do reator. Os principais parâmetros de operação são a temperatura, o tempo de reação, a razão biomassa/água e a presença de catalisadores. A temperatura está relacionada com as reações que ocorrem simultaneamente no reator. Diversos estudos possuem maiores rendimentos de bio-óleo em temperaturas superiores a 300°C. Em temperaturas inferiores, as reações de polimerização podem ainda não dominar em relação às reações de hidrólise (GRANDE et al., 2021). Contudo, a temperatura que vai propiciar maior rendimento é dependente das características da biomassa. Em temperaturas próximas a 250°C, os constituintes do bio-óleo são oriundos da degradação de lipídeos, enquanto em temperaturas maiores, acima dos 300°C, ocorre a conversão de carboidratos e proteínas (GOLLAKOTA; KISHORE; GU, 2018). Isso pode inclusive, ter influência na qualidade do bio-óleo, uma vez que mais moléculas de nitrogênio são liberadas com a degradação de aminoácidos.

O tempo de reação deve ser suficiente para que ocorra a conversão da matéria orgânica da biomassa. No entanto, em tempos demasiadamente longos, os compostos formados podem continuar reagindo e, consequentemente, reduzir o rendimento de bio-óleo. Algumas pesquisas apontam rendimento máximo de bio-óleo entre 30 e 60 minutos (ZHANG, 2010). Entretanto, quanto menor o tempo de reação, para um máximo rendimento, menores são os custos operacionais envolvidos no processo.

A importância da razão biomassa/água, também denotada como porcentagem de sólidos no material a entrar no reator, está diretamente relacionada a característica dos processos hidrotérmicos, onde a água assume papel importante nas reações, participando como catalisador. Dessa forma, uma razão elevada pode prejudicar a conversão da matéria orgânica (COUTO; CALIJURI; ASSEMANY, 2020). Ademais, o excesso de água no reator pode influenciar no consumo de energia para o aquecimento (GUO et al., 2015). Dessa forma, o ganho de rendimento com a redução da razão biomassa/água deve ser ponderado com essa questão e também com a demanda energética do processo de concentração da biomassa.

4.2.8. Uso de catalisadores para refino do bio-óleo

COUTO et al. (2020) apontam que os catalisadores utilizados na LHT de algas são divididos em duas categorias: homogêneos e heterogêneos. Os catalisadores homogêneos podem ser ácidos minerais, ácidos orgânicos e bases, enquanto os catalisadores heterogêneos são principalmente óxidos metálicos. O propósito da utilização dos catalisadores é melhorar o rendimento e a qualidade do bio-óleo. Da mesma forma que para outros parâmetros, a utilização de catalisadores deve ser ponderada em relação aos custos envolvidos, uma vez que implica em gastos de operação e também na separação dos produtos.

JIN et al. (2019) destacam que o processo catalítico mais promissor para estabilizar o bio-óleo é a hidrodesoxigenação (HDO). A HDO catalítica combina processos de hidrogenação e remoção de oxigênio, melhorando as propriedades do produto LHT, a densidade e estabilidade energética, aproximando o bio-óleo dos combustíveis derivados do petróleo ou biodiesel. Na Tabela 4.4 são apresentados trabalhos que realizaram o processo de LHT utilizando biomassa de microalgas.

Tabela 4.4. Estudos que realizaram liquefação hidrotérmica (LHT) e refino do bio-óleo produzido a partir das microalgas.

Microalga	Condições de LHT	Produção de bio-óleo e características	Referência
Nannochloropsis sp.	Temperatura de 320 °C por 30 min	50% de produção com %C de 64,1%	PONGSIRIYAKUL et al. (2021)

Microalga	Condições de LHT	Produção de bio-óleo e características	Referência
Spirulina platensis	Catalisador CeO_2. Temperatura de 250 °C por 30 min	33% de produção, PCS de 35,64 MJ kg^{-1} e %C de 69,75%	KANDASAMY et al. (2021)
Spirulina platensis	Catalisador Fe_3O_4. Temperatura de 320° C por 37 min	32.33% de produção, PCS de 30,98 MJ kg^{-1}, e %C de 69,36%	KANDASAMY et al. (2019)
Tetradesmus obliquus	250 a 350 °C, Catalisador Zr-HZSM-5	52,8% de produção, PCS de 43,56 MJ kg^{-1} e %C de 45,03%	MUSTAPHA et al. (2022)
Chlorella pyrenoidosa	340 °C, 60 min, –COOH modificado	77,9% de produção, PCS de 37,6 MJ kg^{-1} e %C de 50,72%	LU et al. (2021)
Chlorella sp.	280 °C- 400 °C. Catalisador Sílica porosa	32,2% de produção, PCS de 36,56 MJ kg^{-1}	LU et al. (2020)
Cultura mista	300°C, 15 min, razão biomassa/água 1/10 (m/m)	44,4% (SCU), PCS = 38,10 MJ kg^{-1}	COUTO et al. (2018)
Spirulina platensis	340 °C, 50 min	30.07% de produção, PCS de 34,76 MJ kg^{-1} e %C de 71,51%	CHEN et al. (2019)

Nota: CeO_2 = Óxido de Cério, Fe_3O_4 = Óxido de Ferro, Zr-HZSM-5 = Zeólita Socony Mobil-5 trocada por prótons, PCS = Poder calorífico superior, SCU = Sem cinzas e umidade.

Por meio da Tabela 4.4, tem-se que a produção de bio-óleo varia amplamente entre os estudos, de 26% a 77,9%, o que pode ser atribuído às diferenças na composição da biomassa das microalgas, nas condições do processo e na eficácia dos catalisadores utilizados. LU et al., (2021) alcançaram a maior produção (77,9%) com *Chlorella pyrenoidosa*, o que pode ser atribuído ao uso do catalisador com a modificação –COOH, sugerindo que o uso de um catalisador adequado pode aumentar a eficiência da conversão em bio-óleo. O PCS é um indicador importante da qualidade energética do bio-óleo. MUSTAPHA et al., (2022) alcançaram o maior PCS (43,56 MJ kg^{-1}) com *Tetradesmus obliquus*. Ressalta-se que um alto PCS implica um maior potencial para geração de energia. Em resumo, a eficiência e a qualidade do bio-óleo produzido a partir de microalgas por

LHT são fortemente influenciadas pela escolha da microalga, das condições do processo e da estratégia de catalisador.

Nesse contexto, este estudo visa avaliar condições reacionais que otimizem a produção de bio-óleo por LHT, bem como o uso de catalisadores em processo de refino desse bio-óleo, buscando aprimorar suas propriedades físico-químicas e torná-lo mais competitivo em relação aos combustíveis convencionais.

4.2.9. Viabilidade ambiental e econômica da produção de bio-óleo a partir das microalgas

Assim como a viabilidade ambiental e econômica do bioH_2 produzido a partir das microalgas, avaliar tal viabilidade para o bio-óleo tem sido objeto de estudos recentes. Dentre os trabalhos avaliados, MORENO-SADER et al. (2019) avaliaram a produção de bio-óleo por processo de LHT utilizando como substrato cacho de banana, palha de milho e biomassa de microalgas. Os autores observaram que, dentre tais substratos, a biomassa de microalgas foi a alternativa mais conveniente com base na eficiência exergética (~24%) e desempenho ambiental. Adicionalmente, estudo realizado por SARAL et al. (2022) apresenta que o bio-óleo, como combustível renovável produzido por processo de LHT de microalga, se torna mais vantajoso quando se retorna a fase aquosa da LHT para o sistema de cultivo de microalgas. Ademais, os autores apontam que o preço mínimo de venda desse biocombustível deve ser de USD 3,94 por galão equivalente de gasolina.

No mesmo contexto, ZHOU et al. (2024) conduziram uma análise de LHT de microalgas de baixo teor lipídico, considerando tanto a viabilidade ambiental quanto econômica de dois sistemas diferentes do refino do bio-óleo. Foi observado que o uso de catalisadores à base de carbono em meio aquoso (caso 2) apresentou vantagens significativas em relação ao uso de catalisadores em solventes orgânicos (caso 1). No caso 2, foi alcançado um rendimento de 62% de bio-óleo, com autossuficiência energética devido à recuperação de 92,05% do calor do processo. Adicionalmente, os catalisadores à base de carbono possibilitaram uma recuperação mais simples, reduzindo custos e impactos ambientais associados. O estudo também apontou que o caso 2 apresentou lucros anuais 41% superiores ao caso 1, destacando a relevância de integrar inovação tecnológica para melhorar a viabilidade econômica e reduzir os impactos ambientais.

Complementarmente, MARANGON et al. (2024) avaliaram a produção de biocombustíveis de aviação a partir de microalgas cultivadas em efluentes, comparando a rota de LHT com a rota de gaseificação seguida de síntese Fischer-Tropsch (G+FT). Os resultados demonstraram que a LHT oferece benefícios ambientais em categorias como potencial de aquecimento global (emissões de -51,6 g CO_2-eq/MJ) e escassez de recursos fósseis, enquanto a rota G+FT apresentou impactos ambientais significativamente maiores, especialmente em toxicidade carcinogênica humana. Os autores também destacaram que a recuperação de catalisadores (até 90%) e a redução no uso de solventes como o diclorometano (DCM), amplamente utilizado no processo de separação do bio-óleo, são estratégias fundamentais para mitigar os impactos ambientais.

Portanto, esses estudos demonstram a importância de estratégias como otimização energética, recuperação de catalisadores e substituição de solventes para melhorar tanto a viabilidade ambiental quanto econômica da produção de bio-óleo a partir de microalgas, reforçando o papel dessa biomassa como alternativa promissora para a produção de biocombustíveis sustentáveis.

4.3.Conclusão

A produção de biocombustíveis a partir de microalgas, especialmente quando cultivadas em águas residuárias, destaca-se como uma alternativa promissora no cenário energético. A sua capacidade não se limita apenas à geração de energia, mas também ao tratamento de efluentes, evidenciando uma abordagem que une sustentabilidade e inovação. No entanto, o caminho para a plena viabilização dessa alternativa enfrenta desafios. Uma das principais frentes de estudo é a otimização da produção e colheita da biomassa. Para que as microalgas se tornem realmente uma fonte viável de energia, é essencial aprimorar técnicas que permitam uma colheita mais eficiente e, consequentemente, uma produção mais robusta. Em paralelo, o bioH_2, um dos produtos que podem ser derivados das microalgas, apresenta seus próprios desafios. Apesar de promissor, é necessário investigar técnicas que possam intensificar a produção, garantindo que o bioH_2 seja não apenas tecnicamente factível, mas também competitivo do ponto de vista econômico e ambiental. No âmbito da produção de bio-óleo, a técnica de LHT surge como uma solução potencial. Contudo, seu sucesso depende da definição das melhores condições de operação e a possibilidade de incorporar catalisadores que otimizem o processo. Assim como o bioH_2, a sustentabilidade e a viabilidade econômica do bio-óleo devem ser avaliadas. Logo, a produção de biocombustíveis a

partir de microalgas pode ser promissora. Entretanto, para que essa alternativa alcance seu potencial máximo, é indispensável um investimento contínuo em pesquisa e desenvolvimento, abordando os desafios técnicos e garantindo uma produção que seja, ao mesmo tempo, sustentável e economicamente atrativa.

4.4.Referências

ADNAN, M. A. et al. Gasification performance of Spirulina microalgae – A thermodynamic study with tar formation. **Fuel**, v. 241, p. 372–381, abr. 2019.

ADNAN, M. A.; HOSSAIN, M. M. Gasification performance of various microalgae biomass – A thermodynamic study by considering tar formation using Aspen plus. **Energy Conversion and Management**, v. 165, p. 783–793, jun. 2018.

AHMED, S. F. et al. Biohydrogen production from wastewater-based microalgae: Progresses and challenges. **International Journal of Hydrogen Energy**, v. 47, n. 88, p. 37321–37342, out. 2022.

ANZOLA-ROJAS, M. DEL P. et al. Hydrogen production from fermented sugarcane vinasse and its utilization by biosynthesis processes in a single-chambered microbial electrolysis cell. **International Journal of Hydrogen Energy**, v. 100, p. 49–57, 27 jan. 2025.

ARIMI, M. M. et al. Strategies for improvement of biohydrogen production from organic-rich wastewater: A review. **Biomass and Bioenergy**, v. 75, abr. 2015.

ASSIS, L. R. DE et al. Microalgal biomass production and nutrients removal from domestic sewage in a hybrid high-rate pond with biofilm reactor. **Ecological Engineering**, v. 106, p. 191–199, set. 2017.

ASSIS, L. R. DE et al. Evaluation of the performance of different materials to support the attached growth of algal biomass. **Algal Research**, v. 39, n. September 2018, p. 101440, 2019.

ASSIS, L. R. DE et al. Innovative hybrid system for wastewater treatment: High-rate algal ponds for effluent treatment and biofilm reactor for biomass production and harvesting. **Journal of Environmental Management**, v. 274, p. 111183, nov. 2020.

BAN, S. et al. Algal-bacterial cooperation improves algal photolysis-mediated hydrogen production. **Bioresource Technology**, v. 251, p. 350–357, mar. 2018.

BAN, S.; LIN, W.; LUO, J. Ca2+ enhances algal photolysis hydrogen production by improving the direct and indirect pathways. **International Journal of Hydrogen Energy**, v. 44, n. 3, p. 1466–1473, jan. 2019.

BERNER, F.; HEIMANN, K.; SHEEHAN, M. Microalgal biofilms for biomass production. **Journal of Applied Phycology**, v. 27, n. 5, p. 1793–1804, 2015.

BESEMER, K. Biodiversity, community structure and function of biofilms in stream ecosystems. **Research in Microbiology**, v. 166, n. 10, p. 774–781, dez. 2015.

BHATIA, S. K. et al. Algal biomass to biohydrogen: Pretreatment, influencing factors, and conversion strategies. Bioresource TechnologyElsevier Ltd, , 1 jan. 2023.

CAPPELLETTI, A.; MARTELLI, F. Investigation of a pure hydrogen fueled gas turbine burner. **International Journal of Hydrogen Energy**, v. 42, n. 15, abr. 2017.

CASTELLO, D.; HAIDER, M. S.; ROSENDAHL, L. A. Catalytic upgrading of hydrothermal liquefaction biocrudes: Different challenges for different feedstocks. **Renewable Energy**, v. 141, p. 420–430, out. 2019.

CHEN, C.-Y.; CHANG, H.-Y.; CHANG, J.-S. Producing carbohydrate-rich microalgal biomass grown under mixotrophic conditions as feedstock for biohydrogen production. **International Journal of Hydrogen Energy**, v. 41, n. 7, p. 4413–4420, fev. 2016.

CHEN, H. et al. Effects of the aqueous phase recycling on bio-oil yield in hydrothermal liquefaction of Spirulina Platensis, α-cellulose, and lignin. **Energy**, v. 179, p. 1103–1113, jul. 2019.

CHOI, J.-A. et al. Enhancement of fermentative bioenergy (ethanol/hydrogen) production using ultrasonication of Scenedesmus obliquus YSW15 cultivated in swine wastewater effluent. **Energy & Environmental Science**, v. 4, n. 9, 2011.

CHOUDHARY, P.; MALIK, A.; PANT, K. K. Algal Biofilm Systems: An Answer to Algal Biofuel Dilemma. Em: GUPTA, S. K.; MALIK, A.; BUX, F. (Eds.). **Algal Biofuels: Recent Advances and Future Prospects**. [s.l: s.n.]. p. 77–96.

COUTO, E. A. et al. Hydrothermal liquefaction of biomass produced from domestic sewage treatment in high-rate ponds. **Renewable Energy**, v. 118, p. 644–653, 2018.

COUTO, E.; CALIJURI, M. L.; ASSEMANY, P. Biomass production in high rate ponds and hydrothermal liquefaction: Wastewater treatment and bioenergy integration. **Science of the Total Environment**, v. 724, 2020.

DUANGJAN, K. et al. Comparison of hydrogen production in microalgae under autotrophic and mixotrophic media. **Botanica Lithuanica**, v. 23, n. 2, p. 169–177, 1 dez. 2017.

FLEMMING, H.-C. EPS—Then and Now. **Microorganisms**, v. 4, n. 4, p. 41, 18 nov. 2016.

FLORIO, C. et al. Biohydrogen production from solid phase-microbial fuel cell spent substrate: A preliminary study. **Journal of Cleaner Production**, v. 227, p. 506–511, ago. 2019.

GHOLKAR, P.; SHASTRI, Y.; TANKSALE, A. Renewable hydrogen and methane production from microalgae: A techno-economic and life cycle assessment study. **Journal of Cleaner Production**, v. 279, jan. 2021.

GOLLAKOTA, A. R. K.; KISHORE, N.; GU, S. A review on hydrothermal liquefaction of biomass. **Renewable and Sustainable Energy Reviews**, v. 81, p. 1378–1392, jan. 2018.

GRANDE, L. et al. Hydrothermal Liquefaction of Biomass as One of the Most Promising Alternatives for the Synthesis of Advanced Liquid Biofuels: A Review. **Materials**, v. 14, n. 18, p. 5286, 14 set. 2021.

GROSS, M. et al. Development of a rotating algal biofilm growth system for attached microalgae growth with in situ biomass harvest. **Bioresource Technology**, v. 150, p. 195–201, 2013.

GULTOM, S.; HU, B. Review of Microalgae Harvesting via Co-Pelletization with Filamentous Fungus. **Energies**, v. 6, n. 11, p. 5921–5939, 12 nov. 2013.

GUO, Y. et al. Hydrothermal liquefaction of Cyanophyta: Evaluation of potential bio-crude oil production and component analysis. **Algal Research**, v. 11, p. 242–247, set. 2015.

IEA. **Hydrogen**. 2021. https://www.iea.org/reports/hydrogen. Acessado em: 20/03/2022.

IEA (INTERNATIONAL ENERGY AGENCY). **HYDROGEN PRODUCTION AND STORAGE - R&D Priorities and Gaps**. Paris, France: Hydrogen Coordination Group, OECD/IEA, 2006.

JEEVANANDAM, J. et al. Microalgal Biomass Generation via Electroflotation: A Cost-Effective Dewatering Technology. **Applied Sciences**, v. 10, n. 24, p. 9053, 18 dez. 2020.

JIN, W. et al. Catalytic Upgrading of Biomass Model Compounds: Novel Approaches and Lessons Learnt from Traditional Hydrodeoxygenation - a Review. **ChemCatChem**, v. 11, n. 3, p. 924–960, 6 fev. 2019.

JOHNSON, M. B.; WEN, Z. Development of an attached microalgal growth system for biofuel production. **Applied Microbiology and Biotechnology**, v. 85, n. 3, p. 525–534, 28 jan. 2010.

KALAMARAS, C. M.; EFSTATHIOU, A. M. Hydrogen Production Technologies: Current State and Future Developments. **Conference Papers in Energy**, v. 2013, 6 jun. 2013.

KANDASAMY, S. et al. Hydrothermal liquefaction of microalgae using Fe3O4 nanostructures as efficient catalyst for the production of bio-oil: Optimization of reaction parameters by response surface methodology. **Biomass and Bioenergy**, v. 131, p. 105417, dez. 2019.

KANDASAMY, S. et al. Accelerating the production of bio-oil from hydrothermal liquefaction of microalgae via recycled biochar-supported catalysts. **Journal of Environmental Chemical Engineering**, v. 9, n. 4, p. 105321, ago. 2021.

KHETKORN, W. et al. Microalgal hydrogen production – A review. **Bioresource Technology**, v. 243, nov. 2017.

KIM, K.-Y.; LOGAN, B. E. Nickel powder blended activated carbon cathodes for hydrogen production in microbial electrolysis cells. **International Journal of Hydrogen Energy**, v. 44, n. 26, p. 13169–13174, maio 2019.

KRISHNAN, S. et al. Accelerated two-stage bioprocess for hydrogen and methane production from palm oil mill effluent using continuous stirred tank reactor and microbial electrolysis cell. **Journal of Cleaner Production**, v. 229, p. 84–93, ago. 2019.

KUMAR, A.; JONES, D.; HANNA, M. Thermochemical Biomass Gasification: A Review of the Current Status of the Technology. **Energies**, v. 2, n. 3, p. 556–581, 21 jul. 2009.

LACROUX, J. et al. Dark fermentation and microalgae cultivation coupled systems: Outlook and challenges. Science of the Total EnvironmentElsevier B.V., , 20 mar. 2023.

LAKSHMIKANDAN, M.; MURUGESAN, A. G. Enhancement of growth and biohydrogen production potential of Chlorella vulgaris MSU-AGM 14 by utilizing seaweed aqueous extract of Valoniopsis pachynema. **Renewable Energy**, v. 96, p. 390–399, out. 2016.

LEE, S.-H. et al. Higher Biomass Productivity of Microalgae in an Attached Growth System, Using Wastewater. **Journal of Microbiology and Biotechnology**, v. 24, n. 11, p. 1566–1573, 28 nov. 2014.

LI, S. et al. Biohydrogen production from microalgae for environmental sustainability. **Chemosphere**, v. 291, 1 mar. 2022.

LIU, C.-H. et al. Fermentative hydrogen production by Clostridium butyricum CGS5 using carbohydrate-rich microalgal biomass as feedstock. **International Journal of Hydrogen Energy**, v. 37, n. 20, p. 15458–15464, out. 2012.

LU, J. et al. Enhancement of microalgae bio-oil quality via hydrothermal liquefaction using functionalized carbon nanotubes. **Journal of Cleaner Production**, v. 285, p. 124835, fev. 2021.

LU, Q. et al. Hydrothermal Catalytic Upgrading of Model Compounds of Algae-Based Bio-Oil to Monocyclic Aromatic Hydrocarbons over Hierarchical HZSM-5. **Industrial & Engineering Chemistry Research**, v. 59, n. 46, p. 20551–20560, 18 nov. 2020.

LUNPROM, S. et al. A sequential process of anaerobic solid-state fermentation followed by dark fermentation for bio-hydrogen production from Chlorella sp. **International Journal of Hydrogen Energy**, v. 44, n. 6, p. 3306–3316, fev. 2019.

MANTZOROU, A.; VERVERIDIS, F. Microalgal biofilms: A further step over current microalgal cultivation techniques. **Science of the Total Environment**, v. 651, p. 3187–3201, 2019.

MARANGON, B. B. et al. Wastewater-grown microalgae biomass as a source of sustainable aviation fuel: Life cycle assessment comparing hydrothermal routes. **Journal of Environmental Management**, v. 360, 1 jun. 2024.

MORENO-SADER, K.; MERAMO-HURTADO, S. I.; GONZÁLEZ-DELGADO, A. D. Computer-aided environmental and exergy analysis as decision-making tools for selecting bio-oil feedstocks. **Renewable and Sustainable Energy Reviews**, v. 112, p. 42–57, set. 2019.

MUSTAPHA, S. I. et al. Catalytic hydrothermal liquefaction of nutrient-stressed microalgae for production of high-quality bio-oil over Zr-doped HZSM-5 catalyst. **Biomass and Bioenergy**, v. 163, p. 106497, ago. 2022.

NAGARAJAN, D.; CHANG, J.-S.; LEE, D.-J. Pretreatment of microalgal biomass for efficient biohydrogen production – Recent insights and future perspectives. **Bioresource Technology**, v. 302, abr. 2020.

NGUYEN, T.-A. D. et al. Enhancement of fermentative hydrogen production from green algal biomass of Thermotoga neapolitana by various pretreatment methods. **International Journal of Hydrogen Energy**, v. 35, n. 23, dez. 2010.

PHANDUANG, O. et al. Improvement in energy recovery from Chlorella sp. biomass by integrated dark-photo biohydrogen production and dark fermentation-anaerobic digestion processes. **International Journal of Hydrogen Energy**, v. 44, n. 43, set. 2019.

PONGSIRIYAKUL, K. et al. Effective Cu/Re promoted Ni-supported γ-Al2O3 catalyst for upgrading algae bio-crude oil produced by hydrothermal liquefaction. **Fuel Processing Technology**, v. 216, p. 106670, jun. 2021.

ROGERI, R. C. et al. Strategies to control pH in the dark fermentation of sugarcane vinasse: Impacts on sulfate reduction, biohydrogen production and metabolite distribution. **Journal of Environmental Management**, v. 325, 1 jan. 2023.

SARAL, J. S.; SATHEESH, A. R.; RANGANATHAN, P. Economic and environmental analysis of algal biorefinery for the production of renewable fuels and co-product. **Energy Conversion and Management: X**, v. 14, p. 100189, maio 2022.

SEHAR, S.; NAZ, I. Role of the Biofilms in Wastewater Treatment. Em: **Microbial Biofilms - Importance and Applications**. [s.l.] InTech, 2016.

SENGMEE, D. et al. Biophotolysis-based hydrogen and lipid production by oleaginous microalgae using crude glycerol as exogenous carbon source. **International Journal of Hydrogen Energy**, v. 42, n. 4, p. 1970–1976, jan. 2017.

SHOW, K. Y. et al. State of the art and challenges of biohydrogen from microalgae. Bioresource TechnologyElsevier Ltd, , 1 out. 2019.

SINGH, H.; DAS, D. Biohydrogen from microalgae. Em: **Handbook of Microalgae-Based Processes and Products**. [s.l.] Elsevier, 2020. p. 391–418.

SINGH, H.; ROUT, S.; DAS, D. Dark fermentative biohydrogen production using pretreated Scenedesmus obliquus biomass under an integrated paradigm of biorefinery. **International Journal of Hydrogen Energy**, v. 47, n. 1, p. 102–116, jan. 2022.

SKJÅNES, K.; REBOURS, C.; LINDBLAD, P. Potential for green microalgae to produce hydrogen, pharmaceuticals and other high value products in a combined process. **Critical Reviews in Biotechnology**, v. 33, n. 2, 6 jun. 2013.

SRIYOD, K.; REUNGSANG, A.; PLANGKLANG, P. One-step multi enzyme pretreatment and biohydrogen production from Chlorella sp. biomass. **International Journal of Hydrogen Energy**, v. 46, n. 80, p. 39675–39687, nov. 2021.

STANISLAUS, M. S. et al. Improvement of biohydrogen production by optimization of pretreatment method and substrate to inoculum ratio from microalgal biomass and digested sludge. **Renewable Energy**, v. 127, p. 670–677, nov. 2018.

WIECZOREK, N.; KUCUKER, M. A.; KUCHTA, K. Fermentative hydrogen and methane production from microalgal biomass (Chlorella vulgaris) in a two-stage combined process. **Applied Energy**, v. 132, p. 108–117, nov. 2014.

XIA, A. et al. Comparison in dark hydrogen fermentation followed by photo hydrogen fermentation and methanogenesis between protein and carbohydrate compositions in Nannochloropsis oceanica biomass. **Bioresource Technology**, v. 138, jun. 2013.

YANG, Z. et al. Fermentative hydrogen production from lipid-extracted microalgal biomass residues. **Applied Energy**, v. 88, n. 10, p. 3468–3472, out. 2011.

YUN, Y.-M. et al. Microalgal biomass as a feedstock for bio-hydrogen production. **International Journal of Hydrogen Energy**, v. 37, n. 20, p. 15533–15539, out. 2012.

ZHANG, Y. Hydrothermal Liquefaction to Convert Biomass into Crude Oil. Em: **Biofuels from Agricultural Wastes and Byproducts**. Oxford, UK: Wiley-Blackwell, 2010. p. 201–232.

ZHOU, S. et al. Study of life cycle assessment: Transforming microalgae to biofuel through hydrothermal liquefaction and upgrading in organic or aqueous medium. **Journal of Cleaner Production**, v. 444, 10 mar. 2024.

ZHUANG, L. L. et al. The characteristics and influencing factors of the attached microalgae cultivation: A review. **Renewable and Sustainable Energy Reviews**, v. 94, n. November 2017, p. 1110–1119, 2018.

ZIARA, R. M. M. et al. Lactate wastewater dark fermentation: The effect of temperature and initial pH on biohydrogen production and microbial community. **International Journal of Hydrogen Energy**, v. 44, n. 2, p. 661–673, jan. 2019.

ZOHURI, B. The Chemical Element Hydrogen. Em: **Hydrogen Energy**. Cham: Springer International Publishing, 2019.

5. Capítulo II. Enhancing Microalgae Biomass Production: Exploring Improved Scraping Frequency in a Hybrid Cultivation System[1]

Abstract: Recently, hybrid systems, such as those incorporating high-rate algal ponds (HRAPs) and biofilm reactors (BRs), have shown promise in treating domestic wastewater while cultivating microalgae. In this context, the objective of the present study was to determine an improved scraping frequency to maximize microalgae biomass productivity in a mix of industrial (fruit-based juice production) and domestic wastewater. The mix was set to balance the carbon/nitrogen ratio. The scraping strategy involved maintaining 1 cm wide stripes to retain an inoculum in the reactor. Three scraping frequencies (2, 4, and 6 days) were evaluated. The findings indicate that a scraping frequency of each 2 days provided the highest biomass productivity (18.75 g total volatile solids m^{-2} d^{-1}). The species' behavior varied with frequency: *Chlorella vulgaris* was abundant at 6-day intervals, whereas *Tetradesmus obliquus* favored shorter intervals. Biomass from more frequent scraping demonstrated a higher lipid content (15.45%). Extrapolymeric substance production was also highest at the 2-day frequency. Concerning wastewater treatment, the system removed 93% of dissolved organic carbon and ~100% of ammoniacal nitrogen. Combining industrial and domestic wastewater sources to balance the carbon/nitrogen ratio enhanced treatment efficiency and biomass yield. This study highlights the potential of adjusting scraping frequencies in hybrid systems for improved wastewater treatment and microalgae production.

Keywords: Microalga, High-rate algal pond, Biofilm reactor, Wastewater Treatment.

5.1. Introduction

Microalgae are recognized as a promising solution for wastewater treatment due to their high biomass productivity and ability to use sunlight as their main energy source (CHOUDHARY et al., 2020). Using microalgae in wastewater treatment removes excess nutrients, reduces the risk of water body eutrophication, and contributes to carbon dioxide (CO_2) sequestration from the

[1] Versão publicada na revista *Journal of Environmental Management* (Apêndice I)

atmosphere. Several studies have demonstrated the effectiveness of microalgae-based wastewater treatment processes (ASSIS et al., 2017; COUTO et al., 2018; MAGALHÃES et al., 2022).

To further enhance these processes, it is crucial to consider the wastewater mix to balance the carbon/nitrogen (C/N) ratio. Previous studies evaluated the optimal C/N ratio. For instance, Chiu et al. (2015) found that a C/N ratio 6 ensures sufficient nutrient availability, enhancing microalgae growth. ZHENG et al. (2018) found a C/N ratio 7.9 optimal for nutrient removal and biomass production. Other works reported the best biomass production at a C/N ratio 5 (XU et al., 2017; YAN et al., 2013). In this context, a balanced C/N ratio is essential for improved microalgal growth, as it affects the metabolic pathways involved in biomass accumulation and nutrient removal (GAMA et al., 2023).

Improving microalgae harvesting through biofilm formation in support material using wastewater as the culture medium was also evaluated (ASSIS et al., 2020; BOELEE et al., 2014; LIU et al., 2013; WANG et al., 2018). Hybrid systems, such as coupling suspended and attached culture systems, have resulted in higher algal yields than conventional high-rate algal ponds (HRAPs), with simpler and cheaper biomass collection (ASSIS et al., 2020). Among these hybrid systems, biofilm reactors (BRs) integrated HRAPs have been proposed to treat domestic effluents, production, and biomass harvesting, as they are more efficient in production and harvesting than conventional systems (ASSIS et al., 2020). In addition, scraping strategies that keep an inoculum within the reactor are important to boost biomass growth. Cheah and Chan (2021) argue that enhancing biomass productivity facilitates continuous and efficient biomass growth in subsequent cycles, allowing the bottom cells to function as an inoculum.

In recent years, efforts have been made to improve microalgae harvesting and the efficiency of wastewater treatment using hybrid systems. GROSS et al. (2013) found that an attached growth system (cotton sheet) was more efficient in removing nutrients from wastewater than a suspended growth system (flat panel photobioreactor). In addition, they demonstrated that the combination of HRAP and BR resulted in higher biomass productivity (3.48 g m^2 d^{-1} in HRAP only and 8.09 g m^2 d^{-1} in HRAP enhanced with the attached growth system). The results of this study demonstrated that a scraping frequency of 7 days (compared to 3, 5, 10, and 14 days) was the best for greater microalgae biomass productivity (3.51 g m^{-2} day^{-1}) in the effluent composed of a mixture of industrial and domestic wastewater.

It is noteworthy that the biofilm reactor design and the harvesting method are identified as key factors influencing the biochemical composition of biomass. Additionally, ZHANG et al. (2018b) state that self-shadowing in biofilm can affect the lipid content of microalgae. This suggests that in attached growth systems, the harvesting frequency could be a critical factor in determining the lipid richness of the biomass. Therefore, adjusting the harvesting frequency presents a promising approach to not only optimize wastewater bioremediation and biomass production but also to enhance the overall value of the biomass generated.

In this context, ASSIS et al. (2020) investigated the challenges of algal biomass harvesting. The authors introduced a hybrid system that combines a BR for algal biomass production and harvesting with an HRAP for wastewater treatment. The hybrid system showcased a 2.6-fold increase in biomass production compared to HRAP. The system improved harvesting efficiency (61% vs. 22% in HRAP only). The BR also enhanced the density and diversity of microalgae, with *Chlorella vulgaris* being the predominant strain. The study emphasizes the potential of integrating BR in wastewater treatment plants to enhance biomass production and harvesting.

In view of these considerations, the study aims to identify the best scraping frequency to enhance microalgae biomass growth in treating mixed industrial (fruit juice production) and domestic wastewater. The wastewater mix aims to improve the C/N ratio to increase biomass production in a hybrid system composed of HRAPs and BRs. The research explores the effects of different scraping frequencies on both the quality and quantity of microalgae biomass, and the overall wastewater treatment efficiency. It includes a novel scraping strategy that maintains part of the biomass as inoculum within the reactor, alongside an examination of species behavior, biochemical composition, and adherence mechanisms.

5.2. Materials and Methods

5.2.1. Experimental area

The experiments were carried out in the experimental area of the Laboratory of Sanitary and Environmental Engineering, Federal University of Viçosa, Brazil (20º45'14" S, 42º52'54" W). In this area, pilot-scale HRAPs and BRs are installed for wastewater treatment, production, and separation of algal biomass.

The HRAPs have the following characteristics: width, 1.28 m; length, 2.86 m; total depth, 0.5 m; surface area, 3.3 m^2. They are made of fiberglass and steel blades with six blades powered

by a 0.5 HP electric motor. The speed is reduced by a speed reducer coupled to the motor and controlled by a frequency inverter (WEG CFW-10 series). The BRs consist of a flat acrylic panel and have the following characteristics: total area of 1 m², considering the front and the back sides, measuring 1.0 m in width and 0.5 m in length. The BRs are kept vertical and in direct contact with the atmospheric air and solar radiation and are installed next to the HRAPs. To allow biofilm growth, the BRs are coated with polyester (SkTextil, Oxford, 100% polyester), as previously studied by ASSIS et al. (2019). Three BRs were connected to an HRAP. The wastewater and biomass within the HRAP were continuously recirculated through the BRs using submersible pumps set at a flow rate of 400 L h^{-1}, configuring a hybrid system (ASSIS et al., 2020). The HRAPs and the BRs are shown in Figure S5.1 (Apêndice II).

5.2.2. Microalgae culture medium

The culture medium used for microalgae production comprises 50% industry wastewater (IW) and 50% domestic wastewater (DW). Regarding the IW, the industry's main activity is producing fruit-based juices. The wastewater is generated at various stages of the production process, especially the washing of floors and equipment at the end of the production process. The IW was collected after a UASB reactor, and the DW was collected after a septic tank. The characteristics of the culture medium used are presented in Table 5.1.

Table 5.1. Characteristics of industrial and domestic wastewater and their mixture.

Parameter	Industrial Wastewater	Domestic Wastewater	Mix
pH	8.28	7.57	7.09
Dissolved organic carbon (mg L^{-1})	1,055.77	35.77	417.00
Total chemical oxygen demand (mg L^{-1})	4,206.75	575.00	2,906.5
Total phosphorus (mg L^{-1})	2.86	11.70	11.54
Ammoniacal nitrogen (mg L^{-1})	<0.1	94.94	42.10
Nitrate (mg L^{-1})	1.30	2.40	0.90

The choice of the mixture was determined to balance the C/N ratio of the culture medium, an important aspect of microalgae growth. The assimilable carbon and nitrogen fractions for microalgae were considered to calculate the wastewater C/N ratio. These fractions were determined, respectively, by the dissolved organic carbon (DOC) and the sum of ammonia nitrogen

(NH_4^+) and nitrate (NO_3^-). The IW used, although rich in assimilable carbon (1,055.77 mg DOC L^{-1}), has a small amount of assimilable nitrogen and only in the form of nitrate (1.30 mg NO_3^- L^{-1}). On the other hand, the DW has a C/N ratio of 0.37. Therefore, the mixture provided an increase in the C/N ratio to 9.70, approaching the optimal ratio reported in the literature for the cultivation of microalgae strains such as *Chlorella vulgaris* and *Tetradesmus obliquus*, between 5:1 and 15:1 (GAMA et al., 2023; MA et al., 2017; ZHENG et al., 2018). It's worth noting that these strains are commonly found in microalgae cultivation within outdoor wastewater treatment systems (ASSIS et al., 2020; SUTHERLAND et al., 2020). The hydraulic retention time was set at 14 days in the HRAP, and the hybrid system was operated in a continuous regime.

5.2.3. Wastewater treatment analysis

The wastewater treatment was monitored weekly for 136 days (from August to December) using the following parameters: total suspended solids (TSS), volatile suspended solids (VSS), chemical oxygen demand (COD), total Kjeldahl nitrogen (TKN), NH_4^+, NO_3^-, total phosphorus (TP), soluble phosphorus (SP), and total coliforms and *Escherichia coli* according to APHA (2012). DOC was measured using Shimadzu TOC SSM 5000 and TOC C CSH equipment. Dissolved oxygen, electrical conductivity, temperature, and pH were measured using the Hach HQ40d probe. The removal efficiency results obtained after the treatment had stabilized, i.e., in its stationary regime, were presented and discussed (mean values and standard deviation).

5.2.4. Biomass scraping

To determine the scraping frequencies, a methodology adapted from ASSIS et al. (2020) was employed. Initially, it took 21 days for cells to adapt and attach to the BRs. Then, the biofilm development was monitored over the subsequent 21 days by measuring chlorophyll-*a* levels following the NEDERLANDS NORM (1982) based on NUSH (1981) and total volatile solids (TVS) using the APHA (2012) method. Then, a toothed scraper with a 1 cm slot spacing and 1 cm spacing between slots was used for biomass scraping in the 3 BRs. The scraper was designed to scrape half of the biofilm. The remaining biofilm was used as inoculum to boost biomass production (Figure 5.1).

Figure 5.1. Biofilm reactor representing the adopted scraping strategy.

After six days, the detachment of cells in the upper layers of the biofilm was observed within the three BRs. Additionally, a decrease in chlorophyll-*a* and TVS was also observed. Then, six days was set as a complete cycle. After that, a different scraping frequency was set for each BR: 2, 4, and 6 days. These frequencies represented one-third, two-thirds, and a complete cycle (described as R1, R2, and R3, respectively, throughout the paper).

Scraping was performed alternately across the BRs. If one half was scraped in a day, the opposite half was scraped in the subsequent day. Biomass production in the three BRs was monitored every 2, 4, and 6 days for R1, R2, and R3, respectively, using chlorophyll-*a* (NEDERLANDS NORM, 1982; NUSH, 1981) and TVS (APHA, 2012) measurements. Six 1 cm^2 samples were scraped from each BR, 3 cm^2 from the front and 3 cm^2 from the back, totaling an area of 6 cm^2. The samples were collected just before scraping the areas. The production for each parameter (Chl-*a* and TVS) was calculated based on this scraped area (mass/area). To calculate daily productivity rates, the R1, R2, and R3 production were divided by 2, 4, and 6 days, respectively.

5.2.5. Characterization of microalgae species in attached and suspended biomass

At the end of the experiment, samples of 20 cm^2 were scraped from each BR and diluted in 50 ml of distilled water. Additionally, a sample of 20 ml was collected from the HRAP. All samples

were kept in a 4% formaldehyde solution. The characterization is represented by density (number of organisms per unit area) and biovolume (amount of physical space occupied by the organisms). It was performed at the genus level, and for dominant genera, the species were identified. For quantitative analysis, the individuals were counted in a sedimentation chamber under an inverted microscope using the UTERMÖHL (1958) method. Organism density was determined using the criteria described in APHA (2012). For qualitative analysis, identification was performed under an inverted microscope, according to PARRA; GONZALEZ; DELLAROSSA (1983) and KOMAREK; FOTT (1983).

5.2.6. Proximate composition of biomass

Proximate composition was determined for the biomass produced in the HRAP and each BR through lipids, carbohydrates, proteins, humidity, and ash content. The protein content was defined by the nitrogen-to-protein conversion factor of 6.25 (ZHONG et al., 2012) using the Kjeldahl method. The carbohydrate content was determined by quantitative acid hydrolysis of the biomass (HOEBLER et al., 1989), followed by the phenol-sulfuric acid method (DUBOIS et al., 1956) and spectrophotometry (490 nm) using the glucose standard curve. The lipid content was determined by the Soxhlet extraction method (AOAC, 1990). After macerating the biomass, neutral lipids were extracted in a fat determination device (Tecnal TE-044-8/50) for 6 h, with 99% hexane as the solvent. Subsequently, in the same equipment, membrane lipids were extracted with 96% ethanol for 3 h and quantified by gravimetry. Ash content was determined according to the ASTM D3174-12 protocol (ASTM, 2002) and FAROOQ et al. (2021). This involved placing the biomass sample in a muffle furnace at 700°C for 4 hours. This procedure aligns with the biomass proximate analysis, which is suitable when microalgae biomass is used for bioenergy applications (FAROOQ et al., 2021).

5.2.7. Extracellular Polymeric Substances (EPS) analysis

Extracellular polymeric substances (EPS) produced by the microorganisms (microalgae and bacteria) were analyzed according to LV et al. (2016). For each scraping frequency, 6 cm^2 (three 1 cm^2 rectangles from the front and back of each BR, totaling 6 cm^2) diluted in deionized water from each of the three panels were dewatered by centrifugation at 5,000 rpm for 5 minutes at room temperature. The pellet was washed with deionized water and centrifuged again at 5,000 rpm for 5

minutes at room temperature. The washed pellet was transferred to a beaker, and sufficient deionized water was added to ensure the transfer of the entire sample. It was then heated in an oven at 80°C for 30 minutes. After heating, the mixture was made up to approximately 50 mL and centrifuged at 10,000 rpm for 10 minutes at room temperature. The supernatant was then filtered with an acetate cellulose membrane with a porosity of 0.45 µm, and the filtrate was considered the EPS fraction. EPS quantification was performed concerning the carbohydrate and protein content of the sample following the same procedure described in section 5.2.6. Proximate composition of biomass.

5.2.8. Morphology analysis

The morphology of the biofilms formed in each BR was analyzed according to BOELEE et al. (2011). After the experiment, a small piece of textile containing microalgae biomass was extracted from each BR. Each piece was delicately rinsed three times with a phosphate buffer solution (composed of 137 mM NaCl, 2.7 mM KCl, 10 mM Na_2HPO_4, 2 mM KH_2PO_4, pH 7.4). The biofilm was then preserved by immersing it in 2.5% glutaraldehyde at room temperature for 2 hours. Following fixation, the sample underwent dehydration through a series of ethanol concentrations: 30%, 50%, 70%, 90%, and 100% (v/v), lasting each step 20 minutes. Subsequently, the samples were dried at 35°C for 15 minutes. To enhance visualization, a thin 5 nm layer of gold was sputter coated onto the sample. The sample was then examined using a scanning electron microscope (SEM) (TESCAN Vega3).

5.2.9. Biomass surface charge

To assess the influence of surface charge on biofilm formation, zeta potential was considered by employing a methodology adapted from TONG et al. (2021). Microalgal cells from each BR were harvested by centrifugation, followed by two washes with filtered HRAP wastewater on an acetate cellulose membrane with a porosity of 0.45 µm to obtain a final concentration of about 10^6 cells mL^{-1}. The Zeta potential was measured by a Zetasizer Nano-ZS (Malvern, UK) analyzer. To minimize the effect of sedimentation, a well-suspended cell culture was selected to avoid any unwanted flocculation. Measurements were performed at least three times.

5.2.10. Statistical analysis

All statistical analyses were performed using Minitab®19 Software. To compare the production, separation, and characterization of biomass among the three BRs, analysis of variance (ANOVA) was used, followed by Tukey's mean test at a 5% probability of error.

5.3.Results and discussion

5.3.1. Effect of scraping frequency on biomass productivity

The chlorophyll-*a* and TVS productivities were higher (p<0.05) in R1 (56.09 mg m^{-2} d^{-1} and 18.75 g m^{-2} d^{-1}, respectively). On the other hand, as the harvesting interval extended to four and six days, there was a decrease in these parameters. One explanation for these peak values at a 2-day scraping frequency is the maximization of light exposure to the algal cells. Since photosynthesis is the primary growth mechanism for microalgae, guaranteeing light access is important to cell development (PERIN et al., 2016). In addition, a scraping frequency of 2 days limits the thickness of the biofilm, reducing self-shading effects. Self-shading prevents light access to deeper layers. Hence, the photosynthetic potential is hindered (ASSIS et al., 2020). In this context, when scraping intervals were elongated to 4 days (R2) and 6 days (R3), a thickened biofilm was formed, leaving those beneath in relative darkness and diminishing their photosynthetic activity. Simultaneously, increased biofilm density could intensify competition for nutrients, thus restricting the overall nutrient absorption rate (ZHUANG et al., 2018). Previous studies explored different methods and materials for cultivating microalgae biofilms, focusing on improving biomass productivity and efficiency in wastewater treatment systems. ASSIS et al. (2020) operated a hybrid system composed of a BR and an HRAP. The authors reported a 6.13 g m^{-2} d^{-1} productivity using mixed microalgae in domestic wastewater. They noted that the hybrid system does not alter the chemical composition of the biomass.

Compared with traditional methods like conventional HRAP, using a hybrid system significantly enhances biomass production and harvesting efficiency. SALEEM et al. (2024) evaluated the productivity of *Scenedesmus* sp. in various dilutions of solid waste leachate with treated municipal wastewater in wetlands. The productivity ranged from 2.1 to 7.4 g m^{-2} d^{-1}, with the lowest leachate dilution (5%) resulting in the highest biomass productivity. This suggests that leachate characteristics might inhibit algal biofilm development. ZHANG et al. (2017) investigated using lignocellulosic materials as supports for algae biofilms for biomass production for biofuels.

Different types of sawdust (pine, oak, and sugarcane bagasse) were tested, with pine sawdust achieving the highest productivity of 10.92 g m^{-2} d^{-1}. The results indicate that the surface roughness of lignocellulosic materials significantly affects biomass production, making them potential low-cost support materials for algae biofilm cultivation. HODGES et al. (2017) presented a comparative study for treating wastewater from oil refineries using RABRs, demonstrating a significant increase in biomass productivity compared to conventional HRAPs treatment, achieving 4.11 g m^{-2} d^{-1}. Finally, CHENG et al. (2017) explored the use of swine wastewater for cultivating *Chlorella pyrenoidosa* in a biofilm reactor, achieving a biomass productivity of 5.03 g m^{-2} d^{-1}. In conclusion, the studies highlight the importance of harvesting frequency and system design in optimizing biomass productivity. Table 5.2 presents the chlorophyll-a and biomass productivity for each reactor.

Table 5.2. Productivity of chlorophyll-*a* and total volatile solids (TVS) in biofilms harvested every 2 (R1), 4 (R2), and 6 (R3) days.

Parameter	R1	R2	R3
Chl-*a* (mg m^{-2} d^{-1})	56.09 (10.43)[a]	31.34 (14.08)[b]	26.48 (8.90)[b]
TVS (g m^{-2} d^{-1})	18.75 (7.23)[a]	9.28 (3.48)[b]	6.36 (1.58)[b]

Note: Significant at the 5% probability of error level by the Tukey test; the numbers followed by the same letter in the line did not differ statistically.

The results found reinforce that balancing growth with improved harvesting can ensure that biomass productivity is maximized while maintaining the health and efficiency of the algal community. This emphasizes the importance of periodic scraping, especially in light and nutrient-limited environments, to improve biomass yield and ensure the sustainability of the proposed system.

5.3.2. Phytoplanktonic community

Chlorella vulgaris shows the highest density in R2 and R3 at 3,984,375 and 3,222,917 org cm^{-2}, respectively (Table 5.3). In R1, the density was 1,527,344 org cm^{-2}. However, it drastically reduces to 456,875 org. cm^{-2} in HRAP. *Tetradesmus obliquus* maintains a relatively stable density in the BRs and HRAP, with 1,394,531 org cm^{-2} in R1 and around 1,062,500 cm^{-2} in R2, R3, and

HRAP. *Limnothrix planctonica*, present in lower densities, peaks in R3 with 212,500 org. cm^{-2}, 22,135 org. cm^{-2} in R1 and 21,250 org. cm^{-2} in HRAP.

Table 5.3. Density of microalgae and cyanobacteria present in R1, R2, R3, and HRAP.

Microalga	Density (org cm^{-2})			
	R1	R2	R3	HRAP
Chlorella vulgaris	1,527,344	3,984,375	3,222,917	456,875
Tetradesmus obliquus	2,501,302	3,453,153	1,062,500	1,051,875
Limnothrix planctonica	22,135	132,813	212,500	21,250

The images obtained through scanning electron microscopy (Figure 5.2) allow the identification of these species incorporated into the EPS matrix of biofilms. The chlorophytes can be observed on the surface of the biofilms. Although the cyanobacterium *Limnothrix planctonica* is less abundant in R1, its presence was more noticeable in the images of this treatment. This result may be related to the preference of filamentous species to grow in deeper biofilm layers, where there is shade from the upper layers (HILLMAN; SIMS, 2020). Lastly, the comparison between the images clearly shows the increase in the density of microorganisms as the scraping frequency decreases.

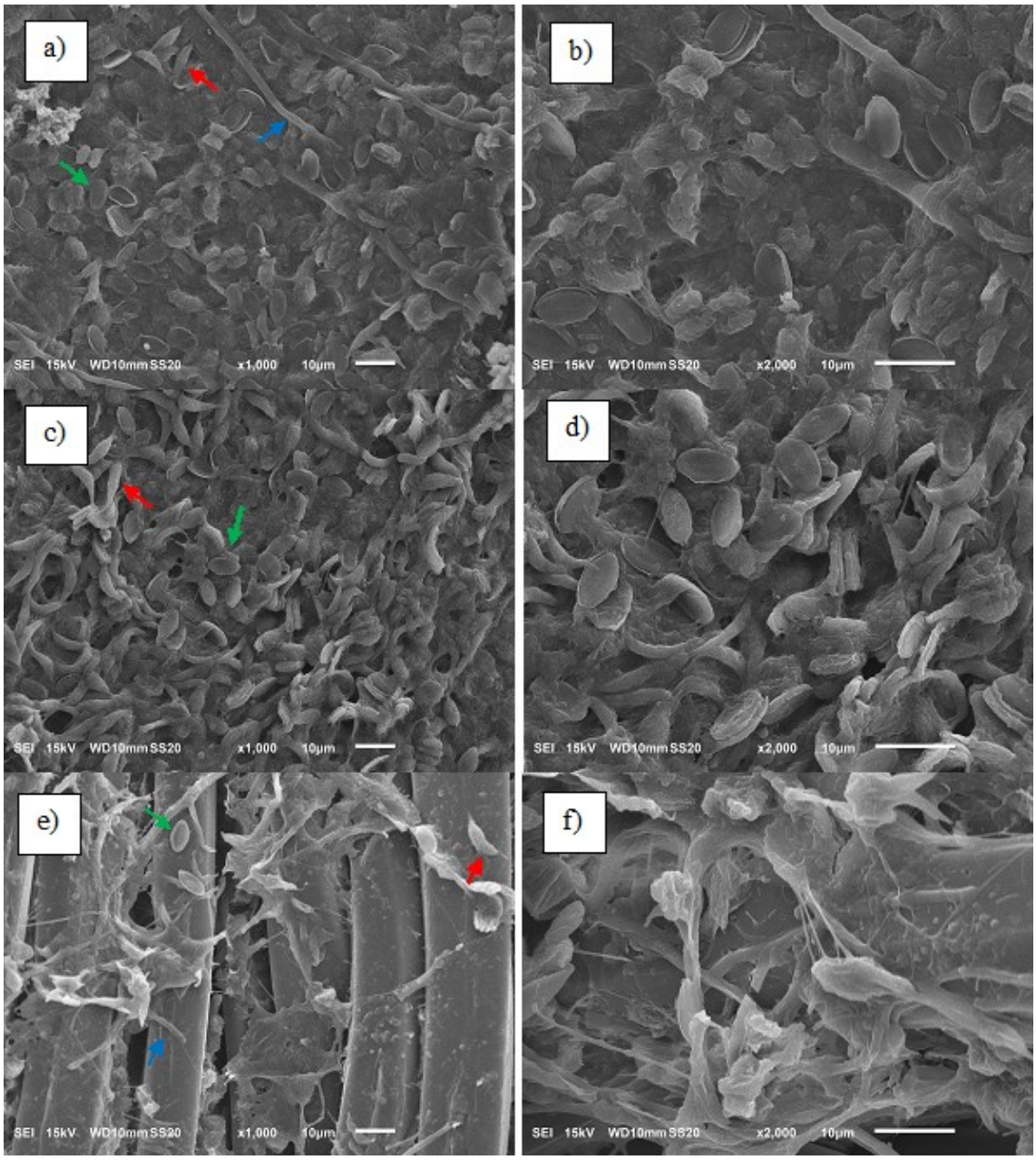

Figure 5.2. Scanning electron microscope pictures of the microalgal biofilm harvested every (a, b) 2, (c, d) 4 and (e, f) 6 days. (Green arrow = Chlorella vulgaris, red arrow = Tetradesmus obliquus, and blue arrow = Limnothrix planctonica).

The highest relative abundance of *Chlorella vulgaris* was observed in R3 (71%). Previous works also reported the predominance of *Chlorella vulgaris* in attached growth when cultivated in domestic wastewater (ASSIS et al., 2020). IRVING; ALLEN (2011) argue that *Chlorella vulgaris* has a lower initial attachment than *Tetradesmus obliquus*. This observation aligns with the current

findings, where in scenarios of higher scraping frequency, indicating more frequent initial attachments, *Tetradesmus obliquus* predominated (61% in R1). Additionally, the higher abundance relative of *Tetradesmus obliquus* in HRAP (69%) indicates its compatibility with suspended growth.

Moreover, the relatively low and stable density of *Limnothrix planctonica* in the BRs and HRAP indicates its limited proliferation in the hybrid system. Although *Limnothrix planctonica* was found in low relative abundance in the present study, ECONOMOU et al. (2015) argue that filamentous cyanobacteria, such as *Limnothrix* species, are known for developing in nutrient-rich environments resulting from the influx of wastewater. They also play a beneficial role in wastewater treatment by efficiently removing nutrients like nitrogen and phosphorus.

The relative biovolume data highlights the dominance of *Tetradesmus obliquus* in the BRs and HRAP. The HRAP and R1 exhibited the highest predominance with 98% and 95% relative biovolume, respectively. R2 and R3, while still showing a strong presence of *Tetradesmus obliquus*, had slightly lower percentages at 91% and 74%. The low relative biovolume is observed in R1, R2, and HRAP for *Limnothrix planctonica* (1%, 3%, and 1%, respectively) and *Chlorella vulgaris* (4%, 6%, and 1%, respectively). As for relative abundance, *Limnothrix planctonica* and *Chlorella vulgaris* exhibit a higher relative biovolume in R3. This suggests that they require more time to thrive compared to *Tetradesmus obliquus*. Consequently, they develop better with less frequent scraping. Figure 5.3 presents the results of the microalgae and cyanobacteria composition in the different reactors: R1, R2, R3, and HRAP. The organisms' relative abundance and relative biovolume are represented in percentage (%).

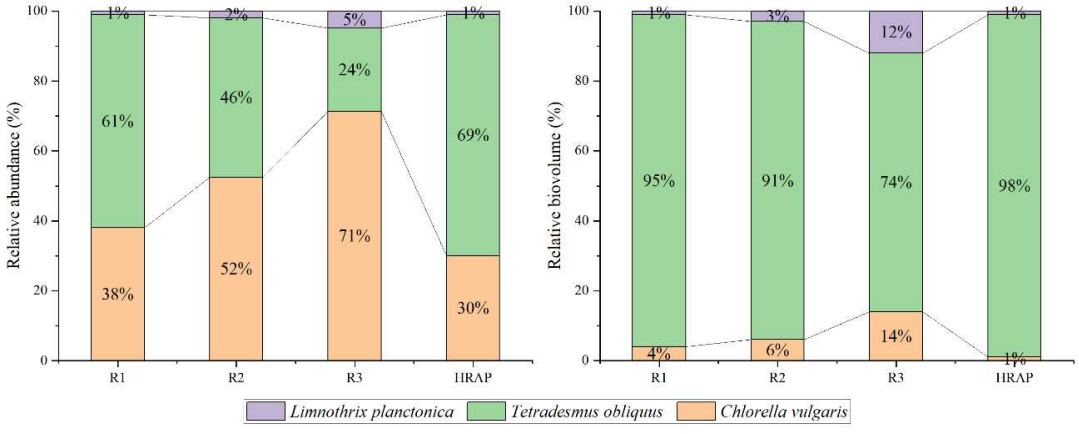

Figure 5.3. a) Relative abundance and b) Relative biovolume of microalgae and cyanobacteria present in R1, R2, R3, and HRAP.

In conclusion, the results emphasize the species-specific responses of microalgae within the hybrid system to different scraping frequencies. Integrating these results with other parameters, such as biochemical composition and structural characteristics, provides a comprehensive understanding of how scraping frequency impacts the composition and structure of microalgae biomass within the hybrid cultivation system.

5.3.3. Biochemical biomass composition

The potential of microalgae for sustainable valorization routes, such as biofuels, is influenced by their biochemical composition, specifically protein, lipids, carbohydrates, and ashes content (CHOUDHARY et al., 2020). The findings suggest that the scraping frequency impacts the composition of the biomass and can potentially influence the production of biofuels. Table 5.4 presents each reactor's proteins, carbohydrates, neutral and membrane lipids, and ashes contents.

Table 5.4. Proteins, carbohydrates, neutral and membrane lipids, and ash content of biofilms harvested every 2 (R1), 4 (R2), and 6 (R3) days and in biomass grown in the high-rate pond (HRAP).

Reactor	Compound				
	Proteins (%)	Neutral lipids (%)	Membrane lipids (%)	Carbohydrates (%)	Ashes (%)
R1	42.29 (0.17)	5.22 (0.13)	10.22 (1.51)	17.15 (1.04)	12.43 (0.19)
R2	38.69 (0.76)	3.62 (0.27)	8.90 (0.46)	14.39 (1.76)	13.39 (0.36)
R3	40.19 (0.42)	3.16 (0.57)	7.49 (0.58)	16.76 (1.85)	15.11 (0.25)
HRAP	58.92 (1.80)	1.40 (0.05)	9.41 (0.76)	10.98 (1.51)	14.83 (0.12)

The protein content in the biomass presented higher results in the HRAP (58.92%) compared to the BRs. Protein accumulation in microalgae is closely linked to nitrogen metabolism (LIU et al., 2016). In the BRs, nitrogen diffusion may be restricted in deeper layers, reducing assimilation efficiency compared to HRAP. Additionally, high cell densities in biofilms, particularly in the upper layers, can increase competition for available nitrogen, limiting assimilation and, consequently, protein synthesis (SINGH; PATIDAR, 2021). Regarding total lipids (membrane and neutral), R1 has a higher content (15.45%) than R2, R3, and HRAP. One

possibility is that frequent scraping may introduce stresses or control the nutrient environment in a way that encourages lipid storage.

Additionally, R1 also presented the highest neutral lipids content. Neutral lipids are more suitable for biofuel production (MEHRABADI; CRAGGS; FARID, 2015). In this context, R1 has greater potential for this purpose. In the present work, with a scraping frequency of every 2 days, there was a more frequent renewal of this top layer compared to scraping intervals of every 4 and 6 days. It may lead to a higher lipid content in R1.

Furthermore, in the HRAP, there was a significant difference between neutral lipids (1.40%) and membrane lipids (9.41%). These findings are consistent with those of Assis et al. (2020), who also observed this greater disparity in HRAP compared to RBs. BRs show the highest carbohydrate content compared to the HRAP (10.98%). One possible explanation for the higher carbohydrate content in BRs is that attached growth leads to EPS production, which is rich in carbohydrates (SHEN et al., 2016). The ash content is highest in reactor R3 (15.11%) and HRAP (14.83%). The less frequent scraping in a 6-day interval allows for a longer settling time for inorganic materials and minerals. This can lead to higher ash content due to the accumulation of these inorganic components over a longer period. Microalgae can incorporate inorganic content from the growth medium into their cells (FOX; ZIMBA, 2018). The wastewater used in the work contains higher levels of inorganic nutrients. When scraping each 6 days and in the HRAP, biofilm has a prolonged exposure time, leading to a higher ash content by microalgae incorporation and particles settling within the cultivation medium.

The findings emphasize the importance of improving scraping frequency to biomass biochemical composition. In this context, HERNÁNDEZ-GARCÍA et al. (2019) argue that a significant advantage of these stored compounds is their potential for biofuel production. For instance, lipids can be used to make biodiesel (COUTO; CALIJURI; ASSEMANY, 2020), and carbohydrates can be converted into biohydrogen (MAÑUNGA et al., 2022).

5.3.4. Extracellular Polymeric Substances (EPS)

Initially, the EPS concentrations across the BRs were 283.35 mg EPS/m² (R1), 243.55 mg EPS m^{-2} (R2), and 255.04 mg EPS m^{-2} (R3). R1, with the highest scraping frequency, showed fluctuations in EPS production, peaking at 651.60 mg EPS m^{-2} on day 10 before diminishing to 592.51 mg EPS m^{-2} by day 18. On the contrary, the peak of EPS concentrations in R2 and R3 was

observed on day 0, registering 243.55 mg EPS/m² and 255.04 mg EPS m^{-2}, respectively (Figure 5.4). In R1, the microalgae may intensify EPS production in response to more frequent scraping. This finding may be due to defense mechanisms, where organisms increase their defensive responses in reaction to stressors or disturbances (CHEN et al., 2013). Additionally, the distinct behaviors between R1 and R2/R3 emphasize the impact of varying scraping frequencies. The lower EPS production in R2 and R3 may indicate less frequent scraping does not incite EPS production as in R1.

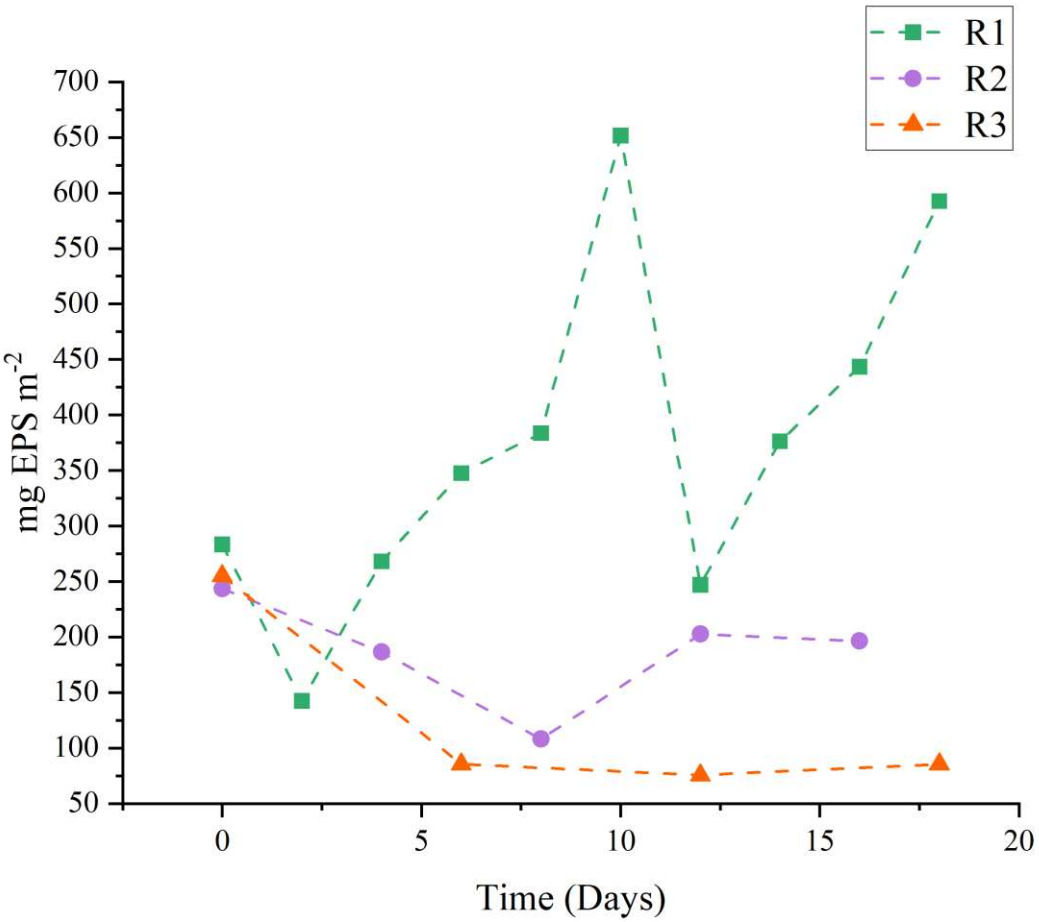

Figure 5.4. Temporal variation of EPS concentration in the different harvesting intervals (2 days (R1), 4 days (R2), and 6 days (R3)).

Notably, the increased EPS production can have significant implications for wastewater treatment efficacy. MELO et al. (2022) discuss the role of EPS in wastewater treatment, forming a

slime matrix that holds microorganisms together in three-dimensional structures. Additionally, EPS aids cell and contaminant aggregation and can enhance pollutant removal from wastewater (HUANG et al., 2022). Xiao and Zheng (2016) argue that in wastewater treatment, beyond helping to concentrate the biomass, simplifying its collection, and reducing costs, EPS produced by microalgae can remove nitrogen, phosphorus, and heavy metals. Hence, the surge in EPS production at higher scraping frequencies (R1) could represent a mechanism to reinforce wastewater treatment efficiency. These aggregates contribute to flocculation, settling, and dewatering processes crucial for biofilm formation and effective wastewater treatment.

5.3.5. Zeta potential

The zeta potential values for the different scraping frequencies were -18.93 mV (R1), -19.25 mV (R2), and -21.02 mV (R3). These values indicate an increasing trend in zeta potential values as the scraping frequency increases. Specifically, the zeta potential becomes more negative as the scraping frequency progresses from R1 to R3. This shift in zeta potential values suggests a change in the surface charge of the microalgae particles or the surrounding medium. This could be attributed to variations in the release of charged molecules, such as EPS, into the medium, which can influence the overall surface charge (CHEN et al., 2013). The reduction in repulsive forces can make the particles more susceptible to aggregation (SHRESTHA; WANG; DUTTA, 2020), potentially affecting the structure of the biofilm and the ease of biomass harvesting. A system with lower absolute zeta potential is more susceptible to aggregation, simplifying the harvesting process (WANG et al., 2022). KRISHNAMOORTHY et al. (2021) discuss that cells with a zeta potential greater than +30 mV or less than −30 mV are considered highly stable.

On the other hand, cells exhibiting low zeta potential values are prone to aggregation. In this context, given that the zeta potential in all three BRs ranged between -30 and +30 mV, there is an increased potential for adhesion. Furthermore, in work conducted by SHI et al. (2017), at a pH of around 10, close to the pH of the system operated in this work, the zeta potential for *Chlorella vulgaris* was approximately -20 mV. In research conducted by OZKAN; BERBEROGLU (2013), the authors observed that the zeta potential of *Chlorella vulgaris* was −23.3 mV, and for *Tetradesmus* sp., it was −18.4 mV. Therefore, the zeta potential values align with the literature, suggesting that the measured zeta potential is consistent with the dominant species in the reactors, namely *Tetradesmus obliquus* in R1 and *Chlorella vulgaris* in R3. However, it is important to

consider other factors that influence harvesting efficiency, such as the biomass's biochemical composition, the biofilm's structural integrity, and external environmental conditions. The biomass production rate and overall system efficiency must also be considered.

5.3.6. Wastewater treatment

The inlet and outlet concentrations throughout the hybrid system are shown in Figure S5.2 (Apêndice II). Real wastewater was used as the culture medium, so there were variations in the influent concentrations, which are common in large-scale municipal wastewater treatment systems. Concentrations of soluble P and nitrogen (NH_4^+ and NO_3^-) were found to be below 5 mg L^{-1} and close to zero, respectively, throughout the operation. The removal of wastewater treatment monitoring variables is shown in

Table 5.5. Organic matter removal of approximately 60% and 77% in total and soluble COD was achieved, respectively. The microalgae assimilate nutrients and carbon, leading to the absorption of about 93% of DOC.

Furthermore, the removal of 50% of TP and 75% of SP from the wastewater was observed. The pH increased from 7.72 to 9.46. It is common in systems that employ microalgae due to the uptake of CO_2 during photosynthesis, which reduces water acidity. This rise in pH aids in the precipitation of pollutants such as phosphorus (DENG; DHAR, 2023) and ammoniacal nitrogen (NH_3) volatilization (CHAI et al., 2021). Hence, the system effectively eliminated NH_4^+, achieving nearly complete removal at approximately 100%.

Regarding DO, there was an increase from 0.89 mg L^{-1} to 10.54 mg L^{-1}, indicative of oxygen production by microalgae via photosynthesis. DO enhances the oxidation of organic contaminants (DUAN et al., 2022), as demonstrated by the decrease in COD and DOC levels. These results emphasize the potential of microalgae and bacteria consortia within the context of wastewater treatment, particularly concerning the removal of organic matter and nutrients. Notably, the high deviations of environmental variables found in this study were linked to the uncontrollable dynamics of the system exposed to climatic conditions (ASSIS et al., 2020).

Table 5.5. Removal of wastewater treatment monitoring variables (mean values, n = 19, and standard deviation in parentheses).

Variable	Mixed wastewater	HRAP	Removal (%)
pH	7.72 (0.53)	9.46 (0.74)	-
DO (mg L^{-1})	0.89 (0.65)	10.54 (2.02)	-
EC (mS cm^{-2})	1,226.21 (182.41)	925.05 (314.08)	-
COD (mg L^{-1})	1,021.92 (888.21)	418.08 (271.28)	59.09%
sCOD (mg L^{-1})	593.52 (534.96)	135.36 (109.17)	77.19%
DOC (mg L^{-1})	382.03 (47.85)	26.92 (17.37)	92.95%
NH_4^+ (mg L^{-1})	48.35 (9.25)	<0.1	100.00%
NO_3^- (mg L^{-1})	1.31 (0.63)	0.94 (0.60)	-
Norg (mg L^{-1})	11.50 (6.90)	28.52 (11.88)	-
TP (mg L^{-1})	7.53 (5.35)	3.76 (1.73)	50.03%
SP (mg L^{-1})	5.21 (5.2)	1.31 (0.79)	74.92%
E. coli (MPN/100ml)	4.92 x 10^4*(9.98 x 10^4)	3.87 x 10^3* (8.49 x 10^4)	1 log unit**

Note: *Geometric mean. **Removal in logarithmic units. DO = Dissolved oxygen, EC = Electrical conductivity, COD = Chemical oxygen demand, sCOD = Soluble chemical oxygen demand, DOC = Dissolved organic carbon, NH_4^+ = Ammonia nitrogen, NO_3^- = Nitrate, Norg = Organic nitrogen, TP = Total phosphorus, SP = Soluble phosphorus, and MPN = Most probable number.

Mixing industrial carbon-rich wastewater and domestic wastewater, including that from the juice industry, can be advantageous for microalgae cultivation as it provides a carbon-rich source for biomass production. Evaluating the performance of the vertical-algal-biofilm-enhanced raceway pond for wastewater treatment and algae biomass production, (ZHANG et al., 2018a) investigated different nutrient loading rates. However, the authors noted that the synthetic wastewater's COD used was insufficient. They suggested mixing wastewaters as an alternative to increasing the COD, thereby enhancing the system's absorption rate during large-scale operations.

Studies show that wastewater mixture provides better treatment. For instance, PARK et al. (2015) investigated the potential of blending DW and swine wastewater (SW) for microalgae cultivation, eliminating the need for pretreatment. The authors discuss that using a mixing ratio of 5-15% (v_{DW}/v_{SW}), microalgae biomass productivity reached 1.03 g total solids L^{-1} d^{-1}. In addition, mixing increased lipid accumulation in the cells, reaching 39.1% (w/w). The study also reported a maximum lipid productivity of 0.19 g fatty acid methyl ester L^{-1} d^{-1}. ZHENG et al. (2018) explored the combination of piggery and brewery wastewaters to boost algal growth and nutrient removal.

The authors found that the most effective ratio was 1:5, resulting in a carbon/nitrogen ratio 7.9. This achieved a biomass concentration of 2.85 g L^{-1}, and removal rates equal to 100% for ammonia, 96% for total nitrogen, 90% for total phosphorus, and 93% for COD.

Additionally, the research conducted by YU et al. (2024) also demonstrated the great potential of the microalgae-bacteria symbiotic biofilm system for treating mixed wastewaters (with a soybean soaking wastewater to domestic wastewater ratio of 1:7). The researchers developed a novel vertical rotating microalgae-bacteria symbiotic biofilm reactor that achieved maximum removal rates of COD, TN, and NH_4^+ (98%, 95%, and 99.9%, respectively) during semi-continuous operation. The maximum biomass productivity of the harvested biofilm at the end of the operation was 2.69 g m^{-2} d^{-1}, with a composition of 22% carbohydrates, 51% proteins, and 10% lipids. In this context, wastewater mixture is a strategic approach that can improve waste treatment processes. However, it is noteworthy that this approach demands a well-structured logistics system to ensure proper mixing and compatibility of the different waste streams. Combining IW and DW with microalgae treatment showcases a forward-thinking strategy that addresses waste disposal and explores the potential for resource recovery. This approach aligns well with sustainability goals and can serve as a model for other industries seeking innovative waste management solutions.

5.4.Conclusion

The improved 2-day scraping frequency yielded the highest biomass productivity, with TVS levels peaking at 18.75 g m^{-2} d^{-1}. *Chlorella vulgaris* succeeded better with less frequent scraping, while *Tetradesmus obliquus* preferred suspended conditions. The biochemical composition also showed differences with the HRAP, indicating a main composition of protein content of 58.92% and R1 demonstrating a lipid content of 15.45%. The results emphasize the need to adjust the scraping frequency to maximize microalgal growth. For future works, it is recommended to evaluate the cost-effectiveness of the proposed systems, considering labor, energy, and equipment durability to develop a scalable and sustainable model. Additionally, it is important to investigate the environmental implications of different scraping frequencies, focusing on wastewater treatment efficiency.

Acknowledgements

The authors gratefully acknowledge the Fundação de Amparo à Pesquisa do Estado de Minas Gerais (FAPEMIG) (grant numbers 02527-18 and 03618-23) and Fundação Coordenação de Aperfeiçoamento de Pessoal de Nível Superior (CAPES).

References

AOAC. **Official methods of analysis**. 11th. ed. Washington: Association of Official Analytical Chemists, 1990.

APHA. **Standard Methods for examination of water and wastewater**. Washington: American Water Work Association, Water Environmental Federation, 2012.

ASSIS, L. R. DE et al. Microalgal biomass production and nutrients removal from domestic sewage in a hybrid high-rate pond with biofilm reactor. **Ecological Engineering**, v. 106, p. 191–199, set. 2017.

ASSIS, L. R. DE et al. Evaluation of the performance of different materials to support the attached growth of algal biomass. **Algal Research**, v. 39, n. September 2018, p. 101440, 2019.

ASSIS, L. R. DE et al. Innovative hybrid system for wastewater treatment: High-rate algal ponds for effluent treatment and biofilm reactor for biomass production and harvesting. **Journal of Environmental Management**, v. 274, p. 111183, nov. 2020.

ASTM. ASTM D3174-02. Standard Test Method for Ash in the Analysis Sample of Coal and Coke from Coal. Wes Conshohocken, PA: ASTM International, 2002.

BOELEE, N. C. et al. Nitrogen and phosphorus removal from municipal wastewater effluent using microalgal biofilms. **Water Research**, v. 45, n. 18, p. 5925–5933, nov. 2011.

BOELEE, N. C. et al. The effect of harvesting on biomass production and nutrient removal in phototrophic biofilm reactors for effluent polishing. **Journal of Applied Phycology**, v. 26, n. 3, p. 1439–1452, 23 jun. 2014.

CHAI, W. S. et al. Microalgae and ammonia: A review on inter-relationship. **Fuel**, v. 303, p. 121303, nov. 2021.

CHEAH, Y. T.; CHAN, D. J. C. Physiology of microalgal biofilm: a review on prediction of adhesion on substrates. **Bioengineered**, v. 12, n. 1, p. 7577–7599, 1 jan. 2021.

CHEN, Y.-P. et al. Functional groups characteristics of EPS in biofilm growing on different carriers. **Chemosphere**, v. 92, n. 6, p. 633–638, jul. 2013.

CHENG, P. et al. Biofilm attached cultivation of Chlorella pyrenoidosa is a developed system for swine wastewater treatment and lipid production. **Frontiers in Plant Science**, v. 8, 21 set. 2017.

CHIU, S.-Y. et al. Cultivation of microalgal Chlorella for biomass and lipid production using wastewater as nutrient resource. **Bioresource Technology**, v. 184, p. 179–189, maio 2015.

CHOUDHARY, P. et al. A review of biochemical and thermochemical energy conversion routes of wastewater grown algal biomass. **Science of the Total Environment**, v. 726, n. 271, p. 137961, 2020.

COUTO, E. A. et al. Effect of depth of high-rate ponds on the assimilation of CO_2 by microalgae cultivated in domestic sewage. **Environmental Technology**, v. 39, n. 20, p. 2653–2661, 18 out. 2018.

COUTO, E.; CALIJURI, M. L.; ASSEMANY, P. Biomass production in high rate ponds and hydrothermal liquefaction: Wastewater treatment and bioenergy integration. **Science of the Total Environment**, v. 724, 2020.

DENG, L.; DHAR, B. R. Phosphorus recovery from wastewater via calcium phosphate precipitation: A critical review of methods, progress, and insights. **Chemosphere**, v. 330, p. 138685, jul. 2023.

DUAN, S. et al. Simultaneous oxidation of trace organic contaminant and Mn(II) by Mn(VII): Accelerating role of dissolved oxygen. **Chemosphere**, v. 308, p. 136321, dez. 2022.

DUBOIS, MICHEL. et al. Colorimetric Method for Determination of Sugars and Related Substances. **Analytical Chemistry**, v. 28, n. 3, p. 350–356, mar. 1956.

ECONOMOU, C. N. et al. Lipid production by the filamentous cyanobacterium Limnothrix sp. growing in synthetic wastewater in suspended- and attached-growth photobioreactor systems. **Annals of Microbiology**, v. 65, n. 4, p. 1941–1948, 15 dez. 2015.

FAROOQ, W. et al. Evolved Gas Analysis and Kinetics of Catalytic and Non-Catalytic Pyrolysis of Microalgae Chlorella sp. Biomass With Ni/θ-Al2O3 Catalyst via Thermogravimetric Analysis. **Frontiers in Energy Research**, v. 9, 25 nov. 2021.

FOX, J. M.; ZIMBA, P. V. Minerals and Trace Elements in Microalgae. Em: **Microalgae in Health and Disease Prevention**. [s.l.] Elsevier, 2018. p. 177–193.

GAMA, R. C. N. DA et al. Influence of C/N ratio on microalgae-bacteria joint culture: Treatment performance and phytoplankton dynamics in mixed wastewaters. **Bioresource Technology Reports**, v. 23, p. 101516, set. 2023.

GROSS, M. et al. Development of a rotating algal biofilm growth system for attached microalgae growth with in situ biomass harvest. **Bioresource Technology**, v. 150, p. 195–201, 2013.

HERNÁNDEZ-GARCÍA, A. et al. Wastewater-leachate treatment by microalgae: Biomass, carbohydrate and lipid production. **Ecotoxicology and Environmental Safety**, v. 174, p. 435–444, jun. 2019.

HILLMAN, K. M.; SIMS, R. C. Struvite formation associated with the microalgae biofilm matrix of a rotating algal biofilm reactor (RABR) during nutrient removal from municipal wastewater. **Water Science and Technology**, v. 81, n. 4, p. 644–655, 15 fev. 2020.

HODGES, A. et al. Nutrient and suspended solids removal from petrochemical wastewater via microalgal biofilm cultivation. **Chemosphere**, v. 174, p. 46–48, 2017.

HOEBLER, C. et al. Rapid acid hydrolysis of plant cell wall polysaccharides and simplified quantitative determination of their neutral monosaccharides by gas-liquid chromatography. **Journal of Agricultural and Food Chemistry**, v. 37, n. 2, p. 360–367, mar. 1989.

HUANG, L. et al. A Review of the Role of Extracellular Polymeric Substances (EPS) in Wastewater Treatment Systems. **International Journal of Environmental Research and Public Health**, v. 19, n. 19, p. 12191, 26 set. 2022.

IRVING, T. E.; ALLEN, D. G. Species and material considerations in the formation and development of microalgal biofilms. **Applied Microbiology and Biotechnology**, v. 92, n. 2, p. 283–294, 8 out. 2011.

KOMAREK, J.; FOTT, B. Das Phytoplankton im Susswasser Chlorophyceae (Grunanlagen) Ordnung: Chlorococcales: Bd 7 1. [s.l.] Schweizerbart'sche, E., 1983.

KRISHNAMOORTHY, N. et al. Recent advances and future prospects of electrochemical processes for microalgae harvesting. **Journal of Environmental Chemical Engineering**, v. 9, n. 5, p. 105875, out. 2021.

LIU, T. et al. Attached cultivation technology of microalgae for efficient biomass feedstock production. **Bioresource Technology**, v. 127, p. 216–222, 2013.

LIU, T. et al. The enhanced lipid accumulation in oleaginous microalga by the potential continuous nitrogen-limitation (CNL) strategy. **Bioresource Technology**, v. 203, p. 150–159, mar. 2016.

LV, J. et al. A comparative study on flocculating ability and growth potential of two microalgae in simulated secondary effluent. **Bioresource Technology**, v. 205, p. 111–117, abr. 2016.

MA, C. et al. Molasses wastewater treatment and lipid production at low temperature conditions by a microalgal mutant Scenedesmus sp. Z-4. **Biotechnology for Biofuels**, v. 10, n. 1, p. 111, 2 dez. 2017.

MAGALHÃES, I. B. et al. Agro-industrial wastewater-grown microalgae: A techno-environmental assessment of open and closed systems. **Science of The Total Environment**, v. 834, p. 155282, ago. 2022.

MAÑUNGA, T. et al. Evaluation of pretreatment methods and initial pH on mixed inoculum for fermentative hydrogen production from cassava wastewater. **Biofuels**, v. 13, n. 3, p. 301–308, 16 mar. 2022.

MEHRABADI, A.; CRAGGS, R.; FARID, M. M. Wastewater treatment high rate algal ponds (WWT HRAP) for low-cost biofuel production. **Bioresource Technology**, v. 184, p. 202–214, maio 2015.

MELO, A. et al. The Role of Extracellular Polymeric Substances in Micropollutant Removal. **Frontiers in Chemical Engineering**, v. 4, 4 maio 2022.

NEDERLANDS NORM. NEN 6520. Spectrophotometric determination of chlorophyll a content. , 1982.

NUSH, E. A. Comparison of different methods for chlorophyll and phaepigment. **Arch. Hydrobiolol. Bech. Stuttgart**, v. 14, p. 14–36, 1981.

OZKAN, A.; BERBEROGLU, H. Physico-chemical surface properties of microalgae. **Colloids and Surfaces B: Biointerfaces**, v. 112, p. 287–293, dez. 2013.

PARK, S. et al. Blending water- and nutrient-source wastewaters for cost-effective cultivation of high lipid content microalgal species Micractinium inermum NLP-F014. **Bioresource Technology**, v. 198, p. 388–394, dez. 2015.

PARRA, O.; GONZALEZ, M.; DELLAROSSA, V. Manual Taxonómico del Fitoplancton de Aguas Continentales. V. Chlorophyceae. n. January, 1983.

PERIN, G. et al. Novel micro-photobioreactor design and monitoring method for assessing microalgae response to light intensity. **Algal Research**, v. 19, p. 69–76, nov. 2016.

SALEEM, S. et al. Eco-friendly cultivation of microalgae using a horizontal twin layer system for treatment of real solid waste leachate. **Journal of Environmental Management**, v. 351, p. 119847, fev. 2024.

SHEN, Y. et al. Biofilm formation in attached microalgal reactors. **Bioprocess and Biosystems Engineering**, v. 39, n. 8, p. 1281–1288, 16 ago. 2016.

SHI, W. et al. Synergy of flocculation and flotation for microalgae harvesting using aluminium electrolysis. **Bioresource Technology**, v. 233, p. 127–133, jun. 2017.

SHRESTHA, S.; WANG, B.; DUTTA, P. Nanoparticle processing: Understanding and controlling aggregation. **Advances in Colloid and Interface Science**, v. 279, p. 102162, maio 2020.

SINGH, G.; PATIDAR, S. K. Development and Applications of Attached Growth System for Microalgae Biomass Production. **BioEnergy Research**, v. 14, n. 3, p. 709–722, 28 set. 2021.

SUTHERLAND, D. L. et al. Effects of nutrient load on microalgal productivity and community composition grown in anaerobically digested food-waste centrate. **Algal Research**, v. 51, p. 102037, out. 2020.

TONG, C. Y. et al. Physico-chemistry and adhesion kinetics of algal biofilm on polyethersulfone (PES) membrane with different surface wettability. **Journal of Environmental Chemical Engineering**, v. 9, n. 6, p. 106531, dez. 2021.

UTERMÖHL, H. Zur vervollkommnung der quantitativen phytoplankton-methodik. **Mitteilung Internationale Vereinigung fuer Theoretische unde Amgewandte Limnologie**, v. 9, p. 1–38, 1958.

WANG, J. H. et al. Microalgal attachment and attached systems for biomass production and wastewater treatment. **Renewable and Sustainable Energy Reviews**, v. 92, n. April, p. 331–342, 2018.

WANG, Q. et al. Insight into the rapid biogranulation for suspended single-cell microalgae harvesting in wastewater treatment systems: Focus on the role of extracellular polymeric substances. **Chemical Engineering Journal**, v. 430, p. 132631, fev. 2022.

XIAO, R.; ZHENG, Y. Overview of microalgal extracellular polymeric substances (EPS) and their applications. **Biotechnology Advances**, v. 34, n. 7, p. 1225–1244, nov. 2016.

XU, J. et al. Effects of influent C/N ratios and treatment technologies on integral biogas upgrading and pollutants removal from synthetic domestic sewage. **Scientific Reports**, v. 7, n. 1, p. 10897, 7 set. 2017.

YAN, C. et al. Effects of various LED light wavelengths and intensities on the performance of purifying synthetic domestic sewage by microalgae at different influent C/N ratios. **Ecological Engineering**, v. 51, p. 24–32, fev. 2013.

YU, M. et al. Treatment of mixed wastewater by vertical rotating microalgae-bacteria symbiotic biofilm reactor. **Bioresource Technology**, v. 393, p. 130057, fev. 2024.

ZHANG, Q. et al. Cultivation of algal biofilm using different lignocellulosic materials as carriers. **Biotechnology for Biofuels**, v. 10, n. 1, 4 maio 2017.

ZHANG, Q. et al. Operation of a vertical algal biofilm enhanced raceway pond for nutrient removal and microalgae-based byproducts production under different wastewater loadings. **Bioresource Technology**, v. 253, p. 323–332, abr. 2018a.

ZHANG, Q. et al. Vertical-algal-biofilm enhanced raceway pond for cost-effective wastewater treatment and value-added products production. **Water Research**, v. 139, p. 144–157, ago. 2018b.

ZHENG, H. et al. Balancing carbon/nitrogen ratio to improve nutrients removal and algal biomass production in piggery and brewery wastewaters. **Bioresource Technology**, v. 249, p. 479–486, fev. 2018.

ZHONG, W. et al. Biogas productivity by co-digesting Taihu blue algae with corn straw as an external carbon source. **Bioresource Technology**, v. 114, p. 281–286, jun. 2012.

ZHUANG, L. L. et al. The characteristics and influencing factors of the attached microalgae cultivation: A review. **Renewable and Sustainable Energy Reviews**, v. 94, n. November 2017, p. 1110–1119, 2018.

6. Capítulo III. Biofuel from Wastewater-Grown Microalgae: A Biorefinery Approach Using Hydrothermal Liquefaction and Catalyst Upgrading[2]

Abstract: Third-generation biofuels from microalgae are becoming necessary for sustainable energy. In this context, this study explores the hydrothermal liquefaction (HTL) of microalgae biomass grown in wastewater, consisting of 30% *Chlorella vulgaris*, 69% *Tetradesmus obliquus*, and 1% cyanobacteria *Limnothrix planctonica*, and the subsequent upgrading of the produced bio-oil. The novelty of the work lies in integrating microalgae cultivation in wastewater with HTL in a biorefinery approach, enhanced using a catalyst to upgrade the bio-oil. Different temperatures (300, 325, and 350°C) and reaction times (15, 30, and 45 minutes) were tested. The bio-oil upgrading occurred with a Cobalt-Molybdenum (CoMo) catalyst for 1 hour at 375°C. Post-HTL, although the hydrogen-to-carbon (H/C) ratio decreased from 1.70 to 1.38-1.60, the oxygen-to-carbon (O/C) ratio also decreased from 0.39 to 0.079-0.104, and the higher heating value increased from 20.6 to 36.4-38.3 MJ kg^{-1}. Palmitic acid was the main component in all bio-oil samples. The highest bio-oil yield was at 300°C for 30 minutes (23.4%). Upgrading increased long-chain hydrocarbons like heptadecane (5%), indicating biofuel potential, though nitrogenous compounds such as hexadecanenitrile suggest a need for further hydrodenitrogenation. Aqueous phase, solid residues, and gas from HTL can be used for applications such as biomass cultivation, bio-hydrogen, valuable chemicals, and materials like carbon composites and cement additives, promoting a circular economy. The study underscores the potential of microalgae-derived bio-oil as sustainable biofuel, although further refinement is needed to meet current fuel standards.

Keywords: Biorefinery approach; Renewable energy; Byproducts reuse; Upgraded bio-oil; Microalga.

6.1. Introduction

Recent developments in sustainable energy alternatives have led to the growing importance of biofuels derived from microalgae cultivated in wastewater (CHOUDHARY et al., 2020).

[2] Versão publicada na revista *Journal of Environmental Management* (Apêndice III)

Microalgae biomass is well-known for its potential as a promising feedstock. They offer advantages like continuous cultivation, adaptability to diverse climates, water and soil quality, minimal land-use conflicts, and mitigation of greenhouse gas emissions (GHG) as they consume carbon dioxide (CO_2) from the atmosphere (SINGH; AHLUWALIA, 2013).

Among the biofuel production strategies, hydrothermal liquefaction (HTL) presents an effective pathway for converting microalgae biomass into bio-oil (COUTO et al., 2018). A previous life cycle assessment (LCA) study for the cultivation of microalgae using food waste revealed that the drying process produced the highest amount of GHGs, contributing to 10.65 kg carbon dioxide equivalent (CO_2-eq) per kg of biomass powder, more than half of the whole emissions attributed to the total production process (19.68 kg CO_2-eq), highlighting how drying can impact negatively microalgal-based processes (THIELEMANN; SMETANA; PLEISSNER, 2021). The process at high pressure and temperature conditions can effectively transform wet biomass into bio-oil, avoiding energy-intensive drying processes (MATHIMANI; MALLICK, 2019). However, the HTL process alone is insufficient for producing a suitable bio-oil from microalgae. Upgrading processes are required to meet current fuel standards (MAGALHÃES et al., 2023). GUO et al. (2015) argued that long-chain fatty acids, such as palmitic acid, lead to the high viscosity of bio-oil, which affects its flow behavior. In this context, viscosity is one factor that highlights the need for bio-oil upgrading. Additionally, bio-oil upgrading involves refining processes to remove undesired components such as oxygen (O), nitrogen (N), and sulfur (S). This is done to decrease oxidative instability, increase the higher heating value (HHV), and reduce future emissions of sulfur oxides (SOx) and nitrogen oxides (NOx) from the resulting drop in biofuel (LIU et al., 2022). In catalytic reactions, the choice of catalyst support, characterized by its morphology, composition, and orientation, crucially influences hydrotreatment processes (ROY et al., 2022). For instance, hydrotreatments can employ bi-metallic sulfided catalysts such as Cobalt-Molybdenum (CoMo) and Nickel-Molybdenum (NiMo), where Mo is the active element and Co and Ni serve as promoters. Additionally, these catalysts are widely used in refineries for hydrodesulfurization (HDS) and hydrodenitrogenation (HDN) due to the presence of coordinated unsaturated sites in their molybdenum disulfide (MoS_2) phase (ROY et al., 2022).

In a study by PRESTIGIACOMO et al. (2019), applying *Chlorella vulgaris* in HTL demonstrated improved bio-oil quality. When using a CoMo catalyst, the bio-oil oxygen to carbon (O/C) ratio decreased from 0.42 in tests without catalysts to 0.19 with CoMo. Additionally, sulfur

levels were reduced to below the detection threshold of the equipment used. These results highlight this catalyst's effectiveness in enhancing the resulting bio-oil's suitability for sustainable fuel applications by reducing undesirable components. The dual capability of CoMo catalysts to efficiently lower sulfur and oxygen in bio-oil highlights their potential to produce cleaner fuel options and supports the sustainable use of microalgae as a renewable energy source.

Recent research has emphasized the importance of reusing byproducts from the HTL process. While the primary focus has been optimizing conditions to produce high bio-oil yields, significant efforts are now being made to valorize the aqueous phase, solid residues, and gas. For instance, recent studies have shown that the HTL aqueous phase can be reused through recirculation back into the HTL process (USMAN et al., 2024) or by generating value-added products such as biofuels, bio-hydrogen and valuable bio-chemicals (SWETHA et al., 2021; YU et al., 2023).

Additionally, the CO_2 produced during HTL biogas can be sequestered by the same microalgae that generated the HTL, reducing greenhouse gas emissions. This integration, as explored by MAGALHÃES et al. (2021), uses CO_2 from industrial emissions in microalgae cultivation, enhancing algal biomass productivity. The microalgae absorb CO_2 through natural carbon capture and utilization (CCU), transforming it into valuable bioresources like biofuels, biofertilizers, and bioplastics (CALIJURI et al., 2022).

Further studies highlight the potential of HTL solid residues. For example, converting them into carbon-silicon dioxide composites for lithium-ion batteries (SHARMA et al., 2022) or blending them with cementitious materials to improve insulation properties (WEI et al., 2024). These applications highlight the importance of optimizing HTL process parameters for enhanced bio-oil production, creating useful byproducts, and promoting circular economy initiatives.

Therefore, considering the importance of process parameters in HTL efficiency, this research studied the effects of varying temperatures and reaction times to identify the conditions that yield the maximum bio-oil from microalgae cultivated in wastewater. Additionally, the bio-oil obtained under the best HTL conditions underwent upgrading. The novelty of the work lies in integrating microalgae cultivation in wastewater with HTL through a biorefinery approach. This process is further enhanced by upgrading the resultant bio-oil using a CoMo catalyst to improve its properties.

6.2.Material and methods

6.2.1. Biomass production

Microalgae biomass was produced in the experimental area of the Laboratory of Sanitary and Environmental Engineering, Federal University of Viçosa, Brazil (20º45'14" S, 42º52'54" W). In this area, pilot-scale high-rate algal ponds (HRAPs) and biofilm reactors (BRs) are installed for wastewater treatment, production, and separation of algal biomass. The HRAPs have the following characteristics: width: 1.28 m; length: 2.86 m; total depth: 0.5 m; surface area: 3.3 m^2. They are made of fiberglass and steel blades with six blades powered by a 0.5 HP electric motor. The speed is reduced by a speed reducer coupled to the motor and controlled by a frequency inverter (WEG CFW-10 series). The BRs consist of flat acrylic panels and have the following characteristics: total area of 0.5 m^2, measuring 1.0 m in width and 0.5 m in length. The BRs are in direct contact with the atmospheric air and solar radiation and are installed next to the HRAPs. To allow biofilm growth, the BRs are coated with polyester (SkTextil, Oxford, 100% polyester), as previously studied by ASSIS et al. (2019) . The wastewater and biomass within the HRAP were continuously recirculated through the BRs using submersible pumps set at a flow rate of 400 L h^{-1}. The experimental arrangement followed the methodology outlined by SILVA et al. (2024).

The culture medium used for microalgae production comprised 50% industry wastewater (IW) and 50% domestic wastewater (DW). The choice of mixture was determined to balance the C/N ratio of the culture medium. Regarding the IW, the industry's main activity is producing fruit-based juice. The wastewater was generated at various stages of the production process, especially the washing of floors and equipment at the end of the production process. The IW was collected after an up-flow anaerobic sludge blanket (UASB) reactor, and the DW was collected after a septic tank.

6.2.2. Biomass characterization

Microalgae biomass was examined at the genus level, and dominant genera were further identified at the species level. The quantitative analysis involved counting individual organisms using the UTERMÖHL (1958) method in a sedimentation chamber with an inverted microscope. The APHA (2012) criteria were employed to determine organism relative abundance. For qualitative assessments, species were identified under an inverted microscope based on guidelines from PARRA; GONZALEZ; DELLAROSSA (1983) and KOMAREK; FOTT (1983). The

phytoplanktonic relative abundance revealed 30% *Chlorella vulgaris*, 69% *Tetradesmus obliquus*, and 1% cyanobacteria *Limnothrix planctonica*.

Ultimate analysis of the biomass was carried out. C, H, and N percentages were measured using a Perkin Elmer Series II 2400 Elemental Analyzer. S percentage was obtained by turbidimetry using a spectrophotometer at 440 nm. The O level in the biomass was determined by difference. The biomass atomic ratios (H/C, O/C, N/C, and S/C) were calculated by dividing the percentage of each element (H, O, N, S) by the percentage of carbon (C) and adjusting for their respective atomic mass ratios (H: 1/12, O: 16/12, N: 14/12, S: 32/12). HHV was determined according to PERRY; CHILTON (1973) (HHV (MJ kg^{-1}) = 33.86C + 144.4 (H – O / 8) + 9.428 S). Proximate analysis was performed according to ASTM (2012) to determine the humidity, volatile matter, fixed carbon, and ash content. The humidity was determined by heating 1g of the sample in an oven at 105°C until the weight stabilized. After humidity removal, the crucible containing the sample was covered with a lid and heated in a muffle furnace at 900°C for seven minutes to determine volatile matter content. After assessing volatile materials, the ash content was established by placing the sample in a muffle furnace at 700°C for 4 hours. Lastly, the fixed carbon content was determined by difference.

Lipid, carbohydrate, and protein content were determined for the biomass harvested from the HRAP and BRs. N content was defined according to APHA (2012). The protein content was defined by the N-to-protein conversion factor of 6.25 (ZHONG et al., 2012). The carbohydrate content was determined by quantitative acid hydrolysis of the biomass (HOEBLER et al., 1989), followed by the phenol-sulfuric acid method (DUBOIS et al., 1956) and spectrophotometry (490 nm) using the glucose standard curve. The lipid content was determined by the Soxhlet extraction method (AOAC, 1990). After macerating the biomass, neutral lipids were extracted in a fat determination device (Tecnal TE-044-8/50) for 6 h, with 99% hexane as the solvent. Subsequently, membrane lipids were extracted with 96% ethanol for 3 h in the same equipment and quantified by gravimetry.

The biomass fatty acid profile was determined using a CP-3800 gas chromatograph (Varian, U.S.A.) equipped with a 30 m SUPELCOWAX 10 capillary column (0.32 mm of internal diameter and 0.25 μm of film thickness). The injector (split 1:50) and the detector (flame ionization) temperatures were kept constant at 250 °C while the oven temperature was programmed to change

from 60 °C, after 2 min, to 200 °C at 10 °C/min and then to 240 °C at 5 °C/min. Helium was used as carrier gas.

Table 6.1 presents biomass characterization, and Table 6.2 presents the biomass fatty acid profile.

Table 6.1. Biomass characterization including ultimate analysis, proximate analysis, biochemical composition, and higher heating value.

Ultimate analysis (%, w w^{-1})	Carbon	45.8
	Hydrogen	6.5
	Oxygen*	25.3
	Nitrogen	6.7
	Sulfur	0.4
Proximate analysis (%, w w^{-1})	Volatile matter	75.7
	Fixed carbon	0.7
	Ashes	15.3
	Humidity	8.2
Biochemical composition (%, w w^{-1})	Carbohydrates	11.3
	Proteins	46.3
	Total Lipids	18.8
Higher heating value (MJ kg^{-1})		20.6

Note: *Oxygen content was defined by difference.

Table 6.2. Microalgae biomass fatty acid profile.

Fatty Acid	Common Name	Type	%
C12:0	Lauric acid	Saturated	1.3
C14:0	Myristic acid	Saturated	1.4
C15:0	Pentadecanoic acid	Saturated	8.5
C16:0	Palmitic acid	Saturated	36.9
C18:0	Stearic acid	Saturated	5.2
C18:1	Oleic acid	Monounsaturated	15.2
C18:2	Linoleic acid	Polyunsaturated	17.8
C18:3	α-Linolenic acid	Polyunsaturated	10.0

C20:0	Arachidic acid	Saturated	2.8
	Total		99.1

6.2.3. Hydrothermal liquefaction (HTL)

The HTL experiments were conducted according to COUTO et al. (2018) at the Bioenergy and Biorefinery Unit (UBB) of the National Laboratory for Energy and Geology (LNEG) in Portugal (38°46'18.1"N 9°10'31.9"W). It was performed in a batch setup, utilizing a 0.16 L reactor made from Hastelloy C276 by Parr Instruments. The reactor cap featured a thermocouple covered in a sheath, which extended deep into the reactor. It also included a stainless-steel Bourdon tube pressure gauge to record internal pressure, gas inlet and outlet valves, and a safety rupture disc. A graphite seal, positioned between the cap and autoclave body, ensured its sealing. For heating, the autoclave was equipped with an oven fitted with an oscillation mechanism for stirring. During the reactor heating phase and test duration, a controller continuously monitored temperature and pressure, connecting to the pressure gauge and thermocouple thermometer. Two variables were evaluated: reaction time and temperature. Times of 15 min, 30 min, and 45 min after reaching operational temperature were examined. The tested temperatures were 300 °C, 325 °C, and 350 °C, with a maximum deviation of ±5 °C allowed. The biomass-to-water ratio was 1/10 (w. w^{-1}), translating to a 9.1% (w. w^{-1}) solid concentration. 55 g of material was consistently present within the reactor. Table 6.3 presents the ID of each combination tested.

Table 6.3. Temperature and reaction time combinations tested for the biomass hydrothermal liquefaction.

Treatment ID	Temperature (°C)	Reaction time (min)
1	300	15
2	300	30
3	300	45
4	325	15
5	325	30
6	325	45
7	350	15
8	350	30
9	350	45

Before each experiment, the autoclave underwent a nitrogen gas (N_2) purge three times and was then pressurized with N_2 to keep the best operational pressure. Initial pressures were derived from preliminary experiments (Table 6.4). The goal was to maintain the pressure within 130–170 bar at the test temperature.

Table 6.4. Initial pressures for each temperature tested in the hydrothermal liquefaction experiments.

Test temperature (°C)	Pressure at room temperature (bar)
300	49
325	38
350	7

After concluding each experiment, the reactor was cooled in an ice bath until it achieved an approximate room temperature of 25 °C for product extraction. The experimental design was completely randomized (CRD) and replicated twice for each set. All statistical analyses were performed using Minitab®19 Software. To compare the yield of bio-oil, water-soluble compounds, gas, and solids residues in each treatment, analysis of variance (ANOVA) was used, followed by the Tukey test at a 5% probability of error.

6.2.4. Separation and characterization of hydrothermal liquefaction products

The procedures adopted for product separation were based on PRESTIGIACOMO et al. (2022). Solid residues, bio-oil, and aqueous phase (water-soluble compounds) yields are presented on a dry weight basis (dwb). Figure 6.1 illustrates the separation process.

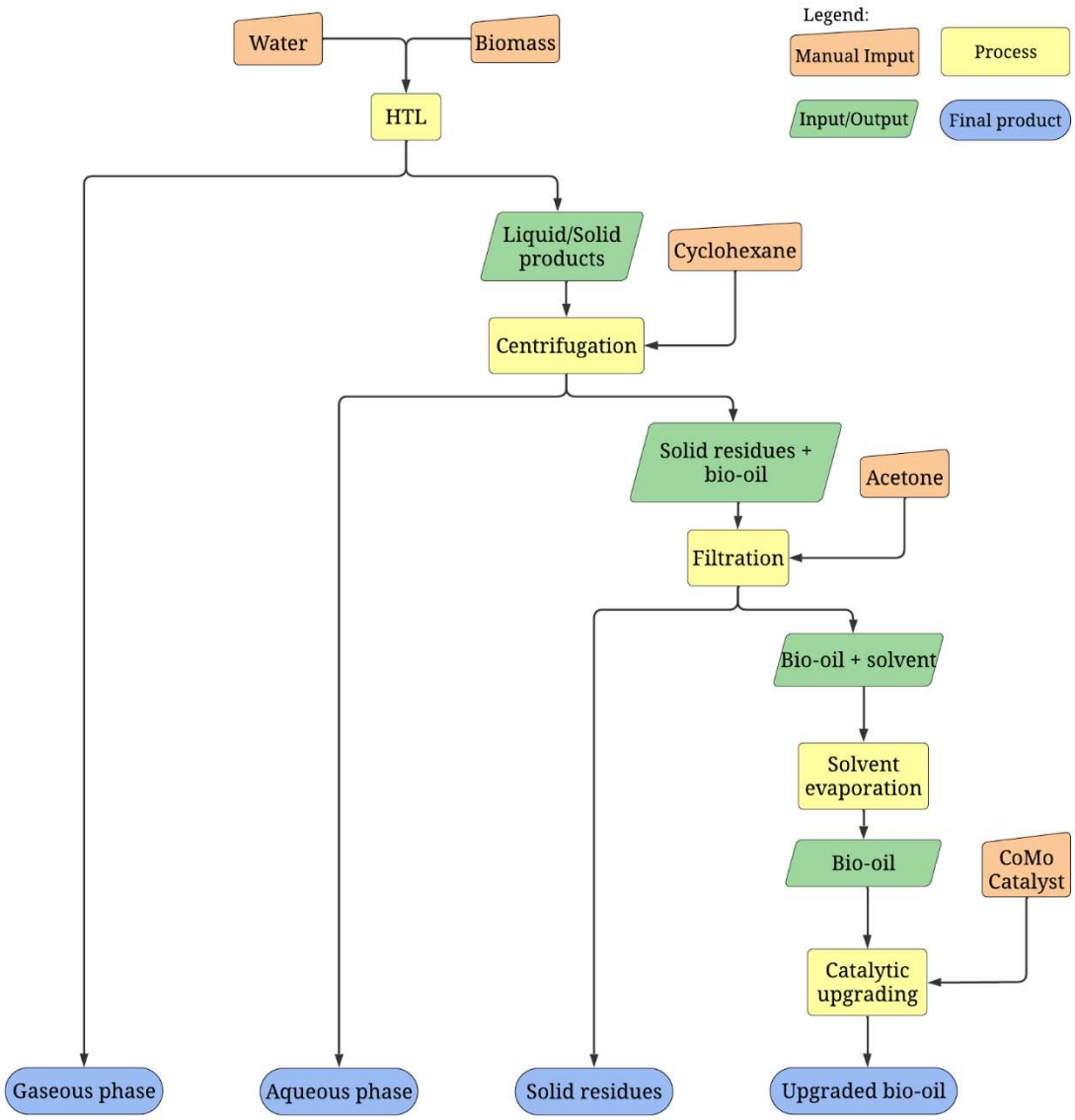

Figure 6.1. Process flowchart for the biomass conversion to bio-oil through hydrothermal liquefaction (HTL) and bio-oil upgrading. *Oxygen (O) content obtained by difference.

6.2.4.1.Gas characterization

After cooling, 1L of gas was collected in a gas sampling bag. An Agilent/HP GC6890 gas chromatograph was utilized for the gas characterization. This equipment boasts a gas sampling valve and two sequential detectors: one for flame ionization (FID) and another for thermal conductivity (TCD). The Molecular Sieve 5 A column was employed to discern CO_2, N_2, H_2, CH_4,

and CO levels, analyzed using the TCD. Additionally, the Porapak Q column was used to detect hydrocarbons ranging from C2 to C5, and these were also evaluated through TCD. The remaining gas was then released, with the Elster BK-G4M gas meter measuring its volume during this release. The N_2 mass added before the test was subtracted to determine the gas mass. Calculations relied on the ideal gas law, considering the starting and ending pressures and temperatures.

6.2.4.2.Separation technique for solid residues, bio-oil, and water-soluble compounds

Product separation proceeded as follows:

(i) The reactor was opened after gas collection and 2 mL cyclohexane. g^{-1} biomass was added;

(ii) The content was transferred to centrifuge tubes and centrifuged in a Sigma 2-7 centrifuge at 3500 rpm for 10 minutes;

(iii) Then, the supernatant (bio-oil, aqueous phase, and cyclohexane) was separated from the sediment (bio-oil mixed with solid residues);

(iv) The sediment was washed from the centrifuge tubes into a beaker with acetone;

(v) Supernatant underwent another centrifugation at 3500 rpm for 10 minutes;

(vi) Then, the supernatant was transferred into a decantation bulb for bio-oil and aqueous phase separation.

(vii) After half an hour, the aqueous phase was transferred to a pre-weighed rotary evaporator flask;

(viii) Bio-oil and solid residues were poured into the same beaker mentioned in step (iv) with acetone.

6.2.4.3.Solid residues characterization

The solid residue was separated from the bio-oil and solvents by filtration using a pre-dried (1 hour at 40°C) nylon membrane filter with a diameter of 47 mm and 0.22 µm pore size. The resultant solid cake was rinsed with acetone to recover any clinging bio-oil. Following a 1-hour oven drying at 40°C, the filter and solid residues were weighed upon returning to room temperature. The solid residues were characterized in terms of C, H, and N using a Perkin Elmer Series II 2400 Elemental Analyzer for biomass characterization (Section 6.2.2).

6.2.4.4.Bio-oil separation and composition analysis

Subsequently, the solvents were separated from the bio-oil using N_2 extraction at a rate of 1 L/min for 6 hours in a pre-weighed impinger. After the 6 hours, the impinger was weighted every 18 hours until its weight stabilized (less than 0.01g weight loss). An Agilent 8890 GC chromatograph (with an Agilent DB-5ms column, 30 m x 250 μm x 0.25 μm) coupled to a 5977B GC/MSD mass spectrometer was used for bio-oil characterization. The compounds in the bio-oil were quantified by dividing the area of each individual peak by the overall chromatogram area (i.e., the sum of the areas of all peaks in the chromatogram). The recovered bio-oil was dissolved in 10 mL of isopropanol and injected using a 1:10 split. Bio-oil C, H, N, S, O, atomic ratios (H/C, O/C, N/C, and S/C), and HHV analysis followed the same procedure described for microalgae biomass (Section 6.2.2).

6.2.4.5.Water-soluble compounds separation and composition analysis

The identification and quantification of the water-soluble compounds (aqueous phase) were carried out by high-performance liquid chromatography (HPLC) in an Agilent 1200 system equipped with an automatic injector, pre-column (Micro-Guard Cation H from Biorad; 30 x 4.6 mm), column (Aminex HPX-87H from Biorad; 300 x 7.8 mm) and refractive index (IR) detector, and with a fixed injection volume of 20 μL. The analysis was carried out at a constant temperature of 50ºC and 35ºC for the column and the detector, respectively. The samples were eluted at 0.5 mL min^{-1} with a 5 mM sulfuric acid solution, previously filtered (filters with a pore size of 0.22 μm and a diameter of 47 mm made of nylon from Filter Labs). For calibration, solutions were prepared with concentrations between 0.1 and 30 g L^{-1} of propionic, acetic, and formic acids and between 0.1 and 2.5 g L^{-1} in cellobiose, glucose, xylose, arabinose, succinic acid, lactic acid, glycerol, isobutyric acid, and butyric acid.

6.2.5. Bio-oil upgrading

The bio-oil upgrading procedure was based on PRESTIGIACOMO et al. (2022). The reactor used for the upgrading was the same as the one used for the HTL process. A 0.16 L autoclave constructed from Hastelloy C276 by Parr Instruments. For the upgrading, 3g of bio-oil and 1g of the CoMo catalyst supported on gamma alumina were introduced into the reactor. The reactor was sealed and purged with hydrogen gas (H_2). The operational parameters were set to

375°C and 1 hour with a reaction pressure of 100 bar. Upgrading experiments were conducted in duplicates.

The produced gas and upgraded bio-oil were analyzed as described in sections 2.4.1 and 2.4.4, respectively. The bio-oil adhered to the CoMo catalyst was recovered using hexane as a solvent in the Soxtec system HT 1043 extraction unit (Velp Scientifica, Europe). Upgraded bio-oil C, H, N, S, O, atomic ratios (H/C, O/C, N/C, and S/C), and HHV analysis followed the same procedure described for microalgae biomass (Section 6.2.2).

6.3.Results and Discussion

6.3.1. Hydrothermal liquefaction products yield

The lowest temperature (300°C) produced the highest bio-oil yields (23.4% - 23.7% dwb) (Table 6.5), which aligns with findings from COUTO et al. (2018). They reported bio-oil yields of approximately 25% (dwb) (or about 44% on a dry-ash-free basis) from HTL of microalgae biomass cultivated in wastewater under optimal conditions (300°C for 15 minutes with a biomass water^{-1} ratio of 1 10^{-1} w w^{-1}). The study by BISWAS et al. (2018) investigated the valorization of the marine algae *Sargassum tenerrimum* through HTL under subcritical conditions, with temperatures ranging between 260 and 300 °C for 15 minutes. The results showed that the maximum bio-oil yield (16.3%) was achieved at 280 °C. The highest conversion rate (75.8%) occurred at 300 °C. This highlights the potential for high-efficiency bio-oil production under controlled HTL conditions. Conversely, Treatment 7, which utilized a higher temperature of 350°C with a shorter reaction time of 15 minutes, resulted in the lowest yield (20.0% dwb). This suggests that higher temperatures may not be conducive to maximizing bio-oil yields in HTL processes. The reduction in bio-oil yield as temperature increases to 350°C may indicate thermal degradation, favoring mainly gas formation over bio-oil (COUTO et al., 2018). MARTINS-VIEIRA et al. (2023) argued that, in HTL, higher temperatures (350 °C) broke down the organic matter further into gas. On the other hand, achieving higher bio-oil yields at lower temperatures (300°C) offers both environmental and economic benefits. According to GOLLAKOTA; KISHORE; GU (2018), operating at reduced temperatures decreased energy consumption, enhancing the efficiency of the energy conversion process. Furthermore, low temperatures, compared to methods like pyrolysis, generate lower quantities of tar.

Table 6.5. Yield of bio-oil, water-soluble compounds, gas, and solids residues in each treatment on a dry weight basis.

Treatment ID	Yield (%, w w^{-1})				
	Bio-oil	Water-soluble compounds	Gas	Solid residue	Total
1	20.4 (0.1)^{bc}	27.4 (1.2)^{a}	11.7 (0.0)^{d}	20.4 (0.2)^{a}	79.9
2	23.4 (0.8)^{a}	27.6 (1.6)^{a}	11.7 (0.0)^{d}	19.6 (0.1)^{ab}	82.3
3	23.7 (0.2)^{a}	25.9 (0.8)^{ab}	19.5 (0.0)^{a}	19.5 (0.5)^{ab}	88.5
4	22.7 (0.5)^{ab}	23.5 (1.2)^{abc}	13.6 (0.0)^{c}	17.9 (0.3)^{bc}	77.7
5	21.3 (0.8)^{abc}	22.0 (2.5)^{bcd}	16.6 (1.4)^{b}	18.5 (0.6)^{abc}	78.4
6	21.5 (0.0)^{abc}	20.8 (0.8)^{cd}	17.4 (0.3)^{b}	18.5 (0.8)^{abc}	78.2
7	19.9 (1.6)^{c}	22.4 (0.6)^{bc}	17.5 (0.1)^{b}	19.0 (0.4)^{abc}	78.8
8	20.5 (0.1)^{bc}	19.1 (0.5)^{cd}	16.2 (0.0)^{b}	17.8 (0.1)^{bc}	73.7
9	22.2 (0.2)^{abc}	17.4 (0.1)^{d}	15.9 (0.1)^{b}	17.4 (0.6)^{c}	72.9

Note: Standard deviation values in parentheses. Significant at the 5% probability of error level by the Tukey test; the numbers followed by the same letter in the column did not differ statistically. Treatment IDs are as follow: 1: 300°C, 15min; 2: 300°C, 30min; 3: 300°C, 45min; 4: 325°C, 15min; 5: 325°C, 30min; 6: 325°C, 45min; 7: 350°C, 15min, 8: 350°C, 30min; 9: 350°C, 45min.

The yield of water-soluble compounds peaked at lower temperatures (300°C) regardless of the reaction time, suggesting a higher solubility at these temperatures. FAN; HORNUNG; DAHMEN (2022) discussed that at lower temperatures (below 300°C), the HTL process tends to hydrolysis reactions. The biomass breaks down during these reactions into smaller, more polar molecules. These smaller molecules often contain functional groups like hydroxyl (-OH) or carboxyl (-COOH) groups, which are polar and hydrophilic, making them more soluble in water. On the other hand, at higher temperatures (above 300°C), the process favors depolymerization and decarboxylation reactions. These reactions tend to break down the biomass, forming gases and compounds that are insoluble in water.

On the gas yield, an increase was noticeable as the temperature rose, suggesting that higher temperatures can facilitate the breaking down of organic matter into gaseous products. COUTO et al. (2018) argued that bio-oil molecules degrade and produce more volatile compounds, which can become gases with increasing temperature. Concerning solid residue yield, it was higher at lower temperatures. Notably, the ash content in the biomass (15.3% (dwb)) contributes to the solid residue yield. The ash remains undissolved or unreacted, contributing to a higher solid residue

content. Furthermore, lower temperatures might not provide enough energy for breaking down stable molecules, thereby retaining them in the solid phase (AKHTAR; AMIN, 2011).

6.3.2. Product Separation and Characterization

6.3.2.1.Bio-oil composition analysis

The bio-oil produced from all the treatments showed a substantial C content increase compared to the initial biomass (45.8%). The C percentage ranged between 74.0% and 76.3%. H content in the bio-oil ranged between 8.7% and 10.0%, showing an enrichment from the initial 6.5% in the biomass. Increased C and H content is favorable for fuel applications due to its correlation with higher HHV (SHAKYA et al., 2017). Additionally, oxygen content decreased, from 25.3% to 8.0-10.3%, in the bio-oil across all treatments compared to the raw biomass. Lower oxygen content is desirable for bio-oil as it indicates fewer oxygenates, which can lead to undesirable reactions during fuel use (REN et al., 2018).

Bio-oil N content varied between 5.1% and 5.5%. Although this range represents a decrease from the original 6.7% in the biomass, it comprises around 80% of the N content present in the raw biomass. LIU et al. (2022) discussed that the bio-oil produced through HTL of microalgae had an N concentration between 5-8%. The authors stated that the elevated N level generates undesirable NOx during combustion, which are harmful emissions. Furthermore, the high N content compromises the stability of the bio-oil. This instability leads to forming larger, more complex molecules from smaller ones. This can further reduce the quality and usability of the bio-oil. In this context, evaluating techniques to remove N content from the bio-oil is important.

Table 6.6 presents the CHNS/O and HHV results for the bio-oil.

Table 6.6. Ultimate analysis and higher heating value in bio-oil treatments.

Treatment ID	Ultimate analysis (%, w w^{-1})					HHV (MJ kg^{-1})
	C	H	N	S	O	
1	74.0	9.6	5.1	1.0	10.3	37.0
2	75.1	10.0	5.5	1.1	8.3	38.3
3	76.0	9.4	5.4	1.2	8.0	37.8
4	75.5	8.7	5.5	1.1	9.2	36.4
5	75.2	9.3	5.4	1.2	8.9	37.7
6	75.8	9.5	5.5	1.1	8.1	37.9
7	75.1	9.5	5.5	1.0	8.9	37.5
8	75.8	9.4	5.4	1.0	8.4	37.7
9	76.3	9.0	5.3	1.0	8.4	37.3

Note: Treatment IDs are as follow: 1: 300°C, 15min; 2: 300°C, 30min; 3: 300°C, 45min; 4: 325°C, 15min; 5: 325°C, 30min; 6: 325°C, 45min; 7: 350°C, 15min, 8: 350°C, 30min; 9: 350°C, 45min.

In the Van Krevelen diagram (H/C vs. O/C) (Figure 6.2), the H/C ratio indicates the aromaticity, and the O/C ratio indicates the polarity of the bio-oil. Notably, the H/C ratio is considered high when it is greater than or equal to 0.7 (CASTRO et al., 2021), which may indicate a reduced presence of aromatic structures. The raw biomass and the obtained bio-oils exhibited H/C values higher than this threshold mentioned. The raw biomass presented an O/C ratio of 0.39 and an H/C ratio of 1.70. Specifically, the atomic H/C ratios for Treatments 1 to 9 ranged from 1.60 to 1.38. The HTL process reduced the O content in the biomass, as evidenced by the decreased O/C ratios across all treatments. The O/C ratios for these treatments are consistently lower than those of the raw biomass, ranging from 0.079 to 0.104. This reduction in the O/C ratio indicates

deoxygenation, which is important for improving bio-oil quality by lowering its oxygen content. Reduced O content enhances the HHV, reduces corrosivity, and improves thermal stability, bringing the bio-oil properties closer to those of conventional fossil fuels (XU et al., 2021).

Comparing the results with conventional fuels, heavy oil has an O/C ratio of 0.01 and an H/C ratio of 1.55 (ANNAMALAI; THANAPAL; RANJAN, 2018). The bio-oils produced through HTL approach the low O/C ratio of heavy oil, indicating deoxygenation. Additionally, the H/C ratios of the bio-oils in Treatment 1 and 2 remain higher than that of heavy oil, suggesting they retain more H. On the other hand, further refinement is needed to match the H/C and O/C ratios of bio-oil with those of conventional fuels. For instance, gasoline has an O/C ratio of 0.00 and a H/C ratio of 2.25, diesel has a O/C ratio of 0.00 and a H/C ratio of approximately 1.92, and biodiesel has a O/C ratio of 0.10 and an H/C ratio of 1.90 (ANNAMALAI; THANAPAL; RANJAN, 2018). In this context, XU et al. (2021) emphasize the importance of optimizing HTL conditions to balance deoxygenation and hydrogen retention, noting that solvents used during the upgrading process can affect the elemental composition of the bio-oil, enhancing its fuel properties. Lastly, MERCKEL; LABUSCHAGNE; HEYDENRYCH (2019) state that reducing oxygen content in biofuels improves their HHV. Their research shows that oxygenates negatively impact fuel properties, making deoxygenation an important step in biofuel production.

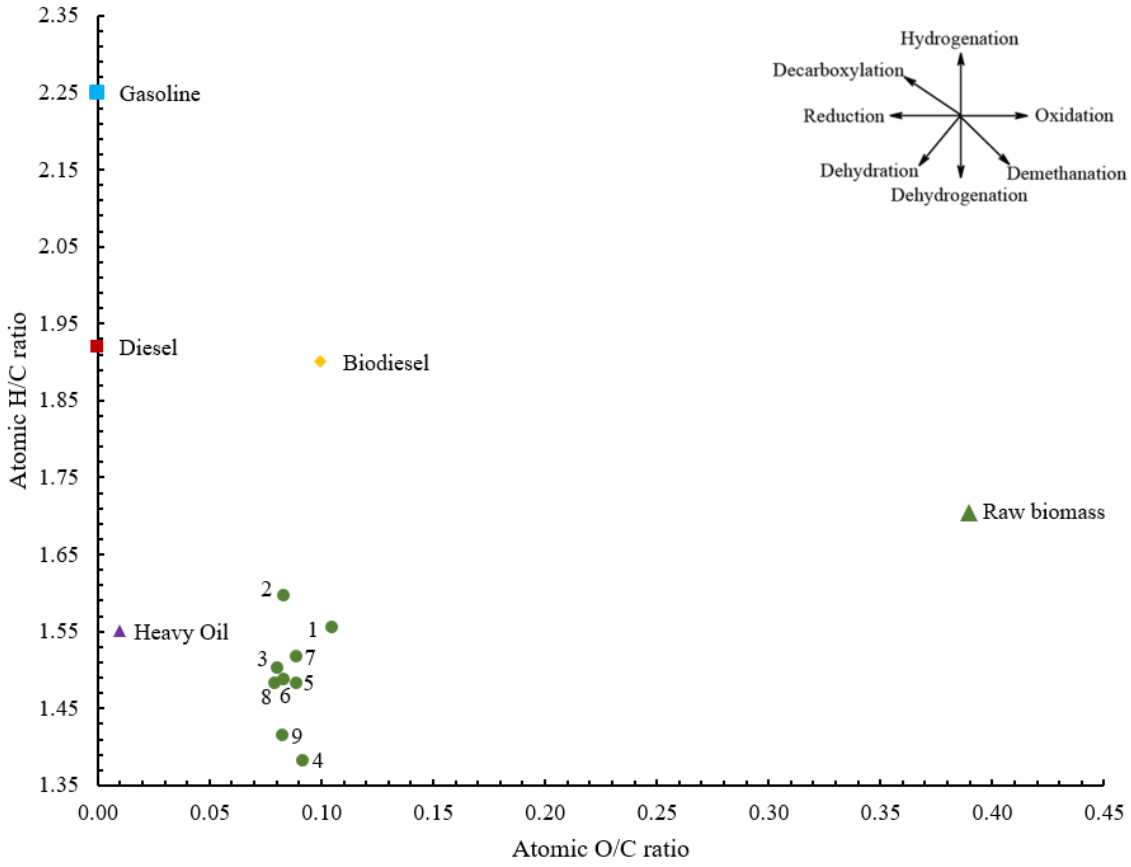

Figure 6.2. Van Krevelen diagram of bio-oil produced in each treatment. Treatment IDs are as follow: 1: 300°C, 15min; 2: 300°C, 30min; 3: 300°C, 45min; 4: 325°C, 15min; 5: 325°C, 30min; 6: 325°C, 45min; 7: 350°C, 15min, 8: 350°C, 30min; 9: 350°C, 45min.

In addition to the H/C and O/C ratios, the N/C and S/C ratios are also important in characterizing bio-oil properties. In the raw biomass, the N/C ratio is 0.125. After treatment, the N/C ratio decreases to 0.06 across all treatments. This consistent N/C reduction demonstrates the effectiveness of the upgrading processes in lowering the N content, thereby improving the quality of the final product. Conversely, the S/C ratio increases from 0.003 in the raw biomass to 0.005-0.006 in the treated bio-oil. Although these values are relatively low, further treatment steps are necessary to remove S to prevent its negative effects during combustion.

Concerning the bio-oil HHV, in all treatments, it was higher than the raw biomass (20.56 MJ kg^{-1}). This is expected due to the increase in C and H content and the decrease in O content. The HHV for the bio-oil treatments lies between 36.43 and 38.34 MJ kg^{-1}, with treatment 2

achieving the highest value. The HHV values obtained are within the range of what is typically reported for bio-oil from HTL (35-40 MJ kg^{-1}) (HAARLEMMER et al., 2016).

Concerning the bio-oil compounds, palmitic and linoleic acids were the main compounds observed in all the treatments. Palmitic acid ranged from 6.9% (Treatment 3) to 14.2% (Treatment 4). The highest linoleic acid content was observed in Treatment 4 (15.4%) (Table S6.1, Apêndice IV). Palmitic and linoleic acids are major constituents of triglycerides in most vegetable oils and animal fats (ORSAVOVA et al., 2015). Additionally, CHEN et al. (2019) discussed that palmitic acid is the main component of the bio-oil from microalgae. These compounds have high oxygen content, which results in a low HHV, and are unsuitable for cold conditions, thus limiting their use as fuel (MIAO et al., 2016). In this context, through bio-oil upgrading, long-chain fatty acids, like palmitic and oleic acid, can be converted into diesel-like alkanes (LIU et al., 2021). The compound 2,6,10,14-tetramethyl-2-hexadecene showed a relatively consistent presence across all treatments (3.5 - 5.9%), indicating its resilience to temperature and time fluctuations. During the HTL process, compounds like 2,6,10,14-tetramethyl-2-hexadecene were formed due to chemical reactions involving fatty acids, esters, and other components naturally present in biomass (GOLLAKOTA; KISHORE; GU, 2018). The unsaturation and the methyl groups in this kind of compound can affect the stability and oxidation tendency of the bio-oil, potentially leading to challenges in storage and transportation (FREIRE et al., 2012). Furthermore, nitrogenous compounds, such as palmitoleamide and hexadecanamide, were present in all treatments. As discussed before, bio-oil upgrading is a strategy to remove such compounds.

Considering the bio-oil stability, KIRAN KUMAR et al. (2018) investigated the aging and polymerization of bio-oil composed of unsaturated and complex organic components like palmitic acid, the main compound found in the study. These chemical alterations impact the oil's chemical structure and composition over time, affecting its stability and usability. The authors explore how additives, specifically antioxidants and metal deactivators, can serve as inhibitors or scavengers of reactive intermediates that promote polymerization, thus mitigating these effects. These additives interact with the free radicals and metal ions that catalyze polymerization, enhancing the oil's storage stability. Their study demonstrates that the presence of these additives effectively reduces the rate of viscosity increase and maintains the acid value below the threshold limit.

The analysis emphasizes the need to refine bio-oil, particularly in reducing N content and converting fatty acids to more suitable forms for fuel applications. This suggests that while bio-oil

production from treatments shows promise as a renewable fuel source, continued research, and development in bio-oil upgrading techniques are essential to address these challenges and achieve the full potential of bio-oil from microalgae biomass as a sustainable energy solution.

6.3.2.2.Analysis of Water-Soluble Compounds (Aqueous phase)

Concerning the aqueous phase (Figure 6.3), the results obtained were analyzed with the purpose not only of verifying whether their composition was related to the variation of the operational parameters but also within the scope of the possible application of technologies for valorizing the HTL-aqueous phase, considering its composition. In general, it was observed that the main compound was glycerol, in which the concentrations varied from 30.1% to 56.8%. This suggests that part of the microalgal lipids was effectively converted into glycerol, an important byproduct in lipid glycerides. On the other hand, the conditions that led to the highest concentration of propionic acid and lowest concentration of glycerol were 300°C and a time reaction of 15 minutes (Treatment 1).

Considering the glycerol applications, MEIER et al. (2020) explored the anaerobic biodigestion of cassava wastewater with added glycerol, focusing on optimizing hydrogen production. They found that glycerol significantly increases hydrogen yields due to its high energy content, enhancing bio-H_2 and biomethane production. The study also examined microbial dynamics, emphasizing the key role of anaerobic *Bacillus* species in converting organic material into hydrogen. Glycerol enhanced microbial pathways favorable to hydrogen production, demonstrating a symbiotic relationship between microbial activity and substrate enhancement. On the other hand, the authors emphasize the challenges like the need for additional treatment of effluents rich in organic acids, prompting recommendations for using physically separated acid and methanogenic phase reactors to improve the treatment process and methane production.

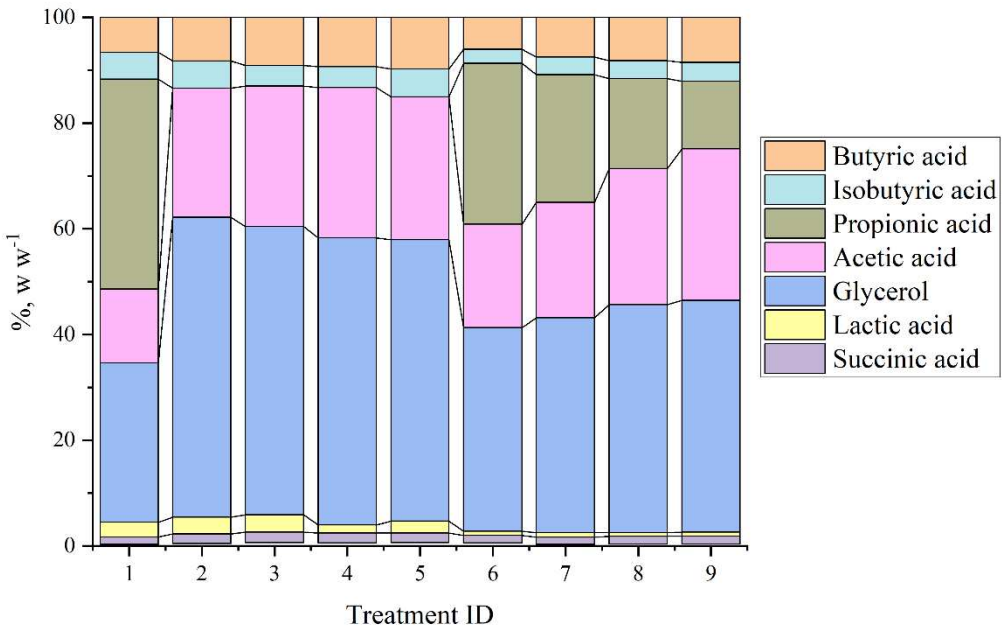

Figure 6.3. Composition of water-soluble compounds. Treatment IDs are as follow: 1: 300°C, 15min; 2: 300°C, 30min; 3: 300°C, 45min; 4: 325°C, 15min; 5: 325°C, 30min; 6: 325°C, 45min; 7: 350°C, 15min, 8: 350°C, 30min; 9: 350°C, 45min.

Furthermore, WANG et al. (2021) focused on optimizing bio-H_2 and bio-CH_4 production through a two-stage co-fermentation process using glycerol and the aqueous phase from HTL. This approach balanced the nutrient profile, mitigated acidic stress, and enhanced microbial tolerance and metabolic capacity, suggesting that adjusting glycerol concentrations can optimize conditions for bioenergy production. The study found that two-stage fermentation improved biogas production by 25.5% compared to single-stage fermentation. Specifically, adding crude glycerol to the HTL aqueous phase at a ratio of 1:1 further enhanced biogas production by 1.85 times. The initial pH value of 5.5 resulted in the highest hydrogen production, and overall, the organic conversion, energy generation, and energy recovery were improved by 48.6%, 84.9%, and 40.1%, respectively . CHACÓN-PARRA et al. (2022) discussed the impact of treatment conditions on acetic acid formation during HTL, noting that operational parameters such as temperature, pressure, and co-solvents influenced the decomposition of carbohydrates and the formation of various organic acids. Optimizing these conditions can control the yield and composition of valuable chemicals like acetic acid, tailoring the HTL process to maximize the production of desired chemicals while minimizing

unwanted byproducts. The effects of temperature and reaction time on carbohydrate breakdown during hydrothermal pretreatment are also significant, particularly in enhancing acetic acid production. Also, SUN et al. (2022) reported that hydrothermal pretreatment at 190°C during 10 and 20 minutes increased acetic acid yield from approximately 3.0% at 10 minutes to about 0.9% at 20 minutes as the reaction time increased. Similarly, the content of hemicelluloses decreased under the same conditions, from 9.5% after 10 minutes to 3.9% after 20 minutes. This breakdown, primarily of hemicelluloses, occurs through the catalytic action of ionized water, which releases acetic acid naturally present as acetyl groups in hemicelluloses. The duration of reaction time allows for more extensive carbohydrate breakdown, optimizing yields in biorefineries and exemplifying green chemistry applications.

REN et al. (2023) have further explored the use of acetic acid for biomass pretreatment, enhancing downstream processing and biomass conversion into valuable products. They demonstrated the effectiveness of acetic acid-rich aqueous phase treatments in reducing ash content in biomass, improving its quality for processes like biomass chemical looping gasification. Acetic acid's role in enhancing biomass conversion by removing impurities and altering chemical properties to favor gasification processes was highlighted, alongside its environmental advantages over stronger inorganic acids. In this context, applying acetic acid in pretreatment processes represents combining chemical engineering principles with renewable energy technology to address contemporary energy challenges.

Overall, the range of water-soluble compounds, including glycerol, organic acids, and short-chain fatty acids, presented a promising option for biofuel production. Moreover, studies have demonstrated that the aqueous phase of an HTL process can be used in versatile applications such as platform chemicals recovery and reaction medium in the HTL process as co-solvent, increasing the bio-oil production yields. Hydrothermal gasification, thermochemical recycling, anaerobic fermentation, and several integrated pathways are such examples that push the fact that the HTL-aqueous phase must be reutilized properly compared to other wastewater treatment processes (SWETHA et al., 2021; USMAN et al., 2024).

6.3.2.3.Analysis of the produced gas during hydrothermal liquefaction

Compared to the varying reaction times and temperatures, the gas composition analysis revealed that these parameters influence the product yields and their composition (Figure 6.4). CO_2

was the predominant gas in all treatments but showed a decreasing trend with increasing reaction temperatures, especially noticeable from treatments 7 to 9. For instance, treatment 2 recorded a 94.6% concentration of CO_2 at 300°C for 15 minutes. On the other hand, in treatment 9, conducted at the highest temperature of 350°C for 45 minutes, the CO_2 concentration dropped to 89.1%, suggesting that under prolonged and hotter conditions, carbon is converted from CO_2 to other components, such as methane, which also showed an increase in these conditions, highlighted by a concentration of 5.8% in the same treatment. This thermal decomposition of CO_2 into other gases under severe conditions aligns with studies suggesting that higher temperatures and prolonged reactions promote the conversion of carbonaceous gases into methane (POSMANIK et al., 2017).

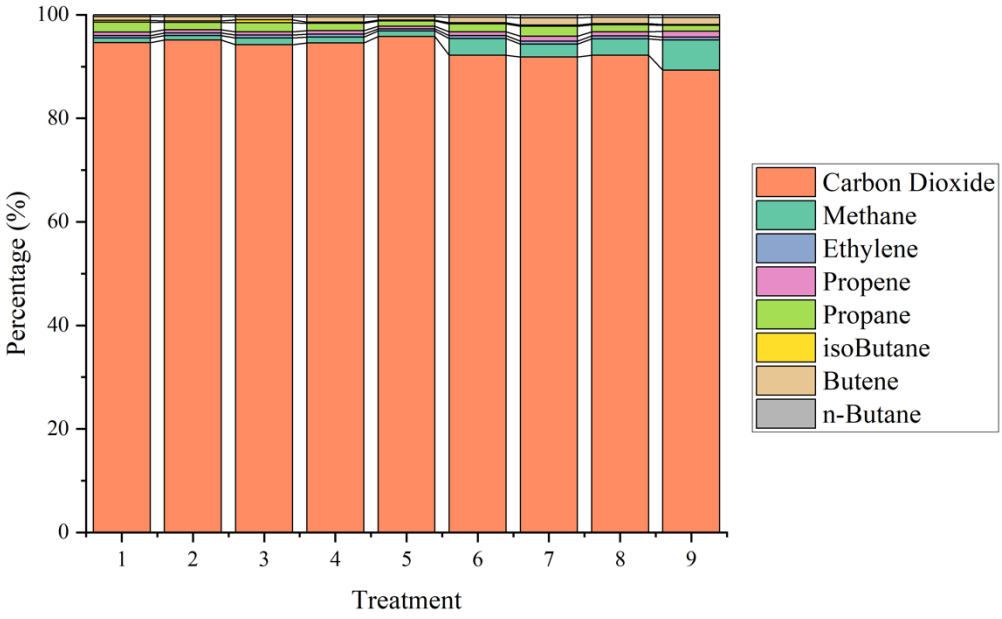

Figure 6.4. Gas composition in all the evaluated treatments. Treatment IDs are as follow: 1: 300°C, 15min; 2: 300°C, 30min; 3: 300°C, 45min; 4: 325°C, 15min; 5: 325°C, 30min; 6: 325°C, 45min; 7: 350°C, 15min, 8: 350°C, 30min; 9: 350°C, 45min.

The CO_2 produced during HTL biogas can be sequestered by the same microalgae that generated the HTL. In this context, MAGALHÃES et al. (2021) explored the environmental benefits of using CO_2 from industrial emissions in microalgae cultivation integrated with wastewater treatment systems. This approach helps to reduce GHG emissions and enhances the productivity of algal biomass, which is crucial for its commercial viability. Microalgae absorb CO_2

through natural carbon capture and utilization (CCU), transforming this industrial byproduct into valuable bioresources such as biofuels, biofertilizers, and bioplastics (CALIJURI et al., 2022).

Furthermore, ASSIS et al. (2019) emphasized the effectiveness of CO_2 supplementation in improving the growth rate of microalgae, highlighting its role in enhancing the efficiency of cultivation. They noted that using CO_2 boosts microalgal growth. This process of recycling CO_2 can reduce greenhouse gas emissions while providing a useful input for biomass production.

6.3.2.4.Analysis of Solid Residues

Solid residues noticeably reduced C, H, and N content as temperatures increased from 300°C to 350°C under similar durations (

Table 6.7). This trend indicates that higher temperatures may lead to a more thorough breakdown of biomass, resulting in higher conversion rates of these elements into gases or liquids. Likewise, extending reaction times at a consistent temperature decreases C, H, and N content. For instance, at 300°C, carbon content drops from 24.0% at 15 minutes to 21.6% at 45 minutes, a pattern at 325°C and 350°C. This suggests that longer durations facilitate more extensive thermal decomposition of organic material. The most significant reductions in CHN content are observed at the highest temperature setting of 350°C, where carbon content diminishes from 19.1% at 15 minutes to 17.2% at 45 minutes. H and N exhibit their lowest percentages at this temperature and duration. These observations align with findings from GOLLAKOTA; KISHORE; GU (2018), which correlate increased temperatures and extended durations with enhanced biomass decomposition and reduced levels of C, H, and N in the residues. The consistent ash content (15.3%) across treatments implies that the inorganic components of the biomass remain largely unaffected by temperature or duration changes, persisting as residual ash after the organic components are converted.

Table 6.7. Carbon, hydrogen, and nitrogen contents in the solid residues.

Treatment	Component (%)

	C	H	N
1	24.0	2.9	2.0
2	21.8	2.7	1.9
3	21.6	2.7	2.0
4	19.9	2.5	1.8
5	20.7	2.6	1.8
6	19.2	2.3	1.8
7	19.1	2.2	1.8
8	17.9	1.9	1.7
9	17.2	1.8	1.6

Treatment IDs are as follow: 1: 300°C, 15min; 2: 300°C, 30min; 3: 300°C, 45min; 4: 325°C, 15min; 5: 325°C, 30min; 6: 325°C, 45min; 7: 350°C, 15min, 8: 350°C, 30min; 9: 350°C, 45min.

Further studies explore various aspects of HTL solid residue management and its potential applications. For example, AKHTAR; AMIN (2011) explored how temperature, moisture, and biomass composition impact char formation and bio-oil yield in HTL. They note that lower temperatures produce more char due to incomplete biomass decomposition, while higher temperatures reduce char formation, thus boosting bio-oil yield. Specifically, temperatures around 280°C are associated with increased char due to the partial breakdown of biomass, whereas temperatures in the range of 300°C to 330°C optimize bio-oil yield by minimizing char production. In the biorefinery sector, SHARMA et al. (2022) highlighted the potential of HTL solid residues by converting them into carbon-silicon dioxide composites used as anode materials in lithium-ion batteries. WEI et al. (2024) investigated blending HTL solid residues with cementitious materials, enhancing their insulation properties and flexibility. These uses emphasize the importance of optimizing HTL process parameters for enhanced bio-oil production and for creating useful byproducts that contribute to circular economy initiatives and environmental sustainability.

6.3.3. Bio-oil Upgrading

6.3.3.1.Analysis of the upgraded bio-oil

Bio-oil upgrading is key to removing O, N, and S from the bio-oil. This process eliminates O as water, while N and S are removed as ammonia (NH_3) and hydrogen sulfide (H_2S), respectively. This process typically occurs under temperatures above 350°C, needing a H source. Considering the high O, N, and S content in the produced bio-oil, the one resulting in the highest

yield and HHV was subjected to an upgrading process (Treatment 2, produced at 300°C for 30 minutes).

The upgraded bio-oil represented 70.5% ± 1.3 of the bio-oil mass before upgrading. Notably, the bio-oil, post-upgrade, exhibited a reduced viscosity (Figure S6.1, Apêndice IV). GUO et al. (2015) discussed the significant role of catalysts in enhancing bio-oil properties. These enhancements include an increased atomic H/C ratio and the removal of heteroatoms, which contribute to a reduction in viscosity. Total gas production during the upgrading process constituted 4.5%, with its composition including 30.9% CH_4, 30.8% CO_2, 15.9% propane (C_3H_8), and 13.6% ethane (C_2H_6). In this scenario, although CO_2 was a significant gas constituent, the majority comprises C and H elements. Therefore, it is important to continually investigate upgrading techniques to minimize the loss of C and H while increasing the removal of O, N, and S content from the bio-oil.

The upgrading process provided a subtle concentration of C content in the bio-oil (from 75.1% to 77.1%). Concerning H content, it was not altered, keeping in 10% before and after the bio-oil upgrading (Table 6.8). N levels decreased from 5.5% before upgrading to 3.7% afterward. The S content decreased from 1.1% before upgrading to 0.0% afterward. S compounds, when combusted, produce harmful SOx emissions ZHANG; CHAMPAGNE; (CHARLES) XU (2011). The reduction in S content can be credited to the HDS activities of the CoMo catalyst (KAZAKOVA et al., 2021). The O content was equal to 8.3% before the upgrading process and equal to 8.0% afterward. These results indicate the need for further investigations to ensure efficient O removal from the bio-oil. RAMIREZ; BROWN; RAINEY (2015) argued that bio-oil from HTL, when containing significant O content, influences CO emissions and particulate matter formation. Concerning the HHV, a slight increase was observed from 38.3 MJ kg^{-1} before upgrading to 38.9 MJ kg^{-1} afterward. HHV is directly influenced by O content, in which higher O values lead to lower HHV. Given this correlation, conducting further research to enhance the upgrading process for O removal could increase the HHV. Concerning atomic ratio analysis, although the H/C ratio slightly decreased from 1.60 to 1.56, the O/C ratio decreased from 0.083 to 0.079, the N/C ratio dropped from 0.06 to 0.04, and the S/C ratio fell from 0.0055 to complete removal. It is noteworthy that further studies are needed to improve the bio-oil properties. These improvements are necessary to enhance the quality and performance of bio-oil, making it a more viable and sustainable alternative to conventional fossil fuels.

Table 6.8. Ultimate analysis and higher heating value of upgraded bio-oil.

Ultimate analysis (%)					HHV (MJ kg^{-1})
C	H	N	S	O*	
77.1	10.0	3.7	0.0	8.0	38.9

Note: *Oxygen (O) content was defined by difference.

The analysis of the upgraded bio-oil (Table S6.2, Apêndice IV) revealed the presence of straight-chain hydrocarbons, including heptadecane (5.1%), pentadecane (4.7%), and hexadecane (3.6%). These compounds are generally desirable in fuels due to their stability and energy content. The presence of heptadecane (C17), pentadecane (C15), and hexadecane (C16) in the bio-oil suggests that it may have properties similar to conventional diesel. PANNUCHAROENWONG et al. (2023) stated that diesel fuels typically comprise straight-chain and branched-chain hydrocarbons, with C-chain lengths usually between C10 and C20. Octane (C8), nonane (C9), and decane (C10) are also observed in the upgraded bio-oil. They are hydrocarbons with relatively low molecular weights and are part of the alkane series. ALGUNAIBET et al. (2016) argued that their presence in any fuel or chemical mixture is important because these compounds are known for their high flammability. The flammability of these hydrocarbons requires careful consideration in terms of storage and transportation. Aromatic compounds such as toluene (2.4%) and ethylbenzene (1.8%) were also detected in the upgraded bio-oil. As stated by HE et al. (2021), aromatics are known for their ability to enhance the performance of engines. This is primarily due to their high energy content and the ability to improve the octane rating of fuels. On the other hand, aromatics, especially in higher concentrations, contribute to air pollution, as they are major precursors to forming ground-level ozone and particulate matter. Nitriles, such as hexadecanenitrile (5.1%) and octadecanenitrile (3.5%), were observed in the upgraded bio-oil.

N compounds in bio-oil, primarily derived from the degradation of proteins and amino acids during HTL, pose challenges for biofuel quality. As MATRICON et al. (2023) discussed, amino acids undergo various transformations under thermal and chemical stresses, leading to nitrogenous byproducts. These increase the N content of biofuels, subsequently elevating NOx emissions during combustion. NOx emissions are environmentally detrimental, contributing to air pollution and ground-level ozone formation. HDN, the most prominent method for nitrogen removal, involves treating bio-oil with H in the presence of catalysts, typically metals such as nickel supported on

alumina or silica (MATRICON et al., 2023). Besides HDN, other methods, such as adsorption and solvent extraction, offer supplementary or alternative means of N removal. Adsorption techniques use materials like zeolites, activated carbon, or silica gel to capture nitrogen compounds, which is particularly effective against basic nitrogen compounds that HDN might not address. Additionally, solvents such as ionic liquids can selectively dissolve N molecules, supporting the HDN process (MATRICON et al., 2023).

Despite the effectiveness of these methods, challenges still need to be addressed. Ongoing research is focused on developing more robust catalysts and energy-efficient processes. Optimizing HDN and understanding the kinetics and mechanisms of nitrogen compound formation during HTL is important to advancing sustainable biofuel technologies. This emphasizes the need for continued research and development to enhance biofuels' sustainability and environmental compatibility derived from microalgae biomass.

Notably, the microalgae strain, HTL process, catalyst, and upgrading process are important to the upgraded bio-oil characteristics. For instance, in the study conducted by MAGALHÃES et al. (2023), the authors evaluated the upgrading process of bio-oil derived from the microalgae *Chlorella sorokiniana* NIES 2273 (CS) and *Chlorella vulgaris* NIES 227 (CV) cultivated in a synthetic medium. The catalyst employed was nickel-tungsten (NiW) supported on alumina. The upgrading process was performed at 375 °C, 10 MPa, and for 5 hours. The study found that for the upgraded bio-oil from CS, HDN and HDO rates were 55% and 90%, respectively. In contrast, these rates were higher for upgraded bio-oil from CV, at 75% and 94%. The authors noted that more N and O compounds could lead to competition for the same catalytic sites. Consequently, the hydrotreated oil from CV had a lower heteroatom content, resulting in biofuel with a higher HHV. BISWAS et al. (2020) investigated the catalytic HTL of the marine algae *Sargassum tenerrimum* using solid base catalysts (calcium oxide/cerium (IV) oxide (CaO/CeO_2), aluminum oxide (Al_2O_3), and zirconium dioxide (ZrO_2)) at different temperatures (260-300°C) and catalyst amounts (5-25 wt%). The highest bio-oil yield (33%) was obtained with CaO/ZrO_2 (10 wt%) in a co-solvent system of water and ethanol at 280 °C. The bio-oil exhibited a high percentage of esters (87.8%) and an HHV of 27.9 MJ kg^{-1}. Catalytic liquefaction improved the bio-oil quality by reducing N and O content, with ultimate analysis indicating up to 58.9% carbon. These results highlight the importance of catalysts, temperature, and solvents in optimizing bio-oil production (BISWAS et al., 2020).

In summary, the upgraded bio-oil composition, including straight-chain hydrocarbons, highlights its potential as a viable biofuel source. However, the presence of N and O contents calls for continued research to optimize the upgrading process, improve the bio-oil environmental profile, and increase the HHV, making it a more efficient and sustainable alternative to conventional fuels.

Concerning CoMo catalyst recovery, it is expected that fresh commercial catalysts have high surface areas and well-defined pore structures, which are important to their catalytic activity. However, after prolonged use in bio-oil upgrading reactions, these catalysts suffer from deactivation due to the deposition of coke and metals such as S and N compounds from crude bio-oil. This deactivation is often characterized by a reduction in surface area and pore volume, as well as changes in the chemical composition of the catalyst's active sites (ABBAS; JUNG, 2024). Advanced methods, including the use of ultrasonic-assisted hydrothermal treatments and solvent extraction with p-xylene and kerosene, have shown promising results in CoMo catalyst recovery. These methods not only enhance oil removal efficiency but also preserve the catalyst's structural integrity, making them suitable for reuse (ABBAS; JUNG, 2024).

6.4.Conclusion

In conclusion, this study demonstrates the potential of integrating microalgae cultivation in wastewater with HTL and catalytic upgrading to produce bio-oil with promising fuel properties. By optimizing HTL conditions and utilizing a CoMo catalyst for upgrading, improvements were observed in the bio-oil's higher heating value and elemental composition, particularly in reducing O and S contents. The process effectively converts wet biomass into valuable bio-oil without energy-intensive drying steps. Furthermore, the byproducts, such as aqueous phase and solid residues, can be repurposed, contributing to a circular economy. However, further research is needed to address the high N content and to optimize upgrading techniques for enhanced HDO and HDN. Additionally, further research is needed to evaluate the environmental and economic feasibility of producing biofuels from microalgae through HTL and subsequent upgrading. Future studies also should evaluate the catalyst's properties and coke formation and their impacts on the catalyst's lifespan. This integrated approach emphasizes the feasibility of wastewater-grown microalgae as a sustainable feedstock for biofuel production, moving towards meeting current fuel standards and environmental goals.

Acknowledgments

The authors gratefully acknowledge the Fundação de Amparo à Pesquisa do Estado de Minas Gerais (FAPEMIG) (grant number 00068-23), Conselho Nacional de Desenvolvimento Científico e Tecnológico (CNPq) (grant number 310319/2020-0), and Fundação Coordenação de Aperfeiçoamento de Pessoal de Nível Superior (CAPES).

References

ABBAS, Z.; JUNG, S. M. A facile method of treating spent catalysts via using solvent for recovering undamaged catalyst support. **PLoS ONE**, v. 19, n. 1 January, 1 jan. 2024.

AKHTAR, J.; AMIN, N. A. S. A review on process conditions for optimum bio-oil yield in hydrothermal liquefaction of biomass. **Renewable and Sustainable Energy Reviews**, v. 15, n. 3, p. 1615–1624, abr. 2011.

ALGUNAIBET, I. M. et al. Flammability and volatility attributes of binary mixtures of some practical multi-component fuels. **Fuel**, v. 172, p. 273–283, maio 2016.

ANNAMALAI, K.; THANAPAL, S. S.; RANJAN, D. Ranking Renewable and Fossil Fuels on Global Warming Potential Using Respiratory Quotient Concept. **Journal of Combustion**, v. 2018, p. 1–16, 2018.

AOAC. **Official methods of analysis**. 11th. ed. Washington: Association of Official Analytical Chemists, 1990.

APHA. **Standard Methods for examination of water and wastewater**. Washington: American Water Work Association, Water Environmental Federation, 2012.

ASSIS, L. R. et al. Evaluation of the performance of different materials to support the attached growth of algal biomass. **Algal Research**, v. 39, 1 maio 2019.

ASTM. ASTM D7582-12 standard test methods for proximate analysis of coal and coke by macro thermogravimetric analysis. , 2012.

BISWAS, B. et al. Valorization of Sargassum tenerrimum: Value addition using hydrothermal liquefaction. **Fuel**, v. 222, p. 394–401, 15 jun. 2018.

BISWAS, B. et al. Solid base catalytic hydrothermal liquefaction of macroalgae: Effects of process parameter on product yield and characterization. **Bioresource Technology**, v. 307, 1 jul. 2020.

CALIJURI, M. L. et al. Bioproducts from microalgae biomass: Technology, sustainability, challenges and opportunities. **Chemosphere**, v. 305, p. 135508, out. 2022.

CASTRO, J. DE S. et al. Hydrothermal carbonization of microalgae biomass produced in agro-industrial effluent: Products, characterization and applications. **Science of The Total Environment**, v. 768, p. 144480, maio 2021.

CHACÓN-PARRA, A. et al. A multi-component reaction kinetics model for the hydrothermal liquefaction of carbohydrates and co-liquefaction to produce 5-ethoxymethyl furfural. **Fuel**, v. 311, 1 mar. 2022.

CHEN, W.-H. et al. A comprehensive analysis of food waste derived liquefaction bio-oil properties for industrial application. **Applied Energy**, v. 237, p. 283–291, mar. 2019.

CHOUDHARY, P. et al. A review of biochemical and thermochemical energy conversion routes of wastewater grown algal biomass. **Science of the Total Environment**, v. 726, n. 271, p. 137961, 2020.

COUTO, E. A. et al. Hydrothermal liquefaction of biomass produced from domestic sewage treatment in high-rate ponds. **Renewable Energy**, v. 118, p. 644–653, 2018.

DUBOIS, MICHEL. et al. Colorimetric Method for Determination of Sugars and Related Substances. **Analytical Chemistry**, v. 28, n. 3, p. 350–356, mar. 1956.

FAN, Y.; HORNUNG, U.; DAHMEN, N. Hydrothermal liquefaction of sewage sludge for biofuel application: A review on fundamentals, current challenges and strategies. **Biomass and Bioenergy**, v. 165, p. 106570, out. 2022.

FREIRE, L. M. S. et al. Evaluation of the oxidative stability and flow properties of quaternary mixtures of vegetable oils for biodiesel production. **Fuel**, v. 95, p. 126–130, maio 2012.

GOLLAKOTA, A. R. K.; KISHORE, N.; GU, S. A review on hydrothermal liquefaction of biomass. **Renewable and Sustainable Energy Reviews**, v. 81, p. 1378–1392, jan. 2018.

GUO, Y. et al. A review of bio-oil production from hydrothermal liquefaction of algae. **Renewable and Sustainable Energy Reviews**, v. 48, p. 776–790, ago. 2015.

HAARLEMMER, G. et al. Analysis and comparison of bio-oils obtained by hydrothermal liquefaction and fast pyrolysis of beech wood. **Fuel**, v. 174, p. 180–188, jun. 2016.

HE, Z. et al. Effects of short chain aromatics in gasoline on GDI engine combustion and emissions. **Fuel**, v. 297, p. 120725, ago. 2021.

HOEBLER, C. et al. Rapid acid hydrolysis of plant cell wall polysaccharides and simplified quantitative determination of their neutral monosaccharides by gas-liquid chromatography. **Journal of Agricultural and Food Chemistry**, v. 37, n. 2, p. 360–367, mar. 1989.

KAZAKOVA, M. A. et al. Boosting hydrodesulfurization activity of CoMo/Al2O3 catalyst via selective graphitization of alumina surface. **Microporous and Mesoporous Materials**, v. 317, p. 111008, abr. 2021.

KIRAN KUMAR, P. et al. Bio oil production from microalgae via hydrothermal liquefaction technology under subcritical water conditions. **Journal of Microbiological Methods**, v. 153, p. 108–117, 1 out. 2018.

KOMAREK, J.; FOTT, B. Das Phytoplankton im Susswasser Chlorophyceae (Grunanlagen) Ordnung: Chlorococcales: Bd 7 1. [s.l.] Schweizerbart'sche, E., 1983.

LIU, H. et al. Evolution pathway of nitrogen in hydrothermal liquefaction polygeneration of Spirulina as the typical high-protein microalgae. **Algal Research**, v. 66, p. 102759, jul. 2022.

LIU, X. et al. Hydrothermal hydrodeoxygenation of palmitic acid over Pt/C catalyst: Mechanism and kinetic modeling. **Chemical Engineering Journal**, v. 407, 1 mar. 2021.

MAGALHÃES, B. DA C. et al. Catalytic hydrotreatment of bio-oil from continuous HTL of Chlorella sorokiniana and Chlorella vulgaris microalgae for biofuel production. **Biomass and Bioenergy**, v. 173, p. 106798, jun. 2023.

MAGALHÃES, I. B. et al. Technologies for improving microalgae biomass production coupled to effluent treatment: A life cycle approach. **Algal Research**, v. 57, 1 jul. 2021.

MARTINS-VIEIRA, J. C. et al. Sugar, hydrochar and bio-oil production by sequential hydrothermal processing of corn cob. **The Journal of Supercritical Fluids**, v. 194, p. 105838, mar. 2023.

MATHIMANI, T.; MALLICK, N. A review on the hydrothermal processing of microalgal biomass to bio-oil - Knowledge gaps and recent advances. **Journal of Cleaner Production**, v. 217, p. 69–84, abr. 2019.

MATRICON, L. et al. The challenge of nitrogen compounds in hydrothermal liquefaction of algae. Journal of Supercritical FluidsElsevier B.V., , 1 maio 2023.

MEIER, T. R. W. et al. Production of biohydrogen by an anaerobic digestion process using the residual glycerol from biodiesel production as additive to cassava wastewater. **Journal of Cleaner Production**, v. 258, 10 jun. 2020.

MERCKEL, R. D.; LABUSCHAGNE, F. J. W. J.; HEYDENRYCH, M. D. Oxygen consumption as the definitive factor in predicting heat of combustion. **Applied Energy**, v. 235, p. 1041–1047, fev. 2019.

MIAO, C. et al. Hydrothermal catalytic deoxygenation of palmitic acid over nickel catalyst. **Fuel**, v. 166, p. 302–308, 15 fev. 2016.

ORSAVOVA, J. et al. Fatty Acids Composition of Vegetable Oils and Its Contribution to Dietary Energy Intake and Dependence of Cardiovascular Mortality on Dietary Intake of Fatty Acids. **International Journal of Molecular Sciences**, v. 16, n. 12, p. 12871–12890, 5 jun. 2015.

PANNUCHAROENWONG, N. et al. Improving fuel quality from plastic bag waste pyrolysis by controlling condensation temperature. **Energy Reports**, v. 9, p. 125–138, set. 2023.

PARRA, O.; GONZALEZ, M.; DELLAROSSA, V. Manual Taxonómico del Fitoplancton de Aguas Continentales. V. Chlorophyceae. n. January, 1983.

PERRY, S. W.; CHILTON, C. N. **Chemical Engineers' Handbook**. 5th. ed. New York, USA: McGraw-Hill, 1973.

POSMANIK, R. et al. Coupling hydrothermal liquefaction and anaerobic digestion for energy valorization from model biomass feedstocks. **Bioresource Technology**, v. 233, p. 134–143, 2017.

PRESTIGIACOMO, C. et al. Sewage sludge as cheap alternative to microalgae as feedstock of catalytic hydrothermal liquefaction processes. **Journal of Supercritical Fluids**, v. 143, p. 251–258, 1 jan. 2019.

PRESTIGIACOMO, C. et al. Effect of transition metals and homogeneous hydrogen producers in the hydrothermal liquefaction of sewage sludge. **Fuel Processing Technology**, v. 237, p. 107452, dez. 2022.

RAMIREZ, J.; BROWN, R.; RAINEY, T. A Review of Hydrothermal Liquefaction Bio-Crude Properties and Prospects for Upgrading to Transportation Fuels. **Energies**, v. 8, n. 7, p. 6765–6794, 1 jul. 2015.

REN, R. et al. High yield bio-oil production by hydrothermal liquefaction of a hydrocarbon-rich microalgae and biocrude upgrading. **Carbon Resources Conversion**, v. 1, n. 2, p. 153–159, 1 ago. 2018.

REN, Y. et al. Effect of water/acetic acid washing pretreatment on biomass chemical looping gasification (BCLG) using cost-effective oxygen carrier from iron-rich sludge ash. **Energy**, v. 272, 1 jun. 2023.

ROY, P. et al. Understanding the effects of feedstock blending and catalyst support on hydrotreatment of algae HTL biocrude with non-edible vegetable oil. **Energy Conversion and Management**, v. 268, 15 set. 2022.

SHAKYA, R. et al. Influence of biochemical composition during hydrothermal liquefaction of algae on product yields and fuel properties. **Bioresource Technology**, v. 243, p. 1112–1120, 2017.

SHARMA, I. et al. Zero-waste: Carbon and SiO2 composite materials from the solid residue of the hydrothermal liquefaction of anaerobic digestion digestate for Li-ion batteries. **Sustainable Materials and Technologies**, v. 31, 1 abr. 2022.

SILVA, T. A. et al. Enhancing microalgae biomass production: Exploring improved scraping frequency in a hybrid cultivation system. **Journal of Environmental Management**, v. 355, p. 120505, mar. 2024.

SINGH, U. B.; AHLUWALIA, A. S. Microalgae: a promising tool for carbon sequestration. **Mitigation and Adaptation Strategies for Global Change**, v. 18, n. 1, p. 73–95, 1 jan. 2013.

SUN, D. et al. Effects of hydrothermal pretreatment on the dissolution and structural evolution of hemicelluloses and lignin: A review. Carbohydrate PolymersElsevier Ltd, , 1 abr. 2022.

SWETHA, A. et al. Review on hydrothermal liquefaction aqueous phase as a valuable resource for biofuels, bio-hydrogen and valuable bio-chemicals recovery. **Chemosphere**, v. 283, p. 131248, nov. 2021.

THIELEMANN, A. K.; SMETANA, S.; PLEISSNER, D. Cultivation of the heterotrophic microalga Galdieria sulphuraria on food waste: A Life Cycle Assessment. **Bioresource Technology**, v. 340, p. 125637, nov. 2021.

USMAN, M. et al. From biomass to biocrude: Innovations in hydrothermal liquefaction and upgrading. **Energy Conversion and Management**, v. 302, p. 118093, fev. 2024.

UTERMÖHL, H. Zur vervollkommnung der quantitativen phytoplankton-methodik. **Mitteilung Internationale Vereinigung fuer Theoretische unde Amgewandte Limnologie**, v. 9, p. 1–38, 1958.

WANG, Z. et al. Enhancing energy recovery via two stage co-fermentation of hydrothermal liquefaction aqueous phase and crude glycerol. **Energy Conversion and Management**, v. 231, 1 mar. 2021.

WEI, Y. et al. Hydrothermal liquefaction of municipal sludge and its products applications. Science of the Total EnvironmentElsevier B.V., , 15 jan. 2024.

XU, D. et al. Biocrude Upgrading in Different Solvents after Microalgae Hydrothermal Liquefaction. **Industrial and Engineering Chemistry Research**, v. 60, n. 21, p. 7966–7974, 2 jun. 2021.

YU, J. et al. Recent advances in the production processes of hydrothermal liquefaction biocrude and aid-in investigation techniques. **Renewable Energy**, v. 218, p. 119348, dez. 2023.

ZHANG, L.; CHAMPAGNE, P.; (CHARLES) XU, C. Supercritical water gasification of an aqueous by-product from biomass hydrothermal liquefaction with novel Ru modified Ni catalysts. **Bioresource Technology**, v. 102, n. 17, p. 8279–8287, set. 2011.

ZHONG, W. et al. Biogas productivity by co-digesting Taihu blue algae with corn straw as an external carbon source. **Bioresource Technology**, v. 114, p. 281–286, jun. 2012.

7. Capítulo IV. Bio-oil from Hydrothermal Liquefaction of Microalgae Cultivated in Wastewater: An Economic and Life Cycle Approach

Abstract: Although microalgae are a promising sustainable biofuel feedstock, their energy-intensive production and most environmental assessments rarely achieve the desired trade-off between productivity and sustainability. In this context, this study aims to evaluate the economic and environmental feasibility of producing bio-oil via hydrothermal liquefaction (HTL) of wastewater-grown microalgae at an industrial scale. Four scenarios varied production scale and steam source: sugarcane bagasse (SCB) in SC1 and SC3, liquefied petroleum gas (LPG) in SC2 and SC4. Each scenario processed microalgae at 300 °C for 30 minutes. Smaller-scale feedstock (1,332.9 kg/h) in SC1 and SC2 produced 34.6 kg/h of bio-oil, while the larger feedstock (85,554.4 kg/h) in SC3 and SC4 yielded 2,222.2 kg/h. Microalgae biomass cultivation costs dominated overall expenses (56-75%). Economic analyses indicated minimum selling prices of 3.82-8.52 USD/kg, exceeding the average literature figure of 1.57 USD/kg. Life Cycle Assessment (LCA) showed SCB reduced fossil resource depletion by 14.97% compared to LPG but increased emissions of nitrogen oxides, particulates, and toxic compounds, which are manageable via selective catalytic reduction and flue gas desulfurization. Cyclohexane as a solvent elevated human carcinogenic toxicity, greener alternatives could reduce toxicity but may cost more, requiring further cost analysis. Advancing this biorefinery route requires optimization of cultivation and processing costs, adoption of environmentally benign solvents, and implementation of emission control strategies to enable economically feasible and environmentally sustainable bio-oil production.

Keywords: Energy efficiency; Biorefinery; Process simulation; Biomass conversion; Feasibility analysis.

7.1. Introduction

The escalating global demand for sustainable energy and the urgent need to mitigate climate change have intensified research into renewable alternatives to fossil fuels (IEA, 2023). Projections indicate that by 2050, the world's energy demand will increase by 50%, highlighting the necessity to develop clean and efficient energy sources (EIA, 2023). Among various renewable options,

microalgae have emerged as a promising feedstock for biofuel production due to their rapid growth rates and high biomass yield, up to 30 times greater per area than traditional terrestrial crops (PARRAY; SINGH; HAGHI, 2024).

In addition to their productivity, microalgae contribute to climate change mitigation by capturing atmospheric carbon dioxide (CO_2) at an estimated rate of about 1.8 kg of CO_2 per kilogram of dry biomass produced (CHEAH et al., 2015). Moreover, cultivating microalgae in wastewater presents an integrated approach that combines effluent treatment with the production of energy-rich biomass (CALIJURI et al., 2022). Studies have demonstrated that microalgal cultivation can remove up to 80-100% of nutrients such as nitrogen (N) and phosphorus (P) from wastewater, thereby addressing environmental pollution while generating valuable biomass (DELGADILLO-MIRQUEZ et al., 2016). This dual functionality supports both environmental remediation and resource recovery, reinforcing the role of microalgae within circular economy frameworks.

Hydrothermal liquefaction (HTL) has been identified as a promising technology for efficiently converting wet microalgal biomass into bio-oil. Operating at temperatures between 280 °C and 374 °C and pressures ranging from 4 to 22 MPa, HTL utilizes the inherent water content of the biomass as the reaction medium, eliminating the need for energy-intensive pre-drying steps (SILVA et al., 2024b). This strategy can reduce the total energy consumption of the process, which is advantageous given that drying microalgal biomass typically accounts for over 80% of production costs (ALJABRI et al., 2023). Moreover, drying often leads to substantial degradation of biomass quality by adversely affecting essential metabolites such as lipids, proteins, and chlorophyll. Conventional drying methods exacerbate these problems further through pigment degradation, increased risk of contamination, and the loss of valuable polyunsaturated fatty acids (PUFAs) (ALJABRI et al., 2023). Thus, processing wet biomass via technologies like HTL is considerably more favorable for biofuel production.

To evaluate the industrial feasibility of HTL, process simulation tools like Aspen Plus are commonly used. For example, through process simulation, ONG et al. (2019) demonstrated that integrating heat recovery into the HTL process can reduce energy consumption by up to 50%. Accurate simulation requires the appropriate selection of thermodynamic models; the Soave–Redlich–Kwong (SRK) equation of state is considered suitable for systems involving water at high

temperatures and pressures, ensuring reliable predictions of phase behavior (CASCIOLI; BARATIERI, 2021).

A key challenge in HTL scale-up is the provision of thermal energy. Among potential sources, sugarcane bagasse (SCB) stands out as a sustainable and abundant agricultural residue. Approximately 700 million tons of SCB are produced annually, representing a significant renewable energy resource (UNGUREANU; VLĂDUȚ; BIRIȘ, 2022). In Brazil, the 2021-2022 harvest generated approximately 170 million tons of SCB, widely utilized in cogeneration systems at sugar and ethanol mills. In 2019, 220 mills exported 22.5 TWh to the national grid, with bagasse contributing 6.4% of the country's installed electrical capacity (FIORANELLI; BIZZO, 2023). SCB also offers operational advantages over residues like rice husk and wheat straw, due to its lower chlorine and potassium content, which reduces the risks of corrosion and fouling in thermal systems (FIORANELLI; BIZZO, 2023). Therefore, comparing energy sources such as SCB and liquefied petroleum gas (LPG), whose global demand reached 342 million tons in 2023, is essential to identify the most sustainable and economically viable option for supplying the thermal energy required in HTL processes (WORLD LIQUID GAS ASSOCIATION, 2023).

From an environmental standpoint, Life Cycle Assessment (LCA) is a critical tool for evaluating the sustainability of HTL-based biofuel production. Studies indicate that HTL bio-oil has a lower global warming potential (GWP) compared to fossil fuels (RANJBAR; MALCATA, 2023). Nonetheless, potential trade-offs in categories such as eutrophication, toxicity, and resource depletion require careful analysis, particularly due to the energy intensity and solvent use in HTL processes (CALIJURI et al., 2023; MARANGON et al., 2022). Energy sourcing is especially impactful; the use of fossil-derived LPG can significantly increase environmental burdens, whereas biomass-based energy sources like SCB align better with circular economy and sustainability goals (FIORANELLI; BIZZO, 2023). For instance, replacing LPG with biomass in the wood panel industry notably reduced fossil fuel dependency (DE CARVALHO ARAÚJO et al., 2022). However, the life cycle implications of using SCB to supply heat in HTL systems for microalgae remain underexplored.

Economic analysis is equally critical in determining the viability of microalgae-based biofuel production. The process is highly sensitive to the cost of biomass cultivation, which can be approximately 3.6 €/kg when microalgae are cultivated in high-rate algal ponds (HRAPs) using wastewater as the cultivation medium (ACIÉN FERNÁNDEZ; FERNÁNDEZ SEVILLA;

MOLINA GRIMA, 2019). Strategies to reduce these costs include increasing biomass productivity, optimizing harvesting and dewatering processes, and valorizing co-products generated during biofuel production (MAGALHÃES et al., 2024).

Despite increasing interest in algae-based biofuels, research gaps persist regarding the integrated assessment of HTL systems using wastewater-grown biomass and alternative heat sources. Previous studies have examined HTL performance and bio-oil yields, but few have evaluated the broader implications of coupling HTL with pre-existing infrastructure, such as wastewater treatment plants, and steam sources like SCB. This study addresses these gaps by assessing different production scenarios to evaluate the technical, economic, and environmental feasibility of bio-oil production from microalgae, while advancing strategies for sustainable resource recovery.

7.2.Material and methods

7.2.1. Experimental Design

Experimental data were obtained from HTL experiments on microalgae cultivated in wastewater (SILVA et al., 2024b). The treatment at 300 °C for 30 minutes yielded bio-oil with a higher heating value (HHV) of 38.34 MJ kg^{-1}. Palmitic and linoleic acids were the main components, with palmitic acid ranging from 6.9% to 14.2% and linoleic acid reaching 15.4%. These results were used to inform and validate the simulation, ensuring that the modeled process conditions and outputs align with experimental observations.

7.2.2. Hydrothermal liquefaction process simulation

Bio-oil production was simulated using the Aspen Plus chemical process simulator version 14.1. The proposed process was divided into three parts: the first stage standardized the effluent generated after the cultivation step to maintain a 1:10 ratio of microalgae to water; the second stage represents the HTL process; and the third involves separating the products obtained. Cyclohexane was used as an extracting solvent to separate the bio-oil from the aqueous phase. Although alternative solvents could be used, cyclohexane was selected based on the technical evaluation by SILVA et al. (2024b). Additionally, the following assumptions were made: (i) The process occurs under steady-state conditions, (ii) The SRK and STEAMNBS models were chosen as the equations of state that best fit for calculating the thermodynamic properties of the HTL process and were

applied to all equipment modules used in the simulation (BORAZJANI; AZIN; OSFOURI, 2024; MOSER; PENKE; BATTEIGER, 2021), (iii) To represent the mixture of conventional and non-conventional components, the flow stream classification was set as 'MIXNC', (iv) The effluent obtained after cultivation, used as feedstock for the proposed processes, was considered a mixture of water (93%) and dry biomass (7%) (ASSIS et al., 2020; SILVA et al., 2024a), (v) For non-conventional components such as microalgae, solids, and residual compounds, the HCOALGEN and DCOALIGT models were selected in Aspen Plus to calculate their enthalpies and densities based on PROXANAL and ULTANAL analyses, (vi) The biomass cultivation step was not simulated, but the cost related to cultivation was estimated from the value presented by MASOUMI; DALAI, (2021), adjusted for inflation, (vii) The yield reactor (RYield) was used for the HTL stage, based on the experimental data by SILVA et al., (2024b) (Table S7.1, Apêndice V).

The simulation of bio-oil production as a biorefinery integrated with a pre-existing industry was evaluated in four scenarios based on the feasibility of biomass cultivation and steam generation using SCB (SC1 and SC3) and LPG (SC2 and SC4) as steam sources. Steam boiler efficiencies were assumed to be 0.77 when fed with SCB and 0.92 with LPG (AGUILAR VIZCARRA; ESENARRO; RODRIGUEZ, 2021; CHANTASIRIWAN, 2021; HASAN, 2024; SAIDUR et al., 2011).

In SC1 and SC2 scenarios, wastewater treatment in HRAPs with biomass conversion into bioproducts was considered. The calculation was based on a full-scale wastewater treatment plant that serves a small community of about one thousand inhabitants and a fruit-based juice production industry (SILVA et al., 2024a, 2024b) with an average effluent flow rate of 1.73 m^3/h (Figure 7.1). In SC1, SCB was selected as the boiler fuel source to meet the steam demand of the biorefinery. This scenario represents a common condition of pre-existing industries with solid residues allowing steam generation in boilers. In SC2, the effluent flow rate used in SC1 was maintained; however, the main difference was the use of LPG as the fuel source to meet the steam demand of the biorefinery, representing pre-existing industries that do not have solid residues for steam generation in boilers.

In scenarios SC3 and SC4 a biomass flow rate of 111.11 m^3/h was considered (BORAZJANI; AZIN; OSFOURI, 2024; MASOUMI; DALAI, 2021; WU; HUANG; TSAI, 2023). Rather than relying exclusively on in-plant production or wastewater-based cultivation, microalgae

biomass in scenarios SC3 and SC4 was assumed to be acquired externally from suppliers to meet the high biomass demand consistent with literature values (BORAZJANI; AZIN; OSFOURI, 2024; MASOUMI; DALAI, 2021; WU; HUANG; TSAI, 2023). For calculation purposes, biomass requirements were expressed on a dry weight basis (7,777.66 kg dry biomass/h), although the actual HTL process utilized wet biomass with a moisture content of approximately 93%. The steam needed for the boilers in SC3 and SC4 was generated using SCB and LPG as fuel sources, respectively.

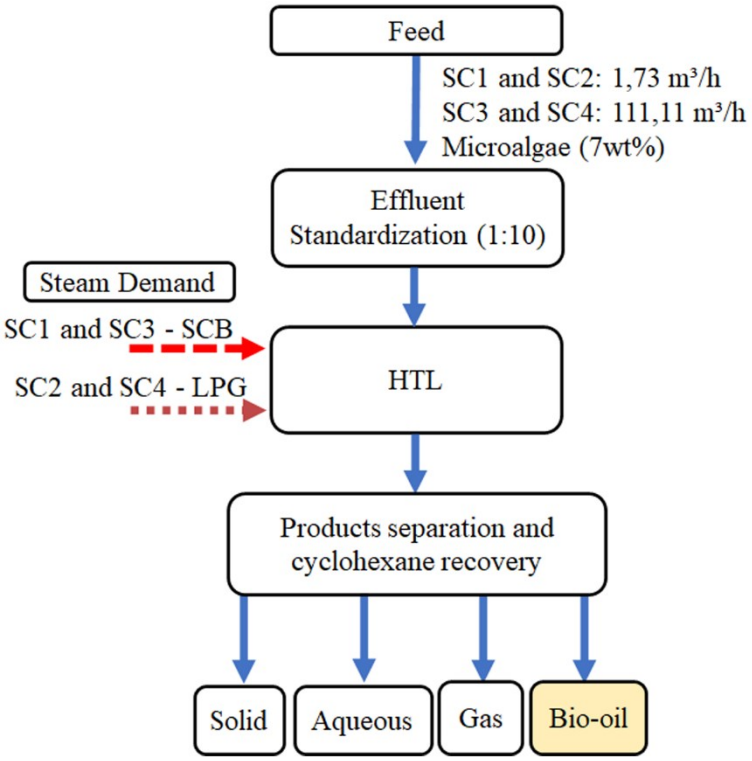

Figure 7.1. Systematic diagram for the conversion of microalgae to bio-oil and co-products.

In scenarios SC1 and SC2, microalgae cultivation was integrated with wastewater treatment, eliminating the need for additional water and sources of N and P required in conventional cultivation. Consequently, the consumption of these resources was accounted as avoided products in the background system. In these scenarios, the infrastructure required for microalgae cultivation was excluded from the scope assuming that it would already be necessary for wastewater treatment.

7.2.3. Economic analysis

For the economic analysis, it was considered a plant operating 24 hours per day, divided into three 8-hour shifts, for 330 days per year, reserving 35 days for maintenance tasks (CHEN; QUINN, 2021; JONES et al., 2014). The plant's useful life was defined as 20 years, with a construction and installation period of 3 years. The equipment acquisition cost was obtained using the Aspen Process Economic Analyzer package. Subsequently, using the economic feasibility spreadsheet formulated by PETERS; TIMMERHAUS; WEST (2003), the selling price of the bio-oil was estimated, achieving a payback period of 3.6 years. The minimum fuel selling price (MFSP) was calculated based on capital investment and processing costs, ensuring zero net present value (NPV). The MFSP was converted from USD/kg to USD/gasoline gallon equivalent (GGE) as presented in Equation 7.1.

$$MFSP\ \left(\frac{USD}{GGE}\right) = \left(\frac{\frac{121\ MJ}{GGE}}{HHV\ \left(\frac{MJ}{kg}\right)}\right)\ x\ MFSP\ \left(\frac{USD}{kg}\right) \qquad \text{(Equation 7.1)}$$

Where,

MFSP (USD/GGE): Minimum Fuel Selling Price in USD per Gasoline Gallon Equivalent (GGE).

121 MJ/GGE: Amount of energy contained in a GGE (SINGH; KUMAR; RAI, 2014).

HHV (MJ/kg): Higher Heating Value of the bio-oil.

MFSP (USD/kg): Minimum Fuel Selling Price in USD per kg.

The fixed capital investment (FCI) was estimated using a Lang factor 4.3, and the working capital cost was calculated as 12% of FCI. Microalgae biomass was assumed to be produced on-site in scenarios SC1 and SC2, while in SC3 and SC4, it was assumed as purchased for 640 USD/ton (ACIÉN FERNÁNDEZ; FERNÁNDEZ SEVILLA; MOLINA GRIMA, 2019). Although the hourly wage rate typically varies based on time and location, an annual salary of 24,000 USD per employee was considered. Economic parameters are summarized in Table 7.1 (Table S7.2, Apêndice V presents the complete economic assessment parameters across all scenarios).

Table 7.1. Summary of cost parameters for the economic analysis of the microalgae biomass to bio-oil conversion process.

Parameter	20 years	References
Internal rate of return	10%	MASOUMI; DALAI, (2021)
Operating hours per year	7920	MASOUMI; DALAI, (2021)
Lang factor	4.3 for fixed capital investment (FCI)	MASOUMI; DALAI, (2021)
Working capital cost	12% of FCI	MASOUMI; DALAI, (2021)
Operating labor	24,000 USD/year per employee	MASOUMI; DALAI, (2021)
Supervisory and clerical labor	15% of labor cost	MASOUMI; DALAI, (2021)
Maintenance and repairs	6% of FCI	MASOUMI; DALAI (2021)
Operating supplies	15% of maintenance and repairs	MASOUMI; DALAI (2021)
Local taxes	1% of FCI	MASOUMI; DALAI (2021)
Insurance	1% of FCI	MASOUMI; DALAI (2021)
Overhead	60% of (operating labor, supervision, and maintenance)	MASOUMI; DALAI (2021)
Capital charge	12% of FCI	MASOUMI; DALAI (2021)
Depreciation	10% of FCI	MASOUMI; DALAI (2021)
Administrative cost	25% of overhead	MASOUMI; DALAI (2021)
Distribution and selling costs	5% of total expenses	PETERS; TIMMERHAUS; WEST (2003)
Research and development	4% of total expenses	PETERS; TIMMERHAUS; WEST (2003)
Income tax rate	21%	PETERS; TIMMERHAUS; WEST (2003)
Feedstock		PETERS; TIMMERHAUS; WEST (2003)

Parameter	20 years	References
Microalgae biomass	650 USD/ton	ACIÉN FERNÁNDEZ; FERNÁNDEZ SEVILLA; MOLINA GRIMA (2019)
Sugarcane bagasse (SCB)	29.96 USD/ton	BROBBEY; LOUW; GÖRGENS (2023)
Liquified petroleum gas (LPG)	750 USD/ton	GLOBAL PETROL PRICES (2024)
Cyclohexane	1.10 USD/kg	CHEMANALYST (2024)
Utilities		
Electricity	0.084 USD/kWh	LIU et al., (2025); QI et al., (2023)

7.2.4. Sensitivity analysis

A sensitivity analysis was conducted to assess the influence of each process and operational parameters on the MFSP. The analysis was performed by varying each parameter by ±25% while keeping the others constant. The parameters evaluated in this study included the processing capacity of the proposed process, bio-oil yield in the HTL reactor, biomass cost, SCB and LPG costs, equipment acquisition cost, utilities, and interest rate.

7.2.5. Life Cycle Assessment (LCA)

The LCA was conducted based on international standards developed by the International Organization for Standardization (ISO), specifically "Environmental Management – Life Cycle Assessment," ISO 14040 – Principles and Framework, and ISO 14044 – Requirements and Guidelines (ISO, 2006a, 2006b). Therefore, the study followed the four steps outlined in these standards: (i) definition of goal and scope; (ii) life cycle inventory analysis; (iii) life cycle impact assessment; and (iv) interpretation.

The LCA goal was to quantify and compare the environmental impacts of valorizing microalgae biomass through HTL for bio-oil production, considering the four scenarios presented in Section 2.2 (SC1, SC2, SC3, and SC4). Two distinct functional units (FUs) were adopted to reflect different system scales: 1.73 m^3 of microalgae biomass per hour for the small-scale scenarios (SC1 and SC2) and 111.11 m^3 per hour for the large-scale scenarios (SC3 and SC4). Within each scale, comparisons were made between different steam sources, sugarcane bagasse (SC1 and SC3) and liquefied petroleum gas (SC2 and SC4), while maintaining the same FU.

Therefore, comparisons were conducted between SC1 vs. SC2 and SC3 vs. SC4, ensuring consistency in the basis of analysis. No cross-scale comparisons were performed.

Primary data on biomass productivity (ASSIS et al., 2020; SILVA et al., 2024a), HTL parameters, bio-oil yield, and avoided products (water, N, and P) (SILVA et al., 2024b) were used to develop the life cycle inventory of the primary processes. Data on the energy consumption of the HRAP was obtained from HERRERA et al. (2021). Additionally, the energy consumption of other equipment (electricity and steam) was estimated based on simulations performed using the Aspen Plus software (described in Section 2.2). This way, the primary processes were defined, while the secondary processes (production of chemicals, electricity, and steam) were obtained from the Ecoinvent v0.30.8 database (Table S7.3, Apêndice V).

The four scenarios were simulated using the SimaPro® software (PRé Sustainability BV, Netherlands, version 9.6.0.1) to evaluate the environmental impacts. The ReCiPe 2016 method (v. 1.09) used the hierarchical perspective. The following impact categories were considered: GWP; Photochemical Ozone Formation Potential, Human Health (POFP-hh); Particulate Matter Formation Potential (PMFP); Photochemical Ozone Formation Potential, Ecosystems (POFP-eco); Terrestrial Acidification Potential (TAP); Freshwater Eutrophication Potential (FEP); Marine Eutrophication Potential (MEP); Terrestrial Ecotoxicity Potential (TETP); Marine Ecotoxicity Potential (METP); Human Toxicity Potential, Cancer Effects (HTP-c); Fossil Resource Scarcity Potential (FRSP); and Water Consumption (WC).

Other studies reported in the literature on topics related to microalgae biomass valorization (CASTRO et al., 2023; MAGALHÃES et al., 2022; MARANGON et al., 2021; SILVA et al., 2022).

Normalized results were presented, along with contribution analyses by stages and processes. The normalized results allowed for identifying impacts with relatively high or low values compared to the average global emissions per person in 2010 (HUIJBREGTS et al., 2017). Through the contribution analysis, significant processes influencing the results were identified. Potential improvements for the environmental performance of the scenarios were also suggested and discussed.

7.3.Results and discussion

7.3.1. Process Flow Diagram (PFD)

Three stages were considered to model and simulate the bio-oil production process from microalgae biomass: (i) standardization of the raw material to a 1:10 microalgae-to-water ratio, (ii) biomass conversion via HTL, and (iii) separation of the obtained products with cyclohexane recovery. Additionally, energy recovery was also considered.

Initially, the effluent obtained after biomass cultivation (FEED) undergoes water removal using a belt filter (FILTER) until a solid-to-liquid ratio of 1:10 is achieved (BOROWITZKA, 2018) (Figure 7.2). Filtration is a more energy-efficient alternative compared to drying (MARANGON et al., 2021).

Subsequently, the standardized feedstock (stream S1) was pressurized using a pump (PUMP) and heated via two heaters (HEAT-1 and HEAT-2) to reach the required reaction conditions of 20 bar and 300 °C before being directed to the HTL stage. This process yielded bio-oil, residual solids, and gas, as described by SILVA et al. (2024b). After the HTL reaction, the output stream (S5) was utilized to preheat the input stream (S2) in HEAT-1, thereby reducing the energy demand in HEAT-2.

The resulting products (stream S6) were then separated using SEP1, SEP2, SEP3, and SEP4. In SEP1, the gaseous fraction (GAS) was separated. In SEP2, the aqueous phase was removed from the bio-oil by adding cyclohexane (2 L/kg of dry biomass) (SILVA et al., 2024b). In SEP3, the solids were separated. Finally, in SEP4, the bio-oil was obtained, and the solvent was recovered at 93.4% (DENG et al., 2018; LYU et al., 2014). Given the complexity of the products generated by HTL technology and the limited studies in the literature on separating these products, SEP-type separators available in the Aspen Plus software are typically used (BORAZJANI; AZIN; OSFOURI, 2024; MAQBOOL; BILLER; ANASTASAKIS, 2024).

Based on the feedstock input to the HTL reactor (stream S4), 1,332.9 kg/h for scenarios SC1 and SC2, and 85,554.4 kg/h for scenarios SC3 and SC4, it was possible to obtain 34.6 kg/h and 2,222.2 kg/h of bio-oil (BIOOIL), 17.3 kg/h and 1,111.1 kg/h of gaseous phase (GAS), and 29.4 kg/h and 1,851.8 kg/h of solid phase (SOLID), respectively. The complete mass and energy balance results for all process streams are provided in the Supplementary Material (Tables S4 and S5 for scenarios SC1/SC2 and SC3/SC4, respectively). Additionally, Table S7.6, Apêndice V summarizes the key operating parameters of each unit operation, further enhancing transparency and reproducibility of the simulation.

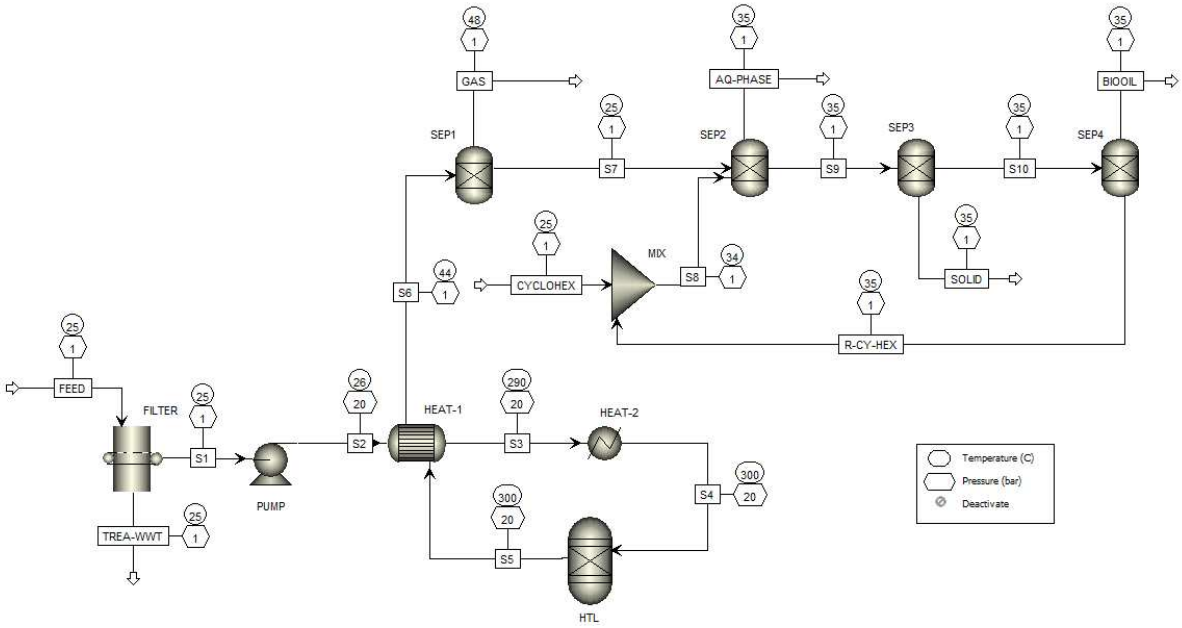

Figure 7.2. Process Flow Diagram (PFD) of bio-oil production process from microalgae biomass.

The SRK thermodynamic model was used for simulation. This equation of state has been widely cited in the literature for HTL technology, both for the conversion of microalgae biomass and other types of feedstocks (BORAZJANI; AZIN; OSFOURI, 2024; MAQBOOL; BILLER; ANASTASAKIS, 2024; QIAN et al., 2021). Furthermore, MAQBOOL; BILLER; ANASTASAKIS (2024) stated that heat recovery is important for scaling up hydrothermal systems to reduce utility costs. The authors compared the impact of several models on property estimation and found that the SRK thermodynamic package best-estimated heat recovery at 350 °C. Figure 7.3 illustrates the Sankey diagram for the conversion process of biomass to bio-oil, showing the mass flow data of wet material for each stream and their respective percentages (in parentheses).

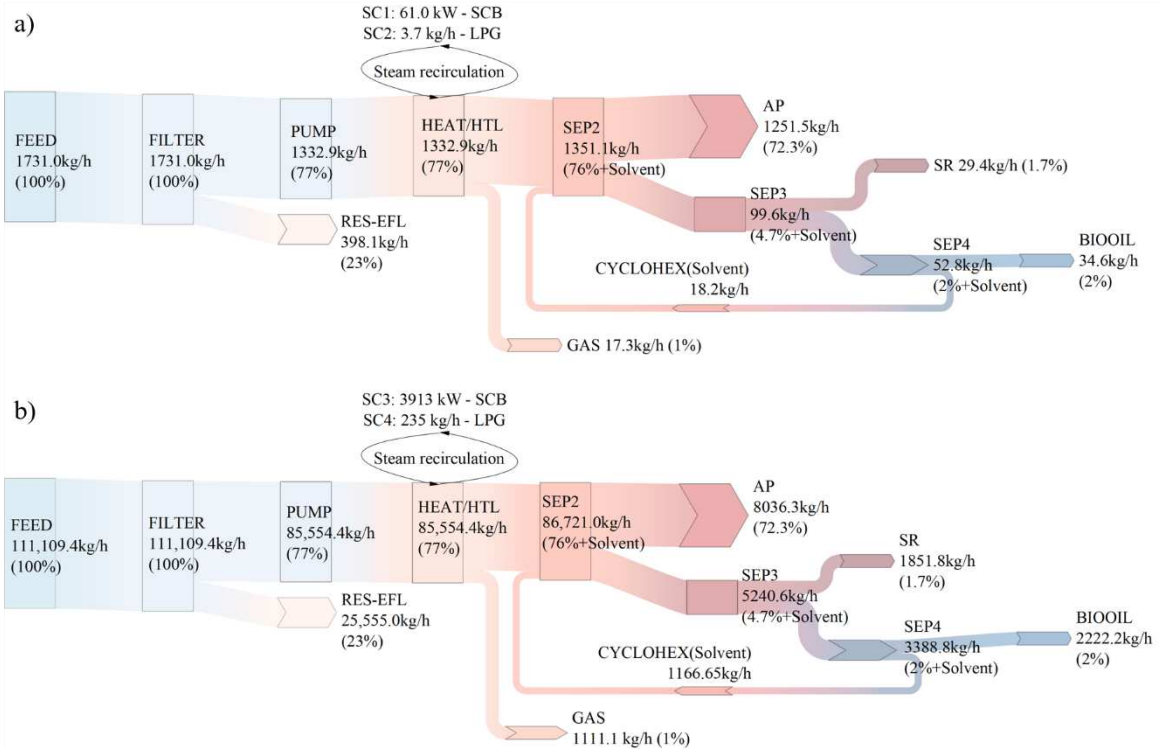

Figure 7.3. Mass flow in the HTL process of microalgae biomass for bio-oil production. a) SC1 and SC2 and b) SC3 and SC4.

FEED represents the biomass used in the simulation, containing approximately 93% moisture. FILTER denotes the standardization step where the dry biomass to water ratio is adjusted to 1:10. The excess treated wastewater obtained in the standardization step, RES-EFL, was considered appropriately discarded.

During the heating and HTL stages, it is assumed that there is no change in the overall mass flow of the stream. After HTL, the separation stage employs equipment SEP1, SEP2, SEP3, and SEP4 to isolate four distinct phases: gaseous (SEP1), aqueous (SEP2) with cyclohexane addition, solid (SEP3), and bio-oil (SEP4) with cyclohexane recovery. These outputs are represented by the streams GAS, AP, SR, and BIOOIL, respectively. Because the thermal load is already recovered in HEAT-1, the gas stream is not utilized for combined heat and power production in that unit. The energy required by each piece of equipment throughout the proposed process is depicted in Figure 7.4.

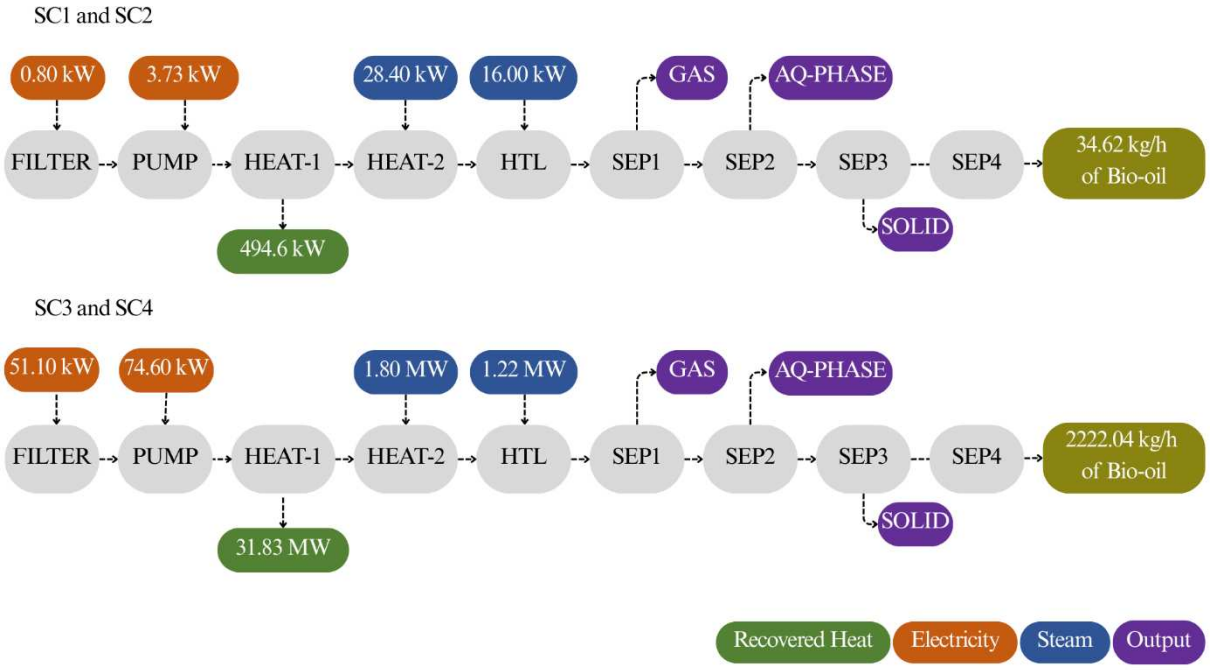

Figure 7.4. Energy power required by each equipment in different scenarios.

In the simulation of the HTL process, the difference between the scenarios regarding the energy power required lies in the input flow rate of feedstock, which directly affects utility expenses. An increase in the input flow rate from SC1 and SC2 to SC3 and SC4 resulted in an approximately 64-fold increase in energy consumption.

7.3.2. Economic analysis

The selling cost of the bio-oil and data related to the initial investment and processing costs were estimated from the simulation of the proposed scenarios. Estimated equipment acquisition costs for each scenario are presented in Table S7, Apêndice V.

As expected, the estimated acquisition cost for SC1 and SC2 is lower than that for SC3 and SC4 because the input flow rate for SC3 and SC4 is 64 times greater than that used in SC1 and SC2. This variation in input flow resulted in an equipment acquisition cost approximately 6.2 times higher in SC3 and SC4.

The total capital investment for the biomass-to-bio-oil conversion process via HTL was 1.26 million USD for SC1 and SC2, while for SC3 and SC4, it was 8.59 million USD. These values are lower than those presented by BORAZJANI; AZIN; OSFOURI (2024) at 13.53 million USD

for producing bio-oil from microalgae, lower than those presented by JIANG et al. (2019) at 56.5 million USD for producing bio-oil from *Tetradesmus* sp., and higher than the HTL of SCB at 3.68 million USD reported by RAMIREZ; BROWN; RAINEY (2018). Figure 7.5 presents the distribution of annual processing costs to evaluate each stage's contribution to the total cost.

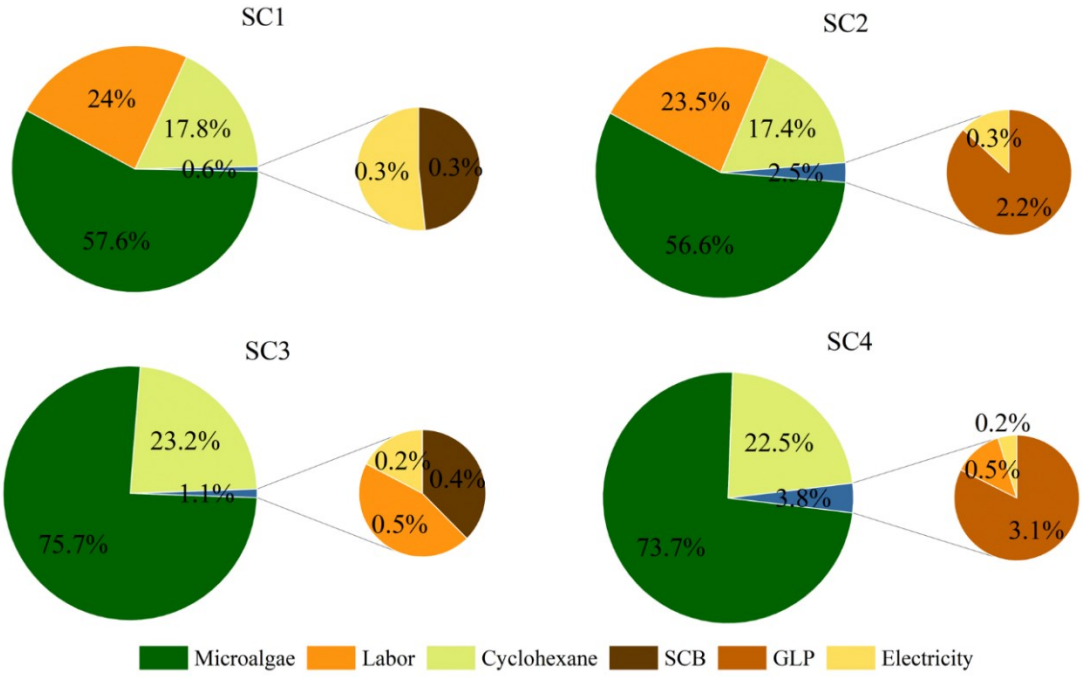

Figure 7.5. Annual distribution of processing costs for the four evaluated scenarios (in million USD/year).

From the results shown in Figure 7.5, the predominant factor in processing costs is related to biomass cultivation, representing 56.5% and 57.6% for SC1 and SC2 and 75.7% and 73.7% for SC3 and SC4, respectively. Another significant element in processing costs is the expense associated with cyclohexane. In all evaluated scenarios, the annual electricity, SCB, and LPG costs contributed less than 4% of the total costs. Labor costs exhibit a strong dependence on production capacity: in lower-capacity processes (SC1 and SC2), they represent 23.5–24.0% of annual costs, whereas in higher-capacity processes (SC3 and SC4), they drop to 0.5%. This reduction is linked to the assumption that, once equipment and systems are scaled up, they can operate without requiring additional supervision, enabling the same workforce to manage increased throughput without the need for extra personnel or extended shifts.

The economic analysis considered two different prices for the bio-oil. The first price, 1.57 USD/kg, represents the average price in the literature (CHEN; QUINN, 2021; JONES et al., 2014; MASOUMI; DALAI, 2021). The second price was calculated to achieve a payback period of 3.6 years (PETERS; TIMMERHAUS; WEST, 2003), reflecting an economic viability target. These prices were used to estimate the income from bio-oil production and determine the overall profitability.

Using the average price of 1.57 USD/kg, all scenarios showed a net return less than zero; that is, the total income of the project is insufficient to cover the total costs. This may have occurred due to the low selling price of bio-oil. The selling price of 1.57 USD/kg described by CHEN; QUINN (2021), JONES et al. (2014), and MASOUMI; DALAI (2021) was obtained with an input feed containing a humidity microalgae biomass content of 80%, which is 2.86 times higher than that used in this work. Achieving a 20% solids content requires additional steps to concentrate the biomass after harvesting, which were not considered in our study. Additionally, in that work, the authors did not account for using solvents to separate the aqueous phase from the bio-oil.

For a payback period of 3.6 years, the selling price of the bio-oil was estimated for SC1, SC2, SC3, and SC4, resulting in values of 8.42 USD/kg (26.95 USD/GGE), 8.52 USD/kg (27.27 USD/GGE), 3.82 USD/kg (12.23 USD/GGE), and 3.93 USD/kg (12.56 USD/GGE), respectively. This analysis concluded that the greater the processing capacity of the process, the lower the selling price of the bio-oil, due to economies of scale. These values are mainly influenced by the costs of algal biomass production/acquisition, representing the largest annual expense in both cases, contributing 56% and 86%, respectively, as illustrated in Figure 7.6. These prices are a benchmark for future cost-reduction efforts, especially compared with other algae-derived biofuel produced via HTL studies.

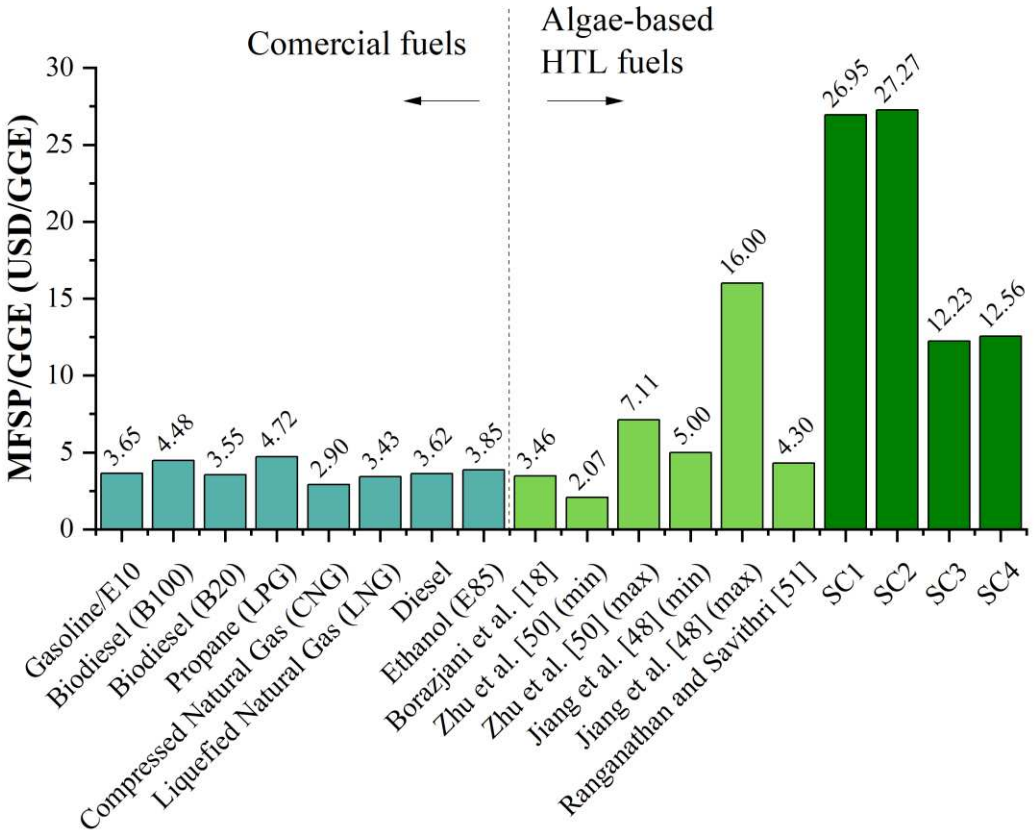

Figure 7.6. Comparison of minimum selling prices for commercial fuels, literature, and the present study, presented as Gasoline Gallon Equivalent (GGE).

The work by BORAZJANI; AZIN; OSFOURI (2024) on HTL with *Aurantiochytrium* sp. reported MFSP values between 2.11 USD and 7.52 USD/GGE, mainly influenced by the cost of biomass. This study focused solely on the HTL process, excluding algae biomass cultivation and the use of solvents for bio-oil separation. The economic results showed that an MFSP of 3.47 USD/GGE could be achieved with a biomass feedstock cost of 50 USD/ton. The sensitivity analysis indicated that an increase of 50 USD/ton in biomass cost could raise the MFSP by 1.35 USD/GGE and generate an increase of 10.3 million USD/year in the total production cost.

JIANG et al. (2019) evaluated the MFSP, disregarding the stages of harvesting, dewatering, and using organic solvents to separate the bio-oil from the aqueous phase. As a result, the MFSP varies between 5 USD and 16 USD/GGE, with an uncertainty margin of ±12%, as algae cost between 400 USD and 1,800 USD/ton (dry basis).

In a study by ZHU et al. (2013), the conversion of microalgae with lipid-extracted algae (LEA) to liquid fuels via HTL and upgrading processes were examined, estimating an MFSP range of 2.07 USD to 7.11 USD/GGE, depending on process parameters. The main factors impacting production costs included the cost of LEA, final product yield, and upgrading equipment. Notably, by excluding feedstock costs, the MFSP was reduced to 0.68 USD/liter (2.56 USD/gallon), reflecting the additional costs of converting LEA to liquid fuel.

As in the present study, the results by ZHU et al. (2013) support focusing on strategies to increase algal biomass productivity and bio-oil yield, such as catalytic processes. The study by RANGANATHAN; SAVITHRI (2019) on wastewater-derived microalgae-based fuels via HTL and hydrotreating reported an MFSP of 4.3 USD/GGE. The study emphasizes that the MFSP of renewable fuels is highly sensitive to biofuel yield via HTL, suggesting improvements in biomass composition, catalyst selection, and heat recycling efficiency as cost-reduction strategies. Although the current MFSP values exceed those of existing commercial fuels, the comparison with the literature highlights viable pathways for cost reduction, especially through increased biomass productivity and process optimization.

7.3.3. Sensitivity analysis

A sensitivity analysis was conducted for scenario SC3 to identify the key parameters influencing the bio-oil MFSP, where SCB was used as the energy source to meet the steam demand of the proposed process. SC3 was chosen for this analysis as it demonstrated the lowest MFSP among all evaluated scenarios. Figure 7.7 illustrates the sensitivity analysis based on a ± 25% fluctuation in economic and operational parameters. The results indicate that bio-oil yield and the cost of microalgae biomass acquisition are the parameters exhibiting the highest sensitivity. When the bio-oil yield varied from -25% to +25% of its base value, the MFSP ranged from 9.64 USD/GGE to 16.05 USD/GGE.

Similarly, varying the biomass production cost by ±25% resulted in the MFSP changing between 9.84 USD/GGE and 14.25 USD/GGE. The cost of cyclohexane was identified as the third most sensitive parameter, with the MFSP varying between 11.37 USD/GGE and 12.72 USD/GGE. The other parameters showed low sensitivity compared to the variations in MFSP caused by changes in bio-oil yield, microalgae acquisition cost, and cyclohexane expenditure.

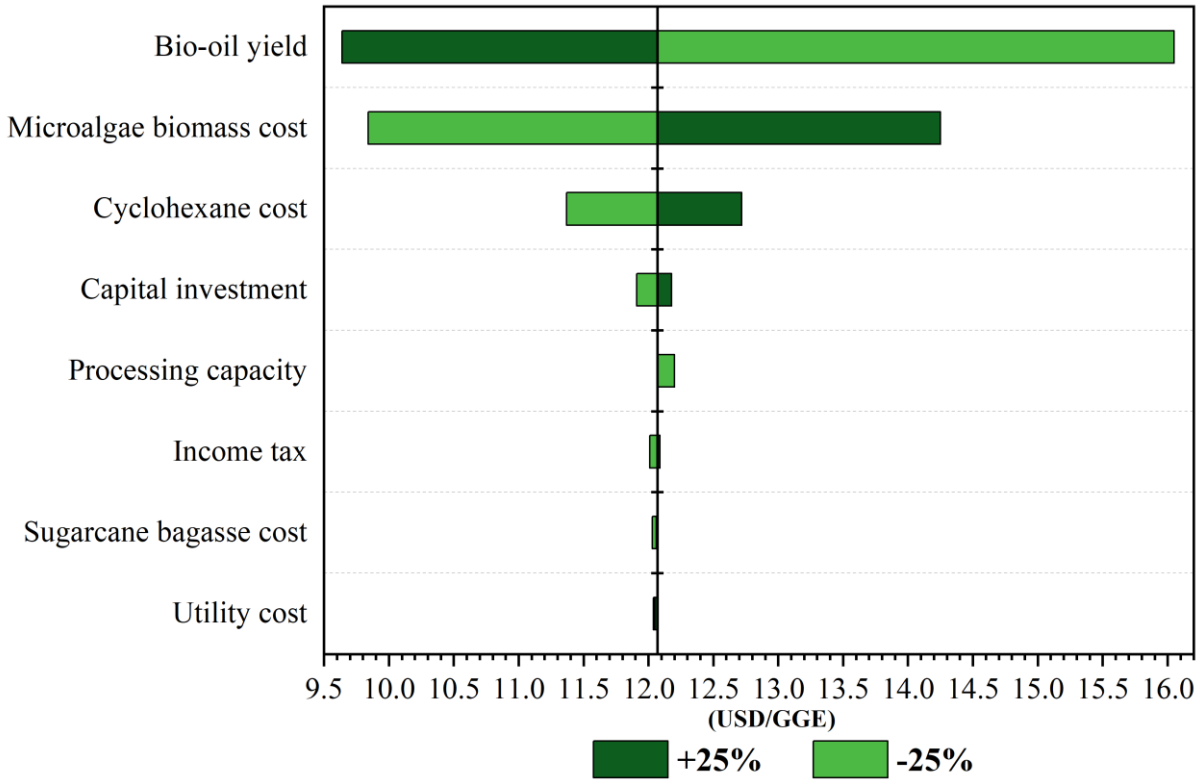

Figure 7.7. Tornado diagram of the minimum selling price of bio-oil when evaluating a fluctuation of ±25% in economic and operational parameters.

The significant effect of variables, microalgae biomass acquisition cost, and bio-oil yield, on the MFSP of bio-oil was also reported by JONES et al. (2014) and JIANG et al. (2019) when simulating bio-oil production from microalgae. Both authors highlight the need for greater efficiency in the cultivation and harvesting stages to reduce production costs. JIANG et al. (2019) concluded that the MFSP of bio-oil varies from 5 USD/GGE to 16 USD/GGE when the price of ash-free microalgae ranges between 400 USD/ton and 1,800 USD/ton.

The simulation and sensitivity analysis of the effect of solvent used in the bio-oil separation stage on the MFSP represents a novel contribution compared to previous studies, as no studies have addressed this specific aspect to date.

7.3.4. Environmental impacts

7.3.4.1.Life cycle inventory

The simplified life cycle inventory for the process is summarized in Table 7.2. For environmental analysis purposes, the inventory was prepared considering the unit in m^3/h. For scenarios SC1 and SC2, the operational data for the biomass harvesting was considered constant throughout the process.

Table 7.2. Simplified life cycle inventory of bio-oil production.

Stage			SC1	SC2	SC3	SC4	Unit
Cultivation	Input	Wastewater	1730.99	1730.99	-	-	m^3/h
		Electricity for paddlewheel	34.20	34.20	-	-	kWh
	Avoided products	Water	1730.99	1730.99	-	-	kg
		N fertilizer	19.98	19.98	-	-	g
		P fertilizer	72.88	72.88	-	-	g
Mechanical dewatering	Input	Electricity	0.80	0.80	51.07	51.07	kWh
Thermal conditioning	Input	Electricity - Pump	3.73	3.73	74.57	74.57	kWh
		Heat Exchanger	541.67	541.67	34,850.66	34,850.66	kWh
	Avoided products	Recovered heat	494.61	494.61	31,829.96	31,829.96	kWh
Steam generation	Input	Heating - SCB	60.96	-	3912.82	-	kWh
		Heating - LPG	-	3.66	-	234.99	kg
	Avoided products	Solid residues incineration	10.74	10.74	3623.11	3623.11	kWh
Products separation	Input	Solvent	18.19	18.19	1166.65	1166.65	kg

Two important aspects are considered to differentiate the scenarios beyond the microalgae biomass source. When SCB is used for steam generation (SC1 and SC3), the dataset considers that SCB is burned in a heat and power cogeneration unit, providing electricity and heat. Emission factors are derived from wood chip combustion data and adjusted to reflect the carbon content of the SCB. The activities include the reception of the SCB at the cogeneration plant and the disposal of the ashes. It includes infrastructure, operational inputs (lubricating oil, ammonia, organic chemicals, sodium chloride, chlorine, and demineralized water), and atmospheric emissions (PRÉ, 2020). For LPG (SC2 and SC4), the dataset is based on a refinery with configurations adjusted to

reflect the average of European refineries in terms of complexity, crude oil sulfur content, and American Petroleum Institute (API) gravity. The activities include introducing crude oil into the refinery to increase the output of refined products. It includes wastewater treatment, freshwater supply, infrastructure, storage, and energy provisioning (PRÉ, 2020).

7.3.4.2.Environmental Impact Assessment

Switching from LPG to SCB lowers the dependence on non-renewable resources: fossil-resource-scarcity scores fall by roughly 13% at smaller scale (from SC1 to SC2) and by 15% from SC3 to SC4. This benefit arises because SCB diminishes reliance on finite fossil fuels and promotes the use of renewable biomass (GOVINDASAMY; SHARMA; SUBRAMANIAN, 2019; KHATRI; PANDIT, 2022; RAMIREZ; BROWN; RAINEY, 2018), whereas LPG impacts come from its extraction, refining, and combustion (PRÉ, 2020). These changes are presented in Figure 7.8, which illustrates the contribution of each life-cycle stage to overall environmental impacts across scenarios.

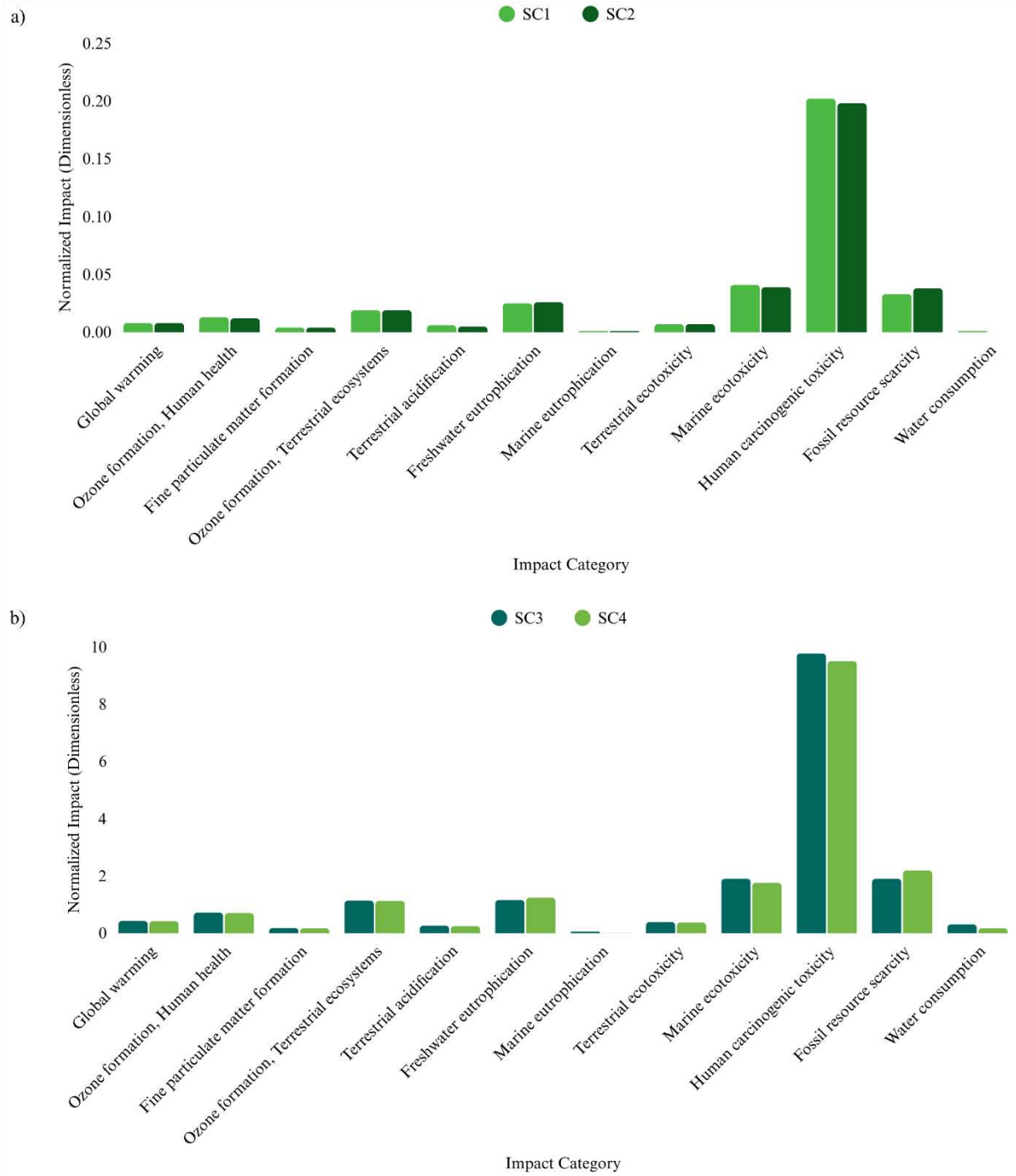

Figure 7.8. Environmental impacts contribution, where a) SC1 and SC2, b) SC3 and SC4.

The trade-off is a modest rise in air-quality indicators: photochemical-ozone formation rises by about 2% and fine-particulate formation by 3-5%, owing to the higher ash and Sulphur content of SCB. Conventional emission-control devices, such as selective catalytic reduction (SCR, for NOx)

and flue-gas desulphurization (FGD, for SOx), would largely neutralize these increments (KHATRI; PANDIT, 2022) while preserving the renewable character of the energy supply.

Regardless of the fuel, a single unit operation, cyclohexane-based liquid/solid separation, dominates the life-cycle impacts. Solvent makes-up and losses account for roughly 70% of every normalized impact score, and for more than 90% of the human-carcinogenic-toxicity load in SC3 and SC4. The increased environmental impacts associated with cyclohexane use are primarily due to the release of benzene and polyaromatic hydrocarbons during its production (MCKEE; ADENUGA; CARRILLO, 2015; PRÉ, 2020). These findings are supported by the flow analysis in Figure 7.9, which depicts the inputs, process stages, and impact categories for the SCB and LPG scenarios.

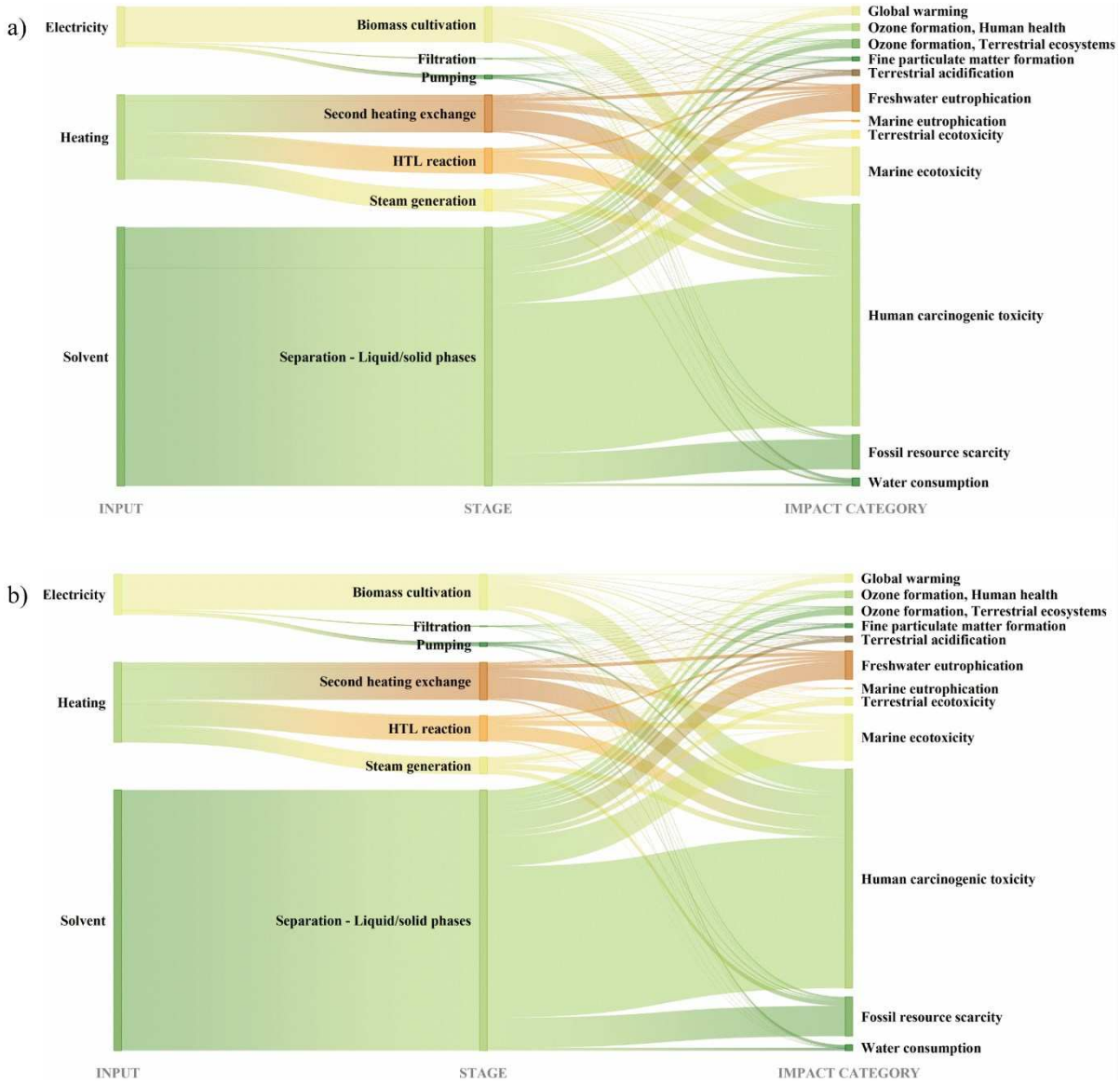

Figure 7.9. Sankey diagram illustrating inputs, process stages, and environmental impact categories for scenarios involving: (a) sugarcane bagasse and (b) liquefied petroleum gas.

The second level of contributions comes from heat demand, split almost evenly between the main heat exchanger and the HTL reactor; together they add another 17-18% to the totals, primarily through CO_2, acidifying gases, and eutrophication associated with fuel combustion and boiler blowdown. Electricity-driven steps, biomass cultivation, pumping, and filtration, become marginal (<2%) once the system scales, though they still represent about one-tenth of the burden at the smaller scale.

Because the separation step overshadows all other contributions, solvent management offers the greatest leverage. Closing the solvent loop with high-efficiency recovery (>95%) or, preferably, substituting cyclohexane with greener alternatives such as ethanol, cyclopentyl-methyl ether, or 2-methyltetrahydrofuran could slash human-toxicity scores while simultaneously reducing global-warming and resource-scarcity impacts (PRASAD et al., 2022). For SCB scenarios, installing FGD and SCR on the furnace could mitigate the small rise observed in ozone and particulate-matter formation. Finally, considering renewable electricity is advisable for small-scale systems, where power use remains a visible contributor. For example, CASTRO et al., (2020) observed a 47% reduction in climate change; 51% in terrestrial ecotoxicity and 19.8% in fossil depletion when switching energy from the grid to photovoltaic panels in an LCA of biofertilizer production from microalgae.

Two refinements could improve subsequent LCAs. First, treating SCB as an avoided product, considering it is not destined for open burning or landfilling, would credit the system for mitigating those alternative emissions and further enhance the attractiveness of SCB. Second, coupling the SCB boiler to carbon-capture technology would allow the process to deliver negative greenhouse-gas emissions, an option that deserves quantitative exploration. In summary, the solvent-based liquid/solid separation step is the overriding environmental hotspot, followed by fossil-fuel-driven heat supply. Prioritizing solvent management and heat integration offers the greatest leverage to reduce the environmental burden of microalgae-based HTL, regardless of the energy source.

7.3.5. Limitations and Future Perspectives

Despite its potential, HTL-based bio-oil production remains constrained by a combination of technical, economic, and environmental limitations that must be overcome for broader deployment. The high cost of microalgae cultivation and harvesting continues to hinder the economic viability of HTL, often accounting for up to 75% of the MFSP (JIANG et al., 2019). Energy requirements for achieving high-pressure and high-temperature conditions also diminish the energy return on investment (EROI) and increase operational expenses (QIAN et al., 2021). Process inputs such as hydrogen for upgrading and solvents for extraction add further cost sensitivity and complicate economic scaling (CHEN; QUINN, 2021).

The use of wastewater as a cultivation medium reduces nutrient input costs and enables biomass production alongside effluent treatment, aligning HTL with circular economy principles. Integrating HTL within existing wastewater treatment infrastructure offers several synergies, including shared utilities (heat, water, land), process water recycling, and centralized waste management (MAGALHÃES et al., 2024). However, challenges persist, such as fluctuations in wastewater composition that affect biomass quality and conversion efficiency (KURNIAWAN et al., 2024), and the accumulation of contaminants like heavy metals or pharmaceuticals in HTL products (KHAN et al., 2023). These issues require effective pretreatment strategies and adaptive process control to ensure consistent performance.

Emerging technical solutions include two-stage cultivation systems in HRAPs, and hybrid configurations using biofilm or membrane reactors to boost productivity while reducing treatment costs (MAGALHÃES et al., 2024). Low-energy harvesting techniques such as gravity sedimentation and bioflocculation can further improve energy balances. A promising avenue lies in diversifying value streams by extracting high-value co-products, proteins, pigments, fatty acids, within an integrated biorefinery framework (PEREIRA et al., 2024).

Beyond the dominant impacts of the separation stage discussed previously, broader environmental concerns persist. Fossil-based heat supply drives significant GHG emissions, and combustion-related pollutants (NOx, SOx, CO_2) continue to pose challenges for air quality (MARANGON et al., 2022). The treatment and valorization of HTL by-products, especially the aqueous phase rich in organic pollutants (KHAN et al., 2023), remains a pressing concern. Similarly, solvent toxicity risks warrant attention, particularly for solvents such as cyclohexane.

Future research should prioritize greener solvent alternatives like ethyl acetate, dimethyl carbonate, and methyl tert-butyl ether, even if associated with trade-offs in cost or efficiency. These options present a significantly lower toxicological profile and could be evaluated via comparative life cycle and techno-economic assessments (NAAZ et al., 2023).

To further decouple HTL systems from fossil dependency, the integration of renewable energy (solar, wind) for process heat and hydrogen production is critical (ZHANG et al., 2022). Innovations such as carbon capture and storage (CCS) concept application or biochar valorization (e.g., as a soil amendment or energy storage material) offer additional sustainability gains (MASOUMI; DALAI, 2021). On the process side, advanced catalysts ($NiMo/Al_2O_3$, noble metals, Fe-HZSM-5) and novel reactor configurations (e.g., Taylor-Couette or tubular reactors) can

increase conversion efficiencies and reduce energy demands (QIAN et al., 2021; RANGANATHAN; SAVITHRI, 2019).

Improved genetic and metabolic engineering of microalgae strains could yield biomass with optimized lipid profiles and faster growth rates, enhancing both fuel yield and productivity (MOSER; PENKE; BATTEIGER, 2021).

There is a clear need for more dynamic, spatially resolved LCAs that consider feedback mechanisms (e.g., nutrient cycling, energy substitution) and reflect uncertainties through sensitivity and scenario analyses. These tools will be essential to guide scale-up and system optimization.

Finally, policy mechanisms, such as carbon credits, renewable fuel mandates, and innovation grants, are necessary to de-risk investments and incentivize industrial deployment. Inclusion of algae-based biofuels in regulatory frameworks like Renewable Energy Directive (RED II) or Low Carbon Fuel Standard (LCFS) can provide crucial momentum for market uptake.

Although this study excluded catalytic upgrading due to marginal gains observed in prior work (SILVA et al., 2024b), other configurations have demonstrated significant improvements in HHV, such as Fe-HZSM-5-catalyzed pyrolysis of *Spirulina* biocrude (LI et al., 2023). If future trials confirm their efficacy, these steps can be integrated into the simulation framework to enable holistic performance assessments.

7.4.Conclusion

This study underscores that producing bio-oil from wastewater-cultivated microalgae through hydrothermal liquefaction (HTL) is technically feasible but still faces economic and environmental barriers. While using sugarcane bagasse as a steam source reduces fossil resource depletion, it also increases pollutant emissions. Likewise, cyclohexane, though effective as a solvent, raises human carcinogenic toxicity risks. To move forward, it is important to focus on lowering cultivation costs, controlling emissions more effectively, and finding greener solvents. By refining operational conditions, improving scale-up methods, and cutting costs, HTL-based bio-oil production can become both more affordable and environmentally competitive. This research provides a framework for future strategies, demonstrating that with integrated optimization, HTL can help turn microalgae into a more competitive and sustainable source of bioenergy.

Acknowledgments

This study was financed in part by the Coordenação de Aperfeiçoamento de Pessoal de Nível Superior – Brasil (CAPES) – Finance Code 001. Furthermore, the authors gratefully acknowledge the financial support of the Conselho Nacional de Desenvolvimento Científico e Tecnológico (CNPq) [Grant Numbers: 405787/2022-7, 406204/2022-5, and 403521/2023-8] and Fundação de Amparo à Pesquisa do Estado de Minas Gerais (FAPEMIG) [Grant Numbers: APQ-03618-23, APQ-00756-23, and RED 00068-23].

References

ACIÉN FERNÁNDEZ, F. G.; FERNÁNDEZ SEVILLA, J. M.; MOLINA GRIMA, E. Costs analysis of microalgae production. Em: **Biofuels from Algae**. [s.l.] Elsevier, 2019. p. 551–566.

AGUILAR VIZCARRA, D.; ESENARRO, D.; RODRIGUEZ, C. Three steps mixed (Fire tube–water tube) vertical boiler to optimize thermal performance. **Fluids**, v. 6, n. 3, 1 mar. 2021.

ALJABRI, H. et al. Evidence of the drying technique's impact on the biomass quality of Tetraselmis subcordiformis (Chlorophyceae). **Biotechnology for Biofuels and Bioproducts**, v. 16, n. 1, 1 dez. 2023.

ASSIS, L. R. DE et al. Innovative hybrid system for wastewater treatment: High-rate algal ponds for effluent treatment and biofilm reactor for biomass production and harvesting. **Journal of Environmental Management**, v. 274, 15 nov. 2020.

BORAZJANI, Z.; AZIN, R.; OSFOURI, S. Kinetics studies and performance analysis of algae hydrothermal liquefaction process. **Biomass Conversion and Biorefinery**, v. 14, n. 16, p. 19257–19284, 1 ago. 2024.

BOROWITZKA, M. A. Biology of Microalgae. Em: **Microalgae in Health and Disease Prevention**. [s.l.] Elsevier, 2018. p. 23–72.

BROBBEY, M. S.; LOUW, J.; GÖRGENS, J. F. Biobased acrylic acid production in a sugarcane biorefinery: A techno-economic assessment using lactic acid, 3-hydroxypropionic acid and glycerol as intermediates. **Chemical Engineering Research and Design**, v. 193, p. 367–382, 1 maio 2023.

CALIJURI, M. L. et al. Bioproducts from microalgae biomass: Technology, sustainability, challenges and opportunities. **Chemosphere**, v. 305, p. 135508, out. 2022.

CALIJURI, M. L. et al. Life cycle assessment of microalgal biomass for valorization. Em: **Valorization of Microalgal Biomass and Wastewater Treatment**. [s.l.] Elsevier, 2023. p. 179–196.

CASCIOLI, A.; BARATIERI, M. Enhanced thermodynamic modelling for hydrothermal liquefaction. **Fuel**, v. 298, p. 120796, ago. 2021.

CASTRO, J. DE S. et al. Microalgae based biofertilizer: A life cycle approach. **Science of The Total Environment**, v. 724, p. 138138, jul. 2020.

CASTRO, J. S. et al. Life cycle assessment and techno-economic analysis for biofuel and biofertilizer recovery as by-products from microalgae. **Renewable and Sustainable Energy Reviews**, v. 187, p. 113781, nov. 2023.

CHANTASIRIWAN, S. **Optimum installation of economizer, air heater, and flue gas dryer in biomass boiler**. **Computers and Chemical Engineering**Elsevier Ltd, , 1 jul. 2021.

CHEAH, W. Y. et al. Biosequestration of atmospheric CO 2 and flue gas-containing CO 2 by microalgae. **Bioresource Technology**, v. 184, p. 190–201, maio 2015.

CHEMANALYST. **Cyclohexane Price Trend and Forecast**. Disponível em: <https://www.chemanalyst.com/Pricing-data/cyclohexane-1148>. Acesso em: 2 out. 2024.

CHEN, P. H.; QUINN, J. C. Microalgae to biofuels through hydrothermal liquefaction: Open-source techno-economic analysis and life cycle assessment. **Applied Energy**, v. 289, 1 maio 2021.

DE CARVALHO ARAÚJO, C. K. et al. Life cycle assessment as a guide for designing circular business models in the wood panel industry: A critical review. **Journal of Cleaner Production**, v. 355, p. 131729, jun. 2022.

DELGADILLO-MIRQUEZ, L. et al. Nitrogen and phosphate removal from wastewater with a mixed microalgae and bacteria culture. **Biotechnology Reports**, v. 11, p. 18–26, set. 2016.

DENG, T. et al. Catalytic distillation for one-step cyclohexyl acetate production and cyclohexene-cyclohexane separation via esterification of cyclohexene with acetic acid over microfibrous-structured Nafion-SiO2/SS-fiber packings. **Chemical Engineering and Processing - Process Intensification**, v. 131, p. 215–226, 1 set. 2018.

EIA. **International Energy Outlook 2023**. , out. 2023.

FIORANELLI, A.; BIZZO, W. A. Generation of surplus electricity in sugarcane mills from sugarcane bagasse and straw: Challenges, failures and opportunities. **Renewable and Sustainable Energy Reviews**, v. 186, p. 113647, out. 2023.

GLOBAL PETROL PRICES. **LPG prices, liter, 25-Nov-2024**. Disponível em: <https://www.globalpetrolprices.com/gasoline_prices/>. Acesso em: 1 dez. 2024.

GOVINDASAMY, G.; SHARMA, R.; SUBRAMANIAN, S. Studies on the effect of heterogeneous catalysts on the hydrothermal liquefaction of sugarcane bagasse to low-oxygen-containing bio-oil. **Biofuels**, v. 10, n. 5, p. 665–675, 2019.

HASAN, K. S. Experimental study on the combustion of gaseous based fuel (LPG) in a tangential swirl burner of a steam boiler. **Journal of Thermal Engineering**, p. 1226–1240, 2024.

HERRERA, A. et al. Sustainable production of microalgae in raceways: Nutrients and water management as key factors influencing environmental impacts. **Journal of Cleaner Production**, v. 287, n. xxxx, p. 125005, mar. 2021.

HUIJBREGTS, M. A. J. et al. ReCiPe2016: a harmonised life cycle impact assessment method at midpoint and endpoint level. **The International Journal of Life Cycle Assessment**, v. 22, n. 2, p. 138–147, 12 fev. 2017.

IEA. **World Energy Outlook 2023**. Disponível em: <https://www.iea.org/reports/world-energy-outlook-2023/overview-and-key-findings#abstract>. Acesso em: 25 set. 2024.

ISO. **ISO 14040 - Environmental Management-Life Cycle Assessment–Principles and Framework**. [s.l: s.n.].

ISO. **ISO 14044 – Environmental Management-Life Cycle Assessment–Requires and Guidelines**. [s.l: s.n.].

JIANG, Y. et al. Techno-economic uncertainty quantification of algal-derived biocrude via hydrothermal liquefaction. **Algal Research**, v. 39, 1 maio 2019.

JONES, S. B. et al. **Process Design and Economics for the Conversion of Algal Biomass to Hydrocarbons: Whole Algae Hydrothermal Liquefaction and Upgrading**. Richland, WA (United States): [s.n.].

KHAN, S. et al. **Microalgal Feedstock for Biofuel Production: Recent Advances, Challenges, and Future Perspective**. **Fermentation**MDPI, , 1 mar. 2023.

KHATRI, P.; PANDIT, A. B. Systematic review of life cycle assessments applied to sugarcane bagasse utilization alternatives. **Biomass and Bioenergy**, v. 158, p. 106365, mar. 2022.

KURNIAWAN, K. I. A. et al. Life cycle assessment of integrated microalgae oil production in Bojongsoang Wastewater Treatment Plant, Indonesia. **Environmental Science and Pollution Research**, v. 31, n. 5, p. 7902–7933, 1 jan. 2024.

LI, H. et al. High-quality bio-oil production via catalytic pyrolysis of biocrude oil from hydrothermal liquefaction of microalgae Spirulina. **Journal of Analytical and Applied Pyrolysis**, v. 173, p. 106057, ago. 2023.

LIU, H. et al. Calcium looping-enhanced biomass gasification for methanol production: Integrating methane dry reforming and carbon utilization. **Separation and Purification Technology**, v. 354, 19 fev. 2025.

LYU, Z. et al. Reprint of: Simulation based ionic liquid screening for benzene-cyclohexane extractive separation. **Chemical Engineering Science**, v. 115, p. 186–194, 1 ago. 2014.

MAGALHÃES, I. B. et al. Agro-industrial wastewater-grown microalgae: A techno-environmental assessment of open and closed systems. **Science of The Total Environment**, v. 834, p. 155282, ago. 2022.

MAGALHÃES, I. B. et al. Advancements in high-rate algal pond technology for enhanced wastewater treatment and biomass production: A review. **Journal of Water Process Engineering**, v. 66, p. 105929, set. 2024.

MAQBOOL, W.; BILLER, P.; ANASTASAKIS, K. A kinetic process model for sewage sludge hydrothermal liquefaction in Aspen Plus: Model validation with pilot-plant data and scale up. **Energy Conversion and Management**, v. 302, 15 fev. 2024.

MARANGON, B. B. et al. Environmental performance of microalgae hydrothermal liquefaction: Life cycle assessment and improvement insights for a sustainable renewable diesel. **Renewable and Sustainable Energy Reviews**, p. 111910, nov. 2021.

MARANGON, B. B. et al. Environmental performance of microalgae hydrothermal liquefaction: Life cycle assessment and improvement insights for a sustainable renewable diesel. **Renewable and Sustainable Energy Reviews**, v. 155, 1 mar. 2022.

MASOUMI, S.; DALAI, A. K. Techno-economic and life cycle analysis of biofuel production via hydrothermal liquefaction of microalgae in a methanol-water system and catalytic hydrotreatment using hydrochar as a catalyst support. **Biomass and Bioenergy**, v. 151, 1 ago. 2021.

MCKEE, R. H.; ADENUGA, M. D.; CARRILLO, J.-C. Characterization of the toxicological hazards of hydrocarbon solvents. **Critical Reviews in Toxicology**, v. 45, n. 4, p. 273–365, 21 abr. 2015.

MOSER, L.; PENKE, C.; BATTEIGER, V. An in-depth process model for FUEL production via hydrothermal liquefaction and catalytic hydrotreating. **Processes**, v. 9, n. 7, 1 jul. 2021.

NAAZ, F. et al. Hydrothermal liquefaction could be a sustainable approach for valorization of wastewater grown algal biomass into cleaner fuel. **Energy Conversion and Management**, v. 283, 1 maio 2023.

ONG, B. H. Y. et al. A heat- and mass-integrated design of hydrothermal liquefaction process co-located with a Kraft pulp mill. **Energy**, v. 189, p. 116235, dez. 2019.

PARRAY, J. A.; SINGH, N.; HAGHI, A. K. Harvesting and Preprocessing Algal Biomass. Em: [s.l: s.n.]. p. 41–64.

PEREIRA, A. S. A. DE P. et al. Municipal and industrial wastewater blending: Effect of the carbon/nitrogen ratio on microalgae productivity and biocompound accumulation. **Journal of Environmental Management**, v. 370, p. 122760, nov. 2024.

PETERS, M. S.; TIMMERHAUS, K. D.; WEST, R. E. **Plant design and economics for chemical engineers**. 5th. ed. [s.l.] McGraw-Hill International, 2003.

PRASAD, W. et al. Green solvents, potential alternatives for petroleum based products in food processing industries. **Cleaner Chemical Engineering**, v. 3, p. 100052, set. 2022.

PRÉ. **Various authors. SimaPro database manual – methods library**. Disponível em: <https://simapro.com/wp-content/uploads/2020/10/DatabaseManualMethods.pdf>. Acesso em: 19 jan. 2021.

QI, J. et al. Hydrogen production from municipal solid waste via chemical looping gasification using CuFe2O4 spinel as oxygen carrier: An Aspen Plus modeling. **Energy Conversion and Management**, v. 294, 15 out. 2023.

QIAN, L. et al. Biocrude production from hydrothermal liquefaction of chlorella: Thermodynamic modelling and reactor design. **Energies**, v. 14, n. 20, 1 out. 2021.

RAMIREZ, J. A.; BROWN, R.; RAINEY, T. J. Techno-economic analysis of the thermal liquefaction of sugarcane bagasse in ethanol to produce liquid fuels. **Applied Energy**, v. 224, p. 184–193, ago. 2018.

RANGANATHAN, P.; SAVITHRI, S. Techno-economic analysis of microalgae-based liquid fuels production from wastewater via hydrothermal liquefaction and hydroprocessing. **Bioresource Technology**, v. 284, p. 256–265, 1 jul. 2019.

RANJBAR, S.; MALCATA, F. X. Hydrothermal Liquefaction: How the Holistic Approach by Nature Will Help Solve the Environmental Conundrum. **Molecules**, v. 28, n. 24, p. 8127, 16 dez. 2023.

SAIDUR, R. et al. **A review on biomass as a fuel for boilers**. **Renewable and Sustainable Energy Reviews**, jun. 2011.

SILVA, T. A. et al. Microalgae from food agro-industrial effluent as a renewable resource for agriculture: A life cycle approach. **Resources, Conservation and Recycling**, v. 186, p. 106575, nov. 2022.

SILVA, T. A. et al. Enhancing microalgae biomass production: Exploring improved scraping frequency in a hybrid cultivation system. **Journal of Environmental Management**, v. 355, p. 120505, mar. 2024a.

SILVA, T. A. et al. Biofuel from wastewater-grown microalgae: A biorefinery approach using hydrothermal liquefaction and catalyst upgrading. **Journal of Environmental Management**, v. 368, p. 122091, set. 2024b.

SINGH, N. B.; KUMAR, A.; RAI, S. Potential production of bioenergy from biomass in an Indian perspective. **Renewable and Sustainable Energy Reviews**, v. 39, p. 65–78, nov. 2014.

UNGUREANU, N.; VLĂDUȚ, V.; BIRIȘ, S.-ȘTEFAN. Sustainable Valorization of Waste and By-Products from Sugarcane Processing. **Sustainability**, v. 14, n. 17, p. 11089, 5 set. 2022.

WORLD LIQUID GAS ASSOCIATION. **WLPGA Annual Report 2023**. Disponível em: <https://www.worldliquidgas.org/publications/>. Acesso em: 2 dez. 2024.

WU, W.; HUANG, C. M.; TSAI, Y. H. Design and validation of a microalgae biorefinery using machine learning-assisted modeling of hydrothermal liquefaction. **Algal Research**, v. 74, 1 jul. 2023.

ZHANG, P. et al. Microalgae cultivated in wastewater catalytic hydrothermal liquefaction: Effects of process parameter on products and energy balance. **Journal of Cleaner Production**, v. 341, 20 mar. 2022.

ZHU, Y. et al. Development of hydrothermal liquefaction and upgrading technologies for lipid-extracted algae conversion to liquid fuels. **Algal Research**, v. 2, n. 4, p. 455–464, out. 2013.

8. Capítulo V. Enhancing microalgal biohydrogen production: Unlocking higher yields with hydrothermal pretreatment with niobium phosphate

Abstract: Microalgae cultivated in wastewater hold promise as a substrate for biohydrogen ($bioH_2$) production. However, their rigid cell walls pose a challenge to fermentability. In this context, this study evaluated hydrothermal pretreatment with niobium phosphate (NbP) at 100-180°C for 0-70 minutes, using up to 75% NbP (relative to the dry weight of microalgal biomass). The combination of 180°C, 10 minutes, and 75% NbP released 7,431 mg total carbohydrates (CHt) L^{-1}, referred to here as PB5, improving subsequent dark fermentation. Fermentation of PB5 at pH 5.0 yielded 1.03 mmol H_2 mol^{-1} CHt and achieved a maximum $bioH_2$ production of 0.17 mmol with an 83.6% CHt conversion efficiency. In contrast, pH 5.5 and 6.0 reduced $bioH_2$ yields and promoted methanogenic activity, while no pH control resulted in negligible $bioH_2$ evolution. In conclusion, hydrothermal pretreatment with niobium phosphate and pH optimization synergize to enhance hydrogenogenesis, integrating wastewater treatment and renewable biohydrogen production.

Keywords: Acidogenic fermentation; Resource Recovery; Wastewater treatment; Biomass valorization; Microalgae biomass.

8.1. Introduction

The global energy transition toward sustainable and low-carbon systems is intensifying, with renewable energy sources such as solar, wind, hydropower, and biofuels expected to play a central role in decarbonizing power, heat, and transportation sectors. Renewable electricity generation is projected to reach over 17,000 TWh by 2030, an increase of almost 90% from 2023 levels, meeting the combined power demand of China and the United States (IEA, 2024). Despite this progress, achieving net-zero carbon emissions necessitates integrating renewable biofuels into the energy mix, particularly in sectors where electrification remains challenging, such as industrial processes and heavy transport (GIELEN et al., 2019). Among renewable energy sources, hydrogen (H_2) stands out as a versatile energy carrier with high energy density, minimal carbon footprint, and diverse production pathways (ARAUJO et al., 2024).

Dark fermentation (DF) of organic biomass has emerged as a promising technology for $bioH_2$ production, leveraging microbial consortia to convert primarily carbohydrates (CHt) into H_2

and volatile fatty acids (VFAs) under anaerobic conditions (ARAUJO et al., 2024; BLANCO; OLIVEIRA; ZAIAT, 2019; FUESS et al., 2021; FUESS; ZAIAT; DO NASCIMENTO, 2019). This process is particularly advantageous due to its ability to valorize diverse feedstocks, including agricultural residues and wastewater-grown biomass, without requiring complex external inputs like high-voltage electricity or pure oxygen (AHMED et al., 2022). However, achieving high H_2 yields is still a challenge.

Microalgae have garnered attention as a feedstock for bioH_2 production owing to their rapid growth rates and ability to be cultivated in wastewater, avoiding competition with arable land and food production (CHEN et al., 2023; FUENTES-SANTIAGO et al., 2023). Furthermore, wastewater-grown microalgae contribute to resource recovery through nutrient removal, reducing the environmental impact of wastewater discharge (MAGALHÃES et al., 2024). The main species commonly found in wastewater, *Chlorella vulgaris* and *Tetradesmus obliquus*, possess robust cell walls composed of proteins, carbohydrates, lipids, and minerals. These resilient structures significantly hinder the bioavailability of intracellular CHt, thereby limiting direct substrate utilization and resulting in low H_2 yields unless effective pretreatment methods are employed (NAGARAJAN; CHANG; LEE, 2020; PRIYA et al., 2023).

Hydrothermal pretreatment has demonstrated effective in addressing the recalcitrance of microalgal biomass. Operating at temperatures between 120°C and 200°C, this process disrupts the structural integrity of cell walls, hydrolyzing polysaccharides and releasing fermentable CHt (NAGARAJAN; CHANG; LEE, 2020; PRIYA et al., 2023). The incorporation of heterogeneous catalysts, such as niobium phosphate ($NbOPO_4 \cdot 3H_2O$, referred to here as NbP), further enhances the efficiency of hydrothermal processes. NbP, with its dual Brønsted and Lewis acidic sites, accelerates glycosidic bond cleavage and cellulose depolymerization while minimizing the formation of inhibitory byproducts such as 5-hydroxymethylfurfural (5-HMF) (GONÇALVES et al., 2024; OLIVEIRA et al., 2023). To date, however, NbP has not been investigated as a catalyst for releasing CHt from microalgae biomass to produce substrates for DF. Its potential to improve CHt accessibility and mitigate pretreatment drawbacks, such as byproduct inhibition, remains unexplored in the context of bioH_2 production.

In addition to pretreatment, the control of fermentation pH plays an essential role in shaping microbial metabolic pathways for H_2 production. Very low pH conditions favor lactic acid accumulation and may promote solventogenic pathways (CASTELLÓ et al., 2020). In contrast,

relatively high pH (>6.0) may lead to propionic acid accumulation and sulfideogenic activity (CASTELLÓ et al., 2020). Acidic conditions (pH 5.0-5.5) generally favor acidogenic bacteria, which convert sugars into VFAs and H_2 while suppressing methanogens that would otherwise consume these intermediates to produce methane (CH_4) (MARTÍNEZ-FRAILE et al., 2024; REGUEIRA-MARCOS; GARCÍA-DEPRAECT; MUÑOZ, 2023).

This study aims to address these challenges by evaluating the interplay between hydrothermal pretreatment conditions (temperature, reaction time, and catalyst loading) and fermentation pH in maximizing bioH_2 yields of wastewater-grown microalgae as substrate. By introducing NbP as a catalyst for the first time in this application, the study explores its ability to enhance CHt solubilization and improve subsequent H_2 production. By integrating an effective pretreatment strategy with process control, this study aims to contribute to the development of sustainable microalgae-based bioH_2 production platforms.

8.2.Material and methods

This section details microalgal cultivation and characterization, hydrothermal pretreatment, preparation of substrates and inoculum, analytical protocols, and the monitoring, kinetic modelling and performance evaluation of batch dark-fermentation assays (Figure 8.1).

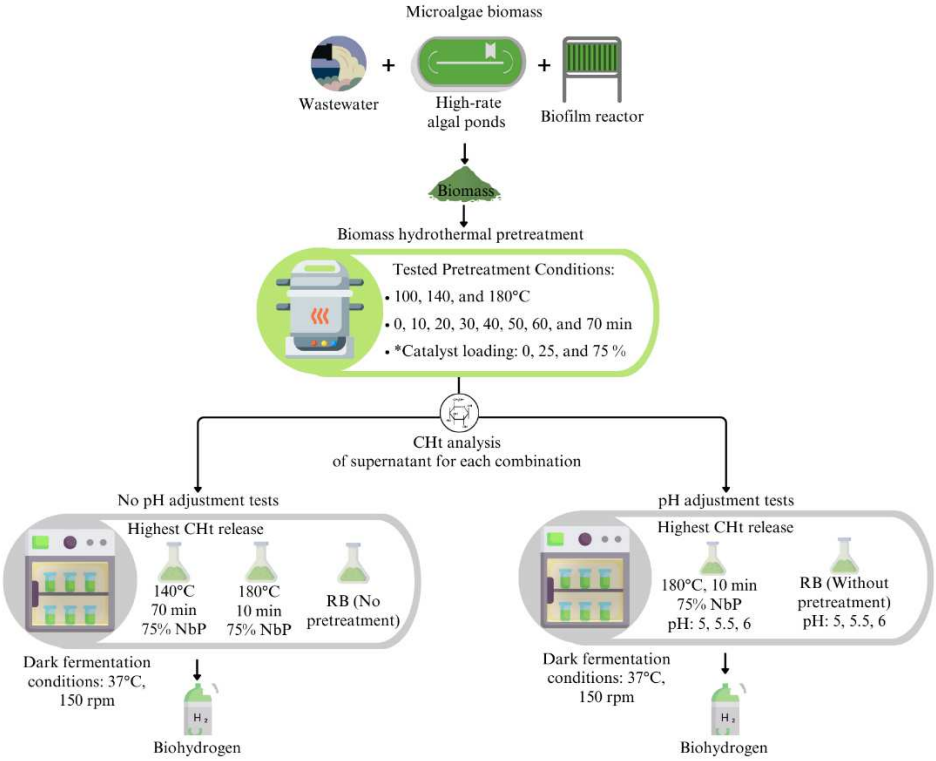

Figure 8.1. Methodological flowchart. Note: CHt – Total carbohydrates, RB – Raw biomass, NbP – Niobium phosphate. *% relative to the dry weight of microalgal biomass.

8.2.1. Biomass production

Microalgae were cultivated at the Laboratory of Sanitary and Environmental Engineering, Federal University of Viçosa (Brazil). The outdoor system comprised twelve raceway-type high-rate algal ponds (HRAPs; 1.28 m × 2.86 m × 0.50 m) fabricated from fibreglass-reinforced plastic and coupled to vertical biofilm reactors (BRs; 1.0 m × 0.5 m; total area = 0.5 m^2) mounted downstream of each pond. Continuous mixing was provided by six stainless-steel blades driven by a 0.5 HP motor whose rotational speed was adjusted with a CFW-10 inverter. Culture liquor (400 L h^{-1}) recirculated between HRAPs and BRs.

The medium consisted of a 50:50 mixture of industrial wastewater from a fruit-juice factory (pre-treated in an up-flow anaerobic sludge blanket reactor) and septic-tank effluent, yielding a C:N ratio of 7:1. After cultivation the suspension was settled, centrifuged (5 000 × g, 10 min) and freeze-dried. Further information is reported in SILVA et al. (2024).

8.2.2. Microalgae biomass characterization

The biomass was analyzed to determine its biochemical composition and species distribution. Species identification was performed using the UTERMÖHL (1958) sedimentation method under an inverted microscope, following morphological criteria described by PARRA; GONZALEZ; DELLAROSSA (1983) and KOMAREK; FOTT (1983). Cell counts were conducted according to APHA (2012) standards, identifying *Tetradesmus obliquus* (69%), *Chlorella vulgaris* (30%), and cyanobacteria (*Limnothrix planctonica*, 1%) as the dominant genera.

The biochemical composition of the biomass was determined for neutral lipids, membrane lipids, proteins, CHt, and ash. Protein content was measured using the Kjeldahl method, with a nitrogen-to-protein conversion factor of 6.25 (APHA, 2012). CHt was quantified via acid hydrolysis followed by the phenol-sulfuric acid method (DUBOIS et al., 1956) and spectrophotometric analysis at 490 nm against a glucose standard curve. Lipid content was measured using Soxhlet extraction with 99% hexane for neutral lipids and 96% ethanol for membrane lipids (AOAC, 1990). The ash content was determined gravimetrically by combusting the biomass at 550°C in a muffle furnace (APHA, 2012). The overall biomass composition was as follows: neutral lipids (11.02% ± 0.22%), membrane lipids (9.46% ± 0.31%), proteins (36.52% ± 0.84%), CHt (24.31% ± 0.69%), and ash (16.79% ± 0.45%). These values represent the average of triplicate analyses.

8.2.3. Microalgae biomass pretreatment (Substrate)

Microalgae biomass pretreatment was conducted using a Parr 5500 series hydrothermal reactor with a 300 mL capacity, equipped with temperature and pressure controls, and operated at a stirring speed of 500 rpm. For each experimental condition, 12 g of dry microalgal biomass was suspended in 200 g of distilled water to achieve a biomass-to-water ratio of 6% (w w^{-1}). This ratio was determined based on prior experiments that accounted for the average moisture content of the wastewater-grown microalgae biomass (ASSIS et al., 2020).

The pretreatment experiments evaluated the combination of three independent variables: temperature (100, 140, and 180°C), reaction time (0, 10, 20, 30, 40, 50, 60, and 70 minutes), and NbP catalyst loading (0, 3, and 9 g, corresponding to 0%, 25%, and 75% of the dry mass of microalgae, respectively). Each combination was tested in duplicate, resulting in a total of 3 × 8 × 3 = 72 experimental conditions, yielding 144 experimental units. Prior to each experiment, the

reactor was purged with nitrogen gas (N_2) to eliminate dissolved oxygen and maintain an anaerobic environment. The NbP catalyst, provided by Companhia Brasileira de Metalurgia e Mineração (CBMM) in Araxá, Minas Gerais, Brazil, is described in its Safety Data Sheet (SDS) as a stable, non-hazardous solid with an absolute density of 2.85 g cm^{-3}. It is insoluble in water and complies with the ABNT-NBR 14725-2:2009 standards (ABNT, 2009).

Following pretreatment, the reactor was cooled to room temperature, and the pretreated biomass suspension was centrifuged at 4,000 rpm for 10 minutes to separate the liquid and solid fractions. The liquid fraction (supernatant) was analyzed for CHt content using the phenol-sulfuric acid method (DUBOIS et al., 1956), with absorbance measured at 490 nm against a glucose standard curve. All experiments were performed in triplicate to ensure reproducibility. To identify the combination of time, temperature, and catalyst loading that maximized CHt release during each treatment, an analysis of variance (ANOVA) was performed, followed by Tukey's post-hoc test at a 5% significance level.

8.2.4. Treatment of anaerobic sludge (inoculum)

The anaerobic sludge used as inoculum was pretreated to inhibit methanogenic archaea and enhance hydrogenogenic activity. The sludge, sourced from an anaerobic digester treating municipal wastewater, was homogenized and subjected to acid treatment based on the protocol by PENTEADO et al. (2013). Initially, the sludge was acidified with 1 N hydrochloric acid (HCl) to adjust the pH to 3.0. The acidified sludge was incubated at 37°C for 24 hours to suppress methanogens, which are sensitive to low pH conditions. After incubation, the pH was neutralized to 7.0 using 1 N sodium hydroxide (NaOH). The treated sludge was centrifuged at 3,500 rpm for 10 minutes to concentrate the microbial biomass, and the supernatant was discarded. The volatile solids (VS) content of the treated inoculum was determined following APHA (2012).

8.2.5. Assembly of batch reactors

The inoculum-substrate mixture was prepared to achieve a food-to-microorganism (F/M) ratio of 5 g total chemical oxygen demand $(CODt)_{substrate}$ g^{-1} $VS_{inoculum}$, according to TUNÇAY et al. (2017). The liquid phase of the pretreated microalgae biomass served as the substrate, and anaerobic sludge was used as the inoculum. Sodium bicarbonate ($NaHCO_3$) was added as a buffering agent to maintain pH stability during fermentation. The concentration of $NaHCO_3$ was

set at 0.4 g $NaHCO_3$ g^{-1} $CODt_{substrate}$, as described by FUESS et al. (2021). The mass calculations required to achieve the specified F/M ratio are detailed in Table S8.1, Apêndice VI. The inoculum and substrate were mixed and the total reaction volume was adjusted to 110 mL of substrate. The final mixture was homogenized and transferred into 500 mL Erlenmeyers flasks for fermentation assays. For each experimental unit, 10 mL samples were taken from the prepared mixture for subsequent analysis. The flasks were sealed with butyl rubber stopper, purged with N_2 for 5 minutes and incubated under anaerobic conditions at 37°C and 150 rpm. Incubation was continued until the accumulated bioH_2 production reached a coefficient of variation below 5%, indicating process stabilization.

Initially, these conditions were tested for raw biomass (RB) and two pretreated biomass samples with the highest CHt content: (1) pretreatment at 180°C for 10 minutes with 75% NbP and (2) pretreatment at 140°C for 70 minutes with 75% NbP. These experiments were performed without pH correction. Subsequently, additional experiments were conducted with pH adjustment to enhance bioH_2 production. The pH was adjusted to 5.0, 5.5, and 6.0 for both RB and the pretreated biomass sample at 180°C for 10 minutes with 75% NbP, which showed the best performance in the initial tests.

8.2.6. Analysis of reaction medium

The analysis of SMPs was conducted to assess the biochemical pathways and metabolic intermediates generated during fermentation. Liquid samples were collected at the beginning and end of the fermentation process and analyzed for organic acids, furans, and other key metabolites.

Prior to analysis, liquid samples were filtered through 0.22 μm pore-size membrane filters to remove particulate matter. Quantitative analysis of SMPs, including formic acid (HFor), acetic acid (HAc), propionic acid (HPr), lactic acid (HLa), butyric acid (HBu), iso-butyric acid (HIBu), levulinic acid (HLe), valeric acid (HVa), iso-valeric acid (HIVa), furfural, and 5-HMF, was performed using high-performance liquid chromatography (HPLC) equipped with a diode array detector (DAD). The HPLC system was configured with a Rezex ROA-Organic Acid H^+ column (Phenomenex) operated at 50°C with 0.005 N sulfuric acid (H_2SO_4) as the mobile phase at a flow rate of 0.6 mL min^{-1} (BLANCO; FUESS; ZAIAT, 2017; PEIXOTO et al., 2011). Calibration curves were generated for each compound using analytical-grade standards to ensure quantification accuracy (ARAUJO et al., 2024). CODt and soluble chemical oxygen demand (CODs) of liquid

samples was measured according to APHA (2012) protocols using a closed reflux colorimetric method. CHt concentration was determined using the phenol-sulfuric acid method (DUBOIS et al., 1956), with spectrophotometric detection at 490 nm against a glucose standard curve. Protein content was determined according to LOWRY et al. (1951). The pH of the fermentation broth was measured using a calibrated digital pH meter.

8.2.7. Reactor monitoring, kinetic investigation, performance assessment, and analytical methods

The reactors were monitored by periodically sampling the gas phase based on quantitative and qualitative measurements of the biogas produced during the incubation period. The headspace pressure of the reactors was tracked using a pressure gauge (Model MDD50, T&S Equipamentos Eletrônicos, São Carlos, SP, Brazil) to quantify the biogas production by measuring internal pressure variation. At the same time, biogas composition analysis (namely H_2, N_2, CH_4, and CO_2) was based on a validated gas chromatography method (ARAUJO et al., 2023). To analyze biogas composition, the biogas samples were collected using 1000 µL insulin syringes fitted with Teflon push-button valves (Supelco™ Analytical – Sigma-Aldrich, Bellefonte, PA, USA). Both procedures utilized a three-way valve to ensure the reactors were properly sealed.

The method used to assess the reactors' bioH_2 production was based on the calculation protocol presented by FUESS et al. (2021). Overall, the calculation protocol used the production of biogas and bioH_2 for the monitoring intervals performed to achieve the cumulative molar bioH_2 production over the incubation period. The modified Gompertz equation (Equation 8.1) (ZWIETERING et al., 1990) was used to fit the experimental cumulative molar bioH_2 production data, and the following kinetic parameters were estimated using the Levenberg Marquardt interaction algorithm in the Origin 2024 version 10.1: The term n_{H2} (t) and *e* are respectively the molar bioH_2 production as a function of the incubation time (t) and the Euler's number (2.71828); P_{maxH_2} is maximum bioH_2 production (mmol); R_{maxH_2} (mmol h^{-1}) is the maximum bioH_2 production rate; λ is the lag phase period (h); and t is the time (h).

$$n_{H_2}(t) = P_{maxH_2} \cdot exp\left\{-exp\left[\frac{R_{maxH_2} \cdot e}{P_{maxH_2}}(\lambda - t) + 1\right]\right\} \qquad \text{(Equation 8.1)}$$

Reactor performance was assessed by calculating the CHt conversion efficiencies (CE_{CHt}) (Equation 8.2) and bioH_2 yields (HY) (Equation 8.3) achieved in each experimental condition tested. The term $[CHt]_i$ is the initial CHt concentration (g L^{-1}); $[CHt]_f$ is the final CHt concentration (g L^{-1}); $n(H_2)_f$ is the total amount of bioH_2 produced at the end of the incubation period (mol); V_f is the final working volume of the reactor (L); and $M_{glucose}$ is the glucose molar mass (180.6 g mol^{-1}). Glucose was used as the reference CHt since it is the primary monosaccharide found in microalgae species such as *Chlorella vulgaris* and *Tetradesmus obliquus* (DO CARMO CESÁRIO et al., 2022; ORTIZ-TENA et al., 2016).

$$CE_{CHt} = \frac{[CHt]_i - [CHt]_f}{[CHt]_i} \cdot 100 \qquad \text{(Equation 8.2)}$$

$$HY = \frac{n(H_2)_f}{\frac{([CHt]_i - [CHt]_f) \cdot V_f}{M_{glucose}}} \qquad \text{(Equation 8.3)}$$

8.3.Results and discussion

8.3.1. Effect of pretreatment conditions on carbohydrate release

The solubilization of fermentable CHt from microalgal biomass was influenced by pretreatment temperature, reaction time, and NbP loading (Figure 8.2). In general, higher temperatures accelerate cell-wall disruption, whereas longer reaction times can degrade the liberated sugars into inhibitory byproducts (NAGARAJAN; CHANG; LEE, 2020). NbP supplementation, in turn, amplifies carbohydrate release by providing Brønsted and Lewis acid sites for hydrolyzing polysaccharides (OLIVEIRA et al., 2023).

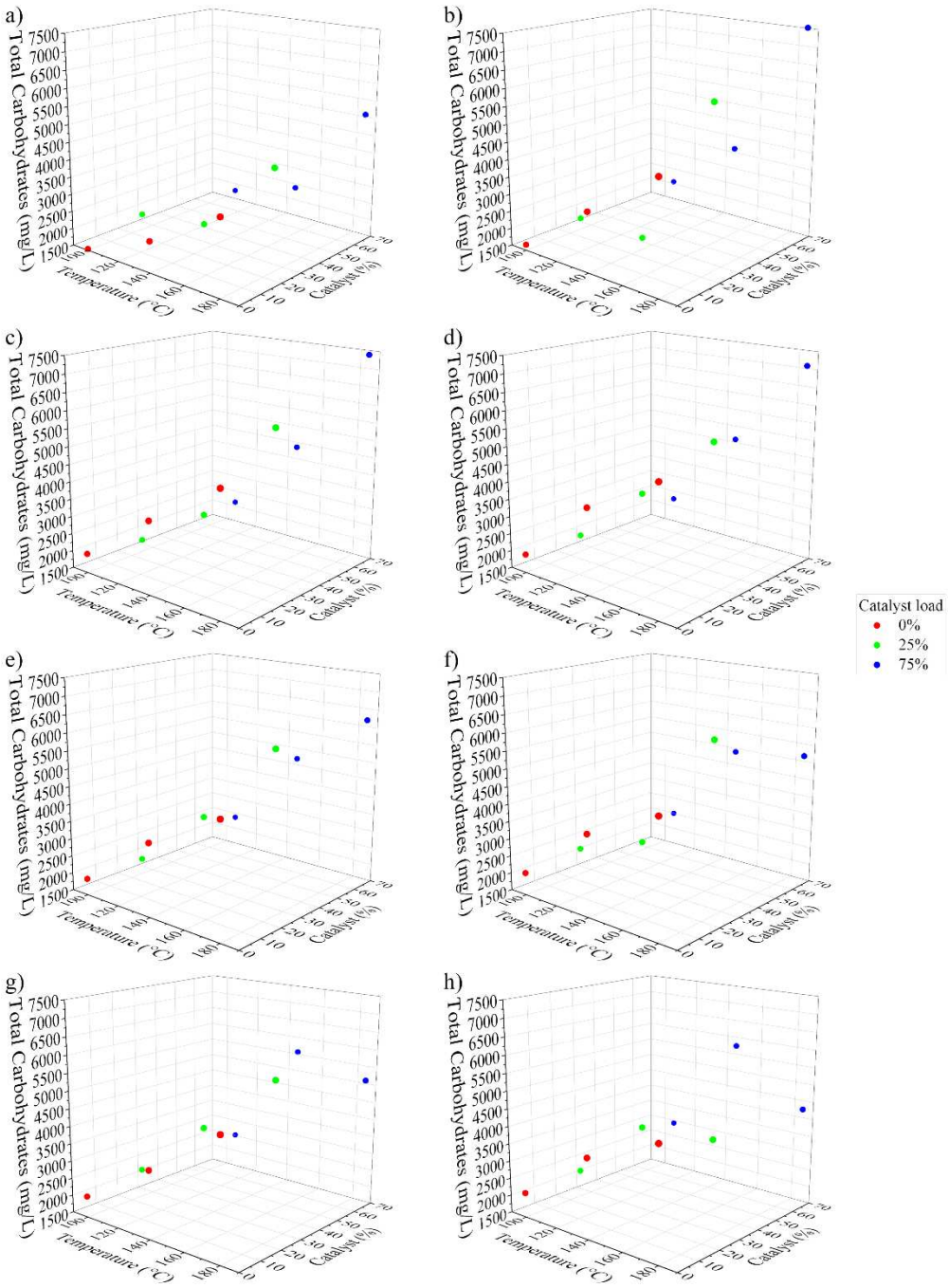

Figure 8.2. Total carbohydrate concentration (mg L^{-1}) as a function of temperature (°C) and catalyst loading (%) at different reaction times: (a) 0 min, (b) 10 min, (c) 20 min, (d) 30 min, (e) 40 min, (f) 50 min, (g) 60 min, and (h) 70 min.

Since the total CHt content in the biomass was 17,019 mg L^{-1}, these solubilized amounts can be translated into overall saccharification yields. CHt release increased steadily as temperatures

rose to 180 °C, peaking at 7,431 ± 226 mg L^{-1} (44% of the total) after 10 min with 75% NbP. These results align with PAL et al. (2024), who observed that microalgal saccharification is comparatively low under mild conditions (120-130 °C, 20-30 min) but rises sharply above 150-160 °C. Likewise, OLIVEIRA et al. (2023) observed that, for sugarcane bagasse, niobium-based catalysis typically operates optimally at 140–200 °C, with sub-140 °C processes often yielding incomplete hydrolysis.

At lower temperatures, such as 100 °C, CHt release was only 2,744 ± 102 mg L^{-1} (16% of the total) after 70 min, indicating that insufficient thermal input fails to break down the microalgal matrix. Intermediate heating of 140 °C yielded 5,460 ± 185 mg L^{-1} (32% of the total) at 70 min. Although higher temperatures favored faster solubilization, prolonged exposure at high severity can degrade the liberated sugars into 5-HMF and furfural (FAHIM; CHENG, 2025). For instance, extending the reaction to 30 min at 180 °C decreased the CHt concentration from 7,431 ± 226 mg L^{-1} (44% of total) to 6,212 ± 189 mg L^{-1} (37% of total) indicating the formation of fermentation inhibitors.

The addition of NbP enhanced CHt release compared to non-catalyzed runs. At 180 °C and 10 min, incrementing the catalyst loading from 0 to 75% boosted CHt by 40% (from 5,315 ± 172 to 7,431 ± 226 mg L^{-1}). Non-catalyzed pretreatment at the same temperature/time yielded 3,942 ± 118 mg L^{-1} (23% of total), illustrating how NbP's Brønsted and Lewis acidic sites effectively split glycosidic bonds (GONÇALVES et al., 2024). Studies show that achieving these efficiency gains frequently requires ≥50% NbP loading (i.e., at least 1:2 w w^{-1} biomass:catalyst), although further increments typically yield diminishing returns once sugar degradation commences (GONÇALVES et al., 2024).

Overall, the most effective condition combined a short reaction time (10 min) with a high temperature (180 °C) and 75% NbP, liberating 7,431 ± 226 mg L^{-1} CHt (44% of the total) while minimizing excessive byproduct formation. Although moderate temperatures (140-160 °C) improve solubilization, stronger thermal inputs can free 20-40% more sugars in far less time, provided that exposure is not prolonged.

8.3.2. Biohydrogen production from pretreated biomass

Dark fermentation of RB yielded only 0.0005 ± 0.02 mmol bioH_2 ($P_{max H_2}$) and 0.00001 ± 0.00 mmol bioH_2 h^{-1} ($R_{max H_2}$), along with a notably extended lag phase of 26.42 ± 1.40 h (Figure 8.3a, Table 8.1). Although these values reflect minimal bioH_2 production, the final CHt

concentration exceeded the initial level, indicating net CHt accumulation. Due to this, a standard HY based on CHt consumption could not be calculated; thus, only the total bioH_2 is reported.

These findings suggest substrate hydrolysis dominated, yet the robust cell wall structure of RB may have hindered the release and fermentation of intracellular sugars, thereby constraining the conversion of hydrolysis products to hydrogen. In line with prior observations for recalcitrant biomasses (AHMAD et al., 2024), this limitation resulted in only modest bioH_2 evolution despite evidence of hydrolysis (increased CHt). However, it is also important to note that the initial microalgal biomass contained about 20% CHt, with the remaining fraction comprising ash and proteins that do not directly contribute to bioH_2 production. Consequently, even if hydrolysis occurs, the limited CHt pool restricts the maximum achievable bioH_2. Thus, although net CHt accumulated, downstream fermentation steps remained insufficient to convert these carbohydrates into hydrogen at higher yields.

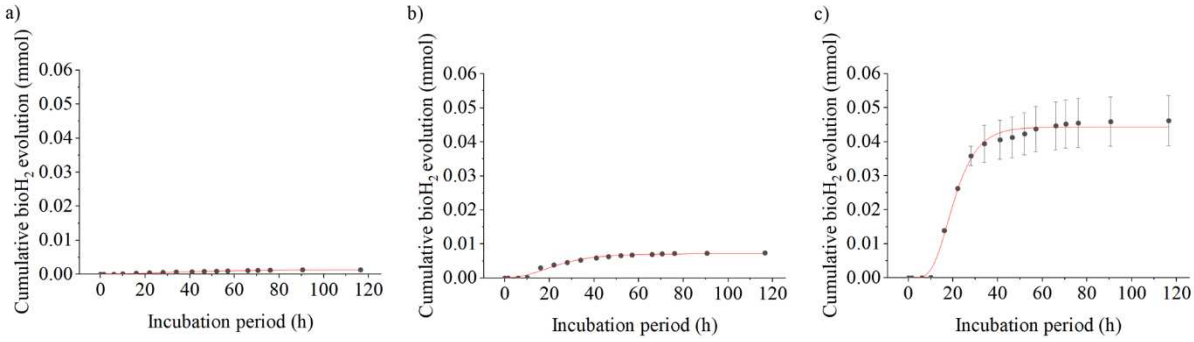

Figure 8.3. Cumulative bioH_2 evolution (mmol) over incubation period under three conditions (without pH adjustment): (a) Raw biomass (RB) without pretreatment, (b) 140 °C with 75% niobium phosphate for 70 min (PB140), and (c) 180 °C with 75% niobium phosphate for 10 min (PB180). Symbols represent experimental data (mean ± standard deviation) and the red lines are the modified Gompertz fits.

Table 8.1. Kinetic parameters from the modified Gompertz equation (P_{maxH2}, R_{maxH2}, λ, R^2), initial and final pH, total carbohydrate conversion efficiency (CE_{CHt}), and bioH_2 yield (HY) for the three experimental conditions (Raw biomass (RB) without pretreatment, 140 °C with 75% niobium phosphate for 70 min (PB140), and 180 °C with 75% niobium phosphate for 10 min (PB180)) without pH adjustment.

Experimental condition		RB	PB140	PB180
Kinetic parameters	PmaxH$_2$ (mmol)	0.0005 ± 0.00002	0.0026 ± 0.0006	0.016 ± 0.0019
	RmaxH$_2$ (mmol h^{-1})	0.00001 ± 0.00	0.00008 ± 0.00001	0.0008 ± 0.00007
	λ (h)	26.42 ± 1.40	18.06 ± 0.99	17.52 ± 0.46
	R^2	0.99	0.98	0.99
Initial pH		7.91 ± 0.15	7.04 ± 0.01	7.06 ± 0.08
Final pH		8.34 ± 0.26	7.16 ± 0.03	6.96 ± 0.04
CECHt (%)		-	70.29 ± 2.79	76.29 ± 3.49
HY (mmol H$_2$ mol^{-1} CHt)		-	0.0035 ± 0.00059	0.016 ± 0.0012

Abbreviations/symbols: P_{maxH_2} – maximum bioH$_2$ production, R_{maxH_2} – maximum bioH$_2$ production rate, λ – lag phase period, R^2 – coefficient of determination used to assess the quality of the fitting, CE_{CHt} – total carbohydrate conversion efficiency, HY – bioH$_2$ yield.

Likewise, SINGH; ROUT; DAS (2022) noted that untreated *Scenedesmus obliquus* showed negligible DF-based hydrogen production. When this microalgal biomass was subjected to an acid-thermal pretreatment at 0.5 N H_2SO_4, 121 °C, for 30 minutes, bioH$_2$ yield jumped to 97.6 mL H_2 g^{-1} VS. This gain in yield was explained by the disruption of rigid algal cell walls, creating easier access to soluble carbohydrates. In the present study, the lag phase of more than 26 h (RB) likely arises from both the intact cell wall structure and any H_2-consuming microbes that persist until accessible substrates become exhausted (AHMAD et al., 2024; D'SILVA et al., 2023). Such constraints severely delay or reduce net bioH$_2$ output under raw conditions.

Treating the biomass at 140 °C for 70 min with NbP raised P_{maxH_2} to 0.0026 ± 0.0006 mmol (Figure 8.3b, Table 8.1), which is approximately five times higher than the raw sample. R_{maxH_2} increased to 0.00008 ± 0.00001 mmol bioH$_2$ h^{-1}, and the lag phase shortened to 18.06 ± 0.99 hours, while CE_{CHt} rose to 70.29 ± 2.79%. This result parallels the gains reported by SINGH; ROUT; DAS (2022), where moderate acid-thermal pretreatments broke down cell structures sufficiently to improve hydrogen production.

However, the overall bioH_2 yield under PB140 (0.0035 ± 0.00059 mmol H_2 mol^{-1} CHt) remained modest compared to previous works. For instance, ROGERI et al. (2023) found a bioH_2 yield of 14 mmol H_2 g^{-1} CHt under optimized conditions, JAIN et al. (2024) achieved 3.0 mol H_2 mol^{-1} glucose in mesophilic digestion of maize stover, and D' SILVA et al. (2021) observed a theoretical maximum of 4 mol H_2 mol^{-1} glucose, with practical yields around 1.84 mol H_2 mol^{-1} glucose. One explanation is that although moderate pretreatment lessens the formation of furfural, 5-HMF, or phenolic inhibitors (JAIN et al., 2024), it may not fully hydrolyze all available polysaccharides. Additionally, because the microalgal biomass has a limited carbohydrate fraction, even complete hydrolysis of those carbohydrates can yield only a finite amount of fermentable sugars. As a result, the remaining resistant fractions and the relatively high protein/ash content limit substrate availability for DF, so despite being better than RB, PB140 still yields suboptimal hydrogen productivity.

By contrast, a higher-severity pretreatment at 180 °C for 10 min with 75% NbP led to more substantial improvements. P_{maxH_2} and R_{maxH_2} increased to 0.016 ± 0.0019 mmol and 0.00084 ± 0.00007 mmol bioH_2 h^{-1}, respectively, marking an order-of-magnitude increase over RB and over six times that of PB140. Furthermore, the bioH_2 yield reached 0.016 ± 0.0012 mmol H_2 mol^{-1} CHt, and the lag phase decreased to 17.52 ± 0.46 hours.

Given that none of the tested pretreatments achieved high yields, further optimization is required. pH, for instance, is widely recognized as a critical factor for balancing the metabolic pathways of bioH_2-producing bacteria and preventing unwanted H_2-consuming processes (D'SILVA et al., 2023; JAIN et al., 2024). Prior studies have found that pH levels between about 5.0 and 6.5 are most favorable for DF of various substrates (ROGERI et al., 2023). Consequently, the next phase of this work focused on DF at different initial pH values (5.0, 5.5, and 6.0) to determine if adjusting acidity can overcome the relatively modest yields observed thus far. Notably, initial pH values in assays RB, PB140, and PB180 were 7.9, 7.0, and 7.1, respectively (Table 8.1).

8.3.3. Analysis of soluble metabolic products in biohydrogen production

Figure 8.4 presents the initial and final levels of CODs, CHt, proteins, and the main SMPs (HAc, HLa, HBu, HPr, HVa, HIVa, and HIBu) during bioH_2 assays with RB and pretreated biomass (PB140 and PB180). Throughout the fermentations, shifts in VFA composition and pH provided insight into the interplay between acidogenesis and methanogenesis.

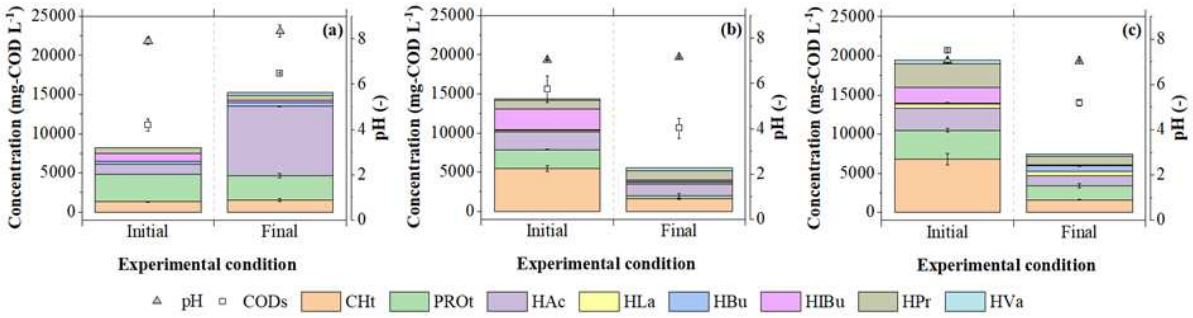

Figure 8.4. Conversion of total carbohydrates (CHt) and production of soluble metabolic products (SMPs) during bioH_2 assays using as substrate raw biomass (RB) and pretreated biomass (PB140 and PB180): (a) RB, (b) PB140, (c) PB180. Legend: CODs = Soluble chemical oxygen demand, CHt = Total carbohydrates, PROt = Total proteins, HAc = Acetic acid, HLa = Lactic acid, HBu = Butyric acid, HPr = Propionic acid, HVa = Valeric acid, HIVa = Isovaleric acid.

Under RB conditions, CODs rose from 11,120 ± 778 to 17,745 ± 35 mg L^{-1}, suggesting that soluble compounds were released from the cells during fermentation. HAc increased substantially (from 1,221 to 8,832 mg COD L^{-1}), while HIVa rose from 111 to 842 mg COD L^{-1}, indicating that even without pretreatment, some hydrolysis still occurred. However, the 5-day incubation period may have been too short to fully convert these VFAs into bioH_2, given the hydrolysis-limiting step in algal biomass fermentation. If more time had been allowed, additional VFA consumption and possibly greater H_2 evolution might have been observed.

In contrast, HBu and HPr declined by 74.7% and 11.4%, respectively, suggesting partial consumption by methanogens. However, the persistence of high HAc levels (rather than being converted to methane) points to the possibility that the methanogenic consortium was predominantly hydrogenotrophic rather than acetoclastic. Indeed, certain inoculum treatments target acetoclastic methanogens more effectively than hydrogenotrophic ones.

The pH shift from 7.91 to 8.34 reflects ammonia (NH_3) release and the consumption of organic acids, commonly associated with methanogenic archaea. This transition drives H_2-consuming pathways, causing any early H_2 generated to be rapidly converted to CH_4 (AMANIDAZ et al., 2023; TREVISAN et al., 2023). Table 8.2 summarizes the data on CH_4 production. Overall, the higher methane production under RB suggests that inoculum pretreatment may not have been

fully effective in suppressing methanogenesis, or that these conditions favored hydrogenotrophic methanogens.

Table 8.2. Kinetic parameters from the modified Gompertz equation for methane (CH_4) (P_{maxCH4}, R_{maxCH4}, λ, R^2), for the three experimental conditions (Raw biomass (RB) without pretreatment, 140 °C with 75% niobium phosphate for 70 min (PB140), and 180 °C with 75% niobium phosphate for 10 min (PB180)) without pH adjustment.

Experimental condition		RB	PB140	PB180
Kinetic parameters	P_{maxCH4} (mmol)	0.080 ± 0.0039	0.0067 ± 0.00091	0.0022 ± 0.00008
	R_{maxCH4} (mmol h^{-1})	0.00093 ± 0.00004	0.00005 ± 0.0000	0.00003 ± 0.0000
	λ (h)	50.20 ± 2.00	82.38 ± 7.33	60.25 ± 1.16
	R^2	0.99	0.98	0.99

Abbreviations/symbols: P_{maxCH4} – maximum methane production, R_{maxCH4} – maximum methane production rate, λ – lag phase period, R^2 – coefficient of determination used to assess the quality of the fitting.

Pretreatment PB140 released 5,445 ± 368 mg COD L^{-1} of CHt, resulting in greater availability of soluble substrates for acidogenic microorganisms compared to RB. Accordingly, the higher initial HAc concentration (2,262 ± 1.51 mg COD L^{-1}), reflected increased acidogenesis. By the end of fermentation, HAc had decreased to 1,514 mg COD L^{-1}, and CODs dropped to 10,620 ± 1,273 mg COD L^{-1}, suggesting more extensive substrate conversion than in the RB trials.

PB180 exhibited an even higher early acidification (2,849 ± 5.18 mg COD L^{-1} of HAc and 3,974 ± 4.67 mg COD L^{-1} of HIBu), which typically correlates with elevated early-stage $bioH_2$ production (COUTO et al., 2025). Despite these strong acidogenesis phases, net $bioH_2$ yields were still relatively low, likely because subsequent methanogenic or other VFA-consuming pathways partially utilized these acids.

In contrast to relying on pH shifts alone, direct CH_4 measurement (Table 8.2) provides clearer evidence of methanogenic activity. RB exhibited the highest maximum CH_4 production

(P_{maxCH_4} = 0.080 ± 0.0039 mmol) and production rate (R_{maxCH_4} = 0.00093 ± 0.00004 mmol h^{-1}), with a lag phase of 50.20 ± 2.00 h. While these values indicate a notable methanogenic route, they do not necessarily mean methanogenesis overwhelmingly dominated; rather, they confirm that the inoculum pretreatment did not fully inhibit the growth or activity of methanogens in the RB condition. By comparison, PB140 and PB180 yielded lower P_{maxCH_4} values (0.0067 ± 0.00091 mmol and 0.0022 ± 0.00008 mmol, respectively) and correspondingly lower CH_4 production rates (R_{maxCH_4} = 0.00005 ± 0.00000 mmol h^{-1} for PB140 and 0.00003 ± 0.00000 mmol h^{-1} for PB180). These data suggest that the severe operating conditions or the presence of niobium phosphate hindered methanogen growth and activity relative to RB.

Taken together, the H_2 and CH_4 production data show that pretreatment increased the pool of readily fermentable substrates, enhancing initial acidogenesis and possibly speeding up early H_2 production by bypassing the prolonged hydrolysis phase. However, pretreatment also appears to suppress methanogenesis to a greater degree than in the RB condition, as evidenced by the lower P_{maxCH_4}. This suppression could be due to the formation of inhibitory compounds, changes in microbial community dynamics, or partial inactivation of methanogens, thereby limiting total methane evolution compared to RB.

8.3.4. pH control on microalgal biohydrogen production

DF of RB at different pH values revealed that pH 5.0 (RB5) was more conducive to bioH_2 production than pH 5.5 (RB5.5) and 6.0 (RB6). Under pH 5.0, P_{maxH_2} and R_{maxH_2} reached 0.058 ± 0.00083 mmol and 0.0035 ± 0.00035 mmol bioH_2 h^{-1}, respectively. CE_{CHt} improved to 52.29 ± 5.32 % (Figure 8.5, Table 8.3). In contrast, when the pH increased to 5.5 and 6.0, P_{maxH_2} dropped to 0.031 ± 0.00047 and 0.021 ± 0.00019 mmol, respectively, and HY likewise decreased from 0.27 ± 0.03 to 0.16 ± 0.01 mmol H_2 mol^{-1} CHt. These findings indicate that pH 5.0 created a more favorable environment for acidogenic bacteria, thereby enhancing bioH_2 production relative to near-neutral conditions.

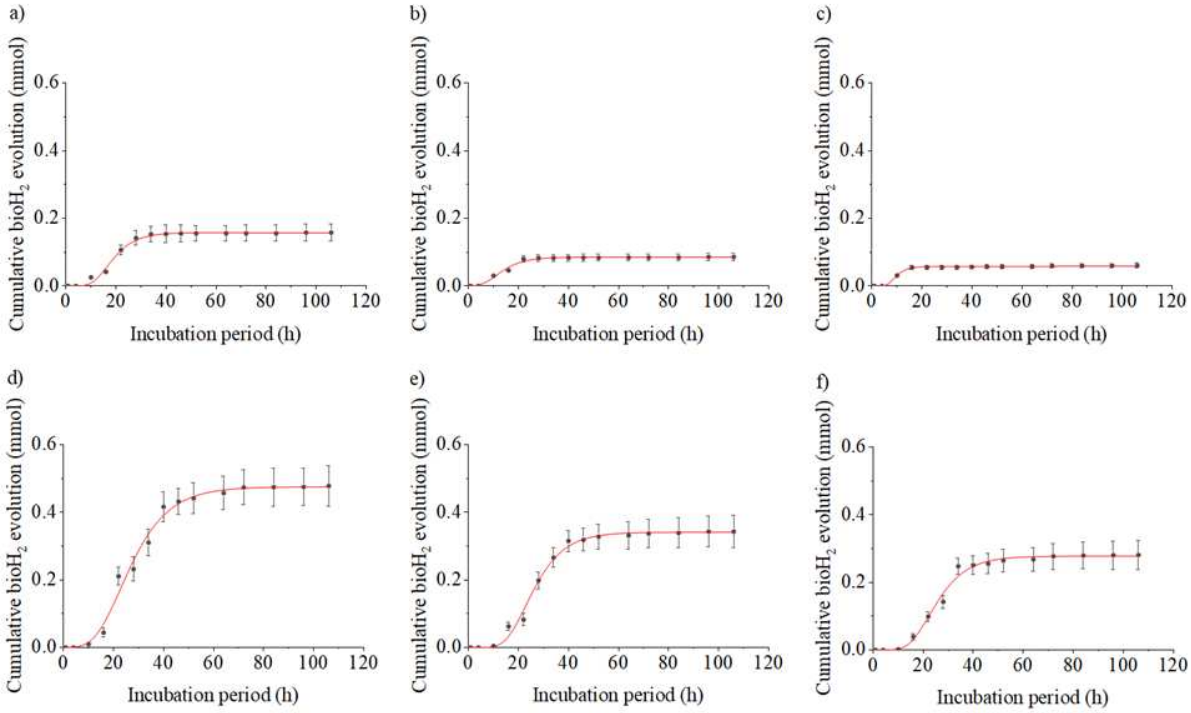

Figure 8.5. Cumulative $bioH_2$ evolution (mmol) for microalgae biomass under six conditions: (a) Raw biomass at pH 5 (RB5), (b) Raw biomass at pH 5.5 (RB5.5), (c) Raw biomass at pH 6 (RB6), (d) Pretreated biomass at 180 °C for 10 minutes, 75 % catalyst, and pH 5 (PB5), (e) Pretreated biomass at 180 °C for 10 minutes, 75 % catalyst, and pH 5.5 (PB5.5), and (f) Pretreated biomass at 180 °C for 10 minutes, 75 % catalyst, and pH 6 (PB6).

Table 8.3. Kinetic parameters from the modified Gompertz equation (P_{maxH2}, R_{maxH2}, λ, R^2), total carbohydrate conversion efficiency (CE_{CHt}), and $bioH_2$ yield (HY) for the experimental conditions (RB5, RB5.5, RB6, PB5, PB5.5, PB6).

Experimental condition		RB5	RB5.5	RB6	PB5	PB5.5	PB6
Kinetic parameters	P_{maxH2} (mmol)	0.058 ± 0.00083	0.031 ± 0.00047	0.021 ± 0.00019	0.175 ± 0.0034	0.125 ± 0.0019	0.102 ± 0.0018
	R_{maxH2} (mmol h^{-1})	0.0035 ± 0.00035	0.0020 ± 0.00023	0.0028 ± 0.00054	0.0061 ± 0.00054	0.0055 ± 0.00046	0.0046 ± 0.00044
	λ (h)	16.46 ± 0.51	11.09 ± 0.56	8.67 ± 0.38	22.84 ± 0.76	23.02 ± 0.57	22.35 ± 0.64
	R^2	0.99	0.99	0.99	0.99	0.99	0.99

CE_{CHt} (%)	52.29 ± 5.32	38.98 ± 2.73	28.04 ± 5.13	83.61 ± 8.51	81.10 ± 9.18	83.37 ± 6.31
HY (mmol H_2 mol^{-1} CHt)	0.44 ± 0.05	0.27 ± 0.03	0.16 ± 0.01	1.03 ± 0.14	0.87 ± 0.06	0.76 ± 0.03

Abbreviations/symbols: P_{maxH2} – maximum bioH_2 production, R_{maxH2} – maximum bioH_2 production rate, λ – lag phase period, R^2 – coefficient of determination used to assess the quality of the fitting, CE_{CHt} – total carbohydrate conversion efficiency, HY – bioH_2 yield.

A key reason pH 5.0 can increase bioH_2 yield is that a more acidic environment fosters acidogenesis and prevents the growth of methanogenic archaea, which typically thrive near neutrality (D'SILVA et al., 2023; ROGERI et al., 2023). Under lower pH, VFAs such as HAc and HBu tend to accumulate, driving hydrogenogenic pathways (JAIN et al., 2024). By maintaining a pH around 5, methanogens, especially those sensitive to acidic conditions, are effectively suppressed. Meanwhile, methanogenic activity can be further controlled or delayed by implementing a sequential fermentation approach, where H_2 production occurs first under acidic conditions (favoring acidogenic bacteria while suppressing methanogens), and methane production is only initiated in a second-stage biomethanation process if desired (SINGH; ROUT; DAS, 2022).

Pretreated biomass at 180 °C for 10 minutes and 75 % NbP exhibited a similar pH-dependent trend. At pH 5.0 (PB5), P_{maxH_2} ascended to 0.175 ± 0.0034 mmol, tenfold higher than that of raw biomass at pH 5.0 (RB5). CE_{CHt} rose to 83.61 ± 8.51 %, and the bioH_2 yield peaked at 1.03 ± 0.14 mmol H_2 mol^{-1} CHt (Table 2, Figure 5). The combined effects of hydrothermal pretreatment and acidic conditions thus enhanced hydrogenogenesis, due to increased substrate availability (from pretreatment) and minimized methanogenic competition (due to pH 5.0). These results parallel findings by MARTÍNEZ-FRAILE et al. (2024) and REGUEIRA-MARCOS; GARCÍA-DEPRAECT; MUÑOZ (2023), who reported that maintaining a pH range of about 5.0 to 5.5 effectively supports acidogenic bacteria while hindering acetoclastic and hydrogenotrophic methanogens.

By contrast, at pH 5.5 (PB5.5) and 6.0 (PB6), P_{maxH_2} decreased to 0.125 ± 0.0019 and 0.102 ± 0.0018 mmol, respectively, accompanied by lower conversion efficiencies and hydrogen yields (0.87 ± 0.06 and 0.76 ± 0.03 mmol H_2 mol^{-1} CHt, respectively). These declines are consistent with partial activation of methanogenic pathways under slightly higher pH, which can divert metabolic flux away from bioH_2 production (ROGERI et al., 2023).

The influence of pH on microbial metabolism is further evidenced by changes in VFA distribution and the presence of potential inhibitors. At pH 5.0, HLa was likely metabolized into HAc and HBu, favoring net bioH_2 yields. This observation aligns with Rogeri et al. (ROGERI et al., 2024), who achieved up to 17.2 mmol H_2 g^{-1} CHt in thermophilic sugarcane vinasse fermentation under acidic conditions, highlighting the important role of pH in maintaining improved bioH_2 production.

8.3.5. Impact of pH adjustment in soluble metabolic products

Applying pH 5.0 to pretreated biomass (PB5) led to an increase in CHt consumption, decreasing from about 7000 mg COD L^{-1} to only 1200-1400 mg COD L^{-1}, demonstrating high hydrolysis and fermentation efficiency (Figure 8.6). The concentration of HAc rose from 2849 ± 5.18 mg COD L^{-1} to over 4000 mg COD L^{-1} during the initial fermentation stages before stabilizing when H_2 production peaked. HBu levels also increased, highlighting its role as a key acidogenic intermediate in bioH_2 production (CHEN et al., 2023). Notably, inhibitory 5-HMF fell from 87 ± 3 mg COD L^{-1} to 22 ± 3 mg COD L^{-1}, indicating effective partial detoxification via microbial metabolism or adsorption onto cells.

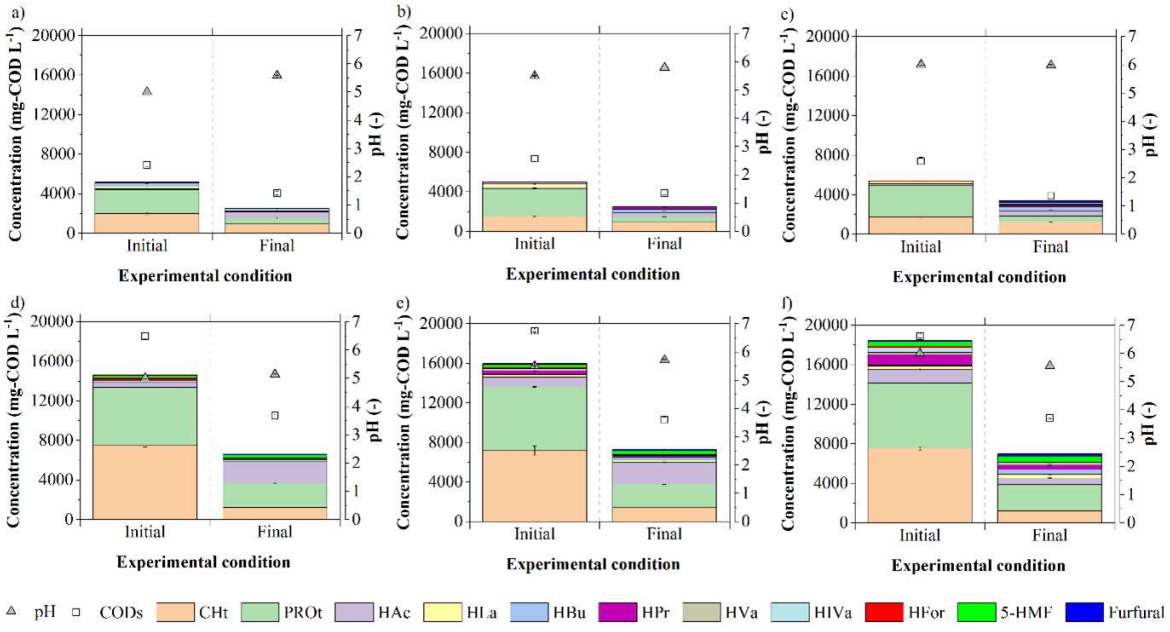

Figure 8.6. Initial vs. final pH, CODs, CHt, proteins, major organic acids (HAc, HLa, HBu, HPr, HVa, HIVa), formic acid (HFor), and furanic compounds (5-HMF, furfural) for (a) RB5, (b) RB5.5,

(c) RB6, (d) PB5, (e) PB5.5, and (f) PB6. Legend: CODs = Soluble chemical oxygen demand, CHt = Total carbohydrates, PROt = Total proteins, HAc = Acetic acid, HLa = Lactic acid, HBu = Butyric acid, HPr = Propionic acid, HVa = Valeric acid, HIVa = Isovaleric acid.

Controlling the pH around 5.0 to 5.2 effectively maintains acidogenic dominance, facilitating the production of VFAs such as HAc and HBu, which are indicative of hydrogenogenic activity (ANZOLA-ROJAS et al., 2025). Lower pH values also minimize methanogenic uptake of VFAs and H_2 (AMANIDAZ et al., 2023). The observed transition from HLa to HAc and HBu at pH 5.0 suggests a metabolic rerouting that enhances HLa consumption and VFA accumulation, indirectly supporting bioH_2 production. This aligns with findings from ROGERI et al. (2023), who reported that maintaining the effluent pH between 5.0 and 5.5 maximized VFA production and bioH_2 yields.

8.3.6. Future perspectives and Limitations

The development of microalgal bioH_2 production systems using hydrothermal pretreatment and NbP presents opportunities for optimization and innovation. However, before contemplating large-scale implementation, fundamental technical challenges, particularly the low bioH_2 yields, must be addressed. Key limitations, such as catalyst recovery, energy efficiency, and byproduct formation, continue to constrain overall performance.

One promising perspective involves improving the recovery and reusability of NbP, a critical component for efficient CHt hydrolysis. Preliminary attempts to physically separate microalgae from niobium phosphate by lyophilizing the solid content revealed that both materials form powders, making separation challenging. In this context, an efficient separation technique must be developed to recover the catalyst and enable its repeated use, thereby reducing both economic and environmental impacts. Advanced techniques such as magnetic immobilization, membrane separation, or the development of alternative, more cost-effective solid acid catalysts could further enhance NbP's economic feasibility (GONÇALVES et al., 2024; SOUZANCHI et al., 2023). Furthermore, long-term studies on the stability of NbP under hydrothermal conditions are needed to verify its viability in repeated cycles.

Energy efficiency is another critical area of improvement. Integrating energy recovery systems, such as waste heat capture from hydrothermal pretreatment, can reduce the energy

footprint of the process. Coupling bioH_2 production with anaerobic digestion of the residual biomass creates a two-stage approach that maximizes energy recovery. However, even with this integration, the high temperatures (e.g., 180 °C) used during pretreatment may still outweigh the gains from the resulting bioH_2, potentially leading to a negative net energy balance. Robust energy assessments are essential to determine whether such integrations are sufficient to achieve net energy gains.

From a biorefinery perspective, integrating bioH_2 production with other processes, such as nutrient recovery from wastewater or the production of co-products like biofertilizers or biochar, could improve economic feasibility and sustainability (FUENTES-SANTIAGO et al., 2023). Nevertheless, the viability of a standalone bioH_2 process remains low unless yields are substantially increased or the process is effectively integrated into a broader circular bioeconomy framework.

Real-time monitoring and advanced control systems using machine learning or artificial intelligence could enhance reactor performance and process stability. These tools can dynamically optimize pH, temperature, and other parameters to maximize bioH_2 yields and minimize inhibitory effects (ANZOLA-ROJAS et al., 2025; MARTÍNEZ-FRAILE et al., 2024).

Finally, life cycle assessment (LCA) and techno-economic analysis (TEA) are indispensable for evaluating the scalability and sustainability of microalgal bioH_2 production. These tools can identify critical points for optimization, such as energy inputs, catalyst costs, and wastewater treatment benefits (FAHIM; CHENG, 2025; ROGERI et al., 2023). Their application can help pinpoint the most impactful areas for improvement and quantify potential benefits associated with wastewater treatment or resource recovery.

In conclusion, although this study has demonstrated the potential for hydrothermal pretreatment, NbP catalysis, and pH control to enhance microalgal bioH_2 production, further work is needed to overcome low yields, optimize catalyst recovery, and improve energy balance. Addressing these technical hurdles is crucial for the development of a truly sustainable and economically viable bioH_2 production platform.

8.4.Conclusions

This study explored the integration of hydrothermal pretreatment, niobium phosphate (NbP) catalysis, and pH control to enhance bioH_2 production from wastewater-grown microalgal biomass. Pretreatment at 180 °C with 75 % NbP solubilized up to 7,431 mg CHt L^{-1}, while

maintaining pH at 5.0 promoted acidogenic pathways, yielding 1.03 mmol H_2 mol^{-1} CHt, a nearly tenfold improvement over untreated biomass. Although the acidic properties of NbP likely facilitated cell wall hydrolysis, the formation and detoxification of potential inhibitory byproducts (e.g., 5-HMF) remain to be fully verified.

To move forward, further efforts should focus on increasing bioH_2 yields via process optimization, integrating energy recovery to address the high thermal requirements, and improving NbP catalyst reusability. Employing life cycle and techno-economic analyses will be crucial for evaluating the overall sustainability and cost-effectiveness of this approach. Ultimately, incorporating biohydrogen production into wastewater valorization holds promise for advancing sustainable energy generation and fostering a circular bioeconomy.

Acknowledgments

This study was financed in part by the Coordenação de Aperfeiçoamento de Pessoal de Nível Superior – Brasil (CAPES) – Finance Code 001. Furthermore, the authors gratefully acknowledge the financial support of the Conselho Nacional de Desenvolvimento Científico e Tecnológico (CNPq) [Grant Numbers: 405787/2022-7, 406204/2022-5, and 403521/2023-8] and Fundação de Amparo à Pesquisa do Estado de Minas Gerais (FAPEMIG) [Grant Numbers: APQ-03618-23, APQ-00756-23, and RED 00068-23].

References

ABNT. Produtos químicos — Informações sobre segurança, saúde e meio ambiente Parte 2: Sistema de classificação de perigo. . 2009, p. 1–106.

AHMAD, A. et al. Biohydrogen production through dark fermentation: Recent trends and advances in transition to a circular bioeconomy. **International Journal of Hydrogen Energy**, v. 52, p. 335–357, 2 jan. 2024.

AHMED, S. F. et al. Biohydrogen production from wastewater-based microalgae: Progresses and challenges. **International Journal of Hydrogen Energy**, v. 47, n. 88, p. 37321–37342, out. 2022.

AMANIDAZ, N. et al. Volatile fatty acids and ammonia recovery, simultaneously cathodic hydrogen production and increasing thermophilic dark fermentation of food waste efficiency. **International Journal of Hydrogen Energy**, v. 48, n. 40, p. 15026–15036, 8 maio 2023.

ANZOLA-ROJAS, M. DEL P. et al. Hydrogen production from fermented sugarcane vinasse and its utilization by biosynthesis processes in a single-chambered microbial electrolysis cell. **International Journal of Hydrogen Energy**, v. 100, p. 49–57, 27 jan. 2025.

AOAC. **Official methods of analysis**. 11th. ed. Washington: Association of Official Analytical Chemists, 1990.

APHA. **Standard Methods for examination of water and wastewater**. Washington: American Water Work Association, Water Environmental Federation, 2012.

ARAUJO, M. N. et al. Rapid method for determination of biogas composition by gas chromatography coupled to a thermal conductivity detector (GC-TCD). **International Journal of Environmental Analytical Chemistry**, p. 1–18, 15 maio 2023.

ARAUJO, M. N. et al. Fixed bed in dark fermentative reactors: is it imperative for enhanced biomass retention, biohydrogen evolution and substrate conversion? **International Journal of Hydrogen Energy**, v. 52, p. 228–245, 2 jan. 2024.

ASSIS, L. R. DE et al. Innovative hybrid system for wastewater treatment: High-rate algal ponds for effluent treatment and biofilm reactor for biomass production and harvesting. **Journal of Environmental Management**, v. 274, 15 nov. 2020.

BLANCO, V. M. C.; FUESS, L. T.; ZAIAT, M. Calcium dosing for the simultaneous control of biomass retention and the enhancement of fermentative biohydrogen production in an innovative fixed-film bioreactor. **International Journal of Hydrogen Energy**, v. 42, n. 17, p. 12181–12196, 2017.

BLANCO, V. M. C.; OLIVEIRA, G. H. D.; ZAIAT, M. Dark fermentative biohydrogen production from synthetic cheese whey in an anaerobic structured-bed reactor: Performance evaluation and kinetic modeling. **Renewable Energy**, v. 139, p. 1310–1319, ago. 2019.

CASTELLÓ, E. et al. Stability problems in the hydrogen production by dark fermentation: Possible causes and solutions. **Renewable and Sustainable Energy Reviews**, v. 119, p. 109602, mar. 2020.

CHEN, C. et al. Screening of microalgae strains for efficient biotransformation of small molecular organic acids from dark fermentation biohydrogen production wastewater. **Bioresource Technology**, v. 390, 1 dez. 2023.

COUTO, P. T. et al. Dynamic modelling of mono- and disaccharide fermentation in an anaerobic fixed-bed reactor. **Renewable Energy**, v. 243, p. 122534, abr. 2025.

D’ SILVA, T. C. et al. Enhancing methane production in anaerobic digestion through hydrogen assisted pathways – A state-of-the-art review. **Renewable and Sustainable Energy Reviews**, v. 151, p. 111536, nov. 2021.

D’SILVA, T. C. et al. Biohydrogen production through dark fermentation from waste biomass: Current status and future perspectives on biorefinery development. **Fuel**, v. 350, p. 128842, out. 2023.

DO CARMO CESÁRIO, C. et al. Biochemical and morphological characterization of freshwater microalga Tetradesmus obliquus (Chlorophyta: Chlorophyceae). **Protoplasma**, v. 259, n. 4, p. 937–948, 13 jul. 2022.

DUBOIS, MICHEL. et al. Colorimetric Method for Determination of Sugars and Related Substances. **Analytical Chemistry**, v. 28, n. 3, p. 350–356, mar. 1956.

FAHIM, R.; CHENG, L. **Biohydrogen production from spent wastewater treatment Substrates: Techno-Economic viability and sustainability**. **Sustainable Energy Technologies and Assessments**Elsevier Ltd, , 1 mar. 2025.

FUENTES-SANTIAGO, V. et al. Carbohydrates/acid ratios drives microbial communities and metabolic pathways during biohydrogen production from fermented agro-industrial wastewater. **Journal of Environmental Chemical Engineering**, v. 11, n. 3, 1 jun. 2023.

FUESS, L. T. et al. Biohydrogen-producing from bottom to top? Quali-quantitative characterization of thermophilic fermentative consortia reveals microbial roles in an upflow fixed-film reactor. **Chemical Engineering Journal Advances**, v. 7, 15 ago. 2021.

FUESS, L. T.; ZAIAT, M.; DO NASCIMENTO, C. A. O. Novel insights on the versatility of biohydrogen production from sugarcane vinasse via thermophilic dark fermentation: Impacts of pH-driven operating strategies on acidogenesis metabolite profiles. **Bioresource Technology**, v. 286, 1 ago. 2019.

GIELEN, D. et al. The role of renewable energy in the global energy transformation. **Energy Strategy Reviews**, v. 24, p. 38–50, abr. 2019.

GONÇALVES, I. M. et al. Use and reuse of niobium phosphate catalyst for the removal of hemicellulose and production of furfural from raw bagasse, straw, and energy sugarcane. **Biomass and Bioenergy**, v. 188, 1 set. 2024.

IEA. **Renewables 2024 - Global overview**. Disponível em: <https://www.iea.org/reports/renewables-2024/global-overview>. Acesso em: 11 fev. 2025.

JAIN, R. et al. **Bio-hydrogen production through dark fermentation: an overview**. **Biomass Conversion and Biorefinery**Springer Science and Business Media Deutschland GmbH, , 1 jun. 2024.

KOMAREK, J.; FOTT, B. **Das Phytoplankton im Susswasser Chlorophyceae (Grunanlagen) Ordnung: Chlorococcales: Bd 7 1.** [s.l.] Schweizerbart'sche, E., 1983.

LOWRY, O. H. et al. Protein Measurement With The Folin Phenol Reagent. **Journal of Biological Chemistry**, v. 193, n. 265, 1951.

MAGALHÃES, I. B. et al. Advancements in high-rate algal pond technology for enhanced wastewater treatment and biomass production: A review. **Journal of Water Process Engineering**, v. 66, p. 105929, set. 2024.

MARTÍNEZ-FRAILE, C. et al. Biohydrogen production by lactate-driven dark fermentation of real organic wastes derived from solid waste treatment plants. **Bioresource Technology**, v. 403, 1 jul. 2024.

NAGARAJAN, D.; CHANG, J. S.; LEE, D. J. **Pretreatment of microalgal biomass for efficient biohydrogen production – Recent insights and future perspectives**. **Bioresource Technology**Elsevier Ltd, , 1 abr. 2020.

OLIVEIRA, L. et al. **Niobium: The Focus on Catalytic Application in the Conversion of Biomass and Biomass Derivatives**. **Molecules**MDPI, , 1 fev. 2023.

ORTIZ-TENA, J. G. et al. Revealing the diversity of algal monosaccharides: Fast carbohydrate fingerprinting of microalgae using crude biomass and showcasing sugar distribution in Chlorella vulgaris by biomass fractionation. **Algal Research**, v. 17, p. 227–235, jul. 2016.

PAL, D. et al. The generation of biohydrogen from pretreated algal biomass in batch fermentation mode. **International Journal of Hydrogen Energy**, fev. 2024.

PARRA, O.; GONZALEZ, M.; DELLAROSSA, V. Manual Taxonómico del Fitoplancton de Aguas Continentales. V. Chlorophyceae. n. January, 1983.

PEIXOTO, G. et al. Hydrogen production from soft-drink wastewater in an upflow anaerobic packed-bed reactor. **International Journal of Hydrogen Energy**, v. 36, n. 15, p. 8953–8966, 2011.

PENTEADO, E. D. et al. **Influence of seed sludge and pretreatment method on hydrogen production in packed-bed anaerobic reactors**. International Journal of Hydrogen Energy. **Anais**...10 maio 2013.

PRIYA, A. et al. **Innovative strategies in algal biomass pretreatment for biohydrogen production**. **Bioresource Technology**Elsevier Ltd, , 1 fev. 2023.

REGUEIRA-MARCOS, L.; GARCÍA-DEPRAECT, O.; MUÑOZ, R. Elucidating the role of pH and total solids content in the co-production of biohydrogen and carboxylic acids from food waste via lactate-driven dark fermentation. **Fuel**, v. 338, 15 abr. 2023.

ROGERI, R. C. et al. Strategies to control pH in the dark fermentation of sugarcane vinasse: Impacts on sulfate reduction, biohydrogen production and metabolite distribution. **Journal of Environmental Management**, v. 325, 1 jan. 2023.

ROGERI, R. C. et al. Methane production from sugarcane vinasse: The alkalinizing potential of fermentative-sulfidogenic processes in two-stage anaerobic digestion. **Energy Nexus**, v. 14, p. 100303, jul. 2024.

SILVA, T. A. et al. Enhancing microalgae biomass production: Exploring improved scraping frequency in a hybrid cultivation system. **Journal of Environmental Management**, v. 355, p. 120505, mar. 2024.

SINGH, H.; ROUT, S.; DAS, D. Dark fermentative biohydrogen production using pretreated Scenedesmus obliquus biomass under an integrated paradigm of biorefinery. **International Journal of Hydrogen Energy**, v. 47, n. 1, p. 102–116, jan. 2022.

SOUZANCHI, S. et al. 5-HMF production from industrial grade sugar syrups derived from corn and wood using niobium phosphate catalyst in a biphasic continuous-flow tubular reactor. **Catalysis Today**, v. 407, p. 274–280, 1 jan. 2023.

TREVISAN, A. P. et al. Reaching the operating limit of the continuous multiple tube reactor: Still a promising technology for maximizing fermentative biohydrogen production? **Biochemical Engineering Journal**, v. 200, 1 nov. 2023.

TUNÇAY, E. G. et al. Dark fermentative hydrogen production from sucrose and molasses. **International Journal of Energy Research**, v. 41, n. 13, p. 1891–1902, 25 out. 2017.

UTERMÖHL, H. Zur vervollkommnung der quantitativen phytoplankton-methodik. **Mitteilung Internationale Vereinigung fuer Theoretische unde Amgewandte Limnologie**, v. 9, p. 1–38, 1958.

ZWIETERING, M. H. et al. Modeling of the Bacterial Growth Curve. **Applied and Environmental Microbiology**, v. 56, n. 6, p. 1875–1881, jun. 1990.

9. Capítulo VI. Wastewater-grown microalgae as substrate for biohydrogen production: An economic and life cycle approach

Abstract: This study evaluates the techno-economic and environmental aspects of biohydrogen ($bioH_2$) production from wastewater-grown microalgae. Two scenarios were examined: direct dark fermentation (SC1) and hydrothermal pretreatment prior to fermentation (SC2). SC1 yielded 0.005 kg h^{-1} of H_2 while requiring moderate steam consumption (108.39 kg h^{-1}). SC2, which includes hydrothermal pretreatment at 180 °C, achieves a higher $bioH_2$ yield of 0.0085 kg h^{-1} but demands more steam (2922.93 kg h^{-1}), leading to elevated capital and operating costs. Despite its improved productivity, SC2's minimum selling price (MSP) remains at 4.98 USD L^{-1}, still above competitive thresholds, while its energy-intensive nature increases global warming potential, tropospheric ozone formation, and particulate matter emissions. Heat recovery (713.7 kg h^{-1}) and renewable energy integration can mitigate some of these impacts. Future research should explore strategies such as catalytic enhancement, co-substrate utilization, and improved energy integration to enhance productivity and commercial feasibility.

Keywords: Dark fermentation; Pretreatment; Niobium phosphate; Economic analysis; Environmental impact.

9.1. Introduction

The growing global demand for cleaner, more sustainable energy sources has driven hydrogen (H_2) into the spotlight as a promising fuel. Unlike traditional fossil fuels, hydrogen combustion produces water rather than carbon dioxide (CO_2), making it a key contender for decarbonizing strategic sectors of the economy, including transportation, industry, and power generation (SALAKKAM et al., 2021). However, most hydrogen in use today is produced via fossil-based process with considerable greenhouse gas (GHG) emissions (KAYFECI; KEÇEBAŞ; BAYAT, 2019). Consequently, there is a need to develop and improve alternative hydrogen production pathways with lower carbon footprints and reduced environmental impact.

Biohydrogen ($bioH_2$) production from wastewater-grown microalgae has attracted attention as a sustainable route for hydrogen generation (AHMED et al., 2022; LEONG et al., 2023; RAZU; HOSSAIN; KHAN, 2019). Microalgae offer several advantages such as (i) rapid growth rates, (ii)

high photosynthetic efficiency, and (iii) the ability to utilize wastewater as a nutrient source (CALIJURI et al., 2022). By integrating algae cultivation with wastewater treatment, it is possible to achieve both biomass production and water remediation in a single platform, thereby reducing or even eliminating the need for external sources of fresh water, nitrogen (N), and phosphorus (P) (MAGALHÃES et al., 2024).

Despite these advantages, practical implementation of microalgal bioH_2 production faces several bottlenecks, especially regarding low hydrogen yields and high operational costs (AHMED et al., 2022). Dark fermentation (DF) has been proposed as a promising method to convert microalgal biomass into H_2 under anaerobic conditions (RADY; ALI; EL-SHEEKH, 2024). However, wastewater-grown microalgae, such as *Chlorella vulgaris* and *Tetradesmus obliquus*, have a robust cell-wall (SHARMA et al., 2025). It can restrict carbohydrate availability for fermentative microbes, thereby limiting H_2 production. Hydrothermal pretreatment (HTP) is one strategy to overcome this barrier by breaking down the microalgal cell wall and enhancing substrate digestibility. Yet, the additional energy and cost associated with high-temperature pretreatment pose economic and environmental trade-offs that need comprehensive evaluation (CHEN; QUINN, 2021).

In this context, this work proposes to perform an integrated techno-economic analysis and life cycle assessment (LCA) of fermentative hydrogen production using wastewater-grown microalgae as the primary substrate, where the microalgal biomass undergoes HTP with niobium phosphate (NbP) as a catalyst. While previous research has investigated fermentative biohydrogen from microalgae, none has combined (i) a catalytic pretreatment step involving NbP to enhance substrate digestibility, (ii) wastewater-grown microalgae biomass to recover feedstock from sanitation and aim for circular economy, and (iii) a parallel TEA-LCA evaluation. By addressing capital investment, processing costs, minimum selling price, and environmental impacts such as global warming potential, tropospheric ozone formation, particulate matter, and resource depletion, this work presents a comprehensive assessment of a novel and potentially more sustainable pathway for bioH_2 production.

9.2.Material and methods

9.2.1. Experimental Design

Experimental data were obtained from DF experiments (Capítulo 5) using microalgae cultivated in wastewater as the substrate and anaerobic sludge from a septic tank as the inoculum. Hydrothermal pretreatment of microalgae biomass at 180°C for 10 minutes with 75% niobium phosphate, followed by fermentation at pH 5.0, resulted in the release of 7,431 mg L^{-1} of total carbohydrates (CHt) and achieved a biohydrogen yield of 1.03 mmol H_2 mol^{-1} CHt. In contrast, fermentation of raw microalgal biomass at pH 5.0 yielded only 0.44 ± 0.05 mmol H_2 mol^{-1} CHt.

9.2.2. Biohydrogen production process simulation

The simulation of bioH_2 production from wastewater-grown microalgae was carried out using Aspen Plus V14. Two distinct scenarios were evaluated. In the first scenario (SC1), fermentation was performed directly from raw microalgae biomass. In the second scenario (SC2), the process occurred in two stages: (1) HTP at 180 °C for 10 minutes with 75% NbP, followed by (2) DF (Figure 9.1).

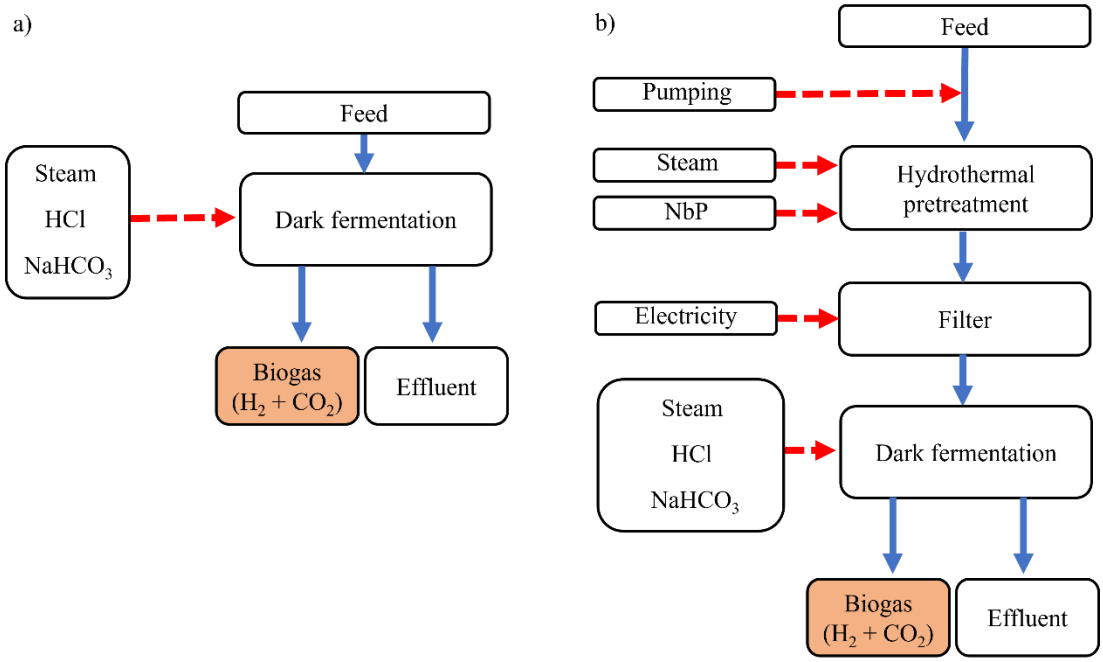

Figure 9.1. Systematic diagram for the conversion of microalgae to biohydrogen. a) SC1 – Raw biomass, b) SC2 – Pretreated biomass. Note: HCl = Hydrochloric acid, $NaHCO_3$ = Sodium bicarbonate, NbP = Niobium phosphate.

The fermentation time was established based on experimental data from SC2, which yielded the highest H_2 production. The chosen criterion focused on production stabilization, considering the time required for the coefficient of variation (CV) in H_2 production between consecutive samples to drop below 4%. The fermentation time determined in this manner was then applied to experiment RB5.

All simulations were performed under steady-state conditions using the Soave-Redlich-Kwong (SRK) thermodynamic model to predict the system's thermodynamic properties. The microalgae were modeled as a nonconventional component, with physicochemical properties estimated using the HCOALGEN model. This estimation employed proximate analysis data (moisture, fixed carbon, volatile matter, and ash content) and ultimate analysis data (carbon, hydrogen, nitrogen, chlorine, sulfur, and oxygen contents), including organic sulfur content (SULTANAL).

For both scenarios, the process was designed to operate with a feed flow rate of 2140.7 kg h^{-1}, composed of microalgae at 6% solids on a dry basis. The pretreatment in SC2 and fermentation reactors were modeled using RYield blocks, which allowed product yields to be specified according to the reactants. During fermentation, the medium's pH was considered as adjusted with hydrochloric acid (HCl) 30% solution, and sodium bicarbonate ($NaHCO_3$) was added as a buffering agent to ensure favorable conditions for microbial conversion (FUESS et al., 2021). In both scenarios, the infrastructure required for microalgae cultivation was excluded from the scope assuming that it would already be necessary for wastewater treatment.

9.2.3. Economic analysis

For the economic analysis, it was considered a plant operating 24 hours per day, divided into three 8-hour shifts, for 330 days per year, reserving 35 days for maintenance tasks (CHEN; QUINN, 2021; JONES et al., 2014). The plant's useful life was defined as 20 years, with a construction and installation period of 3 years. The equipment acquisition cost was obtained using the Aspen Process Economic Analyzer package. Subsequently, using the economic feasibility spreadsheet formulated by PETERS; TIMMERHAUS; WEST (2003), the selling price of the bioH_2 was estimated, achieving a payback period of 3.6 years. The MSP was calculated based on capital investment and processing costs, ensuring zero net present value (NPV). The fixed capital investment (FCI) was estimated using a Lang factor 4.3, and the working capital cost was

calculated as 12% of FCI. Although the hourly wage rate typically varies based on time and location, an annual salary of 24,000 USD per employee was considered. Microalgae biomass was assumed to be produced on-site for 640 USD ton^{-1} (ACIÉN FERNÁNDEZ; FERNÁNDEZ SEVILLA; MOLINA GRIMA, 2019). Concerning HCl, in 2021, the price of HCl 33% was reported to be approximately 300 USD m^{-3} (ABDEL-FATAH; HAWASH; SHAARAWY, 2021). Adjusting for concentration, a 30% HCl solution would cost proportionally less, being 90.9% of the 33% solution price, equating to 273 USD m^{-3}. This adjustment was necessary because, in the tool used for environmental analysis, the process related to HCl is only available for HCl at 30% concentration (PRÉ, 2020). Based on an inflation calculation from 2021 to 2025 (U.S. BUREAU OF LABOR STATISTICS, 2025), the projected price of 30% HCl in 2025 would be approximately 330 USD m^{-3}. The price of $NaHCO_3$ was considered as 435 USD ton^{-1} according to CHEMANALYST (2025). Additionally, the cost of steam was taken as 6 USD ton^{-1}, as referenced by PETERS; TIMMERHAUS; WEST (2003). Economic parameters are summarized in Table 9.1 (Table S9.1, Apêndice VII presents the complete economic assessment parameters across both scenarios).

Table 9.1. Summary of cost parameters for the economic analysis of the microalgae biomass to biohydrogen conversion process.

Parameter	20 years horizon	References
Internal rate of return	10%	MASOUMI; DALAI (2021)
Operating hours per year	7920	MASOUMI; DALAI (2021)
Lang factor	4.3 for fixed capital investment (FCI)	MASOUMI; DALAI (2021)
Working capital cost	12% of FCI	MASOUMI; DALAI (2021)
Operating labor	24,000 USD/year per employee	MASOUMI; DALAI (2021)
Supervisory and clerical labor	15% of labor cost	MASOUMI; DALAI (2021)
Maintenance and repairs	6% of FCI	MASOUMI; DALAI (2021)
Operating supplies	15% of maintenance and repairs	MASOUMI; DALAI (2021)
Local taxes	1% of FCI	MASOUMI; DALAI (2021)

Parameter	20 years horizon	References
Insurance	1% of FCI	MASOUMI; DALAI (2021)
Overhead	60% of (operating labor, supervision, and maintenance)	MASOUMI; DALAI (2021)
Capital charge	12% of FCI	MASOUMI; DALAI (2021)
Depreciation	10% of FCI	MASOUMI; DALAI (2021)
Administrative cost	25% of overhead	MASOUMI; DALAI (2021)
Distribution and selling costs	5% of total expenses	PETERS; TIMMERHAUS; WEST (2003)
Research and development	4% of total expenses	PETERS; TIMMERHAUS; WEST (2003)
Income tax rate	21%	PETERS; TIMMERHAUS; WEST (2003)
Feedstock		PETERS; TIMMERHAUS; WEST (2003)
Microalgae biomass	650 USD ton^{-1}	ACIÉN FERNÁNDEZ; FERNÁNDEZ SEVILLA; MOLINA GRIMA (2019)
Hydrochloric acid (30%)	330 USD m^{-3}	ABDEL-FATAH; HAWASH; SHAARAWY (2021)
Sodium bicarbonate	435 USD ton^{-1}	CHEMANALYST (2025)
Utilities		
Steam	6 USD ton^{-1}	PETERS; TIMMERHAUS; WEST (2003)
Electricity	0.084 USD kWh^{-1}	LIU et al. (2025); QI et al. (2023)

9.2.4. Life Cycle Assessment (LCA)

The LCA was conducted based on international standards developed by the International Organization for Standardization (ISO), specifically "Environmental Management – Life Cycle Assessment," ISO 14040 – Principles and Framework, and ISO 14044 – Requirements and Guidelines (ISO, 2006a, 2006b). Therefore, the study followed the four steps outlined in these

standards: (i) definition of goal and scope; (ii) life cycle inventory analysis; (iii) life cycle impact assessment; and (iv) interpretation.

The LCA objective was to quantify and compare the environmental impacts of valorizing microalgae biomass through DF for bioH_2 production, considering the two scenarios presented in Section 9.2.2 (SC1 and SC2). Accordingly, a functional unit (FU) was defined: 2.14 m^3 of microalgae biomass with a solid content of 6% per hour in both scenarios.

Primary data on biomass productivity (ASSIS et al., 2020; SILVA et al., 2024a), hydrothermal pretreatment and DF parameters, bioH_2 yield, and avoided products (water, N, and P) (SILVA et al., 2024b) were used to develop the life cycle inventory of the primary processes. In both scenarios, microalgae cultivation was integrated with wastewater treatment, thereby eliminating the need for additional water and nutrients that are typically required in conventional cultivation. As a result, the consumption of water, N, and P was accounted for as avoided products in the background system. Data on the energy consumption of the HRAP was obtained from HERRERA et al. (2021). Additionally, the energy consumption of other equipment (electricity and steam) was estimated based on simulations performed using the Aspen Plus software (described in Section 9.2.2). This way, the primary processes were defined, while the secondary processes (production of chemicals, electricity, and steam) were obtained from the Ecoinvent v0.30.8 database (Table S9.2, Apêndice VII).

The two scenarios were simulated using the SimaPro® software (PRé Sustainability BV, Netherlands, version 9.6.0.1) to evaluate the environmental impacts. The ReCiPe 2016 method (v. 1.09) used the hierarchical perspective. The following impact categories were considered: Global Warming Potential (GWP); Photochemical Ozone Formation Potential, Human Health (POFP-hh); Particulate Matter Formation Potential (PMFP); Photochemical Ozone Formation Potential, Ecosystems (POFP-eco); Terrestrial Acidification Potential (TAP); Freshwater Eutrophication Potential (FEP); Marine Eutrophication Potential (MEP); Terrestrial Ecotoxicity Potential (TETP); Marine Ecotoxicity Potential (METP); Human Toxicity Potential, Cancer Effects (HTP-c); Fossil Resource Scarcity Potential (FRSP); Mineral Resource Scarcity (MRS); and Water Consumption (WC). Other studies reported these impact categories on topics related to microalgae biomass valorization (CASTRO et al., 2023; MAGALHÃES et al., 2022; MARANGON et al., 2021; SILVA et al., 2022).

Normalized results were presented, along with contribution analyses by stages and processes. The normalized results allowed for identifying impacts with relatively high or low values compared to the average global emissions per person in 2010 (HUIJBREGTS et al., 2017). Through the contribution analysis, environmental hotspots and process bottlenecks were identified. Potential improvements for the environmental performance of the scenarios were also suggested and discussed.

9.3.Results and discussion

9.3.1. Process Flow Diagram (PFD)

The bioH_2 production process was modeled and simulated for two scenarios (SC1 and SC2), each with distinct processing stages (Figure 9.2). In SC1, the effluent obtained after biomass cultivation (FEED) is mixed with $NaHCO_3$ and HCl (MIX) before being heated (HEAT) to reach the required operating temperature for the dark fermentation reactor (DF). Following fermentation, the output stream (S3) is directed to a separator (SEP), where the produced gas (S4) is separated from the effluent (S5).

In SC2, the process begins with the effluent from biomass cultivation (FEED) being pumped (PUMP) and sequentially heated using two heat exchangers (HEAT-1 and HEAT-2) to reach the required reaction temperature of 180°C. The preheated stream is then introduced into the pretreatment reactor (HTP). After pretreatment, the output stream (S4) is utilized to preheat the input stream (S1) in HEAT-1, reducing the energy demand in HEAT-2. The resulting stream (S6) undergoes filtration (FILTER) to separate solubilized carbohydrates in the supernatant. Finally, the filtered stream (S6) proceeds to the dark fermentation (DF) stage, following the same process described for SC1.

a)

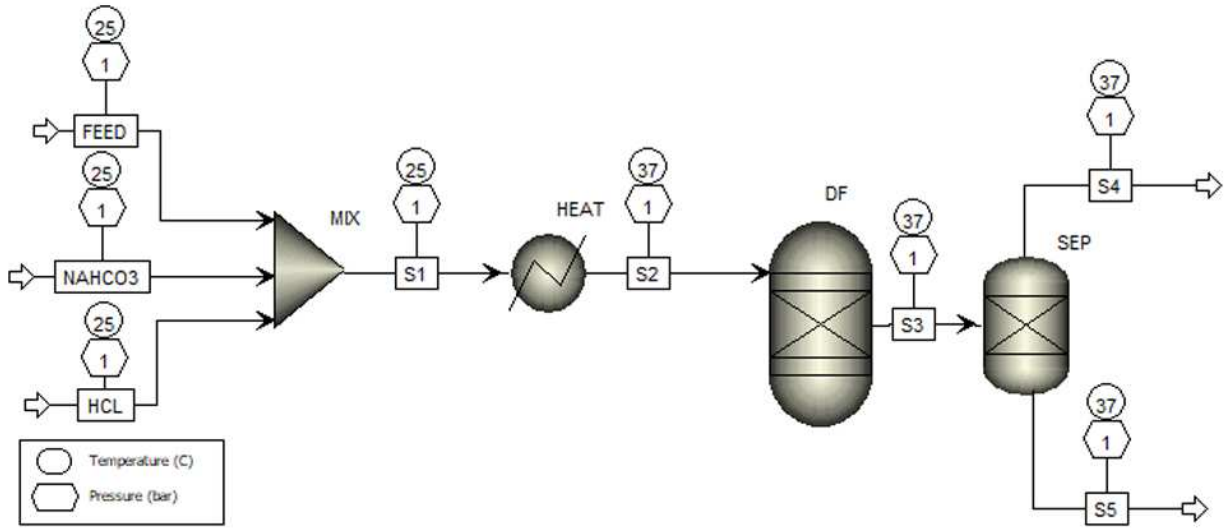

b)

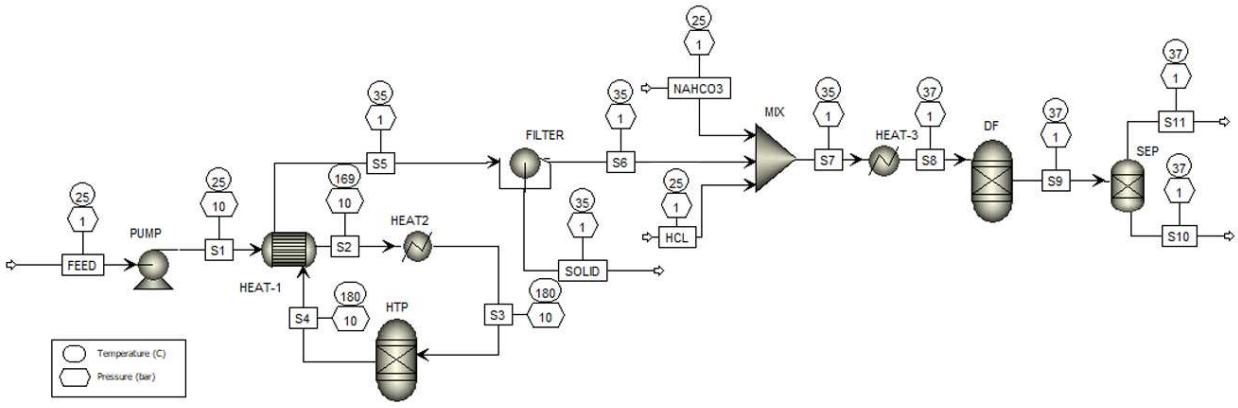

Figure 9.2. Process Flow Diagram (PFD) of biohydrogen production process from microalgae biomass. a) SC1 (Raw biomass as substrate) and b) SC2 (Pretreated biomass as substrate).

The mass balance (Figure 9.3) shows that in SC1, the process began with a feed stream of 2140.7 kg h^{-1} of microalgae biomass. To maintain a pH of 5, 21.34 kg h^{-1} of 30% HCl was added, along with 46.63 kg h^{-1} of $NaHCO_3$ for buffering. The fermentation reactor operated with a total mass flow of 2208.7 kg h^{-1}, comprising the input biomass and chemical additives. This process resulted in the production of 0.005 kg h^{-1} of bioH_2, accounting for 0.0002% of the total output.

Additionally, CO_2 was produced at a rate of 0.45 kg h^{-1}, representing 0.02% of the total mass flow. The effluent stream had a total mass of 2208.65 kg h^{-1}. To maintain the fermentation temperature at 37 °C, the process required 108.39 kg h^{-1} of steam.

a)

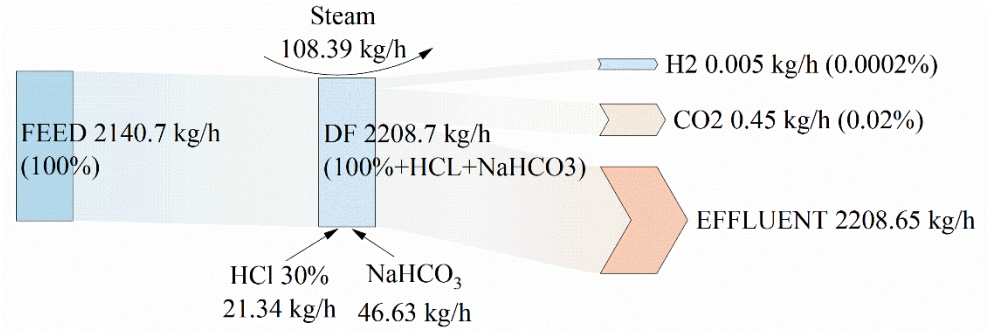

b)

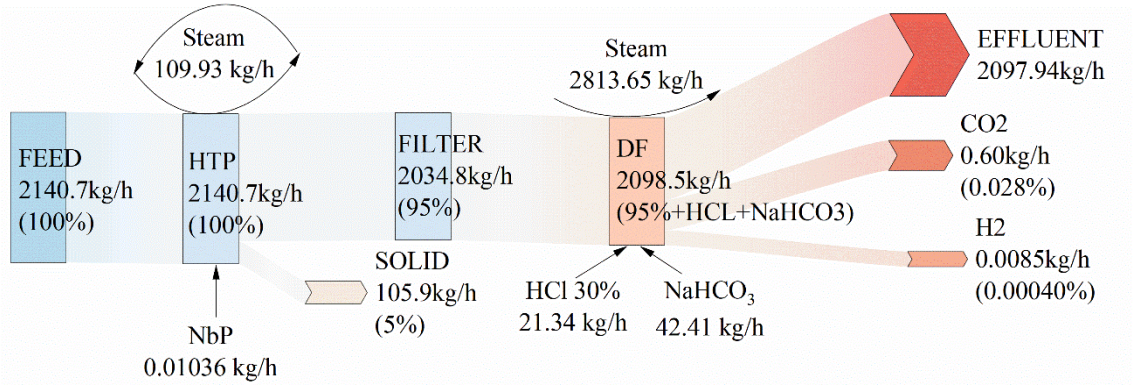

Figure 9.3. Mass flow in the dark fermentation process of microalgae biomass for bioH2 production. a) SC1 – Raw biomass. b) SC2 – Pretreated biomass.

In SC2, the initial feed stream remained the same as in SC1, consisting of 2140.7 kg h^{-1} of microalgae biomass. The hydrothermal pretreatment stage operated under identical input conditions, incorporating 0.01036 kg h^{-1} of NbP. After pretreatment, the biomass underwent a filtration step, which removed 105.9 kg h^{-1} of solids, equivalent to 5% of the initial feed mass. The remaining filtrate, totaling 2034.8 kg h^{-1}, was then introduced into the DF reactor. Similar to SC1, 21.34 kg h^{-1} of 30% HCl was added to maintain a pH of 5, while 42.41 kg h^{-1} of $NaHCO_3$ was used for buffering. The DF reactor in SC2 processed a total mass of 2098.5 kg/h.

The inclusion of hydrothermal pretreatment resulted in a slight increase in H_2 production, reaching 0.0085 kg/h, equivalent to 0.0004% of the total output. CO_2 production also increased slightly to 0.60 kg h^{-1} (0.028% of the total output. The effluent stream in SC2 totaled 2097.94 kg h^{-1}, slightly lower than in SC1 due to the removal of solids during pretreatment.

In terms of energy balance (Figure 9.4), SC1 represents a simpler energy flow, where the feedstock directly enters the DF reactor, requiring 108.39 kg h^{-1} of steam to maintain the operating conditions. The energy input is directly utilized for fermentation, with minimal additional processing steps.

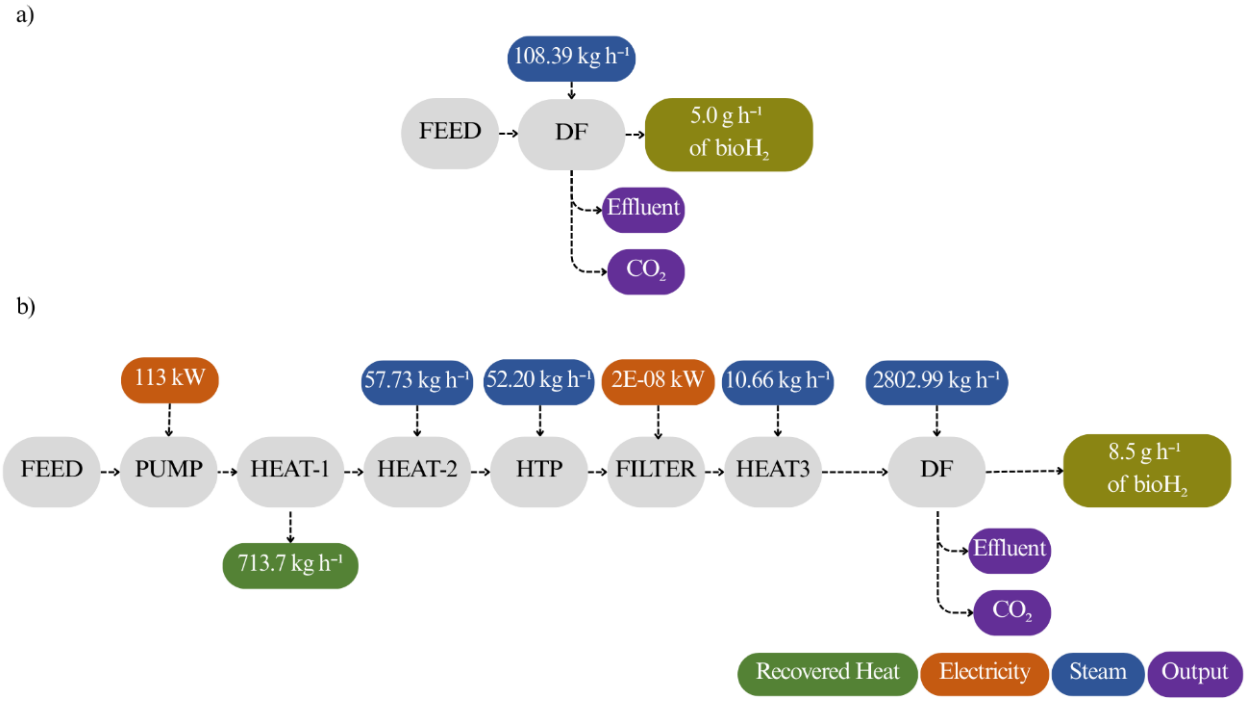

Figure 9.4. Energy power required by each equipment in different scenarios. a) SC1 – Raw biomass. b) SC2 – Pretreated biomass.

SC2, in contrast, exhibits a more complex energy profile due to the inclusion of HTP, additional heating stages, and filtration. One of the differences is the requirement for a pumping stage (113 kW), which ensures that the biomass feedstock enters the pretreatment reactor at 180°C under the necessary pressure conditions. This step is important to maintain a continuous flow and prevent phase separation or boiling within the reactor. To support heat integration between the pretreatment and fermentation stages, 713.7 kg h^{-1} of recovered heat is utilized, reducing the overall

external heating demand. However, multiple heating stages (HEAT-1, HEAT-2, HEAT-3) are still required, contributing to a higher total steam demand of 2802.99 kg h^{-1}, compared to SC1. The filtration stage introduces a minor electricity input (2E-08 kW), which is negligible compared to the total energy consumption.

9.3.2. Economic analysis

The selling cost of the bioH_2 and data related to the initial investment and processing costs were estimated from the simulation of the proposed scenarios. The total capital expenditures (CapEx) were 5.31 million USD for SC1 and 5.88 million USD for SC2. SC2 is more expensive due to the addition of a pretreatment step. Estimated equipment acquisition costs for both scenarios are presented in Table S9.3, Apêndice VII. In comparison, BOSHAGH; VAN NIEL; LEE (2025) report total CapEx of 2.15-2.44 million USD for dark fermentation–anaerobic digestion (DF-AD) systems that utilize coffee wastewater. Likewise, RANI et al. (2024) highlight that algae or lignocellulosic feedstocks often necessitate robust equipment (e.g., high-pressure reactors or specialized pretreatment systems) and advanced cultivation setups, which drive up capital costs.

Turning to operating expenditures (OpEx), the shift from 0.97 million USD $year^{-1}$ (SC1) to 1.17 million USD $year^{-1}$ (SC2) (Figure 9.5), a 20.6% increase, related predominantly from elevated steam (2802.99 kg h^{-1} vs. 108.39 kg h^{-1} in SC1) and electricity (113 kW pumping) needs for hydrothermal pretreatment. These costs for utilities align with PADIGALA et al. (2024), who report that high-temperature or high-pressure pretreatment steps can push costs (especially for steam) to 30% or more of OpEx. Simpler pretreatments, like mild acid hydrolysis, might lower steam requirements but often yield fewer fermentable carbohydrates from hard-to-degrade microalgal cells (CHEN; QUINN, 2021). In that sense, the choice between milder yet potentially less effective pretreatments and more intensive hydrothermal processes involves balancing higher energy inputs against the benefit of improved hydrolysis (AHMED et al., 2021).

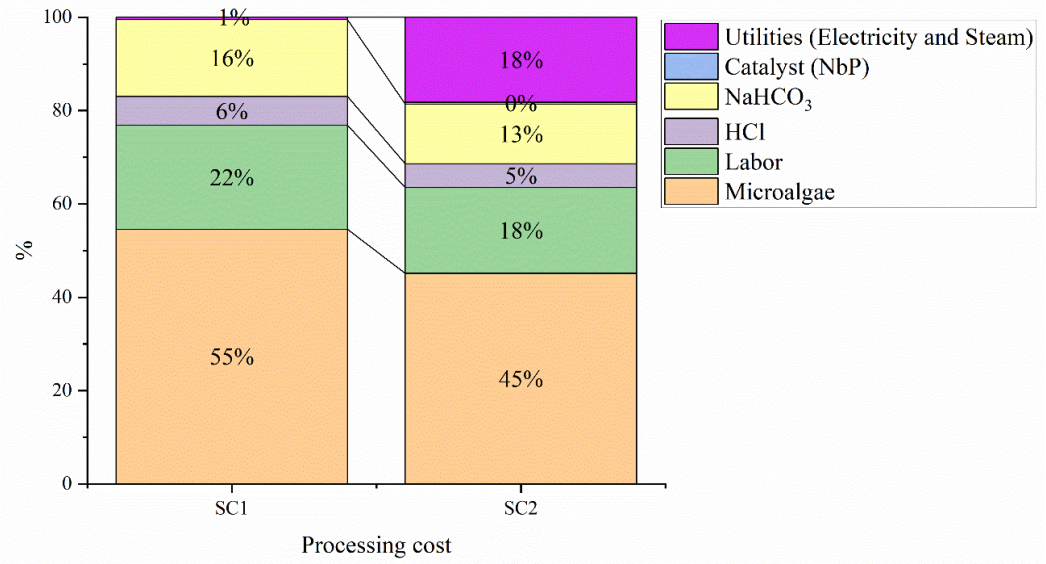

Figure 9.5. Annual distribution of processing costs for the two evaluated scenarios (in %).

Biomass cultivation remains the largest single cost driver, 54.6% in SC1 and 45.3% in SC2 (Figure 9.5), mirroring reports that microalgae production and harvesting can account for up to 76% of total expenses (AHMED et al., 2021). Cultivation costs in SC1 and SC2 remain the same. However, in SC2, they account for a smaller fraction of the total expenses because newly introduced cost components, such as utilities (18.3%) and the NbP catalyst (0.4%), dilute the relative share of cultivation costs. Meanwhile, labor outlays remain fixed at 0.216 million USD $year^{-1}$ in both scenarios but drop proportionally from 22.3% in SC1 to 18.5% in SC2, reflecting the larger total cost base.

SC2's hydrogen yield increases by 33%, which in turn lowers the MSP for bioH_2 to 4.98 USD L^{-1}, relative to 6.53 USD L^{-1} in SC1. This inverse relationship between yield and MSP is consistent with data from other DF studies. For instance, PADIGALA et al. (2024) observed that a 20-25% jump in DF yields could yield a 10-15% reduction in per-kilogram costs, even with additional energy inputs. Direct comparison of MSP must account for the different units and the specifics of microalgae-based processing (which is typically costlier due to cultivation and robust pretreatment). That said, H_2 production from natural gas-based methods costs 0.77-1.70 USD kg^{-1} (BOSHAGH; VAN NIEL; LEE, 2025). By comparison, the DF-AD system from BOSHAGH; VAN NIEL; LEE (2025), had a bioH_2 production cost of 3.84 USD kg^{-1} under thermophilic conditions and 3.86 USD kg^{-1} under mesophilic conditions, approximately 2.3–5 times higher than

SMR-based hydrogen production. The higher bioH_2 production rate compared to the present work can be attributed to key process differences. For instance, their feedstock was coffee-manufacturing wastewater. It contains readily fermentable carbohydrates (71% w w^{-1} dry basis), primarily hexoses, which are directly metabolized by fermentative bacteria into H_2 and volatile fatty acids (VFAs). In contrast, microalgal biomass has a recalcitrant structure composed of cellulose, hemicellulose, and proteins, which require previous hydrolysis for bioavailability (CHEN; QUINN, 2021). Even with hydrothermal pretreatment (180°C) in SC2, the H_2 yield remained lower than in BOSHAGH; VAN NIEL; LEE (2025), where AD was integrated to maximize substrate utilization and energy recovery. They considered a large-scale DF-AD system processing 800 m^3 d^{-1} of wastewater, higher than the scale of the present study, which inherently limits H_2 generation. In this context, approaches such as heat integration, steam recirculation, waste heat recovery (AHMED et al., 2021), and integrating DF-AD (BOSHAGH; VAN NIEL; LEE, 2025) could further mitigate utility costs, potentially rendering high-yield, increasing competitive in a carbon-constrained marketplace.

9.3.3. Environmental impacts

9.3.3.1.Life cycle inventory

The simplified life cycle inventory for the process is summarized in Table 9.2. For environmental analysis purposes, the inventory was prepared considering the unit in m^3 h^{-1} for both scenarios.

Table 9.2. Simplified life cycle inventory of biohydrogen production for SC1 – Raw biomass and SC2 – Pretreated biomass.

Stage			SC1	SC2	Unit
Cultivation	Input	Wastewater	2.14	2.14	m^3 h^{-1}
		Electricity for paddlewheel	34.20	34.20	kWh
	Avoided products	Water	2140.70	2140.70	kg
		N fertilizer	90.12	90.12	g
		P fertilizer	24.70	24.70	g
Hydrothermal pretreatment	Input	Electricity	-	62.00	kWh
	Input	Catalyst (Niobium phosphate)	-	0.01036	kg

Stage			SC1	SC2	Unit
Dark fermentation	Avoided products	Heating (as steam)	-	823.63	kg
		Recovered heat	-	713.70	kg
	Input	Heating (as steam)	108.39	2813.65	kg
		pH adjustment (Hydrochloric acid 30%)	21.34	21.34	kg
		Buffering (Sodium bicarbonate)	46.63	42.41	kg

In the cultivation stage, both scenarios utilized the same amount of wastewater (2140.7 kg h^{-1}) and electricity for paddlewheels (34.2 kWh), with equivalent contributions from avoided products such as water (2140.7 kg), N fertilizer (90.12 g), and P fertilizer (24.7 g). HTP stage, exclusive to SC2, introduced additional inputs, including 62 kWh of electricity, 0.01036 kg of NbP catalyst, and 823.63 kg of steam. However, this stage also recovered an amount of heat (713.7 kg), partially offsetting the energy demand. In the DF stage, SC2 required significantly more steam for heating (2813.65 kg) compared to SC1 (108.39 kg). However, SC2 utilized slightly less buffering agent (42.41 kg of sodium bicarbonate) than SC1 (46.63 kg), attributed to improved substrate digestibility post-pretreatment. Both scenarios required the same amount of HCl for pH adjustment (21.34 kg).

9.3.3.2.Environmental Impact Assessment

The normalized impacts across multiple environmental categories are illustrated in Figure 9.6, revealing trade-offs between the two approaches.

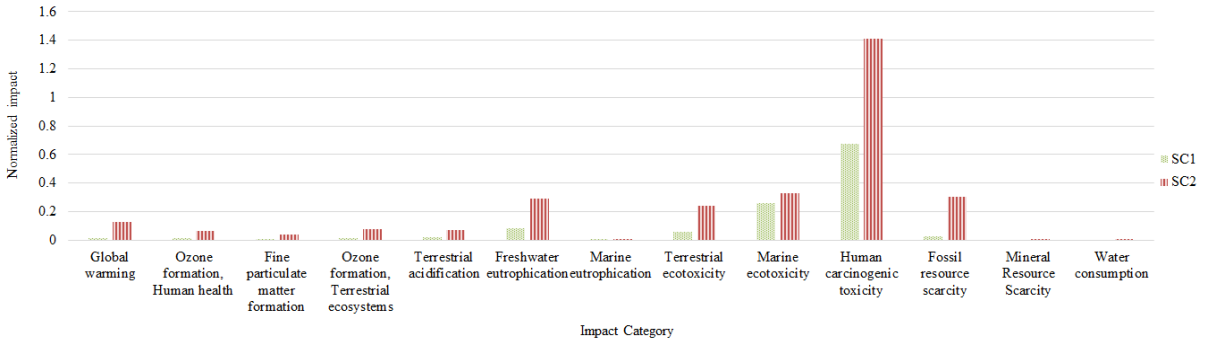

Figure 9.6. Environmental impacts of SC1 (Raw biomass) and SC2 (Pretreated biomass) across impact categories.

SC2 exhibits a 751% higher global GWP than SC1. While HTP, which requires 823.63 kg h^{-1} of steam, contributes to the overall heat demand, the DF stage in SC2 needs an even larger 2,813.65 kg h^{-1} of steam, compared to just 108.39 kg h^{-1} in SC1. Consequently, the combustion of fossil fuels to generate this steam increases GHG emissions. BECERRA-QUIROZ et al. (2024) similarly found that fossil-based thermal energy (5.85 kg CO_2-eq kg^{-1} H_2) was a major contributor to DF's carbon footprint. Likewise, ÖZEN DAŞ; ÖZMIHÇI; BÜYÜKKAMACI (2024) identified heat provision as a principal driver of GWP in waste-to-H_2 processes. Although SC2 improves bioH_2 yields, its heavy reliance on fossil-based steam highlights the need for integrating renewable or low-carbon heat sources, a challenge also emphasized by BOSHAGH; VAN NIEL; LEE (2025) in thermophilic DF–AD systems.

SC2's 403% higher tropospheric ozone impact likely results from increased emissions of nitrogen oxides (NO_x) and volatile organic compounds (VOCs), which are associated with the higher thermal input. Similarly, $PM_{2.5}$ emissions increase by 312%, reflecting the extensive combustion of fossil fuels to generate a total of 3,637.28 kg h^{-1} of steam (pretreatment + DF), despite some offset from the 713.70 kg h^{-1} of recovered heat. While BECERRA-QUIROZ et al. (2024) reported that up to 98.77% of total energy consumption in large-scale DF systems is allocated to mixing, the SC2 data demonstrate that steam requirements, particularly for DF, can be equally or even more energy-intensive. Substituting fossil-fueled steam generation with renewable or waste-heat sources, such as sugarcane bagasse (SCB) (KHATRI; PANDIT, 2022), could reduce ozone-precursor and particulate emissions.

SC2's 109% higher human carcinogenic toxicity is partly due to emissions from fossil fuel combustion driven by high steam demand, but also to the 0.01036 kg h^{-1} of NbP catalyst used in pretreatment. Moreover, SC2's fossil resource scarcity impact is 906% higher than SC1, primarily due to its extensive steam consumption (3,637.28 kg h^{-1}) and reliance on fossil fuels to meet that demand. Finally, SC2 requires 45% more water than SC1, primarily for steam generation in both hydrothermal pretreatment and DF.

While SC2 improves productivity, its reliance on fossil-fueled steam generation results in higher GWP, air pollution, fossil resource depletion, and water consumption. These findings highlight the need for integrating renewable or low-carbon heat sources to mitigate environmental impacts. Optimizations should focus on process efficiency, waste-heat recovery, and sustainable energy integration to ensure that biohydrogen production aligns with decarbonization goals and resource conservation strategies.

9.3.3.3.Analysis of process contribution

SC2 introduces an additional electricity and steam demand for hydrothermal pretreatment, a requirement absent in SC1, leading to increased environmental impacts across multiple categories, including global warming and carcinogenic toxicity (Figure 9.7). This escalation is particularly concerning given that the considered utilities are sourced from fossil-heavy grids, reinforcing findings by BECERRA-QUIROZ et al. (2024), who reported that high-temperature pretreatment can substantially elevate system-wide footprints when powered by non-renewable energy.

a)

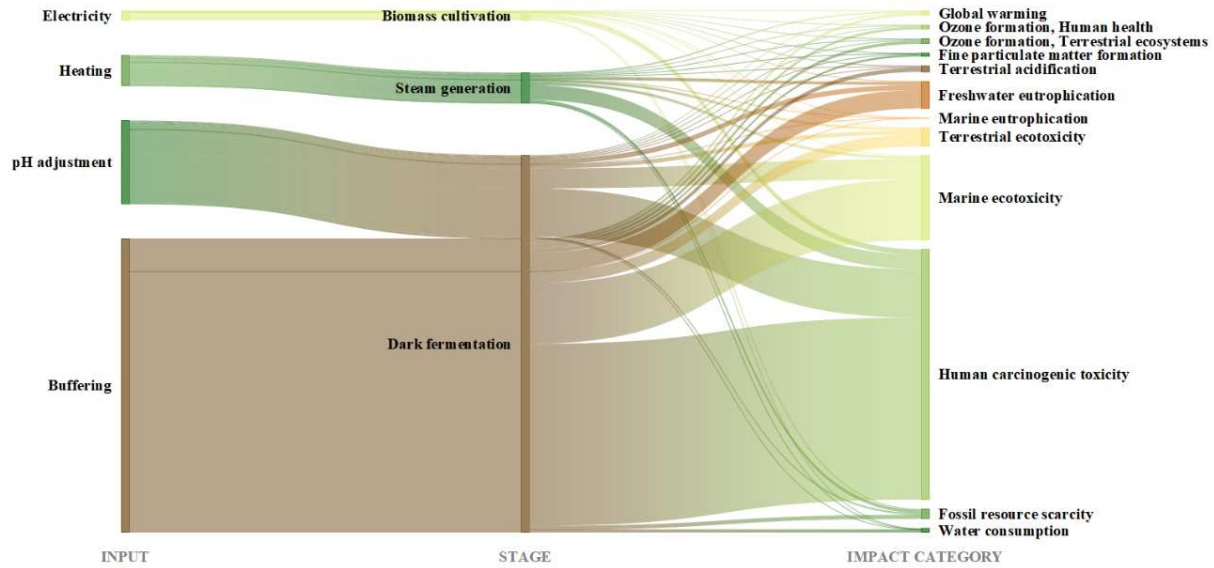

b)

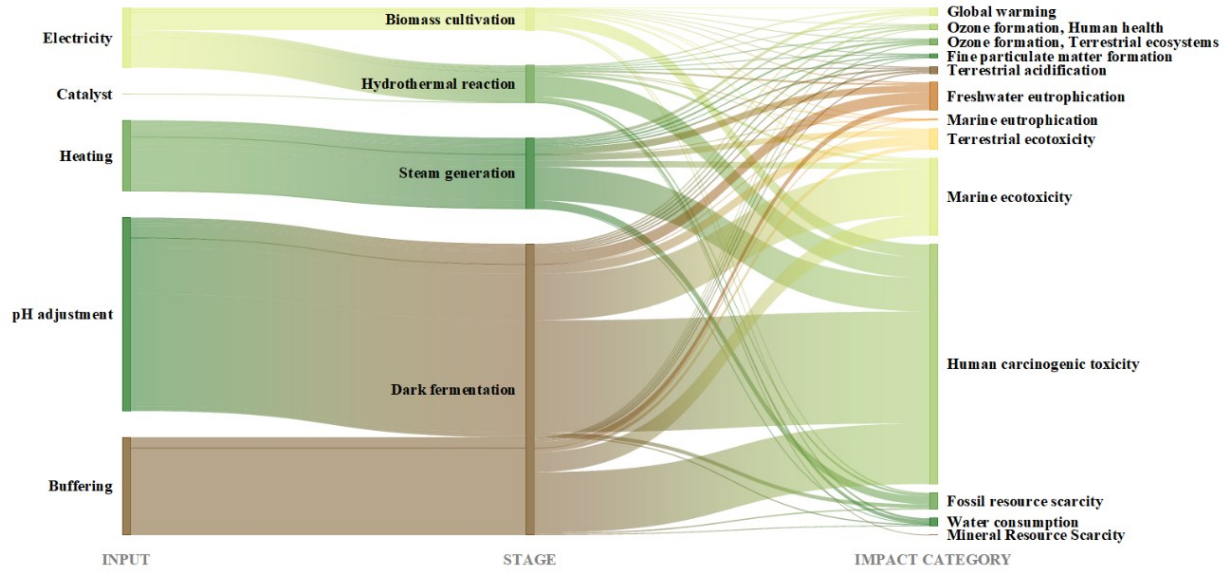

Figure 9.7. Sankey diagram representing process contributions to environmental impacts in a) SC1 (raw microalgae biomass without pretreatment) and b) SC2 (hydrothermal pretreatment with niobium phosphate catalyst).

Another distinguishing factor in SC2 is the use of NbP catalyst, which is not present in SC1, contributing to a higher mineral resource scarcity impact at the hydrothermal stage. Although the absolute quantity of catalyst used is small, BOSHAGH; VAN NIEL; LEE (2025) similarly

observed that even low-dose specialty chemicals can significantly influence resource depletion metrics, underscoring the importance of assessing their long-term sustainability.

SC2 demonstrates an advantage in the buffering stage, where its impacts on global warming, human carcinogenic toxicity, and ecotoxicity are 70–90% lower than in SC1. These findings align with BOSHAGH; VAN NIEL; LEE (2025), who highlighted that process chemicals, particularly pH buffers, can be major contributors to environmental impact when their lifecycle involves intensive energy or material inputs.

SC2 enhances bioH_2 yields but at a higher environmental cost due to increased fossil-based steam and electricity consumption, mineral resource depletion from NbP usage, and greater overall emissions. These findings emphasize the need for renewable energy integration, optimized resource use, and improved process efficiency to balance productivity with sustainability in biohydrogen production.

9.3.3.4.Damage assessment

The results of the damage category analysis for bioH_2 production under scenarios SC1 and SC2 are presented in Figure 9.8.

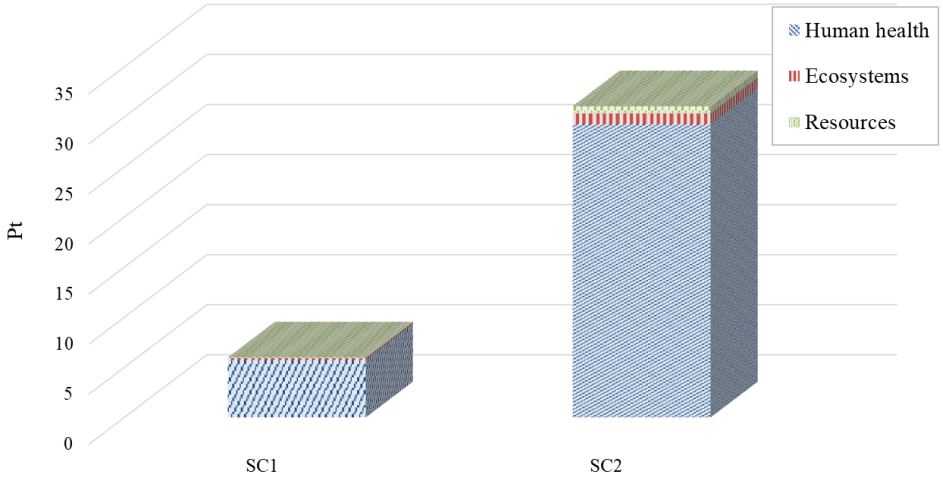

Figure 9.8. Damage category results for SC1 (raw microalgae biomass without pretreatment) and SC2 (hydrothermal pretreatment with niobium phosphate catalyst).

The analysis reveals an increase in environmental damage across all categories in SC2, particularly in human health impact. These findings align with ÖZEN DAŞ; ÖZMIHÇI;

BÜYÜKKAMACI (2024), who highlighted that $bioH_2$ production's environmental footprint is highly dependent on energy consumption, process configurations, and resource efficiency. The fourfold increase in human health impact in SC2 is primarily driven by fossil-fueled steam generation and increased electricity demand. SC2's fivefold increase in ecosystem damage is likely due to NOx emissions, VOCs, and acidifying substances due to elevated fossil fuel combustion. These results emphasize that transitioning to low-carbon heat sources and resource-efficient strategies is essential to balance productivity with environmental responsibility.

9.4.Conclusion

The comparative analysis of SC1 and SC2 highlights a trade-off between improved $bioH_2$ yield and environmental concerns. While SC2's hydrothermal pretreatment increases $bioH_2$ production by 33% and lowers the minimum selling price to 4.98 USD L^{-1}, it also raises energy consumption, intensifying global warming, acidification, and resource depletion impacts. Efficient heat recovery can help offset some of these drawbacks, but the process remains constrained by its reliance on fossil-based utilities and high operational costs. Furthermore, continued investigation into production-enhancing strategies is mandatory. Future efforts should also incorporate a sensitivity analysis to account for fluctuations in operational costs, feedstock availability, and policy changes, ensuring robust economic evaluations of emerging technologies. In addition, these efforts should prioritize advanced heat integration, renewable energy adoption, and catalyst optimization to improve process efficiency. Co-digestion with organic waste and microbial consortia engineering could further boost $bioH_2$ output. Addressing these challenges will be key to making $bioH_2$ from wastewater-grown microalgae a viable and sustainable alternative in the renewable energy landscape.

Acknowledgments

This study was financed in part by the Coordenação de Aperfeiçoamento de Pessoal de Nível Superior – Brasil (CAPES) – Finance Code 001. Furthermore, the authors gratefully acknowledge the financial support of the Conselho Nacional de Desenvolvimento Científico e Tecnológico (CNPq) [Grant Numbers: 405787/2022-7, 406204/2022-5, and 403521/2023-8] and Fundação de Amparo à Pesquisa do Estado de Minas Gerais (FAPEMIG) [Grant Numbers: APQ-03618-23, APQ-00756-23, and RED 00068-23].

References

ABDEL-FATAH, M. A.; HAWASH, S. I.; SHAARAWY, H. H. Cost-effective Clean Electrochemical Preparation of Ferric Chloride and its Applications. **Egyptian Journal of Chemistry**, v. 0, n. 0, p. 0–0, 6 jun. 2021.

ACIÉN FERNÁNDEZ, F. G.; FERNÁNDEZ SEVILLA, J. M.; MOLINA GRIMA, E. Costs analysis of microalgae production. Em: **Biofuels from Algae**. [s.l.] Elsevier, 2019. p. 551–566.

AHMED, S. F. et al. Biohydrogen Production From Biomass Sources: Metabolic Pathways and Economic Analysis. **Frontiers in Energy Research.** Frontiers Media S.A., , 10 set. 2021.

AHMED, S. F. et al. Biohydrogen production from wastewater-based microalgae: Progresses and challenges. **International Journal of Hydrogen Energy**, v. 47, n. 88, p. 37321–37342, out. 2022.

ASSIS, L. R. DE et al. Innovative hybrid system for wastewater treatment: High-rate algal ponds for effluent treatment and biofilm reactor for biomass production and harvesting. **Journal of Environmental Management**, v. 274, 15 nov. 2020.

BECERRA-QUIROZ, A. P. et al. Evaluation of the Dark Fermentation Process as an Alternative for the Energy Valorization of the Organic Fraction of Municipal Solid Waste (OFMSW) for Bogotá, Colombia. **Applied Sciences (Switzerland)**, v. 14, n. 8, 1 abr. 2024.

BOSHAGH, F.; VAN NIEL, E.; LEE, C. J. Techno-economic and life-cycle analyses of dark fermentative hydrogen production integrated with anaerobic digestion from coffee-manufacturing wastewater under thermophilic and mesophilic conditions. **Bioresource Technology**, v. 416, 1 jan. 2025.

CALIJURI, M. L. et al. Bioproducts from microalgae biomass: Technology, sustainability, challenges and opportunities. **Chemosphere**, v. 305, p. 135508, out. 2022.

CASTRO, J. S. et al. Life cycle assessment and techno-economic analysis for biofuel and biofertilizer recovery as by-products from microalgae. **Renewable and Sustainable Energy Reviews**, v. 187, p. 113781, nov. 2023.

CHEMANALYST. **Sodium Bicarbonate Price Trend and Forecast**. Disponível em: <https://www.chemanalyst.com/Pricing-data/sodium-bicarbonate-1186#:~:text=The%20latest%20quarter%2Dending%20price,costs%20amid%20ongoing%20geopolitical%20tensions.>. Acesso em: 15 fev. 2025.

CHEN, P. H.; QUINN, J. C. Microalgae to biofuels through hydrothermal liquefaction: Open-source techno-economic analysis and life cycle assessment. **Applied Energy**, v. 289, 1 maio 2021.

FUESS, L. T. et al. Biohydrogen-producing from bottom to top? Quali-quantitative characterization of thermophilic fermentative consortia reveals microbial roles in an upflow fixed-film reactor. **Chemical Engineering Journal Advances**, v. 7, 15 ago. 2021.

HERRERA, A. et al. Sustainable production of microalgae in raceways: Nutrients and water management as key factors influencing environmental impacts. **Journal of Cleaner Production**, v. 287, n. xxxx, p. 125005, mar. 2021.

HUIJBREGTS, M. A. J. et al. ReCiPe2016: a harmonised life cycle impact assessment method at midpoint and endpoint level. **The International Journal of Life Cycle Assessment**, v. 22, n. 2, p. 138–147, 12 fev. 2017.

ISO. ISO 14040 - Environmental Management-Life Cycle Assessment–Principles and Framework. [s.l: s.n.].

ISO. ISO 14044 – Environmental Management-Life Cycle Assessment–Requires and Guidelines. [s.l: s.n.].

JONES, S. B. et al. Process Design and Economics for the Conversion of Algal Biomass to Hydrocarbons: Whole Algae Hydrothermal Liquefaction and Upgrading. Richland, WA (United States): [s.n.].

KAYFECI, M.; KEÇEBAŞ, A.; BAYAT, M. Hydrogen production. Em: **Solar Hydrogen Production**. [s.l.] Elsevier, 2019.

KHATRI, P.; PANDIT, A. B. Systematic review of life cycle assessments applied to sugarcane bagasse utilization alternatives. **Biomass and Bioenergy**, v. 158, p. 106365, mar. 2022.

LEONG, Y. K. et al. Integrated biohydrogen production and dairy manure wastewater treatment via a microalgae platform. **International Journal of Hydrogen Energy**, fev. 2023.

LIU, H. et al. Calcium looping-enhanced biomass gasification for methanol production: Integrating methane dry reforming and carbon utilization. **Separation and Purification Technology**, v. 354, 19 fev. 2025.

MAGALHÃES, I. B. et al. Agro-industrial wastewater-grown microalgae: A techno-environmental assessment of open and closed systems. **Science of The Total Environment**, v. 834, p. 155282, ago. 2022.

MAGALHÃES, I. B. et al. Advancements in high-rate algal pond technology for enhanced wastewater treatment and biomass production: A review. **Journal of Water Process Engineering**, v. 66, p. 105929, set. 2024.

MARANGON, B. B. et al. Environmental performance of microalgae hydrothermal liquefaction: Life cycle assessment and improvement insights for a sustainable renewable diesel. **Renewable and Sustainable Energy Reviews**, p. 111910, nov. 2021.

MASOUMI, S.; DALAI, A. K. Techno-economic and life cycle analysis of biofuel production via hydrothermal liquefaction of microalgae in a methanol-water system and catalytic hydrotreatment using hydrochar as a catalyst support. **Biomass and Bioenergy**, v. 151, 1 ago. 2021.

ÖZEN DAŞ, İ. T.; ÖZMIHÇI, S.; BÜYÜKKAMACI, N. Environmental impact analysis of different wastes to biohydrogen, biogas and biohytane processes. International Journal of Hydrogen EnergyElsevier Ltd, , 22 fev. 2024.

PADIGALA, C. T. et al. Nanotechnological advancement in green hydrogen production from organic waste: Recent developments, techno–economic, and life cycle analyses. **International Journal of Hydrogen Energy**Elsevier Ltd, , 26 nov. 2024.

PETERS, M. S.; TIMMERHAUS, K. D.; WEST, R. E. **Plant design and economics for chemical engineers**. 5th. ed. [s.l.] McGraw-Hill International, 2003.

PRÉ. Various authors**. SimaPro database manual – methods library**. Disponível em: <https://simapro.com/wp-content/uploads/2020/10/DatabaseManualMethods.pdf>. Acesso em: 19 jan. 2021.

QI, J. et al. Hydrogen production from municipal solid waste via chemical looping gasification using CuFe2O4 spinel as oxygen carrier: An Aspen Plus modeling. **Energy Conversion and Management**, v. 294, 15 out. 2023.

RADY, H. A.; ALI, S. S.; EL-SHEEKH, M. M. Strategies to enhance biohydrogen production from microalgae: A comprehensive review. **Journal of Environmental Management**, v. 356, p. 120611, abr. 2024.

RANI, P. et al. Frontier in dark fermentative biohydrogen production from lignocellulosic biomass: Challenges and future prospects. **Fuel**, v. 366, 15 jun. 2024.

RAZU, M. H.; HOSSAIN, F.; KHAN, M. Advancement of Bio-hydrogen Production from Microalgae. Em: **Microalgae Biotechnology for Development of Biofuel and Wastewater Treatment**. Singapore: Springer Singapore, 2019.

SALAKKAM, A. et al. Valorization of microalgal biomass for biohydrogen generation: A review. **Bioresource Technology**, v. 322, p. 124533, fev. 2021.

SHARMA, A. K. et al. Biofuels from Microalgae: A Review on Microalgae Cultivation, Biodiesel Production Techniques and Storage Stability. **Processes**, v. 13, n. 2, p. 488, 10 fev. 2025.

SILVA, T. A. et al. Microalgae from food agro-industrial effluent as a renewable resource for agriculture: A life cycle approach. **Resources, Conservation and Recycling**, v. 186, p. 106575, nov. 2022.

SILVA, T. A. et al. Enhancing microalgae biomass production: Exploring improved scraping frequency in a hybrid cultivation system. **Journal of Environmental Management**, v. 355, p. 120505, mar. 2024a.

SILVA, T. A. et al. Biofuel from wastewater-grown microalgae: A biorefinery approach using hydrothermal liquefaction and catalyst upgrading. **Journal of Environmental Management**, v. 368, p. 122091, set. 2024b.

U.S. BUREAU OF LABOR STATISTICS. **CPI Inflation Calculator**. Disponível em: <https://www.bls.gov/data/inflation_calculator.htm>. Acesso em: 17 fev. 2025.

10.CONCLUSÕES GERAIS

Esta tese apresenta, de forma integrada, a viabilidade técnica da produção de bio-óleo e biohidrogênio (bioH_2) a partir de microalgas cultivadas em águas residuárias, com foco na otimização produtiva, avaliação econômica e impacto ambiental. A primeira hipótese, de que raspagens menos frequentes em reatores de biofilme promovem maior produtividade e acúmulo de lipídios e carboidratos, foi parcialmente comprovada. A raspagem a cada dois dias resultou na maior produtividade de biomassa (18,75 g SVT m^{-2} d^{-1}) e teor lipídico (15,45%), favorecendo sua valorização energética, especialmente para *Chlorella vulgaris*. No entanto, o desempenho foi espécie-dependente, indicando que a frequência ideal deve considerar as características da comunidade de microalgas e os objetivos de aproveitamento da biomassa.

A segunda hipótese, que propunha que o pré-tratamento hidrotérmico com fosfato de nióbio (NbP) favorece a liberação de carboidratos fermentáveis e aumenta a produção de bioH_2, foi comprovada. O tratamento a 180 °C por 10 minutos, com 75% de NbP, liberou até 7.431 mg CHt L^{-1}, elevando significativamente os rendimentos de bioH_2 (1,03 mmol H_2 mol^{-1} CHt), especialmente quando combinado ao controle de pH em 5,0, o que favoreceu a conversão acidogênica.

A terceira hipótese, de que a liquefação hidrotérmica (LHT), seguida de aprimoramento catalítico, aumenta a fração de hidrocarbonetos no bio-óleo, também foi comprovada. A LHT a 300 °C por 30 minutos gerou bio-óleo com até 76,3% de carbono e poder calorífico de 38,34 MJ kg^{-1}. O uso do catalisador CoMo promoveu o enriquecimento do produto em hidrocarbonetos de cadeia longa, como o heptadecano. No entanto, a presença de compostos nitrogenados ainda limita sua aplicação direta como combustível, exigindo etapas adicionais de refino.

Por fim, a quarta hipótese, que postulava que a substituição de insumos e a integração energética reduzem custos e impactos ambientais, foi parcialmente comprovada. A utilização de resíduos agroindustriais, como o bagaço de cana, contribuiu para reduzir a depleção de recursos fósseis, embora tenha elevado outros impactos, como emissões e toxicidade humana, especialmente no uso de solventes como o ciclohexano. As análises econômicas indicaram que o cultivo de microalgas representa o maior custo nas rotas de produção de bio-óleo e bioH_2. A integração de estratégias como recuperação de calor, uso de energias renováveis e substituição de reagentes críticos mostrou-se essencial para melhorar a viabilidade ambiental e econômica dos processos.

Em síntese, os resultados confirmam que a valorização energética de microalgas cultivadas em efluentes é tecnicamente viável, com alto potencial para integração em biorrefinarias sustentáveis. No entanto, desafios econômicos e ambientais ainda demandam soluções integradas e avanços tecnológicos para permitir a aplicação em larga escala.

11.SUGESTÕES PARA PESQUISAS FUTURAS

A produção de biomassa de microalgas cultivadas em águas residuárias ainda é limitada, o que reforça a necessidade de continuar investigando técnicas para aumentar a quantidade de biomassa gerada e aprimorar a colheita de forma eficiente. Estratégias como a otimização das condições de cultivo devem ser exploradas para tornar o processo mais viável em larga escala.

No contexto da produção de bio-óleo por liquefação hidrotérmica (LHT) e posterior atualização catalítica, é fundamental otimizar técnicas de hidrodesoxigenação (HDO) e hidrodenitrogenação (HDN) para reduzir o teor de nitrogênio no bio-óleo, aproximando suas características das de combustíveis fósseis. Estudos adicionais devem avaliar o desempenho do catalisador quanto à sua vida útil, contribuindo para processos mais sustentáveis e economicamente viáveis. Além disso, pesquisas futuras devem focar na recuperação de nutrientes da fase aquosa para reduzir custos e impactos ambientais, além de explorar a reutilização dessa fração como meio de cultivo para microalgas e como substrato para a produção de biohidrogênio por fermentação escura.

Para sistemas de bioH_2 com pré-tratamento hidrotérmico e inserção de catalisador como o fosfato de nióbio, futuros estudos devem abordar a recuperação e reutilização do catalisador para reduzir custos operacionais e impactos ambientais. A integração de sistemas de recuperação energética e digestão anaeróbia dos resíduos pode melhorar a eficiência energética do processo. Além disso, a mitigação de compostos inibidores gerados no pré-tratamento, como 5-HMF e furfural, é essencial para garantir rendimentos elevados de bioH_2. O uso de monitoramento em tempo real e otimização via inteligência artificial pode aprimorar o controle operacional, tornando o processo mais eficiente e escalável.

Por fim, trabalhos futuros devem priorizar a integração de abordagens sustentáveis, considerando não apenas a eficiência produtiva, mas também a viabilidade econômica e os impactos ambientais dos processos.

12.REFERÊNCIAS BIBLIOGRÁFICAS

AHMED, S. F. et al. Biohydrogen production from wastewater-based microalgae: Progresses and challenges. **International Journal of Hydrogen Energy**, out. 2021.

ASSIS, L. R. DE et al. Innovative hybrid system for wastewater treatment: High-rate algal ponds for effluent treatment and biofilm reactor for biomass production and harvesting. **Journal of Environmental Management**, v. 274, p. 111183, nov. 2020.

BALA AMUTHA, K.; MURUGESAN, A. G. Biological hydrogen production by the algal biomass Chlorella vulgaris MSU 01 strain isolated from pond sediment. **Bioresource Technology**, v. 102, n. 1, jan. 2011.

BOELEE, N. C. et al. The effect of harvesting on biomass production and nutrient removal in phototrophic biofilm reactors for effluent polishing. **Journal of Applied Phycology**, v. 26, n. 3, p. 1439–1452, 23 jun. 2014.

CASTELLO, D.; HAIDER, M. S.; ROSENDAHL, L. A. Catalytic upgrading of hydrothermal liquefaction biocrudes: Different challenges for different feedstocks. **Renewable Energy**, v. 141, p. 420–430, out. 2019.

CASTRO, J. S. et al. Life cycle assessment and techno-economic analysis for biofuel and biofertilizer recovery as by-products from microalgae. **Renewable and Sustainable Energy Reviews**, v. 187, p. 113781, nov. 2023.

CHANG, F. Biohydrogen production using an up-flow anaerobic sludge blanket reactor. **International Journal of Hydrogen Energy**, v. 29, n. 1, jan. 2004.

CHOI, J.-A. et al. Enhancement of fermentative bioenergy (ethanol/hydrogen) production using ultrasonication of Scenedesmus obliquus YSW15 cultivated in swine wastewater effluent. **Energy & Environmental Science**, v. 4, n. 9, 2011.

CHOUDHARY, P.; MALIK, A.; PANT, K. K. Algal Biofilm Systems: An Answer to Algal Biofuel Dilemma. Em: GUPTA, S. K.; MALIK, A.; BUX, F. (Eds.). **Algal Biofuels: Recent Advances and Future Prospects**. [s.l: s.n.]. p. 77–96.

COUTO, E.; CALIJURI, M. L.; ASSEMANY, P. Biomass production in high rate ponds and hydrothermal liquefaction: Wastewater treatment and bioenergy integration. **Science of the Total Environment**, v. 724, 2020.

GOLLAKOTA, A. R. K.; KISHORE, N.; GU, S. A review on hydrothermal liquefaction of biomass. **Renewable and Sustainable Energy Reviews**, v. 81, p. 1378–1392, jan. 2018.

GRANDE, L. et al. Hydrothermal Liquefaction of Biomass as One of the Most Promising Alternatives for the Synthesis of Advanced Liquid Biofuels: A Review. **Materials**, v. 14, n. 18, p. 5286, 14 set. 2021.

GROSS, M. et al. Development of a rotating algal biofilm growth system for attached microalgae growth with in situ biomass harvest. **Bioresource Technology**, v. 150, p. 195–201, 2013.

HEMSCHEMEIER, A.; MELIS, A.; HAPPE, T. Analytical approaches to photobiological hydrogen production in unicellular green algae. **Photosynthesis Research**, v. 102, n. 2–3, 17 dez. 2009.

HOEBLER, C. et al. Rapid acid hydrolysis of plant cell wall polysaccharides and simplified quantitative determination of their neutral monosaccharides by gas-liquid chromatography. **Journal of Agricultural and Food Chemistry**, v. 37, n. 2, p. 360–367, mar. 1989.

JIN, W. et al. Catalytic Upgrading of Biomass Model Compounds: Novel Approaches and Lessons Learnt from Traditional Hydrodeoxygenation - a Review. **ChemCatChem**, v. 11, n. 3, p. 924–960, 6 fev. 2019.

MAÑUNGA, T. et al. Evaluation of pretreatment methods and initial pH on mixed inoculum for fermentative hydrogen production from cassava wastewater. **Biofuels**, v. 13, n. 3, p. 301–308, 16 mar. 2022.

NGUYEN, T.-A. D. et al. Enhancement of fermentative hydrogen production from green algal biomass of Thermotoga neapolitana by various pretreatment methods. **International Journal of Hydrogen Energy**, v. 35, n. 23, dez. 2010.

ONCEL, S. S. et al. Biohydrogen production using mutant strains of Chlamydomonas reinhardtii: The effects of light intensity and illumination patterns. **Biochemical Engineering Journal**, v. 92, p. 47–52, nov. 2014.

PHANDUANG, O. et al. Improvement in energy recovery from Chlorella sp. biomass by integrated dark-photo biohydrogen production and dark fermentation-anaerobic digestion processes. **International Journal of Hydrogen Energy**, v. 44, n. 43, p. 23899–23911, set. 2019.

RAZU, M. H.; HOSSAIN, F.; KHAN, M. Advancement of Bio-hydrogen Production from Microalgae. Em: **Microalgae Biotechnology for Development of Biofuel and Wastewater Treatment**. Singapore: Springer Singapore, 2019.

SINGH, H.; DAS, D. Biohydrogen from microalgae. Em: **Handbook of Microalgae-Based Processes and Products**. [s.l.] Elsevier, 2020. p. 391–418.

XIA, A. et al. Comparison in dark hydrogen fermentation followed by photo hydrogen fermentation and methanogenesis between protein and carbohydrate compositions in Nannochloropsis oceanica biomass. **Bioresource Technology**, v. 138, p. 204–213, jun. 2013.

ZHANG, Y. Hydrothermal Liquefaction to Convert Biomass into Crude Oil. Em: **Biofuels from Agricultural Wastes and Byproducts**. Oxford, UK: Wiley-Blackwell, 2010. p. 201–232.

13.APÊNDICE I

Journal of Environmental Management 355 (2024) 120505

Contents lists available at ScienceDirect

Journal of Environmental Management

journal homepage: www.elsevier.com/locate/jenvman

Research article

Enhancing microalgae biomass production: Exploring improved scraping frequency in a hybrid cultivation system

Thiago Abrantes Silva [a,*], Alexia Saleme Aona de Paula Pereira [a], Jéssica Ferreira [a], Juliana Ferreira Lorentz [a], Marília Luise de Assis [a], Paula Peixoto Assemany [b], Alberto José Delgado dos Reis [c], Maria Lúcia Calijuri [a]

[a] Civil Engineering Department, Federal University of Viçosa, Campus Universitário, Viçosa, Minas Gerais, Brazil
[b] Environmental Engineering Department, Federal University of Lavras, Campus Universitário, Lavras, Minas Gerais, Brazil
[c] Bioenergy and Biorefineries Unit, National Laboratory of Energy and Geology, Lisbon, Portugal

ARTICLE INFO

Handling Editor: Prof Raf Dewil

Keywords:
Microalgae
High-rate algal pond
Biofilm reactor
Wastewater treatment

ABSTRACT

Recently, hybrid systems, such as those incorporating high-rate algal ponds (HRAPs) and biofilm reactors (BRs), have shown promise in treating domestic wastewater while cultivating microalgae. In this context, the objective of the present study was to determine an improved scraping frequency to maximize microalgae biomass productivity in a mix of industrial (fruit-based juice production) and domestic wastewater. The mix was set to balance the carbon/nitrogen ratio. The scraping strategy involved maintaining 1 cm wide stripes to retain an inoculum in the reactor. Three scraping frequencies (2, 4, and 6 days) were evaluated. The findings indicate that a scraping frequency of each 2 days provided the highest biomass productivity (18.75 g total volatile solids m^{-2} d^{-1}). The species' behavior varied with frequency: *Chlorella vulgaris* was abundant at 6-day intervals, whereas *Tetradesmus obliquus* favored shorter intervals. Biomass from more frequent scraping demonstrated a higher lipid content (15.45%). Extrapolymeric substance production was also highest at the 2-day frequency. Concerning wastewater treatment, the system removed 93% of dissolved organic carbon and ~100% of ammoniacal nitrogen. Combining industrial and domestic wastewater sources to balance the carbon/nitrogen ratio enhanced treatment efficiency and biomass yield. This study highlights the potential of adjusting scraping frequencies in hybrid systems for improved wastewater treatment and microalgae production.

1. Introduction

Microalgae are recognized as a promising solution for wastewater treatment due to their high biomass productivity and ability to use sunlight as their main energy source (Choudhary et al., 2020). Using microalgae in wastewater treatment removes excess nutrients, reduces the risk of water body eutrophication, and contributes to carbon dioxide (CO_2) sequestration from the atmosphere. Several studies have demonstrated the effectiveness of microalgae-based wastewater treatment processes (Assis et al., 2017; Couto et al., 2018; Magalhães et al., 2022).

To further enhance these processes, it is crucial to consider the wastewater mix to balance the carbon/nitrogen (C/N) ratio. Previous studies evaluated the optimal C/N ratio. For instance, Chiu et al. (2015) found that a C/N ratio 6 ensures sufficient nutrient availability, enhancing microalgae growth. Zheng et al. (2018) found a C/N ratio 7.9 optimal for nutrient removal and biomass production. Other works reported the best biomass production at a C/N ratio 5 (Xu et al., 2017; Yan et al., 2013). In this context, a balanced C/N ratio is essential for improved microalgal growth, as it affects the metabolic pathways involved in biomass accumulation and nutrient removal (Gama et al., 2023).

Improving microalgae harvesting through biofilm formation in support material using wastewater as the culture medium was also evaluated (Assis et al., 2020; Boelee et al., 2014; Liu et al., 2013; Wang et al., 2016). Hybrid systems, such as coupling suspended and attached culture systems, have resulted in higher algal yields than conventional high-rate algal ponds (HRAPs), with simpler and cheaper biomass collection (Assis et al., 2020). Among these hybrid systems, biofilm reactors (BRs)

* Corresponding author.
E-mail addresses: thiago.abrantes@ufv.br (T. Abrantes Silva), alexia.pereira@ufv.br (A.S.A.P. Pereira), jessica.f.ferreira@ufv.br (J. Ferreira), juliana.lorentz@ufv.br (J.F. Lorentz), marilia.luise@ufv.br (M.L. de Assis), paula.assemany@ufla.br (P.P. Assemany), alberto.reis@lneg.pt (A.J.D. dos Reis), calijuri@ufv.br (M.L. Calijuri).

https://doi.org/10.1016/j.jenvman.2024.120505
Received 1 December 2023; Received in revised form 31 January 2024; Accepted 25 February 2024
Available online 4 March 2024
0301-4797/

14.APÊNDICE II

Supplementary Information for Enhancing Microalgae Biomass Production: Exploring Improved Scraping Frequency in a Hybrid Cultivation System

Authors: Thiago Abrantes Silva [a,*], Alexia Saleme Aona de Paula Pereira [a], Jéssica Ferreira [a], Juliana Ferreira Lorentz [a], Marília Luise de Assis [a], Paula Peixoto Assemany [b], Alberto José Delgado dos Reis [c], Maria Lúcia Calijuri [a]

[a] Department of Civil Engineering, Federal University of Viçosa (Universidade Federal de Viçosa/UFV), Av. Peter Henry Rolfs, s/n, Campus Universitário, Viçosa, Minas Gerais, 36570-900, Brazil.

[b] Department of Water Resources and Sanitation, Federal University of Lavras (Universidade Federal de Lavras/UFLA), Campus Universitário, Lavras, Minas Gerais, 37200-900, Brazil.

[c] Bioenergy and Biorefineries Unit, National Laboratory of Energy and Geology (UBB/LNEG), Lisbon, Portugal.

***Corresponding author:** thiago.abrantes@ufv.br (T.A. Silva)

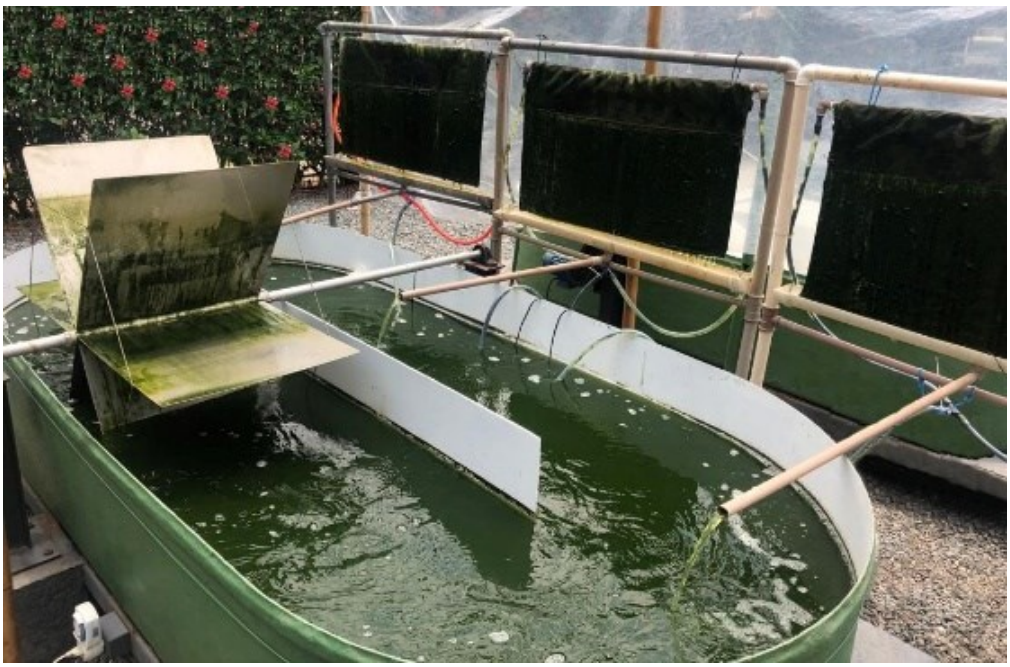

Figure S5.1. BRs integrated into a HRAP, composing the hybrid system.

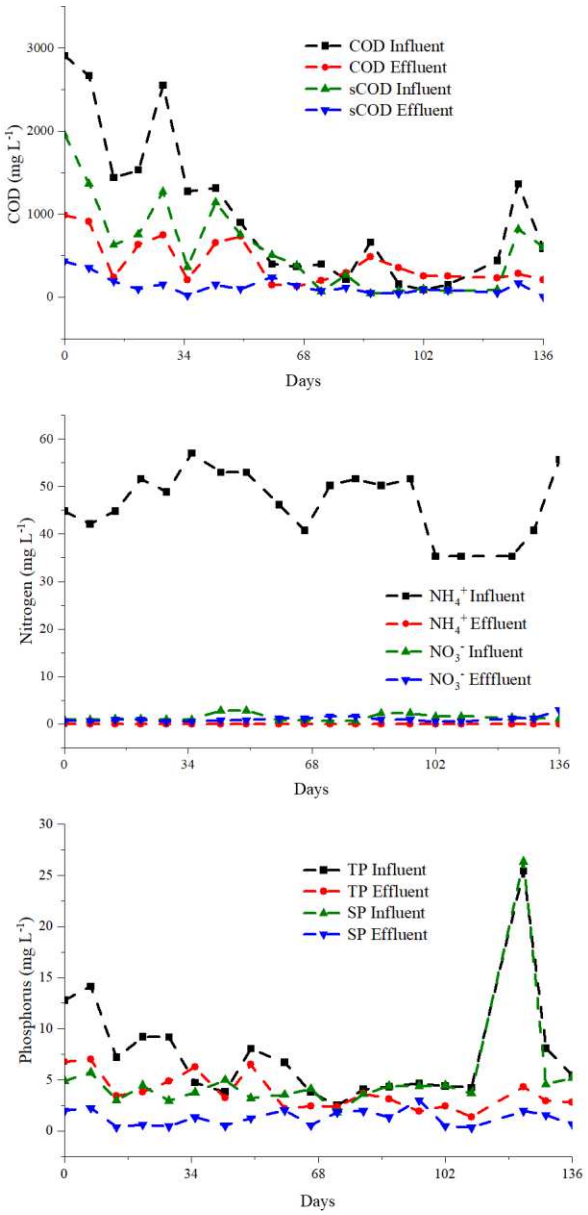

Figure S5.2. Influent and effluent concentrations of a) total chemical oxygen demand (COD), soluble COD (sCOD); b) ammonia nitrogen (NH_4^+), nitrate (NO_3^-); c) total phosphorus (TP), soluble phosphorus (SF) during the experimental period.

15.APÊNDICE III

Journal of Environmental Management 368 (2024) 122091

Contents lists available at ScienceDirect

Journal of Environmental Management

journal homepage: www.elsevier.com/locate/jenvman

Research article

Biofuel from wastewater-grown microalgae: A biorefinery approach using hydrothermal liquefaction and catalyst upgrading

Thiago Abrantes Silva [a,*], Eduardo de Aguiar do Couto [b], Paula Peixoto Assemany [b], Paula Alexandra Conceicao Costa [c], Paula A.S.S. Marques [c], Filipe Paradela [c], Alberto Jose Delgado dos Reis [c], Maria Lucia Calijuri [a]

[a] Department of Civil Engineering, Federal University of Vicosa (Universidade Federal de Vicosa/UFV), Av. Peter Henry Rolfs, s/n, Campus Universitario, Vicosa, Minas Gerais, 36570-900, Brazil

[b] Department of Water Resources and Sanitation, Federal University of Lavras (Universidade Federal de Lavras/UFLA), Campus Universitario, Lavras, Minas Gerais, 37200-900, Brazil

[c] Bioenergy and Biorefineries Unit, National Laboratory of Energy and Geology (LNEG/LNEG), Lisbon, Portugal

ARTICLE INFO

Keywords:
Biorefinery approach
Renewable energy
Byproducts reuse
Upgraded bio-oil
Microalga

ABSTRACT

Third-generation biofuels from microalgae are becoming necessary for sustainable energy. In this context, this study explores the hydrothermal liquefaction (HTL) of microalgae biomass grown in wastewater, consisting of 30% *Chlorella vulgaris*, 69% *Tetradesmus obliquus*, and 1% cyanobacteria *Limnothrix planctonica*, and the subsequent upgrading of the produced bio-oil. The novelty of the work lies in integrating microalgae cultivation in wastewater with HTL in a biorefinery approach, enhanced using a catalyst to upgrade the bio-oil. Different temperatures (300, 325, and 350 °C) and reaction times (15, 30, and 45 min) were tested. The bio-oil upgrading occurred with a Cobalt-Molybdenum (CoMo) catalyst for 1 h at 375 °C. Post-HTL, although the hydrogen-to-carbon (H/C) ratio decreased from 1.70 to 1.38–1.60, the oxygen-to-carbon (O/C) ratio also decreased from 0.39 to 0.079–0.104, and the higher heating value increased from 20.6 to 36.4–38.3 MJ kg^{-1}. Palmitic acid was the main component in all bio-oil samples. The highest bio-oil yield was at 300 °C for 30 min (23.4%). Upgrading increased long-chain hydrocarbons like heptadecane (5%), indicating biofuel potential, though nitrogenous compounds such as hexadecanenitrile suggest a need for further hydrodenitrogenation. Aqueous phase, solid residues, and gas from HTL can be used for applications such as biomass cultivation, bio-hydrogen, valuable chemicals, and materials like carbon composites and cement additives, promoting a circular economy. The study underscores the potential of microalgae-derived bio-oil as sustainable biofuel, although further refinement is needed to meet current fuel standards.

1. Introduction

Recent developments in sustainable energy alternatives have led to the growing importance of biofuels derived from microalgae cultivated in wastewater (Choudhary et al., 2020). Microalgae biomass is well-known for its potential as a promising feedstock. They offer advantages like continuous cultivation, adaptability to diverse climates, water and soil quality, minimal land-use conflicts, and mitigation of greenhouse gas emissions (GHG) as they consume carbon dioxide (CO_2) from the atmosphere (Singh and Ahluwalia, 2013).

Among the biofuel production strategies, hydrothermal liquefaction (HTL) presents an effective pathway for converting microalgae biomass into bio-oil (Couto et al., 2018). A previous life cycle assessment (LCA) study for the cultivation of microalgae using food waste revealed that the drying process produced the highest amount of GHGs, contributing to 10.65 kg carbon dioxide equivalent (CO_2-eq) per kg of biomass powder, more than half of the whole emissions attributed to the total production process (19.68 kg CO_2-eq), highlighting how drying can impact negatively microalgal-based processes (Thielemann et al., 2021). The process at high pressure and temperature conditions can effectively transform wet biomass into bio-oil, avoiding energy-intensive drying processes (Mathimani and Mallick, 2019). However, the HTL process

* Corresponding author.
E-mail addresses: thiago.abrantes@ufv.br (T.A. Silva), eduardo.couto@ufla.br (E.A. do Couto), paula.assemany@ufla.br (P.P. Assemany), paula.costa@lneg.pt (P.A.C. Costa), paula.marques@lneg.pt (P.A.S.S. Marques), filipe.paradela@lneg.pt (F. Paradela), alberto.reis@lneg.pt (A.J.D. Reis), calijuri@ufv.br (M.L. Calijuri).

https://doi.org/10.1016/j.jenvman.2024.122091
Received 16 January 2024; Received in revised form 16 July 2024; Accepted 26 July 2024

16.APÊNDICE IV

Supplementary Information for Biofuel from Wastewater-Grown Microalgae: A Biorefinery Approach Using Hydrothermal Liquefaction and Catalyst Upgrading

Authors: Thiago Abrantes Silva[a,*], Eduardo de Aguiar do Couto[b], Paula Peixoto Assemany[b], Paula Alexandra Conceição Costa[c], Paula A.S.S. Marques[c], Filipe Paradela[c], Alberto José Delgado dos Reis[c], Maria Lúcia Calijuri[a]

[a] Department of Civil Engineering, Federal University of Viçosa (Universidade Federal de Viçosa/UFV), Av. Peter Henry Rolfs, s/n, Campus Universitário, Viçosa, Minas Gerais, 36570-900, Brazil.

[b] Department of Water Resources and Sanitation, Federal University of Lavras (Universidade Federal de Lavras/UFLA), Campus Universitário, Lavras, Minas Gerais, 37200-900, Brazil.

[c] Bioenergy and Biorefineries Unit, National Laboratory of Energy and Geology (UBB/LNEG), Lisbon, Portugal.

***Corresponding author:** thiago.abrantes@ufv.br (T.A. Silva)

Table S6.1. Percentage of bio-oil compounds in the treatments evaluated.

Compound	Treatment (%)								
	1	2	3	4	5	6	7	8	9
Palmitic Acid	11.24	11.34	6.94	14.21	11.56	9.69	10.77	7.25	8.01
Linoleic Acid	8.27	7.74	1.98	15.45	10.59	3.17	1.70	-	3.06
2,6,10,14-Tetramethyl-2-hexadecene	5.36	4.27	5.88	3.54	4.04	5.71	4.72	3.81	3.57
Palmitoleic acid	4.79	4.76	3.46	3.32	4.22	2.05	2.29	-	-
2,6-Dihydroxyacetophenone, 2TMS derivative	4.70	0.90	4.11	-	-	-	-	-	-
Neophytadiene	3.15	2.57	-	-	-	-	-	-	-
3,7,11,15-Tetramethyl-2-hexadecen-1-ol	2.31	1.55	5.04	1.55	1.70	5.52	2.00	1.98	3.67
Palmitoleamide	3.61	3.57	1.65	4.53	3.96	1.82	1.90	1.70	2.44
Heptadecaneamide	-	-	1.90	1.58	5.46	1.70	-	-	-
p-Cresol	-	1.10	-	1.35	-	3.24	4.08	3.33	2.14
1-Pentadecene	1.55	1.93	2.67	2.37	1.65	4.00	3.54	2.57	1.68
3,7,11,15-Tetramethylhexadec-2-ene	2.51	2.50	4.88	2.04	1.75	3.61	1.30	1.75	1.50
Bicyclo[10.8.0]eicosane, (E)-	-	2.30	3.26	1.20	2.45	-	-	-	-
Hexadecanamide	2.95	2.85	1.70	2.56	2.74	2.30	1.65	1.50	1.65
Phenol, 4-ethyl-	-	-	-	-	-	1.84	2.40	2.72	1.55
2-Aminonaphthalene, N-trimethylsilyl-	-	-	-	-	-	-	-	1.60	2.55
9H-Pyrido[3,4-b]indole, 1-methyl-	2.30	1.79	1.72	1.67	1.90	1.67	1.86	2.58	2.27
1H-Indole, 2-methyl-	1.10	1.30	1.50	1.30	-	1.78	3.42	2.80	1.90
Indole	-	0.90	0.90	1.20	-	1.60	3.32	2.85	1.50
Heptadecanamide	2.56	-	-	-	2.28	1.90	1.20	1.05	1.40
Margaric acid	1.60	1.96	2.54	0.80	1.45	2.96	1.10	1.20	1.80
Octadecanamide	2.66	-	1.60	-	1.90	1.35	1.00	-	-
1,7-Trimethylene-2,3-dimethylindole	-	-	-	-	-	-	1.80	1.20	1.74
Phenol	-	0.90	-	0.70	-	2.20	2.21	2.20	1.10
9H-Pyrido[3,4-b]indole	1.40	-	1.30	0.80	2.06	1.40	1.60	1.60	2.23
9-Tricosene, (Z)-	-	-	-	0.90	2.60	-	1.15	1.20	-

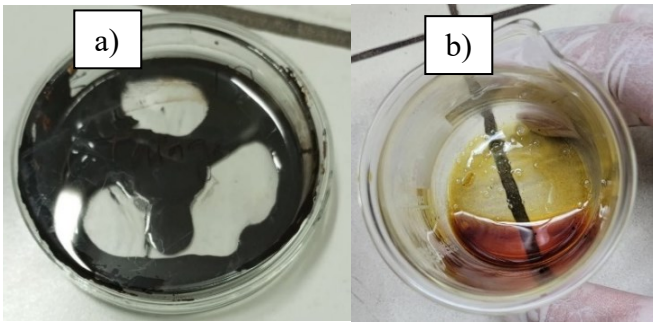

Figure S6.1. Visual aspect of bio-oil a) before and b) after upgrading.

Table S6.2. Compounds in the upgraded bio-oil.

Compounds	%
Hexadecanenitrile	5.14
Heptadecane	5.07
Pentadecane	4.70
Hexadecane	3.58
Octadecanenitrile	3.50
Octadecane	2.76
Hexadecane, 2,6,10,14-tetramethyl-	2.76
Toluene	2.39
Benzestrol, 2TMS derivative	2.24
Ethylbenzene	1.79
Tetradecane	1.79
Anthracene, 1-methyl-	1.79
Nonadecane	1.57
Icosane	1.57
Pentane, 2,3,4-trimethyl-	1.49
9H-Pyrido[3,4-b]indole, 1-methyl-	1.49
Dodecane	1.27
Tridecane	1.27
D-Galactitol, 2-(acetylmethylamino)-2-deoxy-3,4,6-tri-O-methyl-, 1,5-diacetate	1.27
Heneicosane	1.27
Octane	1.12
Nonane	1.12
Decane	1.12
Cyclotrisiloxane, hexamethyl-	1.12
1H-Cyclopropa[l]phenanthrene,1a,9b-dihydro-	1.12
N-Desmethylmirtazapine	1.12
Docosane	1.12
p-Cresol	1.04
Octacosane	1.04
Undecane	0.97
Anthracene, 9-ethyl-9,10-dihydro-10-hydroxy-	0.97
Hexadecanamide	0.97

17.APÊNDICE V

Supplementary Material for

Bio-oil from Hydrothermal Liquefaction of Microalgae Cultivated in Wastewater: An Economic and Life Cycle Approach

Table S7.1. Parameters and results for economic assessment in bio-oil production from microalgae biomass.

Parameter, units	SC1 and SC2	SC3 and SC4
Plant capacity, tons/year biomass	959.66	61599.07
Plant capacity, tons/year bio-oil	274.19	17599.77
Direct cost, million USD		
Purchased equipment	0.23	1.58
Delivery	0.023	0.159
Purchased equipment installation	0.100	0.680
Instrumentation and controls	0.067	0.454
Piping	0.080	0.541
Electrical	0.026	0.174
Buildings	0.074	0.506
Yard improvements	0.031	0.209
Service facilities	0.141	0.959
Indirect cost, million USD		
Engineering	0.082	0.558
Construction	0.087	0.593
Legal expenses	0.010	0.070
Contractor's fee	0.049	0.331
Contingency	0.095	0.645
Fixed capital investment (FCI). million USD	1.10	7.465
Working capital. million USD	0.17	1.120
Total capital investment (TCI). million USD	1.26	8.585
Raw Materials. million USD/year		
Microalgae feedstock	0.52	33.23
SCB or LPG	0.0028 (SCB), 0.0200 (LPG)	0.18 (SCB), 1.40 (LPG)
Cyclohexane	0.16	10.16
Products and Coproducts. million USD/year		
Bio-Oil	2.34	67.33
Carbon Credit	0.02	1.11
Utilities – Electricity. Million USD/year	0.003	0.083
Variable cost. million USD/year		
Operating labor	0.216	0.216

Parameter, units	SC1 and SC2	SC3 and SC4
Operating supervision	0.032	0.032
Maintenance and repairs	0.066	0.448
Operating supplies	0.010	0.067
Laboratory charges	0.032	0.032
Royalties (if not on lump-sum basis)	0.015	0.502
Fixed Charges. million USD/year		
Taxes (property)	0.011	0.075
Insurance	0.011	0.075
Plant Overhead. million USD/year	0.189	0.418
Manufacturing cost. million USD/year	1.264	45.525
General Expense. million US USD/year		
Administrative cost	0.079	0.174
Distribution and selling costs	0.074	2.511
Research development	0.059	2.009
Total production costs. million USD/year	1.475	50.219
Income tax rate	21%	21%

Table S7.2. Foreground processes obtained from Ecoinvent database v3.8.

Input/Avoided product	Process name
N fertilizer	Inorganic nitrogen fertiliser, as N {RoW} | nutrient supply from urea | APOS, S
P fertilizer	Inorganic phosphorus fertiliser, as P_2O_5 {RoW}| nutrient supply from diammonium phosphate | APOS, S
Water	Tap water {BR} | tap water production, conventional treatment | APOS, S
Electricity	Electricity, high voltage {BR}| production mix | APOS, S
Solvent	Cyclohexane {RoW}| production | APOS, S
Steam (Liquified petroleum gas)	Heat, central or small-scale, other than natural gas {RoW}| heat production, at heat pump 30kW, allocation exergy | APOS, S
Steam (Sugarcane bagasse)	Heat, district or industrial, other than natural gas {RoW}| treatment of bagasse, from sugarcane, in heat and power co-generation unit, 6400kW thermal | APOS, S

Table S7.3. Estimation of Equipment Acquisition Cost (USD).

Equipment	SC1 e SC2	SC3 e SC4
Filter	12400.00	34200.00
PUMP	20600.00	42300.00
HEAT-1	25800.00	938100.00
HEAT-2	11400.00	130800.00
HTL	72700.00	321200.00
SEP1	23500.00	42400.00
SEP2	22300.00	27200.00
SEP3	22300.00	27200.00
SEP4	22300.00	27200.00
Total	233300.00	1590600.00

Table S7.4. Normalized results considering relatively high or low values compared to the average global emissions per person in 2010.

IMPACT	INPUT	PROCESS	SC1	SC2	SC3	SC4
Global warming	Electricity	Biomass cultivation	0.00086647	0.000866	0	0
Ozone formation, Human health	Electricity	Biomass cultivation	0.000607087	0.000607	0	0
Ozone formation, Terrestrial ecosystems	Electricity	Biomass cultivation	0.000729822	0.00073	0	0
Fine particulate matter formation	Electricity	Biomass cultivation	0.000456637	0.000457	0	0
Terrestrial acidification	Electricity	Biomass cultivation	0.000850686	0.000851	0	0
Freshwater eutrophication	Electricity	Biomass cultivation	0.001526991	0.001527	0	0
Marine eutrophication	Electricity	Biomass cultivation	0.000404659	0.000405	0	0
Terrestrial ecotoxicity	Electricity	Biomass cultivation	0.000664001	0.000664	0	0
Marine ecotoxicity	Electricity	Biomass cultivation	0.002238107	0.002238	0	0
Human carcinogenic toxicity	Electricity	Biomass cultivation	0.022433072	0.022433	0	0
Fossil resource scarcity	Electricity	Biomass cultivation	0.001702877	0.001703	0	0
Water consumption	Electricity	Biomass cultivation	0.002600858	0.002601	0	0
Global warming	Electricity	Filtration	2.02683E-05	2.03E-05	0.001294	0.001294
Ozone formation, Human health	Electricity	Filtration	1.42009E-05	1.42E-05	0.000907	0.000907
Ozone formation, Terrestrial ecosystems	Electricity	Filtration	1.70719E-05	1.71E-05	0.00109	0.00109
Fine particulate matter formation	Electricity	Filtration	1.06816E-05	1.07E-05	0.000682	0.000682
Terrestrial acidification	Electricity	Filtration	1.98991E-05	1.99E-05	0.00127	0.00127
Freshwater eutrophication	Electricity	Filtration	3.57191E-05	3.57E-05	0.00228	0.00228
Marine eutrophication	Electricity	Filtration	9.4657E-06	9.47E-06	0.000604	0.000604
Terrestrial ecotoxicity	Electricity	Filtration	1.55322E-05	1.55E-05	0.000992	0.000992
Marine ecotoxicity	Electricity	Filtration	5.23534E-05	5.24E-05	0.003342	0.003342
Human carcinogenic toxicity	Electricity	Filtration	0.00052475	0.000525	0.033499	0.033499
Fossil resource scarcity	Electricity	Filtration	3.98334E-05	3.98E-05	0.002543	0.002543
Water consumption	Electricity	Filtration	6.08388E-05	6.08E-05	0.003884	0.003884
Global warming	Electricity	Pumping	9.45009E-05	9.45E-05	0.001889	0.001889
Ozone formation, Human health	Electricity	Pumping	6.62115E-05	6.62E-05	0.001324	0.001324
Ozone formation, Terrestrial ecosystems	Electricity	Pumping	7.95975E-05	7.96E-05	0.001591	0.001591
Fine particulate matter formation	Electricity	Pumping	4.98028E-05	4.98E-05	0.000996	0.000996

IMPACT	INPUT	PROCESS	SC1	SC2	SC3	SC4
Terrestrial acidification	Electricity	Pumping	9.27795E-05	9.28E-05	0.001855	0.001855
Freshwater eutrophication	Electricity	Pumping	0.00016654	0.000167	0.003329	0.003329
Marine eutrophication	Electricity	Pumping	4.41338E-05	4.41E-05	0.000882	0.000882
Terrestrial ecotoxicity	Electricity	Pumping	7.24188E-05	7.24E-05	0.001448	0.001448
Marine ecotoxicity	Electricity	Pumping	0.000244098	0.000244	0.00488	0.00488
Human carcinogenic toxicity	Electricity	Pumping	0.002446648	0.002447	0.048913	0.048913
Fossil resource scarcity	Electricity	Pumping	0.000185723	0.000186	0.003713	0.003713
Water consumption	Electricity	Pumping	0.000283661	0.000284	0.005671	0.005671
Global warming	Heating	Second heating exchange	0.000628003	0.000628	0.040308	0.040308
Ozone formation, Human health	Heating	Second heating exchange	0.000540381	0.00054	0.034684	0.034684
Ozone formation, Terrestrial ecosystems	Heating	Second heating exchange	0.000630703	0.000631	0.040481	0.040481
Fine particulate matter formation	Heating	Second heating exchange	0.000433593	0.000434	0.02783	0.02783
Terrestrial acidification	Heating	Second heating exchange	0.000412116	0.000412	0.026451	0.026451
Freshwater eutrophication	Heating	Second heating exchange	0.003431985	0.003432	0.22028	0.22028
Marine eutrophication	Heating	Second heating exchange	3.42187E-05	3.42E-05	0.002196	0.002196
Terrestrial ecotoxicity	Heating	Second heating exchange	0.000565972	0.000566	0.036327	0.036327
Marine ecotoxicity	Heating	Second heating exchange	0.007782341	0.007782	0.499505	0.499505
Human carcinogenic toxicity	Heating	Second heating exchange	0.020895458	0.020895	1.341164	1.341164
Fossil resource scarcity	Heating	Second heating exchange	0.001250886	0.001251	0.080287	0.080287
Water consumption	Heating	Second heating exchange	0.000118424	0.000118	0.007601	0.007601
Global warming	Heating	HTL reaction	0.000424483	0.000424	0.027249	0.027249
Ozone formation, Human health	Heating	HTL reaction	0.000365258	0.000365	0.023447	0.023447
Ozone formation, Terrestrial ecosystems	Heating	HTL reaction	0.000426309	0.000426	0.027366	0.027366
Fine particulate matter formation	Heating	HTL reaction	0.000293077	0.000293	0.018814	0.018814
Terrestrial acidification	Heating	HTL reaction	0.00027856	0.000279	0.017882	0.017882
Freshwater eutrophication	Heating	HTL reaction	0.002319767	0.00232	0.148915	0.148915
Marine eutrophication	Heating	HTL reaction	2.31293E-05	2.31E-05	0.001485	0.001485
Terrestrial ecotoxicity	Heating	HTL reaction	0.000382555	0.000383	0.024558	0.024558
Marine ecotoxicity	Heating	HTL reaction	0.005260286	0.00526	0.337678	0.337678

IMPACT	INPUT	PROCESS	SC1	SC2	SC3	SC4
Human carcinogenic toxicity	Heating	HTL reaction	0.014123782	0.014124	0.90666	0.90666
Fossil resource scarcity	Heating	HTL reaction	0.000845506	0.000846	0.054276	0.054276
Water consumption	Heating	HTL reaction	8.0046E-05	8E-05	0.005138	0.005138
Global warming	Heating	Steam generation	0.000349796	0.000276	0.022452	0.017708
Ozone formation, Human health	Heating	Steam generation	0.000635337	0.000405	0.04078	0.026025
Ozone formation, Terrestrial ecosystems	Heating	Steam generation	0.000756111	0.000501	0.048532	0.032175
Fine particulate matter formation	Heating	Steam generation	0.000367803	0.000241	0.023608	0.015478
Terrestrial acidification	Heating	Steam generation	0.000670785	0.000445	0.043055	0.028598
Freshwater eutrophication	Heating	Steam generation	0.001488545	0.002874	0.095545	0.184525
Marine eutrophication	Heating	Steam generation	0.000850772	2.46E-06	0.054608	0.000158
Terrestrial ecotoxicity	Heating	Steam generation	0.000722084	0.000555	0.046348	0.035613
Marine ecotoxicity	Heating	Steam generation	0.003011194	0.000769	0.193279	0.049361
Human carcinogenic toxicity	Heating	Steam generation	0.01013206	0.005902	0.650343	0.378908
Fossil resource scarcity	Heating	Steam generation	0.000289916	0.004723	0.018609	0.303231
Water consumption	Heating	Steam generation	0.002293041	1.02E-05	0.147183	0.000653
Global warming	Solvent	Separation - Liquid/solid phases	0.00584172	0.005842	0.37467	0.37467
Ozone formation, Human health	Solvent	Separation - Liquid/solid phases	0.004626614	0.004627	0.296737	0.296737
Ozone formation, Terrestrial ecosystems	Solvent	Separation - Liquid/solid phases	0.005877089	0.005877	0.376938	0.376938
Fine particulate matter formation	Solvent	Separation - Liquid/solid phases	0.002524442	0.002524	0.16191	0.16191
Terrestrial acidification	Solvent	Separation - Liquid/solid phases	0.003564038	0.003564	0.228586	0.228586
Freshwater eutrophication	Solvent	Separation - Liquid/solid phases	0.017587739	0.017588	1.128023	1.128023
Marine eutrophication	Solvent	Separation - Liquid/solid phases	0.000127435	0.000127	0.008173	0.008173
Terrestrial ecotoxicity	Solvent	Separation - Liquid/solid phases	0.005441111	0.005441	0.348976	0.348976
Marine ecotoxicity	Solvent	Separation - Liquid/solid phases	0.02915307	0.029153	1.869787	1.869787
Human carcinogenic toxicity	Solvent	Separation - Liquid/solid phases	0.147915633	0.147916	9.486848	9.486848
Fossil resource scarcity	Solvent	Separation - Liquid/solid phases	0.029671312	0.029671	1.903026	1.903026
Water consumption	Solvent	Separation - Liquid/solid phases	0.002456781	0.002457	0.15757	0.15757

18.APÊNDICE VI

Supplementary Information for

Enhancing microalgal biohydrogen production: Unlocking higher yields with hydrothermal pretreatment with niobium phosphate

Table S8.1. Preparation of the inoculum-substrate mixture for anaerobic fermentation: Food-to-microorganism (F/M) and buffering agent.

Sample	Reaction volume based on the substrate (L)	CODt mass in the substrate (g)	VS mass of the inoculum (g)	Inoculum mass (g)	$NaHCO_3$ (g)
RB	0.11	6.35	1.27	14.18	2.54
140	0.11	1.38	0.28	3.08	0.55
180	0.11	1.88	0.38	4.20	0.75

19.APÊNDICE VII

Supplementary Material for

Wastewater-grown microalgae as substrate for biohydrogen production: An economic and life cycle approach

Table S9.1. Parameters and results for economic assessment in biohydrogen production from microalgae biomass.

Parameter, units	SC1	SC2
Plant capacity, tons/year biomass	18,751.66	18,751.66
Plant capacity, m³/year biohydrogen	573.00	850.00
Direct cost, million USD		
Purchased equipment	0.98	1.09
Delivery	0.098	0.109
Purchased equipment installation	0.421	0.466
Instrumentation and controls	0.281	0.311
Piping	0.334	0.370
Electrical	0.108	0.120
Buildings	0.313	0.347
Yard improvements	0.129	0.143
Service facilities	0.593	0.657
Indirect cost, million USD		
Engineering	0.345	0.382
Construction	0.367	0.406
Legal expenses	0.043	0.048
Contractor's fee	0.205	0.227
Contingency	0.399	0.442
Fixed capital investment (FCI). million USD	4.618	5.115
Working capital. million USD	0.693	0.767
Total capital investment (TCI). million USD	5.310	5.882
Raw Materials. million USD/year		
Microalgae feedstock	0.53	0.53
Niobium phosphate	-	0.0045
Sodium bicarbonate	0.16	0.15
Hydrochloric acid	0.06	0.06
Products and Coproducts. million USD/year		
Biohydrogen	3.74	4.24
Carbon Credit	0.00048	0.00048
Utilities – Steam. Million USD/year	0.0050	0.139
Utilities – Electricity. Million USD/year	-	0.075
Variable cost. million USD/year		
Operating labor	0.216	0.216

Parameter, units	SC1	SC2
Operating supervision	0.032	0.032
Maintenance and repairs	0.277	0.307
Operating supplies	0.042	0.046
Laboratory charges	0.032	0.032
Royalties (if not on lump-sum basis)	0.021	0.024
Fixed Charges. million USD/year		
Taxes (property)	0.046	0.051
Insurance	0.046	0.051
Plant Overhead. million USD/year	0.315	0.333
Manufacturing cost. million USD/year	1.777	2.041
General Expense. million US USD/year		
Administrative cost	0.131	0.139
Distribution and selling costs	0.105	0.120
Research development	0.084	0.096
Total production costs. million USD/year	2.097	2.396
Income tax rate	21%	21%

Table S9.2. Foreground processes obtained from Ecoinvent database v3.8.

Input/Avoided product	Process name
N fertilizer	Inorganic nitrogen fertiliser, as N {RoW} | nutrient supply from urea | APOS, S
P fertilizer	Inorganic phosphorus fertiliser, as P_2O_5 {RoW}| nutrient supply from diammonium phosphate | APOS, S
Water	Tap water {BR} | tap water production, conventional treatment | APOS, S
Electricity	Electricity, high voltage {BR}| production mix | APOS, S
Steam	Steam, in chemical industry {RoW} | market for steam, in chemical industry | APOS, S
Niobium phosphate	Niobium, in ground
Sodium bicarbonate	Sodium bicarbonate {GLO} | market for sodium bicarbonate | APOS, S
Hydrochloric acid	Hydrochloric acid, without water, in 30% solution state {RoW} | market for | APOS, S

Table S9.3. Estimation of Equipment Acquisition Cost (USD).

Equipment	SC1	SC2
PUMP	-	20,000.00
HEAT	10,500.00	-
HEAT-1	-	23,800.00
HEAT-2	-	11,600.00
HEAT-3	-	11,200.00
HTP	-	68,000.00
FILTER	-	12,400.00
DF	948,00.00	917,100.00
SEP	22,300.00	22,300.00
Total	**980,800.00**	**1,086,400.00**